AT RISK MENTAL STATES, PRECISION MEDICINE AND EARLY BIOMARKERS IN MENTAL ILLNESSES

EDITED BY: Panteleimon Giannakopoulos, Sven Haller and Alessio Squassina
PUBLISHED IN: Frontiers in Psychiatry

frontiers Research Topics

frontiers

ISSN 1664-8714
ISBN 978-2-88966-890-8
DOI 10.3389/978-2-88966-890-8

About Frontiers

Frontiers is more than just an open-access publisher of scholarly articles: it is a pioneering approach to the world of academia, radically improving the way scholarly research is managed. The grand vision of Frontiers is a world where all people have an equal opportunity to seek, share and generate knowledge. Frontiers provides immediate and permanent online open access to all its publications, but this alone is not enough to realize our grand goals.

Frontiers Journal Series

The Frontiers Journal Series is a multi-tier and interdisciplinary set of open-access, online journals, promising a paradigm shift from the current review, selection and dissemination processes in academic publishing. All Frontiers journals are driven by researchers for researchers; therefore, they constitute a service to the scholarly community. At the same time, the Frontiers Journal Series operates on a revolutionary invention, the tiered publishing system, initially addressing specific communities of scholars, and gradually climbing up to broader public understanding, thus serving the interests of the lay society, too.

Dedication to Quality

Each Frontiers article is a landmark of the highest quality, thanks to genuinely collaborative interactions between authors and review editors, who include some of the world's best academicians. Research must be certified by peers before entering a stream of knowledge that may eventually reach the public - and shape society; therefore, Frontiers only applies the most rigorous and unbiased reviews.
Frontiers revolutionizes research publishing by freely delivering the most outstanding research, evaluated with no bias from both the academic and social point of view. By applying the most advanced information technologies, Frontiers is catapulting scholarly publishing into a new generation.

What are Frontiers Research Topics?

Frontiers Research Topics are very popular trademarks of the Frontiers Journals Series: they are collections of at least ten articles, all centered on a particular subject. With their unique mix of varied contributions from Original Research to Review Articles, Frontiers Research Topics unify the most influential researchers, the latest key findings and historical advances in a hot research area! Find out more on how to host your own Frontiers Research Topic or contribute to one as an author by contacting the Frontiers Editorial Office: frontiersin.org/about/contact

AT RISK MENTAL STATES, PRECISION MEDICINE AND EARLY BIOMARKERS IN MENTAL ILLNESSES

Topic Editors:
Panteleimon Giannakopoulos, Université de Genève, Switzerland
Sven Haller, Rive Droite SA, Switzerland
Alessio Squassina, University of Cagliari, Italy

Citation: Giannakopoulos, P., Haller, S., Squassina, A., eds. (2021). At Risk Mental States, Precision Medicine and Early Biomarkers in Mental Illnesses. Lausanne: Frontiers Media SA. doi: 10.3389/978-2-88966-890-8

Table of Contents

frontiers in Psychiatry

ORIGINAL RESEARCH
published: 04 May 2020
doi: 10.3389/fpsyt.2020.00278

Hippocampal Resting State Functional Connectivity in Patients With Schizophrenia and Unaffected Family Members

E. Kale Edmiston[1,2†], Yanzhuo Song[1,3†], Miao Chang[1,3,4], Zhiyang Yin[1,3], Qian Zhou[1,3], Yifang Zhou[1], Xiaowei Jiang[1,4], Shengnan Wei[1,4], Ke Xu[1,4], Yanqing Tang[1,3] and Fei Wang[1,3,4*]*

[1] Brain Function Research Section, The First Affiliated Hospital of China Medical University, Shenyang, China, [2] Department of Psychiatry, University of Pittsburgh School of Medicine, Pittsburgh, PA, United States, [3] Department of Psychiatry, The First Affiliated Hospital of China Medical University, Shenyang, China, [4] Department of Radiology, The First Affiliated Hospital of China Medical University, Shenyang, China

OPEN ACCESS

Edited by:
Panteleimon Giannakopoulos, Université de Genève, Switzerland

Reviewed by:
Hao He, Mind Research Network (MRN), United States
Dimitri Van De Ville, Federal Institute of Technology in Lausanne, Switzerland

***Correspondence:**
Fei Wang
fei.wang@yale.edu
Yanqing Tang
yanqingtang@163.com

[†]These authors have contributed equally to this work

Specialty section:
This article was submitted to Neuroimaging and Stimulation, a section of the journal Frontiers in Psychiatry

Received: 02 December 2019
Accepted: 23 March 2020
Published: 04 May 2020

Citation:
Edmiston EK, Song Y, Chang M, Yin Z, Zhou Q, Zhou Y, Jiang X, Wei S, Xu K, Tang Y and Wang F (2020) Hippocampal Resting State Functional Connectivity in Patients With Schizophrenia and Unaffected Family Members. Front. Psychiatry 11:278. doi: 10.3389/fpsyt.2020.00278

The hippocampus is an important candidate region in the study of functional connectivity alterations in schizophrenia (SZ) given its role as a functional hub for multiple brain networks. Although studies have implicated the hippocampus in SZ, no studies have compared hippocampal functional connectivity in healthy participants, patients with SZ, and unaffected family members (UAFMs). Patients and UAFM likely share biomarkers associated with susceptibility to SZ; the study of UAFM may also reveal compensatory markers. Patients with SZ, UAFM, and healthy control (HC) participants underwent resting state magnetic resonance imagingty and completed the Wisconsin Card Sort Task (WCST) as a measure of general cognitive function. We compared functional coupling with a hippocampus seed across the three groups. SZ and UAFM groups shared reductions in connectivity between the hippocampus and the striatum relative to HC. We also identified a significant positive correlation between WCST errors and hippocampal-striatal connectivity in the UAFM group. Hippocampal-striatal rsFC may be associated with familial susceptibility to SZ and with subtle cognitive deficits in the UAFM of individuals with SZ.

Keywords: resting state functional connectivity, hippocampus, unaffected family members, striatum, schizophrenia

INTRODUCTION

Schizophrenia (SZ) is a highly heritable psychiatric disorder characterized by disruptions in multiple cognitive domains, including attention, associative learning, and set shifting(1). These deficits are also often present in the unaffected family members (UAFMs) of patients with SZ and are likely due to shared alterations in brain functional networks (2). Therefore, the study of UAFM can elucidate endophenotypes associated with susceptibility to SZ. Although there is an established neuroimaging literature comparing UAFM to either HC or SZ, there are few studies designed to assess differences among the three groups.

Comparison of patients relative to UAFM and HC could elucidate functional network alterations specific to illness onset (i.e., when a feature is present only in SZ relative to UAFM and HC), illness susceptibility (i.e., when a feature is present in both UAFM and SZ relative to HC), as well as compensatory factors (i.e., differences that are present in UAFM compared to HC, but that are not present in SZ).

Hippocampal functional differences are prominent and consistent findings in SZ (3). The hippocampus is connected with a host of neocortical regions *via* reciprocal functional loops. Input from sensory, associative, and prefrontal cortices enters the hippocampus *via* the entorhinal cortex and outputs to subcortical and cortical structures. Thus, the hippocampus serves as an important functional hub associated with many cognitive processes that are also disrupted in SZ (4). Indeed, alterations in the functional coupling of such a densely connected region may best explain the wide range of cognitive deficits in SZ (5). There is evidence for hippocampal deficits in SZ that are present early in illness course, but worsen as the illness progresses (6). Others have shown that hippocampal functional deficits predict transition to psychosis in at-risk subjects (7). While this literature implicates the hippocampus in the pathophysiology of SZ, it is unclear if functional deficits are related to susceptibility or conversion to psychosis. It could be that alterations in hippocampal functional networks underlie the cognitive impairment that is observed in both at-risk cohorts and patients with SZ, i.e., that hippocampal alterations are a matter of degree and not of kind.

Altered connectivity between temporal and prefrontal regions are among the earliest findings in SZ neuroimaging research (8). Patients with SZ show reduced hippocampus-dorsolateral prefrontal cortex (DLPFC) coupling at rest (9). Reduced hippocampus-DLPFC coupling is also associated with impaired performance on associative learning and memory encoding tasks in patients with SZ (10–12). In addition to the literature implicating hippocampal functional connectivity alterations in SZ, a meta-analytic review of functional neuroimaging studies comparing UAFM to HC found functional activation differences in the DLPFC and hippocampus (2). There are fewer rsFC studies in at-risk cohorts, although task-based studies have reported altered hippocampus-DLPFC connectivity in people with risk alleles associated with SZ, and that these alterations are correlated with performance on cognitive tasks (13–15) Thus, altered coupling of the hippocampus and DLPFC during cognitive tasks may represent an "intermediate phenotype" for SZ (16). Given the important role of hippocampal-PFC coupling in cognitive processes that are disrupted in SZ, and to a lesser extent, in UAFM, shared hippocampal-DLPFC connectivity differences may represent a risk endophenotype associated with cognitive dysfunction. However, most studies of at-risk cohorts have employed task-based approaches, and results regarding the relationship between regional functional coupling and task performance have been mixed (16). To our knowledge, no studies have compared three groups (UAFM, HC, SZ) using an rsFC approach to assess hippocampal-DLPFC connectivity.

The striatum is also a key region in the pathophysiology of SZ (17). The striatum may be related to the pathophysiology of schizophrenia *via* its role in associative learning. Associative learning is thought to be facilitated by a hippocampal-striatal loop (18) and models of striatal dysfunction in schizophrenia posit that altered hippocampal-striatal coupling contributes to impaired associative learning (19). Specifically, disrupted striatal function facilitates incorrect associations between environmental stimuli, resulting in impaired cognition in SZ (20). Patients with SZ show reduced rsFC between the hippocampus and striatum, with higher baseline connectivity predicting better treatment response (21, 22). Fewer studies have assessed hippocampal-striatal coupling in at-risk or family cohorts, but there is evidence for resting cerebral blood flow alterations in at-risk cohorts that persist in those that convert to psychosis and resolve in those who remain unaffected (23) Taken together, this evidence suggests that hippocampal-striatal connectivity is a biomarker for susceptibility to SZ, although no studies have compared a sample of patients early in illness course to at-risk and healthy cohorts.

By using rsFC methods in a sample of patients with SZ at first episode or early in illness course, UAFM, and HC, we can better characterize neural networks associated with risk for and development of SZ, as well as potential compensatory mechanisms. Furthermore, given the prominent differences in performance that often confound SZ studies using task-based fMRI, resting state functional connectivity (rsFC) is a powerful tool for characterizing the coordinated activity of brain regions in SZ and UAFM. In the present study, we tested the hypothesis that patients with SZ would show reduced rsFC between the hippocampus and both the DLPFC and the ventral striatum relative to HC, and that UAFM would show connectivity values between those of the SZ and HC groups. Given that broad differences in cognitive function, including associative learning, set shifting, and attention, are present in both patients and UAFM, we also hypothesized that functional coupling of the hippocampus would be correlated with performance on the Wisconsin Card Sort Task (WCST), a measure of general cognitive function. Finally, because we were also interested in ascertaining if there were regions associated with compensatory mechanisms, we performed exploratory analyses to determine if there were hippocampal connectivity differences in the UAFM group relative to both HC and SZ.

MATERIALS AND METHODS

Participant Characteristics

This study was approved by the Institutional Review Board of China Medical University, Shenyang, China and was conducted in accordance with ethical standards set forth by the Declaration of Helsinki. Participants with SZ and their family members were recruited from inpatient and outpatient services at Shenyang Mental Health Center and the Department of Psychiatry, First Affiliated Hospital of China Medical University in Shenyang,

China. Control participants were recruited from the local Shenyang community by advertisement. All participants 18 and older provided written informed consent after a detailed description of the study. All participants under the age of 18 provided written informed assent and their parent or guardian provided written informed consent after a detailed description of the study.

Study procedures were conducted on a sample of 88 HC, 89 patients with SZ, and 71 UAFM ages 13 to 35. The three participant groups were matched for age (**Table 1A**). Two trained psychiatrists determined the presence or absence of Axis I disorders *via* the Structured Clinical Interview for DSM-IV Axis I Disorders (SCID) in participants ages 18 and older, and for those under the age of 18, the Schedule for Affective Disorders and Schizophrenia for School-Age Children-Present and Lifetime Version (K-SADS-PL). All SZ participants met DSM-IV diagnostic criteria for SZ, and all UAFM and HC participants did not have a current or lifetime Axis I disorder as determined by the SCID or the K-SADS. UAFM all had at least one parent who met DSM-IV criteria for SZ as determined by a detailed family history. In order to match for age, UAFMs enrolled in this study were not the children of the participants in the SZ group. HC participants also did not have a history of psychotic, mood, or other Axis I disorders in their first-degree family members, as determined by a detailed history. Participants were excluded for presence of substance or alcohol dependence or abuse, any major medical or neurological disorder, contraindications for MRI, or history of head trauma with loss of consciousness greater than 5 min. Because of cultural differences in the assessment and treatment of SZ in China versus western countries, as well as differences in psychosocial support systems, a sample of SZ patients without co-occurring substance or alcohol abuse or dependence is representative of the local population.

Interviewers completed the Brief Psychiatric Rating Scale (BPRS), a clinician-observational scale of psychiatric symptom severity designed for use in transdiagnostic psychiatric samples. A subset of 54 HC, 65 UAFM, and 43 SZ participants also completed the Wisconsin Card Sorting Test (WCST). For each participant, we calculated scores for total errors, non-perseverative errors, perseverative errors, and categories completed.

MRI Data Acquisition and Preprocessing

MRI data were acquired with a GE MR Signa HDX 3.0 T MRI scanner at the First Affiliated Hospital, China Medical University, Shenyang, China. A standard head coil was used for radio frequency transmission and reception of the nuclear magnetic resonance signal. All participants were instructed to keep their eyes closed but remain awake during the scan and restraining foam pads minimized head motion. FMRI images were acquired using a spin echo planar imaging (EPI) sequence, parallel to the anterior–posterior commissure (AC–PC) plane with the following scan parameters: repetition time (TR) = 2,000 ms; echo time (TE) = 40 ms; image matrix = 64 × 64; field of view (FOV) = 24 × 24 cm^2; 35 contiguous slices of 3 mm and without gap; scan time 6 min 40 s.

Resting-state fMRI data preprocessing was carried out using Data Processing Assistant for Resting-state fMRI (DPARSF), a program based in SPM8 and Resting-state f-MRI Data Analysis Toolkit (REST). For each participant, the first 10 scan volumes were discarded to allow for steady-state magnetization. Data were then slice time and motion corrected. Head motion parameters were computed by estimating translation in each direction and the angular rotation about each axis for each volume. Participants were excluded if their head motion was >2.5 mm in any of the x, y, or z directions or 2.5° or greater of angular motion in any direction throughout the course of the scan. Nineteen subjects were excluded due to motion, for a final sample of 82 HC, 73 patients with SZ, and 71 UAFM. Spatial normalization was performed using EPI templates with a resampling voxel size of 3 mm^3. Spatial smoothing was done with a 6 mm full-width at half-maximum (FWHM) Gaussian kernel. Preprocessing in REST consisted of linear detrending and filtering and nuisance covariate regression. Linear detrending and temporal bandpass (0.01–0.08 Hz) filtering were carried out to remove low-frequency drift and physiological high-frequency noise. Finally, linear regression of head motion parameters, global signal, white matter signal, and cerebrospinal fluid signal was performed to remove the effects of nuisance covariates. For completeness, we preprocessed images identically, but without global signal regression. We additionally preprocessed the images identically, but with less stringent bandpass filtering (0.01–0.15 Hz, see Supplemental Materials).

The bilateral hippocampal seed region of interest (ROI) was determined using stereotaxic, probabilistic maps of cytoarchitectonic boundaries, which included fascia dentate, subregions of the cornu ammonis (CA 1-CA 4), and subiculum (**Figure 1**). The ROI was created in standard space and based on voxels with at least 50% probability of belonging to the hippocampus (24). For each subject, a mean time series for the hippocampal seed was calculated by averaging the time series for all voxels within the ROI. Correlational analyses were then

TABLE 1A | Participant Characteristics (Total Sample).

	HC (N = 82)	UAFM (N = 71)	SZ (N = 73)	Statistics
Mean age in years ± SD	21.54 ± 5.31	22.93 ± 6.75	20.51 ± 6.06	F=2.92; p=0.056
Gender (male/female)	43:39	47:28	28:45	$\chi2$ = 8.16; p=0.017
Mean years of education ± SD	13.13 ± 2.69	12.00 ± 3.14	11.11 ± 2.62	F=10.19; p < 0.001
Medication (yes/no)	–	–	38:35	
First episode (yes/no)	–	–	64:9	
Mean BPRS total score ± SD	18.18 ± 0.54	18.62 ± 1.61	37.40 ± 13.40	F=110.14; p < 0.001

BPRS, Brief Psychiatric Rating Scale.

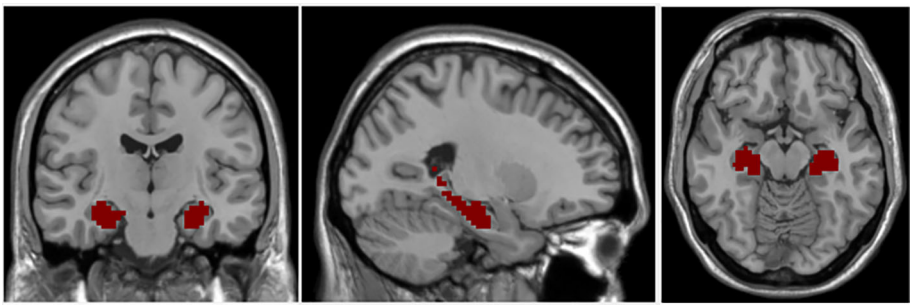

FIGURE 1 | Coronal, axial, and sagittal views of hippocampal seed region of interest.

performed between the hippocampal ROI time series and the time series for each brain voxel. The correlation coefficients in each map were transformed to Z values using Fisher r-to-z transformation for statistical testing.

Statistical Analysis

We used three-group ANOVA to compare demographic variables, including age and gender, as well as clinical (BPRS) and cognitive (WCST) variables.

For fMRI data, we created a binary mask of hippocampus functional connectivity by performing a one-sample t-test of the entire sample with a statistical threshold set to $p < 0.05$. We then used the general linear model function in SPM to perform a three-group comparison, covarying for age, gender, and years of education. To correct for multiple comparisons, we ran Monte Carlo Simulations using Alpha Sim ($p < 0.005$) and determined a threshold of 49 voxels for a corrected $p < 0.05$.

We extracted values from significantly different clusters and then performed *post hoc* pairwise t-tests to compare activity in these significant clusters by group.

We performed Pearson's partial correlations, controlling for age, educational attainment, and gender, between WCST total, non-perseverative, and perseverative errors scores and extracted correlation coefficients to test for relationships between hippocampal functional connectivity and cognitive function in each of the three diagnostic groups separately.

RESULTS

Demographic Data

The three groups did not differ with respect to age ($F = 2.945$, $p = 0.056$). There was a significant difference in the gender compositions of the group ($\chi^2 = 8.16$, $p = 0.017$) and in educational attainment ($F = 10.19$ $p < 0.001$, **Tables 1A**, **B**); all subsequent group-wise statistical testing included age, gender, and years of education as covariates of no interest. As expected, there were significant between-group differences in BPRS scores ($F = 110.14$, $p < 0.001$) and in performance on the WCST (all ps < 0.05, **Table 1B**).

Thirty-eight of the SZ patients were prescribed medications at the time of the scan. Specifically, 24 patients were prescribed a single atypical antipsychotic. Three patients were prescribed an antidepressant and an atypical antipsychotic. Three patients were prescribed only a mood stabilizer, and one patient was prescribed an atypical antipsychotic, an antidepressant, and a mood stabilizer. Seven participants were not able to provide specific information about the class of medication they were prescribed. All but nine patients were experiencing their first psychotic episode (**Table 1A**).

Neuroimaging Data

Three-way ANOVA revealed significantly different between-group hippocampal connectivity with the right and left striatum (**Figure 2**, **Table 2**).

TABLE 1B | Participant Characteristics and WCST Scores for the WCST Subsample.

	HC (N = 54)	UAFM (N = 65)	SZ (N = 43)	Statistics
Mean age in years ± SD	20.83 ± 5.40	23.23 ± 6.64	19.77 ± 5.71	F=4.83; p=0.01
Gender (male/female)	27:27	41:24	19:24	$\chi2 = 4.16$; p=0.13
Mean years of education ± SD	12.65 ± 2.86	12.03 ± 3.21	11.00 ± 2.45	F=3.88; p=0.023
Medication (yes/no)	–	–	23:20	
First episode (yes/no)	–	–	36:7	
Mean BPRS total score ± SD	18.18 ± 0.52	18.67 ± 1.69	35.98 ± 11.58	F=105.13; p < 0.001
Mean WCST categories completed ± SD	3.89 ± 2.02	3.20 ± 1.99	1.84 ± 1.86	F=13.26; p < 0.001
Mean WCST total errors ± SD	17.85 ± 10.93	21.94 ± 11.40	28.65 ± 12.57	F=10.50; p < 0.001
Mean WCST perseverative errors ± SD	8.93 ± 6.16	9.28 ± 9.59	12.81 ± 12.60	F=4.55; p=0.012
Mean WCST nonperseverative errors ± SD	10.94 ± 6.15	12.66 ± 7.32	15.84 ± 8.94	F=5.26; p=0.006

BPRS, Brief Psychiatric Rating Scale; WCST, Wisconsin Card Sorting Test.

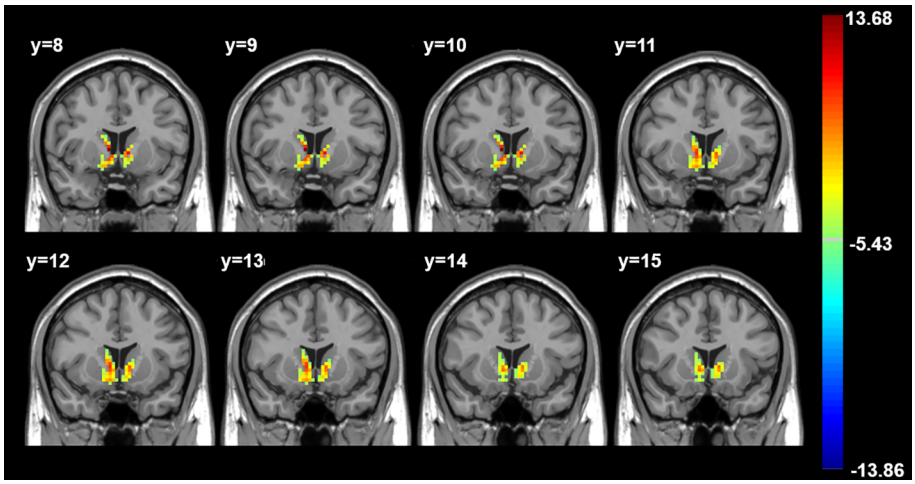

FIGURE 2 | Three-group differences, controlling for age, gender, and years of education. Color bar indicates F values. All findings p < 0.05 corrected for multiple comparisons using AlphaSim (p < 0.005, cluster > 49 voxels). R, Right. Axial images shown in radiological convention with MNI coordinates.

TABLE 2 | Significant Cluster Coordinates.

Brain Region	Cluster Size	MNI Coordinates			F Value
		X	Y	Z	
Right striatum	89	9	9	3	13.68
Left striatum	63	-9	9	0	11.38

All results p < 0.05, corrected.

Between-group *post hoc* analyses revealed significant between-group effects such that functional connectivity in the right striatum cluster was significantly higher in the HC group compared to both the UAFM and the SZ; there was no significant difference between hippocampus-right striatum functional connectivity between the UAFM and SZ groups. Connectivity between the hippocampus and the left striatum cluster was significantly higher in the HC compared to the SZ group, and in the UAFM compared to the SZ; there was no significant difference between the HC and UAFM groups (**Figure 3**).

For neuroimaging findings in data preprocessed without global signal regression, we examined correlations between the hippocampus and regions identified in the original analyses (left and right striatum). The overall pattern of findings persisted, although results no longer met criteria for significance (all *p*s > 0.05).

Additional Analyses

We also performed partial correlations controlling for age and gender between Z values in significant clusters and clinical symptoms as measured by the BPRS. We limited correlation analyses to the SZ group due to insufficient variability of BPRS scores in the HC and UAFM groups. Results were considered significant after correction for multiple comparisons (0.05/2 = 0.03333) (25). There were no significant correlations between

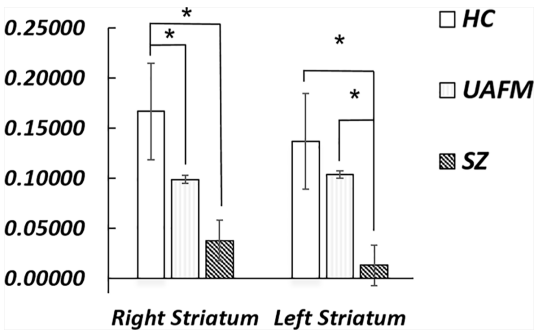

FIGURE 3 | *Post hoc* groupwise comparisons of hippocampal resting state connectivity. HC, healthy control; SZ, schizophrenia; UAFM, unaffected family member; R, right; L, left. Error bars are ± 2 standard error. *p < 0.05. All results Bonferroni corrected for multiple comparisons.

BPRS total score and connectivity between the hippocampus and the right striatum (r = 0.13) or the left striatum (r = 0.17, all *p*s > 0.05).

We performed *post hoc* comparisons in the SZ group only to test for effects of medication or first episode status in each of the significant clusters. There were no significant medication or episode status effects (medicated vs. not medicated, first episode vs. not first episode, all *p*s > 0.10).

Resting State Functional Connectivity Associations With WCST

For each of the three participant groups, we performed partial correlations, controlling for age, gender, and educational attainment, between either WCST total, non-perseverative, or perseverative errors and functional connectivity between the

hippocampus and each region (right and left striatum). Results were considered significant after correction for multiple comparisons (0.05/6 = 0.02041) (25). For the UAFM group, there was a significant positive association between nonperseverative errors and hippocampal-left ventral striatal connectivity (r = 0.34, p = 0.007, **Table 3B**, **Figure 4**) that survived correction. There were no additional significant correlations in the UAFM groups or any in either the SZ or the HC groups (all ps > 0.05, **Tables 3A**, **C**).

DISCUSSION

Consistent with our hypothesis, we found significant differences in hippocampal-striatal rsFC among individuals with SZ, UAFM, and HC. Connectivity differed between groups such that connectivity was highest in the HC group, followed by the UAFM group, and then the SZ group, although *post hoc* analysis showed that the left striatal connectivity finding only significantly differed between the SZ and HC groups. These findings suggest that hippocampal-striatal connectivity is associated with susceptibility to SZ. Contrary to our *a priori* hypothesis but similarly to McHugo and colleagues (26), we did not find group differences in rsFC between the hippocampus and the DLPFC, or associations between WCST performance and hippocampal-striatal connectivity in the SZ group. We did, however, find evidence for an association between WCST nonperseverative error frequency and hippocampal-left striatum connectivity in the UAFM, such that increased connectivity was associated with more errors. The significance of these findings is discussed in detail below.

Hippocampal-Striatal rsFC Findings

We found that hippocampal-striatum connectivity was reduced in patients with SZ compared to HC, while UAFM had intermediate connectivity values. Aberrant hippocampal-striatal connectivity has been implicated in SZ (27) and higher baseline hippocampal-striatal connectivity has been associated with symptom improvement and response to medication (21, 22). Given longstanding reports of dopaminergic alterations in SZ, as well as evidence for striatal functional alterations following treatment with atypical antipsychotics (21), we speculate that our findings of altered connectivity between the hippocampus and striatum could be related to function of the dopaminergic system. Disrupted dopaminergic modulation of the hippocampal-striatal circuit is associated with deficits in reward and associative learning, core deficits in SZ (28). A path analysis study found that motivation deficits in SZ mediate the relationship between cognition and functional outcome, suggesting that although SZ impacts a variety of domains, motivational deficits may be particularly important (29).

Correlation With Set Shifting Performance

We observed a significant correlation between hippocampal-left striatum resting state functional connectivity and nonperseverative errors in a subset of the UAFM group who completed the WCST. This relationship was such that increased connectivity was

TABLE 3A | Partial correlations between wisconsin card sort errors and regional hippocampal connectivity, patients with schizophrenia.

	Left Ventral Striatum	Right Ventral Striatum
Total Errors	0.03	0.13
Perseverative Errors	0.18	0.24
Nonperseverative Errors	-.20	-.15

Pearson partial correlations, controlling for age, educational attainment, and gender.

TABLE 3B | Partial correlations between wisconsin card sort errors and regional hippocampal connectivity, unaffected family members.

	Left Ventral Striatum	Right Ventral Striatum
Total Errors	0.05	0.15
Perseverative Errors	-0.19	-0.002
Nonperseverative Errors	0.34**	0.24

*Pearson partial correlations, controlling for age, educational attainment, and gender. **p < 0.01.*

TABLE 3C | Partial correlations between wisconsin card sort errors and regional hippocampal connectivity, healthy control participants.

	Left Ventral Striatum	Right Ventral Striatum
Total Errors	0.09	0.09
Perseverative Errors	-0.02	-0.06
Nonperseverative Errors	0.18	0.22

Pearson partial correlations, controlling for age, educational attainment, and gender.

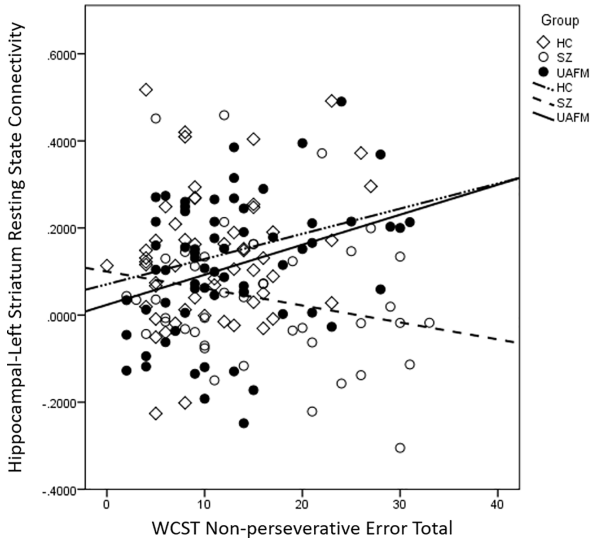

FIGURE 4 | Scatter plot depicting correlations between nonperseverative error totals and hippocampal-left striatum resting state functional connectivity by group. Values are plotted without adjustments for demographic covariates for ease of interpretation. HC, healthy control; SZ, schizophrenia; UAFM, unaffected family member.

associated with more errors. We did not observe this relationship in either the SZ or HC participants. A previous study of healthy individuals identified a frontal-striatal-hippocampal network involved during performance of the WCST. Specifically, lateral prefrontal cortex and striatum activity was associated with rule learning, while activity in the hippocampus and medial prefrontal cortex was associated with application of learned rules. Thus, the hippocampus and striatum have dissociable roles during set shifting/associative learning tasks (30). Another task-based fMRI study showed that, in healthy controls, hippocampal-striatal connectivity is associated with WCST performance, but that this coupling is mediated by medial prefrontal cortices. In this model, the striatum supports acquisition of a new rule, while the hippocampus is associated with maintaining these associations and the medial prefrontal cortices are involved in the shift from rule acquisition to rule maintenance (31). It is unclear why increased resting state connectivity would be associated with more errors in the UAFM only, although it is worth noting that the pattern of association is similar for the HC group, albeit not significant. We speculate that reduced coupling between these regions, which likely have differing roles during set shifting, may promote appropriate switching between rule learning and rule maintenance, and that this relationship is not present in SZ. Future studies that used task-based paradigms and generalized psychophysiological interaction approaches with samples of unaffected family members may help to clarify the nature of this functional circuit during associative learning and set shifting.

Our findings of altered functional coupling between the striatum and the hippocampus at rest corroborate the literature regarding striatal alterations in SZ, and extend this literature by implicating such alterations in the UAFM of patients with SZ. Striatal alterations in UAFM could indicate that striatal connectivity differences are related to genetic risk for SZ. There is some evidence for a relationship between genetic risk for schizophrenia and reduced striatal function during reward and associative learning (32, 33). However, this is the first study of which we are aware to demonstrate shared hippocampal-striatal resting state hypoconnectivity in both schizophrenia and UAFM. Longitudinal studies will better characterize the relationship between hippocampal-striatal connectivity and risk for the development of SZ versus conversion to psychosis.

Limitations

Because of the large sample size in this study, we opted to streamline self-report batteries for feasibility. As such, the BPRS was our only metric of symptom severity. We did not find any relationship between BPRS scores and rsFC of the hippocampus. The gender composition and educational attainment varied by group in our sample. However, we controlled for these factors statistically in all of our analyses and performed additional, secondary analyses that support the conclusions of our primary analysis. A portion of our sample was medicated at the time of the scan, although participants were early in treatment course. We performed *post hoc* analyses that showed no significant effects of medication status. However, it is still possible that medication class contributed to our findings, which we were underpowered to test. Despite these minor limitations, an important strength of this study is the recruitment of a SZ sample that was nearly entirely first episode, thereby avoiding confounding effects of illness course and treatment that limit much of the SZ literature. Furthermore, this study benefits from a sample without co-occurring addictive disorders. Finally, the age range of our sample was relatively large. Even though we controlled statistically for age in all analyses, the wide age range may have contributed to the lack of prefrontal findings, which was contrary to our hypothesis. Particularly because the adolescent and young adult period is critical for the development of prefrontal regions, studies designed to look at differences in rsFC developmental trajectories between patients and their family members are needed.

Conclusions

Our findings suggest that rsFC between the hippocampus and the striatum is associated with susceptibility to SZ. Longitudinal, prospective neuroimaging studies of UAFM, particularly when combined with detailed neuropsychological and behavioral evaluation, will help to elucidate compensatory neural mechanisms as well as the more subtle cognitive deficits and symptoms in UAFM. Taken together, this study highlights the importance of hippocampal-striatal functional networks in the pathophysiology of SZ; these findings could help to inform eventual identification of endophenotypic markers for SZ risk to facilitate early intervention.

DATA AVAILABILITY STATEMENT

The datasets generated for this study are available on request to the corresponding author.

ETHICS STATEMENT

The studies involving human participants were reviewed and approved by China Medical University Institutional Review Board. Written informed consent to participate in this study was provided by the participants' legal guardian/next of kin.

AUTHOR CONTRIBUTIONS

EE drafted the manuscript and analyzed and interpreted data. YS and MC analyzed and preprocessed data. ZY, QZ, YZ, XJ, SW, KX, and YT collected data. FW drafted the manuscript, interpreted data, and designed the study. All authors reviewed the manuscript prior to submission.

REFERENCES

1. Sambataro F, Mattay VS, Thurin K, Safrin M, Rasetti R, Blasi G, et al. Altered cerebral response during cognitive control: a potential indicator of genetic liability for schizophrenia. *Neuropsychopharmacology* (2013) 38(5):846–53. doi: 10.1038/npp.2012.250
2. Fusar-Poli P, Perez J, Broome M, Borgwardt S, Placentino A, Caverzasi E, et al. Neurofunctional correlates of vulnerability to psychosis: a systematic review and meta-analysis. *Neurosci Biobehav Rev* (2007) 31(4):465–84. doi: 10.1016/j.neubiorev.2006.11.006
3. Jaaro-Peled H, Ayhan Y, Pletnikov MV, Sawa A. Review of pathological hallmarks of schizophrenia: comparison of genetic models with patients and nongenetic models. *Schizophr Bull* (2010) 36(2):301–13. doi: 10.1093/schbul/sbp133
4. Lavenex P, Amaral DG. Hippocampal-neocortical interaction: a hierarchy of associativity. *Hippocampus* (2000) 10(4):420–30. doi: 10.1002/1098-1063(2000)10:4<420::AID-HIPO8>3.0.CO;2-5
5. Heckers S, Konradi C. Hippocampal pathology in schizophrenia. *Curr Top Behav Neurosci* (2010) 4:529–53. doi: 10.1007/7854_2010_43
6. McHugo M, Talati P, Woodward ND, Armstrong K, Blackford JU, Heckers S. Regionally specific volume deficits along the hippocampal long axis in early and chronic psychosis. *NeuroImage Clin* (2018) 20:1106–14. doi: 10.1016/j.nicl.2018.10.021
7. Schobel SA, Chaudhury NH, Khan UA, Paniagua B, Styner MA, Asllani I, et al. Imaging patients with psychosis and a mouse model establishes a spreading pattern of hippocampal dysfunction and implicates glutamate as a driver. *Neuron* (2013) 78(1):81–93. doi: 10.1016/j.neuron.2013.02.011
8. Friston KJ. The disconnection hypothesis. *Schizophr Res* (1998) 30(2):115–25. doi: 10.1016/S0920-9964(97)00140-0
9. Li B, Cui LB, Xi YB, Friston KJ, Guo F, Wang HN, et al. Abnormal effective connectivity in the brain is involved in auditory verbal hallucinations in schizophrenia. *Neurosci Bull* (2017) 33(3):281–91. doi: 10.1007/s12264-017-0101-x
10. Hanlon FM, Houck JM, Klimaj SD, Caprihan A, Mayer AR, Weisend MP, et al. Frontotemporal anatomical connectivity and working-relational memory performance predict everyday functioning in schizophrenia. *Psychophysiology* (2012) 49(10):1340–52. doi: 10.1111/j.1469-8986.2012.01448.x
11. Bahner F, Demanuele C, Schweiger J, Gerchen MF, Zamoscik V, Ueltzhoffer K, et al. Hippocampal-dorsolateral prefrontal coupling as a species-conserved cognitive mechanism: a human translational imaging study. *Neuropsychopharmacology* (2015) 40(7):1674–81. doi: 10.1038/npp.2015.13
12. Ragland JD, Ranganath C, Harms MP, Barch DM, Gold JM, Layher E, et al. Functional and neuroanatomic specificity of episodic memory dysfunction in schizophrenia: a functional magnetic resonance imaging study of the relational and item-specific encoding task. *JAMA Psychiatry* (2015) 72(9):909–16. doi: 10.1001/jamapsychiatry.2015.0276
13. Rasetti R, Sambataro F, Chen Q, Callicott JH, Mattay VS, Weinberger DR. Altered cortical network dynamics: a potential intermediate phenotype for schizophrenia and association with ZNF804A. *Arch Gen Psychiatry* (2011) 68(12):1207–17. doi: 10.1001/archgenpsychiatry.2011.103
14. Zheng F, Yan H, Liu B, Yue W, Fan L, Liao J, et al. ALDH2 Glu504Lys confers susceptibility to schizophrenia and impacts hippocampal-prefrontal functional connectivity. *Cereb Cortex* (2017) 27(3):2034–40. doi: 10.1093/cercor/bhw056
15. Zhang Z, Yan T, Wang Y, Zhang Q, Zhao W, Chen X, et al. Polymorphism in schizophrenia risk gene MIR137 is associated with the posterior cingulate Cortex's activation and functional and structural connectivity in healthy controls. *NeuroImage Clin* (2018) 19:160–6. doi: 10.1016/j.nicl.2018.03.039
16. Bahner F, Meyer-Lindenberg A. Hippocampal-prefrontal connectivity as a translational phenotype for schizophrenia. *Eur Neuropsychopharmacol* (2017) 27(2):93–106. doi: 10.1016/j.euroneuro.2016.12.007
17. Goghari VM, Sponheim SR, MacDonald ,AW3rd. The functional neuroanatomy of symptom dimensions in schizophrenia: a qualitative and quantitative review of a persistent question. *Neurosci Biobehav Rev* (2010) 34(3):468–86. doi: 10.1016/j.neubiorev.2009.09.004
18. Calabresi P, Castrioto A, Di Filippo M, Picconi B. New experimental and clinical links between the hippocampus and the dopaminergic system in Parkinson's disease. *Lancet Neurol* (2013) 12(8):811–21. doi: 10.1016/S1474-4422(13)70118-2
19. Moustafa AA, Gluck MA. Computational cognitive models of prefrontal-striatal-hippocampal interactions in Parkinson's disease and schizophrenia. *Neural Netw* (2011) 24(6):575–91. doi: 10.1016/j.neunet.2011.02.006
20. Kapur S. Psychosis as a state of aberrant salience: a framework linking biology, phenomenology, and pharmacology in schizophrenia. *Am J Psychiatry* (2003) 160(1):13–23. doi: 10.1176/appi.ajp.160.1.13
21. Sarpal DK, Robinson DG, Lencz T, Argyelan M, Ikuta T, Karlsgodt K, et al. Antipsychotic treatment and functional connectivity of the striatum in first-episode schizophrenia. *JAMA Psychiatry* (2015) 72(1):5–13. doi: 10.1001/jamapsychiatry.2014.1734
22. Kraguljac NV, White DM, Hadley N, Hadley JA, Ver Hoef L, Davis E, et al. Aberrant hippocampal connectivity in unmedicated patients with schizophrenia and effects of antipsychotic medication: a longitudinal resting state functional MRI study. *Schizophr Bull* (2016) 42(4):1046–55. doi: 10.1093/schbul/sbv228
23. Allen P, Chaddock CA, Egerton A, Howes OD, Bonoldi I, Zelaya F, et al. Resting hyperperfusion of the hippocampus, midbrain, and basal ganglia in people at high risk for psychosis. *Am J Psychiatry* (2016) 173(4):392–9. doi: 10.1176/appi.ajp.2015.15040485
24. Amunts K, Kedo O, Kindler M, Pieperhoff P, Mohlberg H, Shah NJ, et al. Cytoarchitectonic mapping of the human amygdala, hippocampal region and entorhinal cortex: intersubject variability and probability maps. *Anat Embryol (Berl)* (2005) 210(5-6):343–52. doi: 10.1007/s00429-005-0025-5
25. Benjamini Y, Drai D, Elmer G, Kafkafi N, Golani I. Controlling the false discovery rate in behavior genetics research. *Behav Brain Res* (2001) 125(1):279–84. doi: 10.1016/S0166-4328(01)00297-2
26. McHugo M, Rogers BP, Talati P, Woodward ND, Heckers S. Increased Amplitude of Low Frequency Fluctuations but Normal Hippocampal-Default Mode Network Connectivity in Schizophrenia. *Front Psychiatry* (2015) 6:92. doi: 10.3389/fpsyt.2015.00092
27. Huang H, Shu C, Chen J, Zou J, Chen C, Wu S, et al. Altered corticostriatal pathway in first-episode paranoid schizophrenia: Resting-state functional and causal connectivity analyses. *Psychiatry Res Neuroimaging* (2018) 272:38–45. doi: 10.1016/j.pscychresns.2017.08.003
28. Floresco SB, Blaha CD, Yang CR, Phillips AG. Modulation of hippocampal and amygdalar-evoked activity of nucleus accumbens neurons by dopamine: cellular mechanisms of input selection. *J Neurosci* (2001) 21(8):2851–60. doi: 10.1523/JNEUROSCI.21-08-02851.2001
29. Gard DE, Fisher M, Garrett C, Genevsky A, Vinogradov S. Motivation and its relationship to neurocognition, social cognition, and functional outcome in schizophrenia. *Schizophr Res* (2009) 115(1):74–81. doi: 10.1016/j.schres.2009.08.015
30. Liu Z, Braunlich K, Wehe HS, Seger CA. Neural networks supporting switching, hypothesis testing, and rule application. *Neuropsychologia* (2015) 77(1):19–34. doi: 10.1016/j.neuropsychologia.2015.07.019
31. Graham S, Phua E, Soon CS, Oh T, Au C, Shuter B, et al. Role of medial cortical, hippocampal, and striatal interactions during cognitive set-shifting. *Neuroimage* (2009) 45(4):1359–67. doi: 10.1016/j.neuroimage.2008.12.040
32. Zandbelt BB, van Buuren M, Kahn RS, Vink M. Reduced proactive inhibition in schizophrenia is related to corticostriatal dysfunction and poor working memory. *Biol Psychiatry* (2011) 70(12):1151–8. doi: 10.1016/j.biopsych.2011.07.028
33. Vink M, de Leeuw M, Luykx JJ, van Eijk KR, van den Munkhof HE, van Buuren M, et al. DRD2 schizophrenia-risk allele is associated with impaired striatal functioning in unaffected siblings of schizophrenia patients. *Schizophr Bull* (2016) 42(3):843–50. doi: 10.1093/schbul/sbv166

Conflict of Interest: The authors declare that the research was conducted in the absence of any commercial or financial relationships that could be construed as a potential conflict of interest.

frontiers in Psychiatry

SYSTEMATIC REVIEW
published: 23 June 2020
doi: 10.3389/fpsyt.2020.00588

Application of Support Vector Machine on fMRI Data as Biomarkers in Schizophrenia Diagnosis: A Systematic Review

Luca Steardo Jr.[1]*, *Elvira Anna Carbone*[1], *Renato de Filippis*[1], *Claudia Pisanu*[2], *Cristina Segura-Garcia*[3], *Alessio Squassina*[2,4], *Pasquale De Fazio*[1] and *Luca Steardo*[5,6]

[1] Department of Health Sciences, School of Medicine and Surgery, University Magna Graecia of Catanzaro, Catanzaro, Italy, [2] Section of Neuroscience and Clinical Pharmacology, Department of Biomedical Sciences, Faculty of Medicine and Surgery, University of Cagliari, Cagliari, Italy, [3] Department of Medical and Surgical Science, University of Magna Graecia, Catanzaro, Italy, [4] Department of Psychiatry, Faculty of Medicine, Dalhousie University, Halifax, NS, Canada, [5] Department of Physiology and Pharmacology, Faculty of Pharmacy and Medicine, Sapienza University of Rome, Rome, Italy, [6] Department of Psychiatry, Giustino Fortunato University, Benevento, Italy

OPEN ACCESS

Edited by:
Katrin H. Preller,
University of Zurich, Switzerland

Reviewed by:
Bingsheng Huang,
Shenzhen University, China
Wenbin Guo,
Second Xiangya Hospital, Central South University, China

***Correspondence:**
Luca Steardo Jr.
steardo@unicz.it

Specialty section:
This article was submitted to Neuroimaging and Stimulation, a section of the journal Frontiers in Psychiatry

Received: 31 January 2020
Accepted: 08 June 2020
Published: 23 June 2020

Citation:
Steardo L Jr., Carbone EA, de Filippis R, Pisanu C, Segura-Garcia C, Squassina A, De Fazio P and Steardo L (2020) Application of Support Vector Machine on fMRI Data as Biomarkers in Schizophrenia Diagnosis: A Systematic Review. Front. Psychiatry 11:588. doi: 10.3389/fpsyt.2020.00588

Non-invasive measurements of brain function and structure as neuroimaging in patients with mental illnesses are useful and powerful tools for studying discriminatory biomarkers. To date, functional MRI (fMRI), structural MRI (sMRI) represent the most used techniques to provide multiple perspectives on brain function, structure, and their connectivity. Recently, there has been rising attention in using machine-learning (ML) techniques, pattern recognition methods, applied to neuroimaging data to characterize disease-related alterations in brain structure and function and to identify phenotypes, for example, for translation into clinical and early diagnosis. Our aim was to provide a systematic review according to the PRISMA statement of Support Vector Machine (SVM) techniques in making diagnostic discrimination between SCZ patients from healthy controls using neuroimaging data from functional MRI as input. We included studies using SVM as ML techniques with patients diagnosed with Schizophrenia. From an initial sample of 660 papers, at the end of the screening process, 22 articles were selected, and included in our review. This technique can be a valid, inexpensive, and non-invasive support to recognize and detect patients at an early stage, compared to any currently available assessment or clinical diagnostic methods in order to save crucial time. The higher accuracy of SVM models and the new integrated methods of ML techniques could play a decisive role to detect patients with SCZ or other major psychiatric disorders in the early stages of the disease or to potentially determine their neuroimaging risk factors in the near future.

Keywords: machine learning, schizophrenia, support vector machine (SVM), resting-state fMRI, biomarkers

INTRODUCTION

Schizophrenia (SCZ) is a major psychiatric disorder characterized by positive and negative symptoms, associated with cognitive impairment, leading to a worse outcome and a high impact on global functioning (1). The lifetime prevalence is 0.40% (2), and it has been estimated that approximately 1 in 200 individuals will be diagnosed with SCZ at some point during their lifetime (3). Even if the diagnosis of schizophrenia is made by observation of the clinical features of the disorder according to the Diagnostic and Statistical Manual of Mental Disorders 5 (DSM-5) (4) or on the ICD (5) criteria, evidences on specific biomarkers that can predict or detect the disease accurately at an early stage are still scarce. (6). It is clear that, considering the biological complexity, the attempt to improve insights into the disease processes is difficult: brain neuroanatomy is intrinsically complex and heterogeneous (7). Non-invasive measurements of brain function and structure, as neuroimaging, are useful and powerful tools for studying discriminatory biomarkers (8, 9) in patients with mental disorders. In this regard, brain imaging studies have revealed that functional and structural brain connectivity in the default mode network (DMN), salience network (SN) and central executive network (CEN) are consistently altered in schizophrenia (10). To date, functional MRI (fMRI) and structural MRI (sMRI) represent the most used techniques to provide a multiple perspective on brain function, structure, and its connectivity. Large amounts of imaging data from magnetic resonance imaging (MRI) need to be analyzed by computerized methods that are able to process information and determine the probability of diseases with great precision (11). Rising attention has been given to machine-learning (ML) techniques (i.e. pattern recognition methods) applied to neuroimaging data (12) to identify phenotypes to be translated into clinical practice for early diagnosis (13, 14). ML techniques applied to fMRI analyze highly complex data sets and assess the importance and interactions between variables, exploring brain functionality and making accurate predictions (15, 16). Machine learning stems from the theory that computers can learn to perform specific tasks without being programmed to do so starting from specific input, thanks to the recognition of patterns in the data. Machine learning uses algorithms that learn from data iteratively. For example, it allows computers to find information, even unknown, without being explicitly told where to look for it (17). Among them, the Support Vector Machine (SVM) represents one of the ML techniques that has shown higher accuracy and precision especially in predicting clinical outcome and severity in schizophrenia patients (14). SVM is a supervised learning model with associated learning algorithms that analyzes data used for classification and regression analysis. This technique has yielded good results applied to fMRI in defining a set of features and information from the various regions of the brain allowing to classify healthy controls and patients affected by SCZ with a potential great translational impact (11).

This review aimed to assess the current state of the evidence about the use of SVM techniques in making diagnostic discrimination in SCZ patients from healthy controls (HC) using as input neuroimaging data from fMRI, according to PRISMA guidelines (18).

MATERIALS AND METHODS

Search Strategy

Articles published until September 27th, 2019 in PubMed, Embase, MEDLINE, PsychINFO, and the Cochrane Library, without language and time limits, were searched by using the following keywords: (*Deep Learning OR DL OR Big data OR Artificial Intelligence OR Machine Learning OR Gaussian process OR Regularized logistic OR Linear discriminant analysis OR LDA OR Random forest OR Least Absolute selection shrinkage operator OR elastic net OR LASSO OR RVM OR relevance vector machine OR pattern recognition OR Computational Intelligence OR Machine Intelligence OR support vector OR SVM OR Pattern classification OR Deep learning*) AND *Schizophrenia* AND (*fMRI OR magnetic resonance imaging OR MRI OR functional MRI OR functional-MRI OR functional magnetic resonance imaging*). All the selected studies were individually reviewed by two researchers. Reference lists from the included articles were screened for additional studies. The eligible publications have been included and cited in this review.

Assessment of Study Quality

In this systematic review we applied the Jadad rating system (19) to check the methodological quality of included studies. Jadad's process allows to qualify selected studies according to their transparency and reproducibility, with great validity and reliability evidence, through the description of three simple and easy items: randomization methods, the double-blinding procedure, and the patient's withdrawal and dropout reports. Scores range from 0 to 5 points. The cut-off for inclusion in this study was a Jadad score ≥3.

Selection Criteria

We selected studies applying SVM as ML techniques with patients diagnosed with Schizophrenia according to the DSM-IV, DSM-IV TR, DSM-5 or ICD-10 criteria, chronic SCZ or at first episode of schizophrenia (FES) regardless of antipsychotic medications. We excluded studies without a control group and trials including patients affected by general medical conditions, neurological or psychiatric comorbidity, substance abuse or alcohol dependence, traumatic brain injuries with loss of consciousness, and unclear or unverified psychiatric diagnoses according to the DSM or ICD criteria.

Data Collection and Extraction

Two authors (RdF and EAC) independently screened all the titles and abstracts of the collected articles, and fully read the texts of papers that met the eligibility criteria. In cases of disagreement, a third researcher (LS) supervised and made the final decision. Data from the extracted article included: publication year, sample size, diagnoses, and all statistical data and features (i.e. accuracy, sensitivity, specificity, brain region or networks).

RESULTS

Initially, 660 items were identified, of which 384 articles were eliminated because they did not fulfill the inclusion criteria. The abstracts of the remaining 276 articles were reviewed. Overall, 226 out of 276 articles were excluded because they were not trials (i.e. editorials, letters to editors, reviews, meta-analyses, case reports or different interventions). Then, 28 manuscripts out of 50 papers were further excluded because they did not fulfill the inclusion criteria (e.g. unclear or unverified psychiatric diagnoses, studies considering outcome, costs or therapy or not using MRI); the remaining 22 studies (**Table 1**) were included in this review (**Figure 1**).

DISCUSSION

Included studies were very heterogeneous, and the samples vary in size and clinical characteristics (**Table 1**). Several features from different brain regions were used as inputs for SVM and focused to investigate how the performance of the model in accuracy, precision, sensitivity, and specificity could be affected by these variables. Studies in this review mostly used and evaluated frontal, temporal, and occipital brain regions. ML techniques were able to detect significantly altered activation patterns or brain connectivity differences in SCZ patients compared to HC. Moreover, this happened quickly, effectively, and efficiently, greatly reducing the number of false negatives, as desirable for a good screening test (42, 43). SVM has achieved good results in terms of accuracy and precision in identifying patients with SCZ. This technique can improve the clinical and research tasks due to the repetitiveness of the data. Computers learn from previous processing to produce results and make decisions that are reliable and replicable (17). SVM presents pros and cons. Specifically, an important advantage is that SVM is the most used and well-known machine learning tool, and even when other techniques are validated, they are compared with SVM. It achieves high accuracy level (e.g. 99%) and is the golden standard to develop new techniques. It can be used for both classification and regression purposes; it allows data repeatability; it can be used in different fields of study, and it represents a great option for future studies. However, it is expensive, and its interpretation is not simple as it requires an experienced and dedicated team (14, 44, 45).

Pläschke et al. used the resting-state Functional Connectivity (FC) to differentiate SCZ patients from matched HC, reaching a remarkable accuracy, equal to 68%. Interestingly, emotional scenes and face processing, empathic processing, and cognitive action control have proven to be the best networks to accurately discriminate patients from HC. Moreover, the age affects network integrity in a more global way so it could be used as a specific flag of functional dysregulation in particular networks affected in SCZ (33). The results of Bae's study reported a decrease in the global and local network connectivity in SCZ patients compared with HC, especially in the superior right temporal region, in the anterior right cingulate cortex, and the inferior left parietal region with an accuracy of 92.1%, sensitivity of 92%, specificity of 92.1% and precision 94% (31). One of the largest studies on SCZ (200 patients vs 200 HC) reported a high diagnostic accuracy (84%) using data from several locations. Otherwise, significantly poorer accuracy was reached with the use of individual sites, showing a lower connectivity in SCZ patients (28). Su et al. recreated the whole brain functional connectivity in SCZ patients (23) vs HC (23) and related the exact spatial location of the activated brain areas to the emerging symptoms. With >80% accuracy authors found an increased FC in SCZ patients group (20). It could probably be explained by an altered cerebral connectivity spread throughout the whole brain, with particular aberrations found in many of the main connections. Altered connectivities in both intra- and inter-hemispherical connections were observed by Li et al. (37), especially in the right hemisphere more than the left hemisphere (temporal, occipital, insula, and limbic regions). Similar data were confirmed in others studies focusing on altered connections (decreased in the basal ganglia, thalamus, lingual gyrus, and cerebellar vermis and increased in medial temporal lobe and posterior cingulate gyri) (39). Koch et al. reached 93% accuracy in identifying SCZ patients and were also able to predict the severity of the negative symptoms of patients based on ventricular striatal activation patterns (24). The results of these studies corroborate the idea of the occurrence of dysconnectivity in schizophrenic patients and deepen our knowledge on the pathological mechanisms.

Functional network connectivity (FNC) to capture the internetwork connectivity pattern and autoconnectivity to capture the temporal connectivity of each brain network were proposed as features for SVM technique (22). The authors manage to achieve particularly high accuracy values in order to discriminate patients with SCZ from HC thanks to the integration of these features (autoconnectivity + FNC). Indeed, the final diagnostic and classification accuracy settles in 88.21% (83.7% for FNC and 80.2% for autoconnectivity alone), with a sensitivity of 86.7% (81.4% for FNC and 78.1% for autoconnectivity alone) and a specificity of 89.5% (85.9% for FNC and 82.2% for autoconnectivity alone). In one of the first studies, the authors were able to analyze the whole functional connectome both in the patient and in the HC groups. They demonstrated many of the main differences, although general and poorly detailed. Indeed, they weighed three series of network-to-network connections (intra-frontoparietal, intra-cerebellar, frontoparietal default) considered to be of major importance for SCZ psychopathology and clinical manifestation (23). Another paper examined the role of long- and short range functional connectivity (lFC) (sFC) in discriminating patients from their own relatives or HC: SCZ group exhibited an spread in sFC and lFC in the DMN with an adequate level of accuracy, sensitivity, and specificity (94%, 92%, 96%, respectively) (27). By analyzing the coherence regional homogeneity (Cohe-ReHo) value, Liu et al. demonstrated that it was decreased in several areas, such as the left postcentral gyrus, right precentral gyrus, left superior temporal gyrus, right middle frontal gyrus, left paracentral lobule, right IPL, and

TABLE 1 | Summary of included studies classifying schizophrenia using SVM.

Author, year	Sample size	Best accuracy	Other measures (sensibility, specificity, AUC)	Data features as input	Brain regions and networks involved	Jadad's score	Comments
Su et al. (20)	N: 64 – 32 SCZ – 32 HC	82,8%	Sp: 81, 2% Sp :84, 4%	90 regions (45 for each hemisphere) and 26 areas (nine in each cerebellar hemisphere and eight in the vermis)	Default mode network, cerebellum, visual network, sensorimotor network, fronto-parietal network, cingulo-opercular network	4	The trial is confined to connectivity analyses.
Yang et al. (21)	N: 40 – 20 SCZ – 20 HC	Hybrid ML 87,3%	Sn: 85,8% Sp: 88.8%	150 SNPs from a database + auditory stimuli	Cingulate gyrus, post-/pre-central gyrus, para-central lobule, precuneus, superior and inferior parietal lobule.	5	Hybrid ML technique using together fMRI and SNP data for more accuracy.
Arbabshirani et al. (22)	N: 370 – 195 SCZ – 175 HC	88,2%	Sn: 86,7% Sp: 89,5%	1128 features for each subject extracted	Control processes, default-mode, cerebellar networks, and subcortical, auditory, visual, somatomotor regions.	5	Functional network connectivity and autoconnectivity improved significantly classification results.
Watanabe et al. (23)	N: 91 – 54 SCZ – 67 HC	77–88.2%	N.A.	Authors described a whole brain resting state functional connectome.	Lateral prefrontal cortex, intra-frontoparietal, frontoparietal default, intracerebellum networks.	3	Authors assessed three sets of network-to-network connections as their role in SZ psychopathology was considered crucial.
Koch et al. (24)	N: 98 – 44 SCZ – 54 HC	69.3–93.2%	Sn: 70.5–100% Sp: 40.9–93.2%	Six fMRI volumes per trial were acquired, resulting in a total of 450 volumes per run	Nucleus accumbens, amygdala, insula, thalamus, ventral striatum, right pallidum, putamen, right inferior frontal gyrus, inferior temporal gyrus	5	Able to use the ventricular striatal activation patterns to predict the severity of the negative symptoms of patients enrolled.
Chyzhyk et al. (25)	N: 147 – 72 SCZ – 75 HC	≈90%	N.A.	rs-fMRI data were collected with single-shot full k-space EPI with ramp sampling correction using the AC-PC as a reference.	Inferior temporal gyrus, para-hippocampal gyrus, planum polare, thalamus, temporal fusiform cortex	4	Application of SVM and RF methods to the data extracted from cross-validation as the ensembles of ELM
Liu et al. (26)	N: 79 – 48 Drug-naïve SCZ – 31 HC	89.9%	Sn: 91.67% Sp: 87.10%	The fMRI scan lasted for 480 s for every pt included, and in total 240 volumes were obtained. The first 10 volumes of each take-over were discarded to certain steady state conditions	Left paracentral lobule, left postcentral gyrus, left superior temporal gyrus, right middle frontal gyrus, bilateral precuneus, right pre-central gyrus, right inferior parietal lobule.	4	Authors enrolled only adolescent onset without previous medication SCZ patients
Guo et al. (27)	N: 96 – 28 SCZ – 40 HC – 28 relatives	94.6%	Sn: 92.9% Sp: 96.4%	Long-range and short-range FCs	Default-mode network, left fusiform gyrus, cerebellum, sensorimotor circuits, right superior parietal lobule	4	The SCZ group was unmedicated and recent onset, so, results may be confounded by their acute positive symptoms
Orban et al. (28)	N: 382 – 191 SCZ – 191 HC	84%	N.A.	Functional brain connectomes included a total of 2016 functional connections among 64 brain parcels	Connectivity of the whole brain	3	Brain imaging data derived from six different and independent studies and databases.
Wang et al. (29)	N: 79 – 48 AOS – 31 HC	90.1%	Sn: 88.2% Sp: 91.9%	Authors used brain regions with significantly different ReHo values between SCZ and HC group	Bilateral superior medial pre-frontal cortex, right inferior parietal lobule, left paracentral lobule, left superior temporal gyrus, right precentral lobule	5	Sample sizes in the two groups were different.
Wang et al. (30)	N: 79 – 48 drug-naïve – 31 HC	92.4%	Sn: 89.6% Sp: 96.8%	Regional homogeneity (ReHo), a measurement that reflects brain local functional connectivity or synchronization	Left superior temporal gyrus, right middle frontal gyrus, right superior medial prefrontal cortex	4	SVM analysis was applied to an independent database
Bae et al. (31)	N: 75 – 21 SCZ – 54 HC	92.1%	Sn: 92.0% Sp: 92.1%	90 ROIs from the image database.	Anterior right cingulate cortex, inferior left parietal region, superior right temporal region	5	Likely interference of pharmacological treatment and disease phase on the

(Continued)

TABLE 1 | Continued

Author, year	Sample size	Best accuracy	Other measures (sensibility, specificity, AUC)	Data features as input	Brain regions and networks involved	Jadad's score	Comments
			Precision: 94%				investigated functional connections. Moreover, authors used only n-back tests without rs-fMRI
Qureshi et al. (32)	N: 144 – 72 SCZ – 72 HC	99.3%	Sn: 100% Sp: 98, 6%	Mean cortical thickness, white matter volume, surface area, volume, cortical thickness standard deviation, mean curvature, subcortical segment volume, subcortical intensity, and overall brain volume and intensity as the structural features	Surface area, cortical thickness, global average functional connectivity , WM/subcortical/ overall volume, curvature	4	Authors developed a specific ELM in this trial
Pläschke et al. (33)	N: 170 – 86 SCZ – 84 HC	61–72%	Sn: 65–77% Sp: 46–69% AUC: 0.61–0.79	12 functional networks.	Emotion-processing, empathy, and cognitive action control networks	3	Young-old classification was grounded on outperformed clinical classification and all networks.
Liu et al. (34)	N: 79 – 48 Drug-Naïve FES – 31 HC	94.93%	Sn: 100% Sp: 87.09%	A total of 240 volumes were acquired. The first 10 volumes of each scan were discarded to certain steady-state conditions at the beginning of acquisition.	Superior temporal gyrus, insula, fusiform gyrus, precentral gyrus, and precuneus	4	Authors assessed also a neurocognitive test battery demonstrating neurocognitive deficits in patients compared to HC
Vacca et al. (35)	N: 201 – 86 SCZ – 115 HC	87,8%	N.A.	Battery tests related to attention, memory, praxic, visuospatial and executive functions	Working memory, executive functions, attention, verbal fluency, memory	3	Data obtained should be integrated thorough neuropsychological evaluation into the more general diagnostic approach of patients with SCZ
Zhuang et al. (36)	N: 69 – 40 drug naïve FES – 29 HC	84,29%	Sn:92.5 Sp: 73.33	Structural MRI , diffusion tensor imaging (DTI) and rs-fMRI data	Altered morphological measurements in both gray matter and white matter, functional connectivity, and regional functional activity	5	A multimodal classification method to discriminate FES schizophrenia patients from HC by a combined structural MRI, DTI, and rs-fMRI data
Li et al. (37)	N: 148 – 60 SCZ – 71 HC	71,8%	Sn: 70 Sp: 73,24	Aberrant connectivities in both intra- and inter-hemispherical connections	Disconnectivities mainly appeared on temporal and occipital regions for the within-large-region connections; connectivity disruption was observed on the connections from temporal region to occipital, insula and limbic regions for the between-large-region connections	4	The findings of this study corroborate previous conclusion of dysconnectivity in SCZ and further shed light on distribution patterns of dysconnectivity, which deepens the understanding of its pathological mechanism.
Jing et al. (38)	N: 153 – 60 SCZ – 43 unaffected FDRs of patients – 50 HC	83,9%	Sn: 87.5% Sp: 80.0% AUC: 0.914	Informative FNs	Cerebellum, default mode network (DMN), ventral frontotemporal network, and posterior DMN with parahippocampal gyrus	5	Pattern classifiers built upon the informative FNs can serve as biomarkers for quantifying brain alterations in SCZ and help to identify FDRs with FN patterns and cognitive impairment similar to those of SCZ patients.
Ramkiran et al. (39)	N: 112 – 56 SCZ – 56 HC	69%	Sn: 68% Sp: 72%	Functional connectivity	The basal ganglia, thalamus, lingual gyrus, and cerebellar vermis showed significantly different, type A (decreased anticorrelation) connections. The medial temporal lobe and posterior cingulate gyri showed	4	Different aberrant functional connectivity in SCZ patients.

(Continued)

TABLE 1 | Continued

Author, year	Sample size	Best accuracy	Other measures (sensibility, specificity, AUC)	Data features as input	Brain regions and networks involved	Jadad's score	Comments
					significantly different, Type B (increased anticorrelation) connections.		
Ji et al. (40)	N: 737 – 240 HC – 161 Bipolar – 131 schizoaffective – 205 SCZ	64%	AUC: 69%	Whole brain ReHo	Inferior/middle temporal area and fusiform gyrus	5	Patterns of higher ReHo abnormalities could be used as robust psychosis biomarker.
Zhu et al. (41)	N: 221 – 76 FES drug naïve – 74 ultra-high risk – 71 HC	74,83%	Sn: 68, 42% Sp: 81, 69%	Parameter of functional asymmetry	Left thalamus/pallidum, right hippocampus/ parahippocampus, right inferior frontal gyrus/insula, right thalamus, and left inferior parietal lobule-right precentral gyrus/postcentral gyrus, and left calcarine, right superior occipital gyrus/middle occipital gyrus.	3	First-episode patients and UHR subjects shared decreased PAS in the left thalamus. This observed pattern of functional asymmetry highlights the involvement of the thalamus in the pathophysiology of psychosis and could be also applied as a very early marker for psychosis.

AOS., adolescent onset SCZ; AUC, area under the curve; DMN, default mode network; DTI, diffusion tensor imaging; ELM, extreme learning machine; FC, functional connectivity; FN, functional network; FDR, first-degree relatives; FES, first episode schizophrenia; HC, healthy controls; ML, machine learning; n, number; NA, not available; PAS, parameter of asymmetry; RF, random forest; ReHo, regional homogeneity; ROI, region of interest; SCZ, schizophrenia; SN, sensibility; SNP, single nucleotide polymorphisms; SP, specificity; SVM, support vector machine; UHR, ultra-high risk.

bilateral praecuneus in 48 SCZ vs 31 HC (26). The Whole brain ReHo measures were used as robust psychosis biomarker: SVM resulted more accurate in identify patterns of higher ReHo abnormalities (inferior/middle temporal area and fusiform gyrus) (40). The integration of the neuropsychological evaluation to detect different aspects related to attention, working memory, praxic, visuospatial, and executive functions was able for the early diagnosis of patients with SCZ (35).

The combination of SVM with other ML techniques can identify anatomic brain areas with major alterations (temporal fusiform cortex, inferior, middle, and medial frontal gyri, inferior temporal gyrus, anterior division of the parahippocampal gyrus, planum polare, cingulate gyrus, superior temporal gyrus, precuneus left, and right thalamus) with an accuracy close to 90% (21, 25). An extreme learning machine (ELM) was developed by Qureshi et colleagues, reaching a maximum accuracy of 99.3%. Main data derived from cortical thickness and surface area, total cerebral volume, and overall volume of cortex features scans. Authors concluded that their ELM technique can be applied to patients offering a solid chance of helping clinicians to make diagnosis of SCZ (32).

Another important field of application of SVM is the evaluation of functional features in first episode schizophrenia (FES). The identification of early-onset schizophrenia remains challenging, and SVM may constitute a promising tool for the early diagnosis for its high accuracy and valuable prognostic implication in FES. Recently, the sFC and lFC in the whole brain were explored in 48 first-episode, drug-naïve patients and 31 HC using SVM. Major abnormalities were found in some brain networks (anterior and posterior Default Mode Network and Sensorimotor Network) classifying patients and controls with > 92% accuracy and high sensitivity and specificity (30). Liu et al. evaluated the alteration in FC in different brain regions in a similar patients' sample and found dysfunctional interhemispheric network within the sensorimotor area among patients with SCZ. It was associated with processing speed deficits, indicating the probable involvement with the neurocognitive alterations of these patients. The application of SVM ML technique analysis reached 100% sensitivity, 87.09% specificity, and 94.93% accuracy (34). Functional alterations could point to a role of DMN and SN in the SCZ psychopathology that is already known in first-psychotic episode patients and SVM seems to be able to discriminate with high accuracy patients from HC in research context. Wang et al. identify brain peculiarities using ReHo input in SVM analysis through resting state-fMRI (rs-fMRI) in drug-naïve patients and 32 HC. ReHo values were significantly amplified in the bilateral superior medial prefrontal cortex, and, otherwise, reduced in the left superior temporal gyrus, right precentral lobule, right inferior parietal lobule, and left paracentral lobule in patient group compared to HC (29). Disrupted functional asymmetry was calculated comparing patients with FES, drug-naïve schizophrenia, ultra-high risk (UHR) for psychosis and HC. SVM classification analysis was applied to analyze the data and showed decreased parameter of asymmetry in the left thalamus/pallidum, right hippocampus/parahippocampus, right inferior frontal gyrus/ insula, right thalamus, and left inferior parietal lobule, and increased PAS in the left calcarine, right superior occipital gyrus/middle occipital gyrus, and right precentral gyrus/postcentral gyrus. First-episode patients and UHR subjects shared decreased pattern of functional asymmetry in the left thalamus underlining the possible involvement of the thalamus in the pathophysiology of psychosis

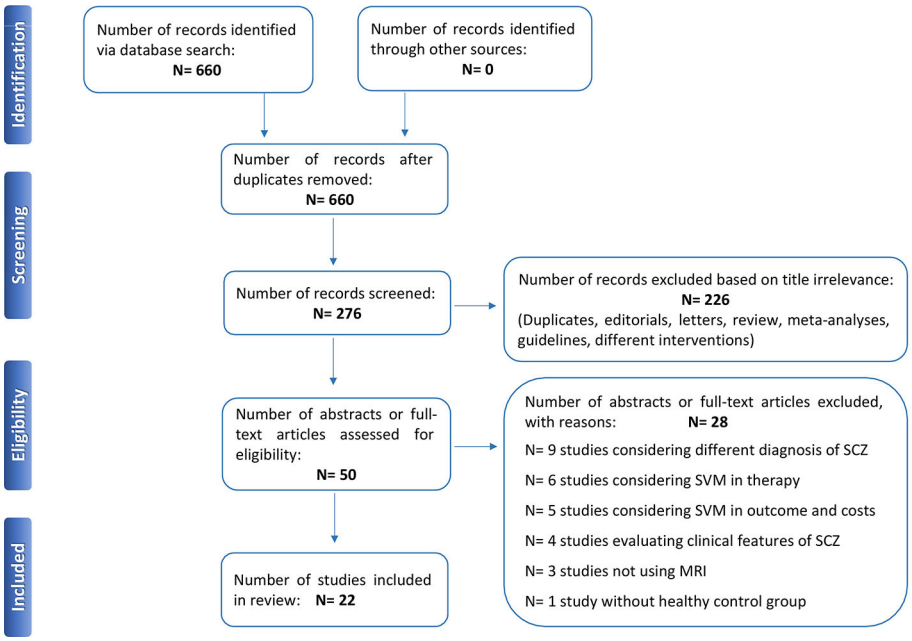

FIGURE 1 | PRISMA flowchart of included studies.

and demonstrating a very early marker for psychosis (41). A multimodal classification method to discriminate FES patients from HC combined structural MRI and rs-fMRI data, and identified functional markers in both gray matter and white matter and altered functional connectivity in DMN and cerebellar connections (36). A recent study identified informative functional networks to distinguish patients from HC and to classify unaffected first-degree relatives (FDRs) with or without functional networks similar to patients. Four informative functional networks (DMN, ventral frontotemporal network, and posterior DMN with parahippocampal gyrus) resulted implicated in brain alterations. They could be probably used as biomarkers to identify FDRs with FN patterns similar to those of SCZ patients (38). The ability to apply complex mathematical calculations to big data is newly developed, and its use is hopefully growing. Now, theoretically, it is possible to create automatically models for analyzing larger and more complex data and to produce more accurate and repeatable results even on a large scale.

The application of these models would allow clinicians to identify new tasks, not merely diagnostic but also preventive, for major psychiatric disorders such as Schizophrenia.

CONCLUSION

Approaches of big data, focusing on classification based on huge biological information rather than the single clinical manifestation, have the greatest advantage to move the field forward faster and with more evidence than before. The application of ML techniques in psychiatry as well, will be useful to routinely classify patients with major psychiatric disorders, and schizophrenia in particular, on the basis of resting state functional MRI data. This technique can be a valid, cheap, and non-invasive support for physicians to detect patients, even in the early stage of the disorder, conferring a crucial diagnostic anticipation, hopefully decisive in changing the natural history of the disease. The results collected in this review allow us to assume that the greater accuracy demonstrated by the SVM models and new integrated methods of ML techniques could play an increasingly decisive role in the future both for the early diagnosis and a more accurate evaluation of the treatment response, and to establish the middle-term prognosis of patients with SCZ.

AUTHOR CONTRIBUTIONS

All authors contributed to the article and approved the submitted version.

FUNDING

This research was co-funded by University "G. Fortunato" Benevento (Italy). Grant: cda N°8/111119.

REFERENCES

1. Owen MJ, Sawa A, Mortensen PB. Schizophrenia. *Lancet* (2016) 388:86–97. doi: 10.1016/S0140-6736(15)01121-6
2. McGrath J, Saha S, Chant D, Welham J. Schizophrenia: a concise overview of incidence, prevalence, and mortality. *Epidemiol Rev* (2008) 30:67–76. doi: 10.1093/epirev/mxn001
3. Simeone JC, Ward AJ, Rotella P, Collins J, Windisch R. An evaluation of variation in published estimates of schizophrenia prevalence from 1990-2013: A systematic literature review. *BMC Psychiatry* (2015) 15:193. doi: 10.1186/s12888-015-0578-7
4. American Psychiatric Association. *Diagnostic and Statistical Manual of Mental Disorders: DSM-5. fifth Ed.* Washington (2013).
5. World Health Organization. The ICD-10 Classification of Mental and Behavioural Disorders. In: *Clinical descriptions and diagnostic guidelines* (1992). Available from: http://www.who.int/classifications/icd/en/bluebook.pdf. Accessed November 02, 2019.
6. Kambeitz J, Kambeitz-Ilankovic L, Leucht S, Wood S, Davatzikos C, Malchow B, et al. Detecting neuroimaging biomarkers for schizophrenia: A meta-analysis of multivariate pattern recognition studies. *Neuropsychopharmacology* (2015) 40:1742–51. doi: 10.1038/npp.2015.22
7. Senthil G, Lehner T. Schizophrenia research in the era of Team Science and big data. *Schizophr Res* (2019) 217:13–16. doi: 10.1016/j.schres.2019.07.008
8. He Y, Chen ZJ, Evans AC. Small-world anatomical networks in the human brain revealed by cortical thickness from MRI. *Cereb Cortex* (2007) 17:2407–19. doi: 10.1093/cercor/bhl149
9. He Y, Wang J, Wang L, Chen ZJ, Yan C, Yang H, et al. Uncovering intrinsic modular organization of spontaneous brain activity in humans. *PloS One* (2009) 4(4):e5226. doi: 10.1371/journal.pone.0005226
10. Han W, Sorg C, Zheng C, Yang Q, Zhang X, Ternblom A, et al. Low-rank network signatures in the triple network separate schizophrenia and major depressive disorder. *NeuroImage Clin* (2019) 22:101725. doi: 10.1016/j.nicl.2019.101725
11. Veronese E, Castellani U, Peruzzo D, Bellani M, Brambilla P. Machine learning approaches: from theory to application in schizophrenia. *Comput Math Methods Med* (2013) 2013:867924. doi: 10.1155/2013/867924
12. Wolfers T, Buitelaar JK, Beckmann CF, Franke B, Marquand AF. From estimating activation locality to predicting disorder: A review of pattern recognition for neuroimaging-based psychiatric diagnostics. *Neurosci Biobehav Rev* (2015) 57:328–49. doi: 10.1016/j.neubiorev.2015.08.001
13. Orrù G, Pettersson-Yeo W, Marquand AF, Sartori G, Mechelli A. Using Support Vector Machine to identify imaging biomarkers of neurological and psychiatric disease: A critical review. *Neurosci Biobehav Rev* (2012) 36:1140–52. doi: 10.1016/j.neubiorev.2012.01.004
14. de Filippis R, Carbone EA, Gaetano R, Bruni A, Pugliese V, Segura-Garcia C, et al. Machine learning techniques in a structural and functional MRI diagnostic approach in schizophrenia: a systematic review. *Neuropsychiatr Dis Treat* (2019) 15:1605–27. doi: 10.2147/NDT.S202418
15. Vapnik VN. An overview of statistical learning theory. *IEEE Trans Neural Networks* (1999) 10:988–99. doi: 10.1109/72.788640
16. Krystal JH, Murray JD, Chekroud AM, Corlett PR, Yang G, Wang X-J, et al. Computational Psychiatry and the Challenge of Schizophrenia. *Schizophr Bull* (2017) 43:473–5. doi: 10.1093/schbul/sbx025
17. Deo R. Machine Learning in Medicine. *Circulation* (2015) 132(20):1920–30. doi: 10.1161/CIRCULATIONAHA.115.001593
18. Liberati A, Altman DG, Tetzlaff J, Mulrow C, Gøtzsche PC, Ioannidis JPA, et al. The PRISMA statement for reporting systematic reviews and meta-analyses of studies that evaluate healthcare interventions: explanation and elaboration. *BMJ* (2009) 339:b2700. doi: 10.1136/bmj.b2700
19. Jadad AR, Moore RA, Carroll D, Jenkinson C, Reynolds DJ, Gavaghan DJ, et al. Assessing the quality of reports of randomized clinical trials: is blinding necessary? *Control Clin Trials* (1996) 17:1–12. doi: 10.1016/0197-2456(95)00134-4
20. Su L, Wang L, Shen H, Feng G, Hu D. Discriminative analysis of non-linear brain connectivity in schizophrenia: An fMRI Study. *Front Hum Neurosci* (2013) 7:702. doi: 10.3389/fnhum.2013.00702
21. Yang H, Liu J, Sui J, Pearlson G, Calhoun VD. A hybrid machine learning method for fusing fMRI and genetic data: Combining both improves classification of schizophrenia. *Front Hum Neurosci* (2010) 4:192. doi: 10.3389/fnhum.2010.00192
22. Arbabshirani MR, Castro E, Calhoun VD. Accurate Classification of Schizophrenia Patients Based on Novel Resting-State fMRI Features. *Conf Proc IEEE Eng Med Biol Soc* (2014) 2014:6691–4. doi: 10.1109/EMBC.2014.6945163
23. Watanabe T, Kessler D, Scott C, Angstadt M, Sripada C. Disease prediction based on functional connectomes using a scalable and spatially-informed support vector machine. *Neuroimage* (2014) 96:183–202. doi: 10.1016/j.neuroimage.2014.03.067
24. Koch SP, Hägele C, Haynes JD, Heinz A, Schlagenhauf F, Sterzer P. Diagnostic classification of schizophrenia patients on the basis of regional reward-related fMRI signal patterns. *PloS One* (2015) 10(3):e0119089. doi: 10.1371/journal.pone.0119089
25. Chyzhyk D, Savio A, Graña M. Computer aided diagnosis of schizophrenia on resting state fMRI data by ensembles of ELM. *Neural Networks* (2015) 68:23–33. doi: 10.1016/j.neunet.2015.04.002
26. Liu Y, Zhang Y, Lv L, Wu R, Zhao J, Guo W. Abnormal neural activity as a potential biomarker for drug-naive first-episode adolescent-onset schizophrenia with coherence regional homogeneity and support vector machine analyses. *Schizophr Res* (2018) 192:408–15. doi: 10.1016/j.schres.2017.04.028
27. Guo W, Liu F, Chen J, Wu R, Li L, Zhang Z, et al. Using short-range and long-range functional connectivity to identify schizophrenia with a family-based case-control design. *Psychiatry Res - Neuroimaging* (2017) 264:60–7. doi: 10.1016/j.pscychresns.2017.04.010
28. Orban P, Dansereau C, Desbois L, Mongeau-Pérusse V, Giguère CÉ, Nguyen H, et al. Multisite generalizability of schizophrenia diagnosis classification based on functional brain connectivity. *Schizophr Res* (2018) 192:167–71. doi: 10.1016/j.schres.2017.05.027
29. Wang S, Zhang Y, Lv L, Wu R, Fan X, Zhao J, et al. Abnormal regional homogeneity as a potential imaging biomarker for adolescent-onset schizophrenia: A resting-state fMRI study and support vector machine analysis. *Schizophr Res* (2018) 192:179–84. doi: 10.1016/j.schres.2017.05.038
30. Wang S, Zhan Y, Zhang Y, Lyu L, Lyu H, Wang G, et al. Abnormal long- and short-range functional connectivity in adolescent-onset schizophrenia patients: A resting-state fMRI study. *Prog Neuropsychopharmacol Biol Psychiatry* (2018) 81:445–51. doi: 10.1016/j.pnpbp.2017.08.012
31. Bae Y, Kumarasamy K, Ali IM, Korfiatis P, Akkus Z, Erickson BJ. Differences Between Schizophrenic and Normal Subjects Using Network Properties from fMRI. *J Digit Imaging* (2018) 31:252–61. doi: 10.1007/s10278-017-0020-4
32. Qureshi MNI, Oh J, Cho D, Jo HJ, Lee B. Multimodal discrimination of schizophrenia using hybrid weighted feature concatenation of brain functional connectivity and anatomical features with an extreme learning machine. *Front Neuroinform* (2017) 11:59. doi: 10.3389/fninf.2017.00059
33. Pläschke RN, Cieslik EC, Müller VI, Hoffstaedter F, Plachti A, Varikuti DP, et al. On the integrity of functional brain networks in schizophrenia, Parkinson's disease, and advanced age: Evidence from connectivity-based single-subject classification. *Hum Brain Mapp* (2017) 38:5845–58. doi: 10.1002/hbm.23763
34. Liu Y, Guo W, Zhang Y, Lv L, Hu F, Wu R, et al. Decreased Resting-State Interhemispheric Functional Connectivity Correlated with Neurocognitive Deficits in Drug-Naive First-Episode Adolescent-Onset Schizophrenia. *Int J Neuropsychopharmacol* (2018) 21:33–41. doi: 10.1093/ijnp/pyx095
35. Vacca A, Longo R, Mencar C. Identification and evaluation of cognitive deficits in schizophrenia using "Machine learning". *Psychiatr Danub* (2019) 31:261–4.
36. Zhuang H, Liu R, Wu C, Meng Z, Wang D, Liu D, et al. Multimodal classification of drug-naïve first-episode schizophrenia combining anatomical, diffusion and resting state functional resonance imaging. *Neurosci Lett* (2019) 705:87–93. doi: 10.1016/j.neulet.2019.04.039
37. Li J, Sun Y, Huang Y, Bezerianos A, Yu R. Machine learning technique reveals intrinsic characteristics of schizophrenia: an alternative method. *Brain Imaging Behav* (2019) 13:1386–96. doi: 10.1007/s11682-018-9947-4
38. Jing R, Li P, Ding Z, Lin X, Zhao R, Shi L, et al. Machine learning identifies unaffected first-degree relatives with functional network patterns and cognitive impairment similar to those of schizophrenia patients. *Hum Brain Mapp* (2019) 40:3930–9. doi: 10.1002/hb

39. Ramkiran S, Sharma A, Rao NP. Resting-state anticorrelated networks in Schizophrenia. *Psychiatry Res - Neuroimaging* (2019) 284:1–8. doi: 10.1016/j.pscychresns.2018.12.013
40. Ji L, Meda SA, Tamminga CA, Clementz BA, Keshavan MS, Sweeney JA, et al. Characterizing functional regional homogeneity (ReHo) as a B-SNIP psychosis biomarker using traditional and machine learning approaches. *Schizophr Res* (2019) 215:430–8. doi: 10.1016/j.schres.2019.07.015
41. Zhu F, Liu Y, Liu F, Yang R, Li H, Chen J, et al. Functional asymmetry of thalamocortical networks in subjects at ultra-high risk for psychosis and first-episode schizophrenia. *Eur Neuropsychopharmacol* (2019) 29:519–28. doi: 10.1016/j.euroneuro.2019.02.006
42. Zhou Y, Zeidman P, Wu S, Razi A, Chen C, Yang L, et al. Altered intrinsic and extrinsic connectivity in schizophrenia. *NeuroImage Clin* (2018) 17:704–16. doi: 10.1016/j.nicl.2017.12.006
43. Li P, Fan TT, Zhao RJ, Han Y, Shi L, Sun HQ, et al. Altered Brain Network Connectivity as a Potential Endophenotype of Schizophrenia. *Sci Rep* (2017) 7 (1):5483. doi: 10.1038/s41598-017-05774-3
44. Bisenius S, Mueller K, Diehl-Schmid J, Fassbender K, Grimmer T, Jessen F, et al. Predicting primary progressive aphasias with support vector machine approaches in structural MRI data. *NeuroImage Clin* (2017) 14:334–43. doi: 10.1016/j.nicl.2017.02.003
45. Pellegrini E, Ballerini L, Hernandez M del CV, Chappell FM, González-Castro V, Anblagan D, et al. Machine learning of neuroimaging for assisted diagnosis of cognitive impairment and dementia: A systematic review. *Alzheimer's Dement Diagnosis Assess Dis Monit* (2018) 10:519–35. doi: 10.1016/j.dadm.2018.07.004

Conflict of Interest: The authors declare that the research was conducted in the absence of any commercial or financial relationships that could be construed as a potential conflict of interest.

frontiers in Psychiatry

ORIGINAL RESEARCH
published: 26 June 2020
doi: 10.3389/fpsyt.2020.00612

Correlation Between Decreased Amygdala Subnuclei Volumes and Impaired Cognitive Functions in Pediatric Bipolar Disorder

Dong Cui[1,2], *Yongxin Guo*[1,2], *Weifang Cao*[1,2], *Weijia Gao*[3], *Jianfeng Qiu*[1], *Linyan Su*[4]*, *Qing Jiao*[1,2]* and *Guangming Lu*[5]

[1] College of Radiology, Shandong First Medical University (Shandong Academy of Medical Sciences), Taian, China, [2] Collaborative Innovation Center of Magnetic Resonance Imaging of Brain Disease, Shandong First Medical University, Shandong Academy of MedicalSciences, Taian, China, [3] Department of Child Psychology, The Children's Hospital, Zhejiang University School of Medicine, Hangzhou, China, [4] Mental Health Institute of The Second Xiangya Hospital, Central South University, Changsha, China, [5] Department of Medical Imaging, Jinling Hospital, Nanjing University School of Medicine, Nanjing, China

OPEN ACCESS

Edited by:
Sven Haller,
Rive Droite SA, Switzerland

Reviewed by:
Gianluca Serafini,
San Martino Hospital (IRCCS), Italy
Luke Norman,
University of Michigan,
United States

***Correspondence:**
Linyan Su
xysulinyan@126.com
Qing Jiao
bingbao17@163.com

Specialty section:
This article was submitted to Neuroimaging and Stimulation, a section of the journal Frontiers in Psychiatry

Received: 27 February 2020
Accepted: 12 June 2020
Published: 26 June 2020

Citation:
Cui D, Guo Y, Cao W, Gao W, Qiu J, Su L, Jiao Q and Lu G (2020) Correlation Between Decreased Amygdala Subnuclei Volumes and Impaired Cognitive Functions in Pediatric Bipolar Disorder. Front. Psychiatry 11:612. doi: 10.3389/fpsyt.2020.00612

Background: The amygdala has been proposed to be involved in the pathophysiology of pediatric and adult bipolar disorder (BD). The goal of this structural magnetic resonance imaging (sMRI) study was to investigate the morphometric characteristics of amygdala subnuclei in patients with pediatric bipolar disorder (PBD) compared to healthy controls (HCs). Simultaneously, we examined correlation between amygdala subnuclei volumes and cognitive dysfunction.

Materials and Methods: We assessed 40 adolescent outpatients, diagnosed with manic or euthymic PBD according to the DSM-5 criteria for BD and 19 HCs. Cognitive functions were evaluated using a Stroop color-word test (SCWT), trail making test (TMT), visual reproduction immediate recall subtest (VR I), and digit span subtest (DST). Amygdala and its subnuclei structures were automated segmented using FreeSurfer software and the volumes of them were compared between groups and correlation with clinical and cognitive outcomes was conducted.

Results: Manic patients exhibited significantly decreased volumes in the bilateral whole amygdala and its basal nucleus, cortico-amygdaloid transition (CAT), and accessory basal nucleus (ABN) compared with HCs. Euthymic patients had decreased volume in the bilateral ABN and left CAT. In addition, we found significant positive associations between VR I scores and the right whole amygdala and its bilateral basal, right lateral, and ABN volumes in the manic group.

Conclusion: These findings support previous reports of smaller amygdala volumes and cognitive dysfunctions in PBD, and further mapping abnormalities to specific amygdala subnuclei. Correlation between basolateral volume and VR I of PBD may expand our understanding of neural abnormalities that could be targeted by treatment.

Keywords: pediatric bipolar disorder, mania, euthymia, amygdala subnuclei, magnetic resonance imaging

INTRODUCTION

Pediatric bipolar disorder (PBD) is characterized by persistent influence dysregulation affects roughly 2% of youth under the age of 18 (1). Like bipolar disorder (BD) in adults, PBD is also characterized by recurring manic or hypomanic episodes and a depressive episode typically separated by periods of relative euthymia (2). Retrospective studies clearly indicate that pathology begins in childhood or adolescence for 50% to 66% of adults with BD (3). Early-onset BD may have worse outcomes including greater cognitive impairment (4), fewer days of euthymia (5), and suicide attempts (6). In these adolescents, the persistent affect dysregulation is often accompanied by increased risk of suicide (7) and severe cognitive impairment (8) leading to considerable deficits in memory, executive, processing speed, and verbal learning (5, 9). Therefore, it is important to have early objective biomarkers to detect cognitive impairment in order to minimize its negative impact on adolescent development. Such a biomarker would allow early and reliable identification and treatment of BD disorder-associated cognitive decline and shed light on the underlying mechanisms of BD development. However, no biomarkers for targeting or tracking the progression of BD in adolescents exist.

The amygdala is a key limbic region in modulating mood and emotions and is potentially involved in the cognitive and affective symptoms of BD (10). Neuropathologic and neuroimaging studies have implicated the amygdala as a central brain structure for processing emotions (11, 12), emotion-related aspects of behavior (13), attention (14), and memory (15). Converging evidence from neuroimaging studies has consistently implicated the dysfunction of the amygdala in the pathophysiology of BD. Kryza-Lacombe and colleagues (16) showed that youth and adult patients with BD had abnormal amygdala-temporo-parietal connectivity. Specifically, amygdala activation is inversely correlated with volume (17).

Numerous structural magnetic resonance imaging (MRI) studies indicate that smaller amygdala volumes may be an age-specific biomarker for BD. Decreased amygdala volumes in patients with PBD as compared with HCs have been reported in most studies (18–21). In contrast, studies of adults BD patients regarding the amygdala are markedly heterogeneous, with increased (22), not significantly different (23, 24), or decreased (25–27) amygdala volumes compared with HCs. These discrepancies likely reflect clinical and treatment heterogeneity. Some researchers speculate that amygdala volume is reduced at the onset of the disease and increases with age (26). A meta-analysis of the functional neural correlates of BD highlighted the amygdala as an area with unique developmental alterations in BD (28). Therefore, structural and functional amygdala abnormalities identified by neuroimaging may serve as useful disease and treatment response biomarker in BD.

The amygdala formation is commonly treated as a single entity in structural MRI; however, it is known to be comprised of multiple nuclei, each exhibiting different connectivities and cellular profiles (29). These subnuclei have diverse functions physiologically and have been shown in disease models of BD to react differentially to pathological mechanisms (30, 31). Due to the small size of the amygdala, few studies focused on volume changes of amygdala subnuclei in patients with PBD. Whether smaller amygdala volume has been localized to specific amygdala subnuclei in different clinical stages is unknown. With substantial advances in structural MRI tools, new amygdala segmentation algorithms have made it possible to label amygdala subnuclei and automatically provide volumetric information for each based on an *in vivo* atlas (32). Given this background, the goal of the current study was to compare amygdala and subnuclei volumes in a sample of manic or euthymic patients with PBD, and HCs. We hypothesized that the volumes of amygdala subnuclei would be smaller in patients with PBD than that of HCs. Moreover, we also hypothesized that worse cognitive abnormalities might be associated with these reduced amygdala subnuclei in patients with mania or euthymia.

MATERIALS AND METHODS

Subjects

In this case-control study, all PBD patients were recruited from the Mental Health Institute of the Second Xiangya Hospital, Key Laboratory of Psychiatry and the Mental Health of Hunan Province of Central South University (Changsha, Hunan, China). We recruited forty right-handed patients with PBD across an age range of 12 to 18 years. All patients met DSM-5 criteria for BD (33), made up of two subgroups, mania (n = 20, 9 male/11 female), and euthymia (n = 20, 11 male/9 female). In addition, 19 right-handed age and sex-matched healthy control (HC) participants (7 male/12 female) were recruited from the local middle school *via* advertisements. All subjects were completed the Wechsler Abbreviated Scale of Intelligence as an overall measure of cognitive ability (34). General exclusion criteria were intellectual disability (IQ ≤ 80), left-handedness, substance abuse, history of seizures, history of electroconvulsive therapy (ECT), severe brain trauma, and MRI scan contraindications (e.g. metallic implants or claustrophobia).

All adolescents were assessed by the Schedule for Affective Disorders and Schizophrenia for School-Age Children-Present and Lifetime (KSADS-PL) (35) and the Washington University in St. Louis Kiddie Schedule for Affective Disorders and Schizophrenia (WASH-U-KSADS) (36). The K-SADS-PL for DSM-5 is a semi-structured diagnostic interview that assesses both current and lifetime diagnostic psychiatric episodes in children and adolescents. WASH-U-KSADS was developed specifically to target the assessment of prepubertal mania and hypomania and to assess the pattern of rapid cycling. Furthermore, severity of depression and mania were evaluated in all subjects by the Mood and Feelings Questionnaire (MFQ) (37), and Young Manic Rating Scale (YMRS) (38) respectively. The MFQ is a widely used screening measure of depressive symptomatology for children 8 to 18 years of age. The YMRS is an instrument used to assess the severity of mania in patients with a diagnosis of BD. The patients in the manic subgroup were required to have a YMRS score > 26 and MFQ score < 18, those in the euthymic subgroup were required to have had no episodes

of illness for at least 1 month and YMRS score < 12 and MFQ score < 18 at the time of scanning. The inclusion criteria for HC included that the participants have no current or past DSM-5 psychiatric diagnosis, as confirmed by KSADS-PL, and no first- or second-degree family history of BD or other psychotic disorders.

This study protocol was approved by the University of Central South Institutional Review Board in compliance with the Declaration of Helsinki. After complete description of the study to adolescents and their parents, written informed consent and assent were obtained.

Cognitive Function Test

To assess different aspects of cognitive functions, the cognitive estimate battery included the following: Stroop color-word test (SCWT), trail making test (TMT), visual reproduction immediate recall subtest (VR I), and digit span subtest (DST). The battery was administered by experienced clinical psychiatrists in a quiet environment. Below is a description of the various test procedures.

Stroop Color-word Test (SCWT)

The SCWT (39), measuring the ability to attention and response inhibition, included three tasks: word reading (SCWT-A), color naming (SCWT-B), and color interference reading (SCWT-C), each set contains 100 visual stimuli. SCWT-A is made up of the number of words that participants completed in 45 s. SCWT-B is made up of the number of symbols that subjects named correctly. SCWT-C is made up of the number of competing colors that participants read in 45 s.

Trail Making Test (TMT)

TMT is administered in the part A (TMT-A) and part B (TMT-B). TMT-A requires the subjects to draw a line between consecutive numbers (1–25) distributed on a piece of paper, and TMT-B requires the subjects to draw lines sequentially connecting 13 numbers (1–13) and 12 letters (A-L) distributed on a piece of paper. Numbers and letters are encircled and must be connected alternately. TMT score was the total times for subjects to complete the task. TMT-A reflect attention and processing speed, and part B reflects cognitive flexibility (40).

Visual Reproduction Immediate Recall Subtest (VR I)

The VR I was used to assessing visual memory, which check immediate recall and learning rate. Three pages of geometric designs are shown, one at a time. After viewing each graphic for 10 s, the participants are instructed to draw the graphics as accurately as possible from memory (41).

Digit Span Subtest (DST)

In the DST, the participant is asked to repeat the same sequence numbers back to the psychiatrists in forward order (DST-A) and in reverse order (DST-B). DST-A and DST-B were scored according to the longest series separately. DST-A was used to assess attention and DST-B measured working memory (34).

MRI Acquisition and Analysis

All MRI scans were collected with a 3.0 T Siemens Trio system (Siemens, Erlangen, German) using a standard whole head coil. High-resolution anatomical scan was acquired using three-dimensional magnetization-prepared rapid acquisition gradient echo (3D MPRAGE) protocol with the following parameters: repetition time (TR) = 2300 ms, echo time (TE) = 2.98 ms, inversion time = 900 ms, thickness = 1 mm, gap = 0 mm, field of view (FOV) = 256 mm ×256 mm, matrix = 256× 256, flip angle = 9°.

T1-weighted images were preprocessed by motion correction and brain extraction using FreeSurfer (version 6.0, https://surfer.nmr.mgh.harvard.edu). Each T1-weighted image was segmented into gray matter (GM), white matter (WM), and cerebrospinal fluid (CSF). Subsequently, the segmentation of subcortical structures was examined by a nonlinear warping atlas, yielding volumetric measures of Deep GM, including the thalamus, caudate, putamen, amygdala, hippocampus, pallidum, and accumbens. Furthermore, the amygdala subnuclei segmentation module, which is only present in the FreeSurfer dev version (ftp://surfer.nmr.mgh.harvard.edu/pub/dist/freesurfer/dev) was used to parcellate the hippocampus, amygdala, and thalamus subnuclei further, as shown in **Figure 1A**. A probabilistic atlas and a modified version of Van Leemput's algorithm was applied on the segmentation of amygdala (32). In total the amygdala was divided into nine nuclei, including lateral, basal, accessory-basal nucleus (ABN), anterior-amygdaloid area (AAA), central, medial, cortical, cortico-amygdaloid transition (CAT), and paralaminar nucleus. Finally, using FreeSurfer's native visualization toolbox, freeview, we visually inspected the segmentation of hippocampal/amygdala, as shown in **Figure 1**.

We used the Statistical Package for the Social Sciences (SPSS) for Windows, version 22.0 (SPSS Statistics, IBM, Armonk, NY, USA) to study the demographic, clinical, cognitive tests, and MRI data. The Shapiro-Wilk test was used to test for normality. Demographic, clinical, and cognitive test scores were evaluated using Pearson's chi-square test, two-sample t-test or one-way ANOVA with a confidence interval of 95% where applicable. A general linear model (GLM) was used for group analysis of each subnuclei. The GLM was fitted with volume as the dependent variable, groups as the categorical predictor, and total intracranial volume (TIV), age, gender, and education were included as covariates. The indices with significant differences across the three groups were examined further by *post-hoc* differences. Multiple comparisons between groups were assessed using the Bonferroni method. We calculated the Spearman correlation coefficients between each subregion volume and each of the clinical and cognitive variables (onset age, illness duration, YMRS scores, and cognitive tests) for the PBD patients. In the correlation calculations, we regressed out the confounding factors of age, gender, education, and TIV. Spearman correlation results were corrected by false discovery rate (FDR) correction. Statistical significance for all tests was set at $p < 0.05$.

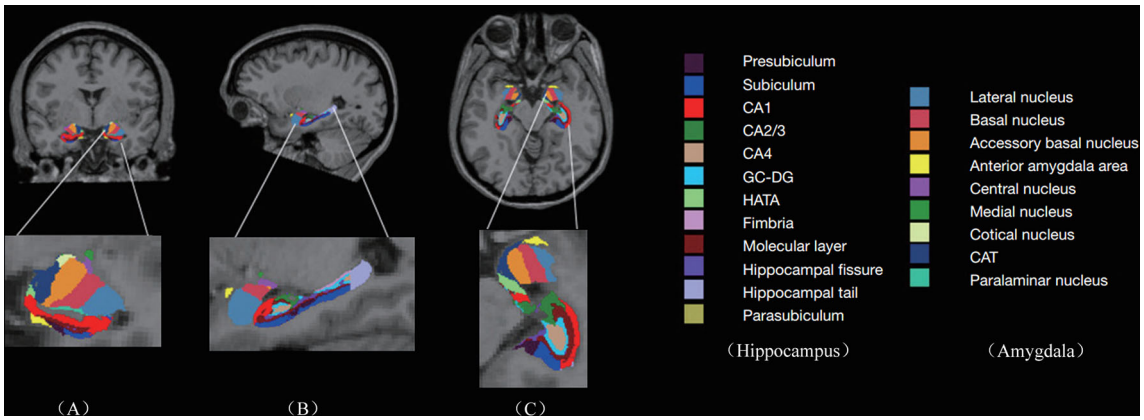

FIGURE 1 | Subregions of hippocampus and amygdala: Columns **(A–C)** represent the image view of coronal, sagittal, and axial, respectively. The second row represents the enlarged subregions on the left. CA, cornus ammonis; GC-DG, granule cell layer of the dentate gyrus; HATA, hippocampal amygdala transition area; CAT, cortico-amygdaloid transition.

RESULTS

Participants' Characteristics and Cognitive Tests

Clinical, demographic, and cognitive test information was collected through self-report questionnaires and clinical interviews by trained psychiatrists. Demographic, clinical, cognitive tests, and medication regimen are summarized in **Table 1**. No group differences were observed in age ($F = 3.118$, $p = 0.052$), gender (chi-square = 1.301, $p = 0.522$), education ($F = 2.153$, p = 0.126), IQ ($F = 1.503$, $p = 0.231$) or MFQ ($F = 0.429$, $p = 0.654$). As expected, significant group differences were observed for YMRS ($F = 356.537$, $p < 0.001$). There were no significant differences in age of onset (t = 0.587, $p = 0.561$), illness duration (t = −1.687, $p = 0.100$), onset frequency (t = −0.983, $p = 0.332$), psychotic symptoms (chi-square = 0.902, $p = 0.342$), type of BD (chi-square = 0.125, $p = 0.723$) or familial BD history (chi-square = 0.476, $p = 0.490$) between two groups of PBD patients. In the mania subgroup, patients were taking the following medications: lithium (n = 8), valproate (n = 11), antipsychotics (n = 13), and antidepressants (n = 2). In the euthymic subgroup, patients were taking lithium (n = 8), valproate (n = 15), and antipsychotics (n = 15). There were significant differences in SCWT-A scores ($F = 4.852$, $p = 0.011$), SCWT-B scores ($F = 8.023$, $p = 0.001$), SCWT-C scores ($F = 9.161$, $p < 0.001$), TMT-A scores ($F = 4.439$, $p = 0.016$), VR I scores ($F = 16.132$, $p < 0.001$), and DST-B scores ($F = 5.412$, $p = 0.007$). Furthermore, the pairwise comparisons demonstrated apparent declines in SCWT, VR I, and DST-B scores in the two PBD groups ($p < 0.05$) compared with the HC group, as well as lower TMT-A scores in the manic patients ($p < 0.05$) compared with HC (**Table 1**). No significant difference was observed for TMT-B scores ($F = 1.455$, $p = 0.242$) or DST-A scores ($F = 1.520$, $p = 0.228$) among the 3 groups.

Subnuclei Volume Analysis

Table 2 summarizes the statistical analysis for the volume of the amygdala subnuclei. There were significant differences in the bilateral whole amygdala, basal nucleus, ABN, and CAT, left cortical nucleus, left paralaminar nucleus, and right central nucleus among the three groups ($p < 0.05$). Histograms in **Figure 2** demonstrate post-hoc pairwise comparisons on amygdala subnuclei volumes. **Table 2** lists the statistical results of *post-hoc* pairwise comparisons in subnuclei with significant differences among the three groups. The strongest effects for bilateral whole amygdala, ABN, and CAT volume decrease were seen in manic patients ($p < 0.01$). In addition, euthymic PBD group exhibited deceased bilateral ABN and left CAT volumes compared with HCs ($p < 0.05$).

Correlation Analysis

Age, gender, and years of education were not significantly correlated with amygdala morphology within the HCs and PBD groups. In the manic PBD group, VR I score was found to be positively correlated with right whole amygdala, bilateral basal nucleus, right lateral nucleus, and right ABN volume ($p < 0.05$; **Figure 3**). The euthymic PBD group had no significant correlation between the subnuclei volume and any of the clinical and cognitive characteristics.

DISCUSSION

To the best of our knowledge, this cross-sectional study is the first work utilizing automated neuroanatomical quantification (FreeSurfer) to evaluate amygdala and subnuclei volumetric differences in PBD patients. The main finding of the present study was the significant differences in the basal nucleus, ABN, and CAT volumes between PBD patients and HCs. Unexpectedly,

TABLE 1 | Sample characteristics.

Characteristics	Manic-PBD (n=20)	Euthymic-PBD (n=20)	HC (n=19)	$F/T/\chi^2$	*p*	Pairwise comparisons (*p* value)		
						Mania vs. Euthymia	Mania vs. HC	Euthymia vs. HC
Gender (male/female)	9/11	11/9	7/12	1.301#	0.522	0.527	0.605	0.256
Age (years)	15.30 ± 1.81	15.60 ± 1.64	14.37 ± 1.30	3.118&	0.052	1.000	0.059	0.224
Education (years)	8.40 ± 1.76	8.70 ± 1.75	7.47 ± 2.22	2.153&	0.126	1.000	0.411	0.152
IQ	103.50 ± 10.67	108.60 ± 9.73	105.32 ± 7.51	1.503&	0.231	0.278	1.000	0.844
YMRS scores	34.30 ± 6.44	5.50 ± 1.70	3.63 ± 2.06	356.537&	<0.001***	<0.001***	<0.001***	0.467
MFQ scores	7.15 ± 2.62	6.65 ± 4.38	6.11 ± 3.33	0.429&	0.654	1.000	1.000	1.000
Onset age (year)	14.05 ± 1.73	13.70 ± 2.03	–	0.587^	0.561	–	–	–
Illness duration (months)	15.90 ± 12.96	24.15 ± 17.62	–	−1.687^	0.100	–	–	–
Onset frequency	3.10 ± 1.68	4.80 ± 7.55	–	−0.983^	0.332	–	–	–
The first episode bipolar disorder (mania/depression)	9/11	7/13	–	0.417#	0.519	–	–	–
Acute or delayed onset (acute/delayed)	10/10	11/9	–	0. 010#	0.752	–	–	–
Psychotic symptoms(yes/no)	9/11	12/8	–	0.902#	0.342	–	–	–
BP-I/BP-II	15/5	14/6	–	0.125#	0.723	–	–	–
Familial BD history(yes/no)	7/13	5/15	–	0.476#	0.490	–	–	–
Medications Lithium	8	8	–	–	–	–	–	
Valproate	11	13	–	–	–	–	–	
Atypical antipsychotics	13	15	–	–	–	–	–	
Antidepressants	2	–	–	–	–	–	–	
SCWT-A	53.35 ± 15.98	54.35 ± 13.53	66.00 ± 12.26	4.852&	0.011*	1.000	0.020*	0.037*
SCWT-B	69.80 ± 19.56	71.80 ± 15.16	87.79 ± 9.08	8.023&	0.001**	1.000	0.002**	0.006**
SCWT-C	29.65 ± 7.36	31.85 ± 9.12	40.74 ± 9.43	9.161&	<0.001***	1.000	<0.001***	0.006**
TMT-A	40.35 ± 12.31	38.15 ± 12.80	29.74 ± 9.63	4.439&	0.016*	1.000	0.019*	0.086
TMT-B	88.90 ± 30.64	101.95 ± 50.89	80.61 ± 31.27	1.455&	0.242	0.844	1.000	0.294
VRT	8.45 ± 3.41	10.30 ± 2.60	13.21 ± 1.48	16.132&	<0.001***	0.091	<0.001***	0.003**
DST-A	8.20 ± 1.51	8.65 ± 1.66	9.00 ± 1.05	1.520&	0.228	0.980	0.264	1.000
DST-B	4.45 ± 1.15	4.75 ± 1.62	5.95 ± 1.68	5.412&	0.007**	1.000	0.009**	0.047*

*Data are presented as mean ± standard deviation. #Pearson chi-square test; &one-way ANOVA (analysis of variance); ^Independent-sample t-test. The pairwise comparisons between groups using Bonferroni method. *p < 0.05, **p < 0.01, ***p < 0.001.*

IQ, intelligence quotient; YMRS, Young Manic Rating Scale; MFQ, Mood and Feelings Questionnaire; BP-I, bipolar disorder type I; BP-II, bipolar disorder type II; SCWT, Stroop color-word test; TMT, trail making test; VR I, visual reproduction immediate recall subtest; DST, digit span test.

amygdala and subnuclei volumes between manic and euthymic patient group were indistinguishable for all structures examined. In addition, this study detected that PBD patients have significant differences in SCWT, TMT-A, VR I, and DST-B compared to HCs. And in the manic PBD group, VR I score was found to be positively correlated with right whole amygdala, bilateral basal nucleus, right lateral nucleus, and right ABN volume.

Neuroimaging studies in PBD have so far supported the key role of amygdala. Alterations in amygdala volumes have been associated with measures of illness duration and disease progression in PBD (20). Consistent with previous finding, the present study specifically found a mean volume reduction of 6.4% in left amygdala, and 7.8% in right amygdala in manic PBD patients compared with that of the HCs, with no significant difference in euthymic PBD patients (**Figure 2A**). Furthermore, the mania and euthymia group showed differences in right whole amygdala volume, but it did not attain the statistical significance ($p = 0.050$). It is worth noting that little evidence of amygdala volumetric alterations was reported in young subjects with schizophrenia (SZ) or other psychotic disorders, indicating that alterations may be specific to BD (42). Post mortem studies had reported the amygdala as a common site for senile plaques and neurofibrillary tangles in Alzheimer's disease (AD) and mild cognitive impairment (43). McGaugh emphasized that the amygdala is critically related with memory consolidation by intermediating the impacts of epinephrine and glucocorticoids and regulating the activities of striatum and hippocampus (44). In healthy individuals, amygdala volume has no connection with memory function, whereas in BD patients, larger amygdala volume was predictive of integrated memory function (24). Consistent with our study, we found that right whole amygdala volume was predictive of cognitive performance in manic group, correlating positively with better immediate recall memory for manic PBD patients (**Figure 3A**).

We determined *in vivo* localization of the volumetric difference within the amygdala. The most affected subnuclei were the bilateral ABN and left CAT in all PBD patients (**Figures 2D, I**), and volume changes in the bilateral basal, left paralaminar nucleus, and right CAT, lateral, and central nucleus were apparent only in manic patients (**Figures 2B, C, I, J**). Originating in the anteromedial temporal lobe, the amygdalofugal tract passes through the basal, lateral, and central amygdala nucleus toward the midline (45), which is believed to apply downstream control over hypothalamus and septal nuclei,

TABLE 2 | The difference among the three groups in the amygdala and subnuclei.

Regions		Manic-PBD (n = 20)	Euthymic-PBD (n = 20)	HC (n = 19)	$F^{\#}$	*p*	Pairwise comparisons (*p* value)		
							Mania vs. Euthymia	Mania vs. HC	Euthymia vs. HC
Left	Whole amygdala	1699.614 ± 193.038	1805.293 ± 195.487	1815.260 ± 174.344	4.669	0.014*	0.145	0.004**	0.121
	Lateral nucleus	647.823 ± 72.738	683.317 ± 70.861	676.520 ± 65.766	1.776	0.180	0.274	0.068	0.447
	Basal nucleus	439.095 ± 54.010	464.978 ± 55.652	468.220 ± 47.291	3.274	0.046*	0.263	0.013*	0.161
	ABN	250.118 ± 27.183	269.462 ± 32.278	275.435 ± 31.274	8.345	0.001**	0.075	<0.001***	0.028*
	AAA	58.851 ± 8.472	60.574 ± 7.341	60.381 ± 6.779	0.113	0.893	0.901	0.644	0.739
	Central nucleus	40.210 ± 6.246	43.291 ± 5.649	42.654 ± 6.794	1.109	0.368	0.306	0.183	0.737
	Medial nucleus	20.219 ± 5.779	20.390 ± 3.818	21.452 ± 3.815	0.811	0.450	0.658	0.396	0.215
	Cortical nucleus	25.228 ± 3.544	27.040 ± 3.934	27.368 ± 3.429	3.288	0.045*	0.324	0.014	0.127
	CAT	168.509 ± 21.032	182.552 ± 25.746	190.128 ± 26.655	6.470	0.003**	0.123	0.001**	0.048*
	Paralaminar nucleus	49.561 ± 5.853	53.688 ± 6.877	53.101 ± 5.820	3.256	0.047*	0.058	0.022*	0.642
Right	Whole amygdala	1741.491 ± 175.730	1856.749 ± 192.371	1859.253 ± 168.184	5.184	0.009**	0.050	0.003**	0.243
	Lateral nucleus	658.386 ± 65.822	699.189 ± 64.786	692.813 ± 65.799	2.860	0.066	0.057	0.038*	0.814
	Basal nucleus	448.180 ± 48.673	478.357 ± 59.766	478.559 ± 45.965	3.508	0.037*	0.114	0.012*	0.313
	ABN	260.065 ± 30.681	278.116 ± 33.518	283.288 ± 25.640	6.825	0.002**	0.115	0.001**	0.042*
	AAA	61.595 ± 6.781	65.147 ± 7.057	64.180 ± 6.641	1.151	0.324	0.168	0.25	0.851
	Central nucleus	41.861 ± 7.571	44.650 ± 5.929	46.013 ± 5.886	3.226	0.048*	0.420	0.015*	0.099
	Medial nucleus	21.761 ± 4.291	23.858 ± 5.181	24.000 ± 4.893	1.203	0.308	0.386	0.130	0.504
	Cortical nucleus	27.501 ± 2.979	28.732 ± 3.444	29.276 ± 3.349	1.730	0.187	0.560	0.072	0.222
	CAT	172.367 ± 20.692	184.866 ± 23.368	188.620 ± 19.389	4.988	0.010*	0.125	0.003**	0.115
	Paralaminar nucleus	49.776 ± 5.556	53.834 ± 7.309	52.502 ± 5.646	2.520	0.090	0.065	0.057	0.911

*Data are presented as mean ± standard deviation. The pairwise comparisons between groups using Bonferroni method. #ANCOVAs (Analysis of covariance). nit: mm^3. *p < 0.05, **p < 0.01, ***p < 0.001.*

ABN, accessory basal nucleus; AAA, anterior amygdaloid area; CAT, cortico-amygdaloid transition.

affecting threat reactivity and memory (46). The central nucleus is a key output area for expressing innate emotional responses and associated physiological responses, and it connects brainstem controlling specific behaviors and physiological responses. The basal nucleus is another important region of output connecting with the central nucleus; and the striatal areas are related with controlling of instrumental behaviors. In addition, connections from the basal amygdala to the striatum are involved in controlling actions. The lateral nucleus in is believed to tie cortical areas account for processing sensory stimuli with structures responsible for eliciting emotional responses to these stimuli. Therefore, we suggested that the ABN and CAT may serve as early image markers for differentiating patients with PBD from HCs and the volume of basal, lateral, and central nucleus for targeting or tracking the progression of illness in adolescents BD.

The amygdala can be generally partitioned into two major subdivisions: the basolateral (BLA), and centrocorticomedial. The ABN, basal, and lateral nucleus constitute the BLA complex (25, 47), which comprises 69% of the total amygdala volume in humans. The BLA group is thought to represent an integration center for coordinating inputs from certain cortical and subcortical regions, including the prefrontal cortex (PFC), hippocampus, thalamus, and visual cortices; the BLA is involved in learning and memory (48). The cortical, medial, and central nucleus belong to the centrocorticomedial group (49), which has been suggested to receive astrictive information from the medial PFC and BLA, thereby serve as the pathway to generate behavioral, motor, and autonomic emotional responses (50). The results showed that the decreased volume of amygdala subnuclei in PBD patients were mainly concentrated in the BLA.

In psychiatric disorders, neurocognitive impairments are prevalent and have been associated with poor outcome (51). The cognitive tests used in this study cover a broad range of cognitive abilities, including attentional capacity measured with DST-A and TMT-A; processing speed measured with TMT-A, SCWT-A (color naming), SCWT-B (word reading); working memory/mental tracking measured with DST-B; visual memory measured with VR I (immediate recall); self-regulation/self-monitoring measured with SCWT-C (inhibition); and cognitive flexibility measured with TMT-B (Number-Letter Switching) (52). In this study, SCWT, TMT-A, VR I, and DST-B completion scores differed significantly between the patients and HCs. The results provide evidence that manic and euthymic patients with PBD have significant cognitive impairment, specifically in processing speed, executive function, visual learning, and working memory.

The Spearman correlation of this study indicated that amygdala subnuclei association with VR I scores are primarily in the right BLA (**Figures 3B–D**). Except for immediate recall memory, VR is also related to visual-perceptual-motor and nonverbal reasoning memory. VR has a widely of clinical and research utility, often employed in AD (53), posttraumatic stress disorder (54), major depressive Disorder (55), autism spectrum disorder (56). Troster et al. (53) found that VR had excellent sensitivity and specificity in differentiating patients with AD from HCs. Mak and colleagues (55) found that unipolar and bipolar patients with depression could be distinguished by a

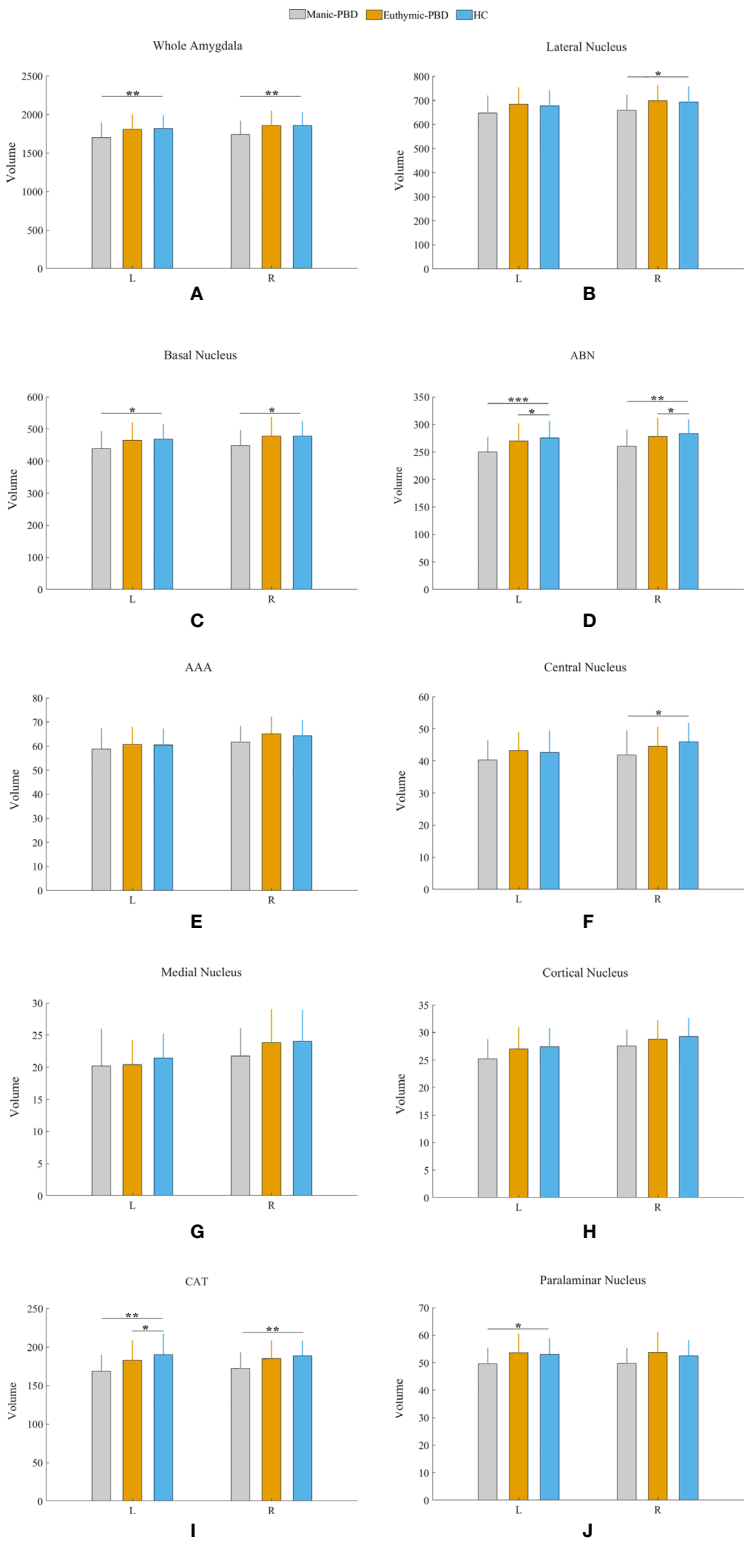

FIGURE 2 | Pairwise comparison of volumes in the manic PBD group, euthymic PBD group, and healthy control group (**A**,Whole Amygdala volume; **B**, Lateral Nucleus volume; **C**, Basal Nucleus volume; **D**, ABN volume; **E**, AAA volume; **F**, Central Nucleus volume; **G**, Medial Nucleus volume; **H**, Cortical Nucleus volume; **I**, CAT volume; **J**, Paralaminar Nucleus volume). The Y-axis represents the mean volume of amygdala and its subnuclei in each group. Unit: mm^3. *$p < 0.05$; **$p < 0.01$. L, left amygdala; R, right amygdala; ABN, accessory basal nucleus; AAA, anterior amygdaloid area; CAT, cortico-amygdaloid transition.

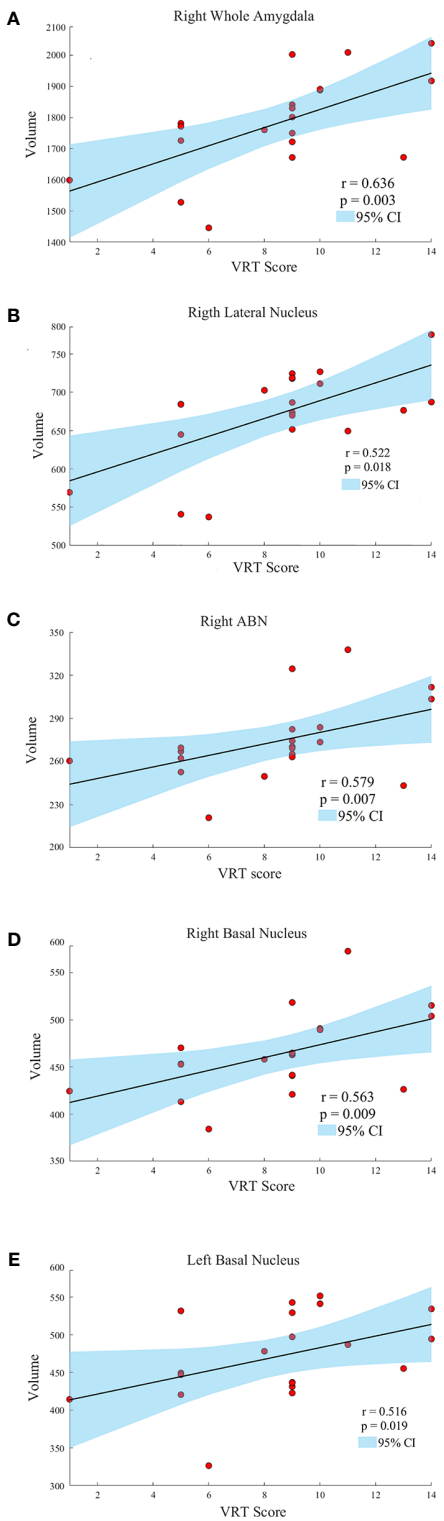

FIGURE 3 | Scatter plots showing the relationships between the amygdala and subnuclei volumes and VR I score in manic patients group (**A**, Right Whole Amygdala; **B**, Right Lateral Nucleus; **C**, Right ABN; **D**, Right Basal Nucleus; **E**, Left Basal Nucleus). ABN, accessory basal nucleus; VR I, visual reproduction immediate recall subtest.

relatively intact cognitive profile, including TMT and VR. As a result, the right BLA group may serve as early imaging markers for the visual memory dysfunction of manic PBD patients. The relationship between scores in VR I, the right whole amygdala and BLA volumes may evoke a long-existing theory of left-right dissociation of memory systems. This controversial hypothesis suggests that the left amygdala may be responsible for verbal information, whereas visuospatial data may be stored within the right amygdala (57).

There are several limitations in our study. Medication (lithium and other mood stabilizers like valproic acid) could influence the amygdala and subnuclei volumes of patients with PBD. In this study, most of the adolescent patients were taking more than one drug, so we could not rule out drug effects on the results. Moreover, this was a cross-sectional study. Future studies would benefit from longitudinal monitoring to determine whether discrete syndromes have different patterns of amygdala and subnuclei volume changes during an individual's clinical progression.

In conclusion, we used a novel, automated approach to segment and evaluate differences in amygdala and subnuclei volumes in patients with PBD. Together our neuroimaging and cognitive function findings suggest that the volumes of amygdala subnuclei were smaller in manic and euthymic patients with PBD than that of HCs, especially the ABN and CAT. In addition, visual memory abnormalities might be associated with right whole amygdala, bilateral basal nucleus, right lateral nucleus, and right ABN volume reductions in patients with manic. Moreover, our findings suggest that smaller BLA group volumes may be an early marker of PBD progression toward weaker cognitive function.

DATA AVAILABILITY STATEMENT

All datasets generated for this study are included in the article/supplementary material.

ETHICS STATEMENT

The studies involving human participants were reviewed and approved by University of Central South Institutional Review Board. Written informed consent to participate in this study was provided by the participants' legal guardian/next of kin. Written informed consent was obtained from the individual(s), and minor(s)' legal guardian/next of kin, for the publication of any potentially identifiable images or data included in this article.

AUTHOR CONTRIBUTIONS

JQ, LS, and GL designed the study. WG and LS acquired the data. DC, YG, and WC processed all neuroimaging data. DC and JQ performed all statistical analyses. DC wrote the article, which all

authors reviewed. All authors contributed to the article and approved the submitted version.

FUNDING

We are grateful for support from the Fundamental Research Funds for the Central Universities (No. 3332018159 to DC), Funds of the National Natural Science Foundation of China (81371531 to QJ, 81901730 to WC), Key Project of Scientific Research of "12th Five-Year Plan" in Medical Research of the Army (BWS11J063 to GL), Academic Promotion Programme of Shandong First Medical University (No. 2019QL009), and JQ was supported by the Taishan Scholars Program of Shandong Province (No. TS201712065).

ACKNOWLEDGMENTS

We thank LetPub (www.letpub.com) for its linguistic assistance during the preparation of this manuscript.

REFERENCES

1. Frias A, Palma C, Farriols N. Comorbidity in pediatric bipolar disorder: prevalence, clinical impact, etiology and treatment. *J Affect Disord* (2015) 174:378–89. doi: 10.1016/j.jad.2014.12.008
2. Leibenluft E, Charney DS, Pine DS. Researching the pathophysiology of pediatric bipolar disorder. *Biol Psychiatry* (2003) 53(11):1009–20. doi: 10.1016/S0006-3223(03)00069-6
3. Perlis RH, Miyahara S, Marangell LB, Wisniewski SR, Ostacher M, DelBello MP, et al. Long-term implications of early onset in bipolar disorder: data from the first 1000 participants in the systematic treatment enhancement program for bipolar disorder (STEP-BD). *Biol Psychiatry* (2004) 55(9):875–81. doi: 10.1016/j.biopsych.2004.01.022
4. Malhi GS, Ivanovski B, Hadzi-Pavlovic D, Mitchell PB, Vieta E, Sachdev P. Neuropsychological deficits and functional impairment in bipolar depression, hypomania and euthymia. *Bip Disord* (2007) 9(1-2):114–25. doi: 10.1111/j.1399-5618.2007.00324.x
5. Elias LR, Miskowiak KW, Vale AM, Kohler CA, Kjaerstad HL, Stubbs B, et al. Cognitive Impairment in Euthymic Pediatric Bipolar Disorder: A Systematic Review and Meta-Analysis. *J Am Acad Child Adolesc Psychiatry* (2017) 56 (4):286–96. doi: 10.1016/j.jaac.2017.01.008
6. Pompili M, Gibiino S, Innamorati M, Serafini G, Del Casale A, De Risio L, et al. Prolactin and thyroid hormone levels are associated with suicide attempts in psychiatric patients. *Psychiatry Res* (2012) 200(2-3):389–94. doi: 10.1016/j.psychres.2012.05.010
7. Pompili M, Shrivastava A, Serafini G, Innamorati M, Milelli M, Erbuto D, et al. Bereavement after the suicide of a significant other. *Indian J Psychiatry* (2013) 55(3):256–63. doi: 10.4103/0019-5545.117145
8. Bora E, Pantelis C. Meta-analysis of Cognitive Impairment in First-Episode Bipolar Disorder: Comparison With First-Episode Schizophrenia and Healthy Controls. *Schizophr Bull* (2015) 41(5):1095–104. doi: 10.1093/schbul/sbu198
9. Frias A, Palma C, Farriols N. Neurocognitive impairments among youth with pediatric bipolar disorder: a systematic review of neuropsychological research. *J Affect Disord* (2014) 166:297–306. doi: 10.1016/j.jad.2014.05.025
10. Brambilla P, Hatch JP, Soares JC. Limbic changes identified by imaging in bipolar patients. *Curr Psychiatry Rep* (2008) 10(6):505–9. doi: 10.1007/s11920-008-0080-8
11. Sotres-Bayon F, Sierra-Mercado D, Pardilla-Delgado E, Quirk GJ. Gating of fear in prelimbic cortex by hippocampal and amygdala inputs. *Neuron.* (2012) 76(4):804–12. doi: 10.1016/j.neuron.2012.09.028
12. Mendez-Bertolo C, Moratti S, Toledano R, Lopez-Sosa F, Martinez-Alvarez R, Mah YH, et al. A fast pathway for fear in human amygdala. *Nat Neurosci* (2016) 19(8):1041–9. doi: 10.1038/nn.4324
13. Asari T, Konishi S, Jimura K, Chikazoe J, Nakamura N, Miyashita Y. Amygdalar enlargement associated with unique perception. *Cortex.* (2010) 46(1):94–9. doi: 10.1016/j.cortex.2008.08.001
14. Jacobs RH, Renken R, Aleman A, Cornelissen FW. The amygdala, top-down effects, and selective attention to features. *Neurosci Biobehav Rev* (2012) 36 (9):2069–84. doi: 10.1016/j.neubiorev.2012.05.011
15. Krause-Utz A, Winter D, Schriner F, Chiu CD, Lis S, Spinhoven P, et al. Reduced amygdala reactivity and impaired working memory during dissociation in borderline personality disorder. *Eur Arch Psychiatry Clin Neurosci* (2018) 268(4):401–15. doi: 10.1007/s00406-017-0806-x
16. Kryza-Lacombe M, Brotman MA, Reynolds RC, Towbin K, Pine DS, Leibenluft E, et al. Neural mechanisms of face emotion processing in youths and adults with bipolar disorder. *Bip Disord* (2019) 21(4):309–20. doi: 10.1111/bdi.12768
17. Kalmar JH, Wang F, Chepenik LG, Womer FY, Jones MM, Pittman B, et al. Relation between amygdala structure and function in adolescents with bipolar disorder. *J Am Acad Child Adolesc Psychiatry* (2009) 48(6):636–42. doi: 10.1097/CHI.0b013e31819f6fbc
18. Kelley R, Chang KD, Garrett A, Alegria D, Thompson P, Howe M, et al. Deformations of amygdala morphology in familial pediatric bipolar disorder. *Bip Disord* (2013) 15(7):795–802. doi: 10.1111/bdi.12114
19. Blumberg HP, Kaufman J, Martin A, Whiteman R, Zhang JH, Gore JC, et al. Amygdala and hippocampal volumes in adolescents and adults with bipolar disorder. *Arch Gen Psychiatry* (2003) 60(12):1201–8. doi: 10.1001/archpsyc.60.12.1201
20. DelBello MP, Zimmerman ME, Mills NP, Getz GE, Strakowski SM. Magnetic resonance imaging analysis of amygdala and other subcortical brain regions in adolescents with bipolar disorder. *Bip Disord* (2004) 6(1):43–52. doi: 10.1046/j.1399-5618.2003.00087.x
21. Pfeifer JC, Welge J, Strakowski SM, Adler CM, DelBello MP. Meta-analysis of amygdala volumes in children and adolescents with bipolar disorder. *J Am Acad Child Adolesc Psychiatry* (2008) 47(11):1289–98. doi: 10.1097/CHI.0b013e318185d299
22. Strakowski SM, Delbello MP, Adler CM. The functional neuroanatomy of bipolar disorder: a review of neuroimaging findings. *Mol Psychiatry* (2005) 10 (1):105–16. doi: 10.1038/sj.mp.4001585
23. Swayze V, Andreasen NC, Alliger RJ, Ehrhardt JC, Yuh WT. Structural brain abnormalities in bipolar affective disorder. Ventricular enlargement and focal signal hyperintensities. *Arch Gen Psychiatry* (1990) 47(11):1054–9. doi: 10.1001/archpsyc.1990.01810230070011
24. Killgore WD, Rosso IM, Gruber SA, Yurgelun-Todd DA. Amygdala volume and verbal memory performance in schizophrenia and bipolar disorder. *Cognit Behav Neurol* (2009) 22(1):28–37. doi: 10.1097/WNN.0b013e318192cc67
25. Aghamohammadi-Sereshki A, Hrybouski S, Travis S, Huang Y, Olsen F, Carter R, et al. Amygdala subnuclei and healthy cognitive aging. *Hum Brain Mapp* (2019) 40(1):34–52. doi: 10.1002/hbm.24353
26. Usher J, Leucht S, Falkai P, Scherk H. Correlation between amygdala volume and age in bipolar disorder - a systematic review and meta-analysis of structural MRI studies. *Psychiatry Res* (2010) 182(1):1–8. doi: 10.1016/j.pscychresns.2009.09.004
27. Hibar DP, Westlye LT, van Erp TG, Rasmussen J, Leonardo CD, Faskowitz J, et al. Subcortical volumetric abnormalities in bipolar disorder. *Mol Psychiatry* (2016) 21(12):1710–6. doi: 10.1038/mp.2015.227
28. Wegbreit E, Cushman GK, Puzia ME, Weissman AB, Kim KL, Laird AR, et al. Developmental meta-analyses of the functional neural correlates of bipolar disorder. *JAMA Psychiatry* (2014) 71(8):926–35. doi: 10.1001/jamapsychiatry.2014.660
29. Ding SL, Royall JJ, Sunkin SM, Ng L, Facer BA, Lesnar P, et al. Comprehensive cellular-resolution atlas of the adult human brain. *J Comp Neurol* (2017) 525 (2):407. doi: 10.1002/cne.24130
30. Kalin NH, Shelton SE, Davidson RJ. The role of the central nucleus of the amygdala in mediating fear and anxiety in the primate. *J Neurosci* (2004) 24 (24):5506–15. doi: 10.1523/JNEUROSCI.0292-04.2004

31. Dong X, Li S, Kirouac GJ. Collateralization of projections from the paraventricular nucleus of the thalamus to the nucleus accumbens, bed nucleus of the stria terminalis, and central nucleus of the amygdala. *Brain Struct Funct* (2017) 222(9):3927–43. doi: 10.1007/s00429-017-1445-8
32. Saygin ZM, Kliemann D, Iglesias JE, van der Kouwe AJW, Boyd E, Reuter M, et al. High-resolution magnetic resonance imaging reveals nuclei of the human amygdala: manual segmentation to automatic atlas. *Neuroimage* (2017) 155:370–82. doi: 10.1016/j.neuroimage.2017.04.046
33. Association AP. *Diagnostic and Statistical Manual of Psychiatric Disorders, fifth ed*. Arlington, MA: American Psychiatric Publishing (2013).
34. Traci W, Olivier E, Mark Mahone Lisa A. Jacobson. Wechsler Intelligence Scale for Children. *Can J Sch Psychol* (2018) 19(Suppl 1):221–34. doi: 10.1007/978-3-319-56782-2_1605-2
35. Kaufman J, Birmaher B, Brent D, Rao U, Flynn C, Moreci P, et al. Schedule for Affective Disorders and Schizophrenia for School-Age Children-Present and Lifetime Version (K-SADS-PL): initial reliability and validity data. *J Am Acad Child Adolesc Psychiatry* (1997) 36(7):980–8. doi: 10.1097/00004583-199707000-00021
36. Geller B, Zimerman B, Williams M, Bolhofner K, Craney JL, DelBello MP, et al. Reliability of the Washington University in St. Louis Kiddie Schedule for Affective Disorders and Schizophrenia (WASH-U-KSADS) mania and rapid cycling sections. *J Am Acad Child Adolesc Psychiatry* (2001) 40(4):450–5. doi: 10.1097/00004583-200104000-00014
37. Wood A, Kroll L, Moore A, Harrington R. Properties of the mood and feelings questionnaire in adolescent psychiatric outpatients: a research note. *J Child Psychol Psychiatry* (1995) 36(2):327–34. doi: 10.1111/j.1469-7610.1995.tb01828.x
38. Young RC, Biggs JT, Ziegler VE, Meyer DA. A rating scale for mania: reliability, validity and sensitivity. *Br J Psychiatry* (1978) 133:429–35. doi: 10.1192/bjp.133.5.429
39. Moran L, Yeates KO. Stroop Color and Word Test, Children's Version. *Encyclopedia of Clinical Neuropsychology*. New York, NY: Springer (2011).
40. Ralph M, Reitan, Deborah, Wolfson. Category test and trail making test as measures of frontal lobe functions. *Clin Neuropsychol* (1995) 9:50–6. doi: 10.1080/13854049508402057
41. Welch LW, Nimmerrichter A, Gilliland R, King DE, Martin PR. "Wineglass" Confabulations Among Brain- Damaged Alcoholics on the Wechsler Memory Scale-Revised Visual Reproduction Subtest. *Cortex*. (1997) 33(3):0–551. doi: 10.1016/S0010-9452(08)70235-1
42. Eggins PS, Hatton SN, Hermens DF, Hickie IB, Lagopoulos J. Subcortical volumetric differences between clinical stages of young people with affective and psychotic disorders. *Psychiatry Res Neuroimag* (2018) 271:8–16. doi: 10.1016/j.pscychresns.2017.11.015
43. Markesbery WR. Neuropathologic alterations in mild cognitive impairment: a review. *J Alzheimers Dis* (2010) 19(1):221–8. doi: 10.3233/JAD-2010-1220
44. McGaugh JL. Memory–a century of consolidation. *Science* (2000) 287 (5451):248–51. doi: 10.1126/science.287.5451.248
45. Trobe DJ. The Human Brain. An Introduction to Its Functional Anatomy, 6th Edition. *J Neuro-Ophthalmol* (2010) 30(1):107. doi: 10.1097/01.wno.0000369168.32606.54
46. Brown SSG, Rutland JW, Verma G, Feldman RE, Schneider M, Delman BN, et al. Ultra-High-Resolution Imaging of Amygdala Subnuclei Structural Connectivity in Major Depressive Disorder. *Biol Psychiatry Cognit Neurosci Neuroimaging* (2020) 5(2):184–93. doi: 10.1016/j.bpsc.2019.07.010
47. LeDoux J. The amygdala. *Curr Biol* (2007) 17(20):R868–74. doi: 10.1016/j.cub.2007.08.005
48. Roozendaal B, McEwen BS, Chattarji S. Stress, memory and the amygdala. *Nat Rev Neurosci* (2009) 10(6):423–33. doi: 10.1038/nrn2651
49. Aggleton J. The amygdala: a functional analysis. New York, NY: Oxford University Press (2000).
50. Pessoa L. Reprint of: Emotion and cognition and the amygdala: from "what is it?" to "what's to be done"?. *Neuropsychologia* (2011) 49(4):681–94. doi: 10.1016/j.neuropsychologia.2011.02.030
51. Joseph MF, Frazier TW, Youngstrom EA, Soares JC. A quantitative and qualitative review of neurocognitive performance in pediatric bipolar disorder. *J Child Adolesc Psychopharmacol* (2008) 18(6):595–605. doi: 10.1089/cap.2008.064
52. Sparding T, Silander K, Palsson E, Ostlind J, Ekman CJ, Sellgren CM, et al. Classification of cognitive performance in bipolar disorder. *Cognit Neuropsychiatry* (2017) 22(5):407–21. doi: 10.1080/13546805.2017.1361391
53. Troster AI, Butters N, Salmon DP, Cullum CM, Jacobs D, Brandt J, et al. The diagnostic utility of savings scores: differentiating Alzheimer's and Huntington's diseases with the logical memory and visual reproduction tests. *J Clin Exp Neuropsychol* (1993) 15(5):773–88. doi: 10.1080/01688639308402595
54. Vasterling JJ, Aslan M, Lee LO, Proctor SP, Ko J, Jacob S, et al. Longitudinal Associations among Posttraumatic Stress Disorder Symptoms, Traumatic Brain Injury, and Neurocognitive Functioning in Army Soldiers Deployed to the Iraq War. *J Int Neuropsychol Soc* (2018) 24(4):311–23. doi: 10.1017/S1355617717001059
55. Mak ADP, Lau DTY, Chan AKW, So SHW, Leung O, Wong SLY, et al. Cognitive Impairment In Treatment-Naive Bipolar II and Unipolar Depression. *Sci Rep* (2018) 8(1):1905. doi: 10.1038/s41598-018-20295-3
56. Funabiki Y, Shiwa T. Weakness of visual working memory in autism. *Autism Res* (2018) 11(9):1245–52. doi: 10.1002/aur.1981
57. Markowitsch HJ. Differential contribution of right and left amygdala to affective information processing. *Behav Neurol* (1998) 11(4):233–44. doi: 10.1155/1999/180434

Conflict of Interest: The authors declare that the research was conducted in the absence of any commercial or financial relationships that could be construed as a potential conflict of interest.

frontiers in Psychiatry

REVIEW
published: 06 August 2020
doi: 10.3389/fpsyt.2020.00769

Proton Magnetic Resonance Spectroscopy in Common Dementias—Current Status and Perspectives

Stephan Maul, Ina Giegling and Dan Rujescu*

University Clinic and Outpatient Clinic for Psychiatry, Psychotherapy and Psychosomatics, Martin Luther University Halle-Wittenberg, Halle, Germany

Dementia occurs mainly in the elderly and is associated with cognitive decline and impairment of activities of daily living. The most common forms of dementia are Alzheimer's disease (AD), vascular dementia (VD), dementia with Lewy bodies (DLB), and frontotemporal dementia (FTD). To date, there are no causal options for therapy, but drug and non-drug treatments can positively modulate the course of the disease. Valid biomarkers are needed for the earliest possible and reliable diagnosis, but so far, such biomarkers have only been established for AD and require invasive and expensive procedures. In this context, proton magnetic resonance spectroscopy (^{1}H-MRS) provides a non-invasive and widely available technique for investigating the biochemical milieu of brain tissue *in vivo*. Numerous studies have been conducted for AD, but for VD, DLB, and FTD the number of studies is limited. Nevertheless, MRS can detect measurable metabolic alterations in common dementias. However, most of the studies conducted are too heterogeneous to assess the potential use of MRS technology in clinical applications. In the future, technological advances may increase the value of MRS in dementia diagnosis and treatment. This review summarizes the results of MRS studies conducted in common dementias and discusses the reasons for the lack of transfer into clinical routine.

Keywords: proton magnetic resonance spectroscopy, Alzheimer's disease, vascular dementia, dementia with Lewy bodies, frontotemporal dementia, biomarker

OPEN ACCESS

Edited by:
Sven Haller,
Rive Droite SA, Switzerland

Reviewed by:
Gabriele Ende,
University of Heidelberg, Germany
Stefan Klöppel,
Universität Bern, Switzerland

****Correspondence:***
Stephan Maul
Stephan.maul@uk-halle.de

Specialty section:
This article was submitted to Neuroimaging and Stimulation, a section of the journal Frontiers in Psychiatry

Received: *07 April 2020*
Accepted: *20 July 2020*
Published: *06 August 2020*

Citation:
Maul S, Giegling I and Rujescu D (2020) Proton Magnetic Resonance Spectroscopy in Common Dementias—Current Status and Perspectives. Front. Psychiatry 11:769. doi: 10.3389/fpsyt.2020.00769

INTRODUCTION

Dementia occurs mainly in the elderly and is associated with cognitive decline and impairment of activities of daily living. This leads to an increased need for care during the course of the disease. Dementia is therefore not only an enormous burden for the affected patients and their relatives, but also confronts social systems with great challenges, as the number of people suffering from dementia is expected to increase in the coming decades (1).

The most common cause of dementia is Alzheimer's disease (AD), followed by vascular dementia (VD), dementia with Lewy bodies (DLB), and frontotemporal dementia (FTD) [for review see Cunningham et al. (2)]. Although these most common types of dementia differ in

etiology, clinical symptoms, diagnostic findings, and treatment approaches, in many cases it is difficult to make a reliable diagnosis. A particular challenge is early detection and classification of cognitive impairments associated with discrete abnormalities that cannot be reliably distinguished clinically from age-related changes. The stage of slight symptoms is called mild cognitive impairment (MCI), MCI does not lead to limitations in activities of daily living, and it is a heterogeneous construct that has many underlying etiologies. In the context of dementia, MCI is seen as an intermediate predementia state of cognitive decline, but there are also stable and even reversible forms of MCI, which are not based on dementia neuropathology (3, 4). Additional tests using positron emission tomography (PET) and cerebrospinal fluid (CSF) are helpful for MCI and dementia diagnostics, but they are expensive, not widely available and invasive (5). However, there is still a lack of biomarkers which are easily available and allow early diagnosis and classification of dementia.

MR spectroscopy is a non-invasive *in vivo* method for measuring metabolite levels in various tissues based on the principles of nuclear magnetic resonance (NMR). More detailed literature on the physical background of MRS and on the clinical application in diseases of the central nervous system is provided by Ulmer and colleagues (6) and Öz et al. (7). Metabolites that are present in the brain at sufficiently high concentrations for quantification by MRS and have been commonly analyzed in dementia include N-acetylaspartate (NAA), myo-Inositol, total choline (tCho; primarily glycerophosphocholine and phosphocholine), and total creatine (tCr; creatine and phosphocreatine). Other metabolites less frequently investigated so far include glutamate+glutamine (Glx), γ-aminobutyric acid (GABA), and the antioxidant glutathione (GSH). NAA is highly concentrated in the brain and is mainly present in neurons, but also in oligodendrocytes. The exact function of NAA has not yet been clarified, and it has been hypothesized that it is involved in the energy metabolism of neuronal mitochondria, in the storage of acetyl coenzyme A, in signaling pathways and neurotransmission and in myelination processes (8–11). NAA is considered a marker of neuronal integrity, and reduced levels are found in various neuropathological conditions. However, it is unknown whether the reduced levels in MRS are due to a neuronal loss, neuronal dysfunction or disturbed NAA metabolism (8, 10). The tCho signal is mainly composed of glycerophosphocholine and phosphocholine, which are metabolites associated with the phospholipid metabolism of the cell membrane, whereby phosphocholine can be both a precursor or a degradation product and glycerophosphocholine is formed as a breakdown product (12). Disturbed tCho levels thus indicate an imbalanced cell membrane phospholipid metabolism, but MRS cannot determine whether this is driven by anabolic or catabolic pathways. In AD, elevated levels of glycerophosphocholine in the CSF were detected, which may indicate an increased membrane breakdown, possibly triggered by the activation of calcium-dependent phospholipase A_2 (13, 14).

The sugar alcohol mI is considered a glial cell marker, as it occurs predominantly in glial cells and is involved in intracellular signaling pathways (15). The tCr peak is composed of creatine and phosphocreatine, which are involved in the energy metabolism, with the phosphorylated form of creatine serving as an energy buffer (16). In earlier studies, the tCr level has been described as relatively stable in dementia, AD and aging and was therefore often used as a reference for calculating metabolite ratios (e.g. NAA/tCr, mI/tCr) (17–19). This is problematic, as deviations in tCr levels were found in later studies [e.g. (20)] and tCr therefore does not appear to be a reliable reference marker. The Glx complex consists of signals of the metabolites glutamate (Glu), glutamine (Gln), and GABA and the individual peaks can only be separated at higher magnetic field strengths (3.0 T and higher) (21). Glu is the most important excitatory neurotransmitter in the brain which, after its release from the synaptic terminals, is transported into astrocytes, where it is converted into Gln and then it is made available to neurons again (Glu-Gln-cycle) (22). Although the functions of the different metabolites are not fully understood, which also makes the interpretation of metabolite abnormalities somewhat difficult, they can be useful as diagnostic markers and facilitate the understanding of disease-related biochemical alterations in brain tissue (8). For example, MRS can be used *in vivo* to determine which brain regions are affected by metabolic alterations particularly early in the course of the disease.

MRS acquisition distinguishes between single-voxel technique, in which signals from a previously selected voxel are obtained, and magnetic resonance spectroscopic imaging (MRSI), in which many voxels are acquired simultaneously (multi-voxel spectroscopy). Single-voxel spectroscopy (SVS) offers the advantage that scan times are shorter and the quantification of metabolites is more accurate, but only one brain region can be examined at a time. MRSI allows simultaneous acquisition of numerous brain regions with the disadvantage of being less precise and it demands a longer imaging time (23). In contrast to anatomical MR imaging, MRS requires suppression of the water signal to obtain measurable signals of the significantly lower concentrated metabolites. For this purpose, it is necessary to define sufficiently large voxels, which also increases scanning time (24). Other imaging parameters that differ between MRS studies include relaxation time (TR) and echo time (TE). A short TE leads to a high signal-to-noise ratio, so that more metabolite peaks can be acquired than with a longer TE. However, a short TE leads to an increased overlap of peaks, whereas some metabolites cannot be detected with a longer TE (e.g. mI and Glx). With higher TR values, better spectra can be acquired, but this is associated with longer imaging times (23, 25).

The use of brain MRS is no longer limited to research applications, but now complements clinical neuroimaging, for example in neuro-oncology and neuro-pediatrics (7). Numerous studies in dementia have been conducted in the past, but MRS has not yet found its way into clinical routine. There are numerous reasons for this and they will be discussed in this review. But first an overview of MRS studies in AD, DLB, VD, and FTD will be provided.

METHODS

For this review, a systematic literature research on PubMed was conducted using the keywords "proton magnetic resonance

spectroscopy" in combination with one of the following terms: "Alzheimer's disease", "dementia with Lewy bodies", "vascular dementia", and "frontotemporal degeneration". For VD (seven studies), DLB (nine studies), and FTD (seven studies) all studies published since 2000 were considered. For AD, significantly more studies have been published that were meta-analyzed in 2015 (26). The present review summarizes the findings of the meta-analysis and only lists MRS studies on AD published since 2015. MRS studies in MCI were only considered when a longitudinal design was used to verify conversion to dementia, which enabled early metabolite alterations to be detected. **Tables 1–8** provide a systematic overview of all identified MRS studies. As some studies report absolute metabolite levels and some provide metabolite ratios, two tables were compiled for each dementia considered. Significant differences between dementia and control groups are indicated by an arrow pointing up or down, whereas a horizontal arrow means that no differences were found. Results appear in several tables if more than one common dementia has been studied within the same study. Significant differences between different dementias are marked with footnotes in the tables. Studies that followed interventional approaches or investigated specific symptoms (e.g. depression) in dementia were not taken into account.

Alzheimer's Disease

AD is by far the most common form of dementia in the elderly and leads to progressive cognitive decline, often initially affecting memory function. Typical histological findings are extracellular amyloid plaques and intracellular neurofibrillary tangles (55). In recent years, it has become increasingly apparent that early detection of AD seems to be an important prerequisite for pharmacological treatment (56). Thus, current clinical trials are focusing on individuals with an increased risk of AD, who do not yet have symptoms (preclinical AD) or who are at the stage of MCI (57). The use of biomarkers increases diagnostic accuracy, which is why the framework on diagnostic criteria for AD published by the National Institute on Ageing–Alzheimer's Association (NIA-AA) in 2018 recommends the use of biomarkers for AD diagnosis, particularly in the context of research projects (58). However, the best validated biomarkers to date can be determined either invasively by lumbar puncture (amyloid-β, tau, phospho-tau) or by using expensive imaging techniques that are not available on a large scale (amyloid PET). The huge dilemma is that there are still no easily and widely available biomarkers that would allow early and reliable diagnosis.

In 2015, a meta-analysis of 38 MRS studies in AD was published, with most MRS studies using 1.5 T MRI (26). Although more studies on this topic have been identified, not all of them could be included in the analyses due to the heterogeneity of the studies (e.g. lack of information on acquisition parameters or missing data needed to calculate effect sizes). Meta-analysis data are available for the four most frequently investigated brain regions, including the posterior cingulate cortex (PCC) (investigated in 17 studies), hippocampus (nine studies), and temporal and parietal lobes (seven studies each). Consistently, the NAA/tCr ratio or NAA level were significantly lowered in the four examined brain regions (Hedges g between −1.29 and −0.83). For the other metabolites analyzed in the meta-analysis, the results were more heterogeneous. Although a significantly increased mI/tCr ratio was found in the PCC (g=0.83), the effect was considerably lower when using absolute mI levels (g=0.32). A moderate increase in the PCC was found for tCho/tCr (g=0.48), while no significant difference was found for absolute tCho levels. In addition, an increased mI level in parietal gray matter was obtained in AD patients, whereas data for the other regions and metabolites were not sufficient for the meta-analysis. In summary, only for NAA a significant decrease in the investigated brain regions has been determined, while for the other metabolites data are less clear (e.g. due to a lack of studies in which these metabolites were acquired and discrepancies between reported metabolite ratios and absolute levels).

Since the publication of the meta-analysis, 14 MRS studies on AD have been published, including four studies with a longitudinal study design (see **Tables 1** and **2**). Consistent with the results of the meta-analysis, altered NAA and mI metabolites in the PCC were observed in four studies (27, 29, 36, 39). However, discrepant results were found in the study conducted by Su et al. (31), which revealed decreased NAA/tCr ratios in several brain areas and, also decreased mI/tCr and tCho/tCr ratios in the PCC, hippocampus, temporal, and frontal cortex. This opposite effect to other studies also occurred in DLB patients investigated in this study and is therefore discussed in the DLB section. Some studies also examined brain areas that were previously less in the focus. The occipital lobe was investigated in three recent studies, with no differences found between AD and controls (31, 35, 39). In the frontal cortex, Zhang et al. (35) detected no metabolite differences. This is consistent with a previous report (59), while the aforementioned study by Su et al. (31) obtained decreased NAA/tCr, mI/tCr, and tCho/tCr ratios.

Further studies focused on metabolites whose levels can be determined at higher field strengths (3.0 T or more) by better spectral resolution. Thus, Bai et al. (34) found a reduced level of γ-aminobutyric acid (GABA+), the major inhibitory neurotransmitter in the brain, in the parietal lobe of AD patients, while no differences between AD patients and healthy controls were found in the frontal lobe, hippocampus and ACC (28, 34). In addition, Mandal et al. (33) detected reduced levels of glutathione (GSH), an important antioxidant present in high concentrations in the brain (60), within the hippocampus and frontal cortex of AD patients. Chiang et al. (61) also investigated GSH levels, but in cognitively unimpaired older volunteers (average age: 63 ± 5 years), and found a negative correlation of amyloid load measured by Pittsburgh Compound B PET imaging with GSH levels in the temporal (r=−0.51) and parietal lobe (r=−0.47). The implementation of modern MRS techniques thus enables the detection of further metabolites in the brain tissue. However, its potential benefit must be verified in further studies.

It is also worth taking a look at recent studies in which the clinical outcome was determined in a prospective study design, with three studies involving patients with MCI (27, 30, 35) and

TABLE 1 | Magnetic resonance spectroscopy studies in Alzheimer's disease (studies reporting metabolite ratios).

Study	Parameters				Results					
	Field strength TR/TE (ms) technique	Sample	Area Voxel size (mm^3)	Cohort	NAA/ tCr	NAA/ ml	ml/ tCr	tCho/ tCr	Glx/ tCr	Others
Mitolo et al. (27)	1.5 T4,000/35 Single-voxel	Baseline: AD (n=25), MCI (n=38), HC (n=18)Clinical follow-up after 2 years:non-converter MCI (n=12), converter MCI (n=26),	Midline PCC (20x20x20)	AD	–	↓a	–	–	–	–
				Converter	–	↓a	–	–	–	–
				Non-converter	–	↔	–	–	–	–
Huang et al. (28)	3.0 T2,000/68 Singe-voxel	AD (n=17),MCI (n=21),HC (N=15)	Midline ACC (40x40x25)	AD	↓b	–	–	–	↓b	GABA+ ↔
				MCI	↔	–	–	–	↔	GABA+ ↔
			Right hippocampus (40x20x20)	AD	↔	–	–	–	↓	GABA+ ↔
				MCI	↔	–	–	–	↔	GABA+ ↔
Waragai et al. (29)	1.5 T2,000/25 Single-voxel	Baseline: HC (n=289)*	Midline PCC (20x20x20)	AD	↓	↓c	↑	–	–	–
				MCI	↓	↓c	↔	–	–	–
		7 years follow-up: AD (n=21), MCI (n=53), DLB (n=7), PD (n=8)		AD	↓	↓	↑d	–	–	–
				MCI	↔	↓	↑d	–	–	–
Fayed et al. (30)	3.0 T1,500/35 Single-voxel	aMCI (n=48) + clinical follow-up after 3 years: AD (n=15), aMCI (n=33)	Midline PCC (20x20x20)	AD converter	↔	–	ml ↔	–	↓	Glu/tCr ↓
			Left occipital cortex (20x20x20)		↔	–	ml ↓	–	↔	Glu/tCr ↔
Su et al. (31)	3.0 T3,450/35 Multi-voxel	AD (n=35),DLB (n=25),HC (n=34)	PCC	AD	↓	–	↓	↓	↓	–
			Thalamus		↓	–	↔	↓	↔	–
			Hippocampus		↔	–	↓	↔	↔	–
			Superior temporal cortex		↓	–	↓	↓	↔	–
			Prefrontal cortex		↓	–	↓	↓	↔	–
			Occipital cortex		↔e	–	↔	↔e	↔	–
			Caudate		↓	–	↓	↓	↔	–
			Corpus callosum		↓	–	↔	↓	↔	–
Guo et al. (32)	3.0 T1,500/35 Multi-voxel	Mild AD (n=15),aMCI (n=13),HC (n=16)	ACC (left+right) (10x10x15)	AD	–	–	-f	-f	–	–
			PCC (left+right) (10x10x15)		–	–	-f	–	–	–
Mandal et al. (33)	3.0 T2,500/120 Single-voxel	AD (n=21), MCI (n=22), HC (n=21)	Frontal cortex (left+right) (15,600)	AD	–	–	–	–	–	GSH ↓
				MCI	–	–	–	–	–	GSH ↓g
		AD (n=19), MCI (n=19), HC (n=28)	Hippocampus (left+right) (15,600)	AD	–	–	–	–	–	GSH ↓
				MCI	–	–	–	–	–	GSH ↓
Delli Pizzi et al. (17)	3.0 T2,000/39 Single-voxel	DLB (n=16), AD (n=16), HC (n=13)	Thalamus (left+right) (15x10x15)	AD	↔	–	–	↔h	–	tCr/H2O ↔
Bai et al. (34)	3.0 T2,000/68 Single-voxel	AD (n=15), HC (n=15)	Midline frontal lobe (30x30x30)	AD	–	–	–	–	–	GABA+/tCr ↔
			Midline parietal lobe (30x30x30)		–	–	–	–	–	GABA+/tCr ↓
Zhang et al. (35)	1.5 T2,000/30 Single-voxel	Baseline: MCI (n=57),Follow-up (after 18–32 months): DLB (n=10), AD (n=27), MCI (n=20)*	Midline frontal lobe (20x20x20)	AD	↔	–	↔	↔	–	–
			Midline PCC (20x20x20)		↔i	–	↔	↔	–	–
			Midline occipital lobe (20x20x20)		↔	–	↔	↔	–	–
Murray et al. (36)	3.0 T2,000/30 Single-voxel	AD (n=24), HC (n=17)	Midline PCC (20x20x20)	AD	↓	↓	↑	↔	–	–

ACC, anterior cingulate cortex; AD, Alzheimer's disease; tCho, total choline; tCr, total creatine; DLB, dementia with Lewy bodies; GABA+, γ-aminobutyric acid, macromolecules and homocarnosine; Glu, glutamate; Glx, glutamate-glutamine; HC, healthy controls; MCI, mild cognitive impairment; ml, myo-Inositol; NAA, N-acetlyaspartate; PCC, posterior cingulate cortex; PD, Parkinson's disease; TR, repetition time; TE, echo time.

↑ increased, ↓ decreased and ↔ unchanged metabolite ratios between AD and controls.

**Baseline differences were calculated on retrospective grouping according to clinical outcome.*

[a]significantly lower ratios in AD and MCI-converter compared to stable MCI.

[b]significantly lower ratios in AD compared to MCI.

[c]significantly lower ratios in AD compared to progressor MCI at baseline.

[d]significantly higher ratios in AD compared to progressor MCI after 7 years.

[e]significantly lower ratios in AD compared to DLB.

[f]No comparisons of patients and controls were reported, but significant bilateral differences (left vs. right ACC, left vs. right PCC) were observed.

[g]significantly lower ratios in AD compared to MCI in the left frontal cortex.

[h]significantly lower ratios in AD compared to DLB in the right thalamus.

[i]significantly reduced ratios in MCI converted to AD compared to MCI converted to DLB.

TABLE 2 | Magnetic resonance spectroscopy studies in Alzheimer's disease (studies reporting absolute metabolite levels).

Study	Parameters				Results					
	Field strength TR/TE (ms) technique	Sample	Area Voxel size (mm^3)	Cohort	NAA	mI	tCho	tCr	Glx	Others
Joe et al. (37)	1.5 T1,500/30 Single-voxel	Preclinical ADAD (n=16),HC (n=11)	Left ACC (11x11x9)	ADAD	↓	↔	↔	↔	↓	–
			Right ACC (11x11x9)		↔	↔	↔	↔	↔	–
			Midline PCC (11x11x12)		↔	↔	↔	↔	↔	–
			Midline precuneus (11x11x12)		↓	↑	↑	↔	↔	–
Glodzik et al. (38)	3.0 T10,000/0 NA	AD (n=53), MCI (n=42), HC (n=102)	Whole brain	AD/MCI	↓	–	–	–	–	–
Zhong et al. (39)	3.0 T2,000/35 Single-voxel	DLB (n=19), AD (n=21), HC (n=18)	Midline PCC (20x20x20)	AD	↓	↔	↔	↔	↓	Glu ↓
			Midline occipital lobe (20x20x20)		↔a	↔	↔	↔a	↓	Glu ↓a

ACC, anterior cingulate cortex; AD, Alzheimer's disease; ADAD, autosomal dominant AD; tCho, total choline; tCr, total creatine; DLB, dementia with Lewy bodies; Glu, glutamate; Glx, glutamate-glutamine; GSH, glutathione; HC, healthy controls; (a)MCI, (amnestic) mild cognitive impairment; mI, myo-Inositol; NAA, N-acetlyaspartate; PCC, posterior cingulate cortex; TR, repetition time; TE, echo time.

↑ increased, ↓ decreased and ↔ unchanged metabolite levels between AD and controls.

[a] significantly higher levels in AD compared to DLB.

TABLE 3 | Magnetic resonance spectroscopy studies in vascular dementia (studies reporting metabolite ratios).

Study	Parameters				Results					
	Field strength TR/TE (ms) technique	Sample	Area Voxel size (mm^3)	Cohort	NAA/ tCr	NAA/ mI	mI/ tCr	tCho/ tCr	Glx/ tCr	Others
Kantarci et al. (40)	NA2,000/30 Single-voxel	FTD (n=41),AD (n=121),DLB (n=20),VD (n=8),HC (n=206)	Midline PCC (20x20x20)	VD	↓	–	↔a	↔	–	–
Herminghaus et al. (41)	1.5 T1,500/20 Single-voxel	VD (n=15),AD (n=28), HC (n=15)	Midline frontal GM (8,000–12,600)	VD	↓b	–	↔	↑c	↔	–
			Midline parietal GM (8,000–12,600)		↓	–	↑	↑c	↑	–
			Left frontal WM (4,200–8,000)		↓	–	↑c	↑c	↔	–
			Left parietal WM (4,200–8,000)		↓	–	↑	↑c	↔	–
			Temporal gyrus (dominant hemisphere)		↓	–	↑	↔	↑	–
Waldman et al. (42)	1.0 T1,500/30 Single-voxel	VD (n=18), AD (n=20),Mixed dementia (n=6), HC (n=3)	Midline occipital lobe	VD	↔	–	↔b	↔	–	–

AD, Alzheimer's disease; tCho, total choline; tCr, total creatine; DLB, dementia with Lewy bodies; FTD, Frontotemporal dementia; Glu, glutamate; Glx, glutamate-glutamine; GM, gray matter; HC, healthy controls; mI, myo-Inositol; NAA, N-acetlyaspartate; PCC, posterior cingulate cortex; TR, repetition time; TE, echo time; VD, vascular dementia; WM, white matter.

↑ increased, ↓ decreased and ↔ unchanged metabolite concentrations between VD and controls.

[a]significantly lower ratios in VD compared to AD and FTD.

[b]significantly lower ratios in VD compared to AD.

[c]significantly higher ratios in VD compared to AD.

TABLE 4 | Magnetic resonance spectroscopy studies in vascular dementia (studies reporting absolute metabolite levels).

Study	Parameters					Results					
	Field strength TR/TE (ms) technique	Sample	Area Voxel size (mm^3)	Cohort	NAA	mI	tCho	tCr	Glx	Others
Shiino et al. (43)	1.5 T2,000/30 Single-voxel	VD (n=30),AD (n=99),HC (n=45)	Left hippocampus (NA)	VD	↓a	↓b	→	→	→	–
			Right hippocampus (NA)		↔a	↓b	↕	↓b	→	–
			Midline PCC (NA)		→	↓b	↕	→	↕	–
Watanabe et al. (44)	1.5 T2,000/30 Single-voxel	VD (n=13),AD (n=30),HC (n=26)	Right hippocampus (3,000)	VD	↓a	↔b	→	↕	–	–
			Left hippocampus (3,000)		↓a	↕	↕	↕	–	–
			Midline PCC (5,000)		↕	↔b	↕	↕	–	–
			Midline occipital lobe (6,000)		→	↔b	↕	↕	–	–
			Right anterior periventricular WM (4,000)		↓b	↓b	↓b	↓b	–	–
			Left anterior periventricular WM (4,000)		↓b	↓b	↓b	↓b	–	–
			Right posterior periventricular WM (4,000)		→	↓b	↓b	→	–	–
			Left posterior periventricular WM (4,000)		↓b	↓b	↓b	↓b	–	–
Schuff et al. (20)	1.5 T2,000/30 Multi-voxel	VD (n=13),AD (n=43),HC (n=52)	Frontal lobe (left+right) (7.8x7.8x15)	VD	↓b	–	↕	↕	–	–
			Parietal lobe (left+right) (7.8x7.8x15)		↓b	–	↕	↕	–	–
			Temporal lobe (left+right) (8.5x8.5x15)		↕	–	↕	↕	–	–
Capizzano et al. (45)	1.5 T1,800/135 Single-voxel+Multi-voxel	AD (n=18), Dementia with lacunes (n=11), MCI with lacunes (n=14), HC (n=20)	Frontal lobe (8x8x15)	Dementia + lacunes	→	–	↕	↕	–	–
			Parietal lobe (8x8x15)		→	–	↕	↕	–	–
			Hippocampus (8.75x8.75x15)		↕	–	↕	↕	–	–
			WM		→	–	↕	↕	–	–

AD, Alzheimer's disease; tCho, total choline; tCr, total creatine; Glx, glutamate-glutamine; GM, gray matter; HC, healthy controls; MCI, mild cognitive impairment; mI, myo-Inositol; NA, Not applicable; NAA, N-acetylaspartate; PCC, posterior cingulate cortex; TR, repetition time; TE, echo time; VD, vascular dementia; WM, white matter.

↑ increased, ↓ decreased and ↔ unchanged metabolite levels between VD and controls.

[a] *significantly higher levels in VD compared to AD.*

[b] *significantly lower levels in VD compared to AD.*

one study involving cognitively healthy elderly individuals (29). The PCC was investigated in all studies. Waragai and colleagues and Mitolo and colleagues found significant metabolite deviations in subjects who progressed to AD, but Zhang et al. and Fayed and colleagues observed no significant differences (except for a lowered Glu level in the latter study). However, in asymptomatic carriers of mutations associated with autosomal dominant AD (ADAD), evidence of early metabolic alterations was found, with decreased NAA and increased mI and tCho levels in the precuneus reported (37).

In summary, there is consistent data on AD associated metabolic deviations that occur predominantly in brain areas typically affected in AD (hippocampus, temporal, and parietal lobe) with evidence of early detectable abnormalities. Replications in larger samples and the investigation of metabolites, which are facilitated by improved MRI technology, are necessary.

Vascular Dementia

VD is the second most common form of dementia after AD and in addition to rare causes, subcortical ischemia (small vessel dementia) and cerebral infarcts (multi-infarct dementia) play the most important role in VD pathology. For both VD and AD, the presence of vascular risk factors is of relevance. There are patients for whom a clear classification is not possible or who suffer from mixed dementia. However, the classification is important for the treatment of patients, as the therapy regimes differ in both diseases [for review see O'Brien and Thomas (62)].

A total of seven MRS studies were identified in which patients with VD were recruited (see **Tables 3** and **4**). Among these studies, frontal and parietal lobes, hippocampus (four studies each) and PCC (three studies) were the most frequently examined. In all studies that examined these four brain regions, a reduction in the NAA/tCr ratio or NAA level was found (20, 40, 41, 43–45). For mI/tCr (or absolute mI level) and tCho/tCr ratios (or absolute tCho level), the results were inconsistent, with one study reporting increased levels in the frontal and parietal lobe (41), two studies reporting decreased levels in the hippocampus and in frontal and parietal white matter respectively (43, 44), and two studies reporting no differences in the frontal and parietal lobe (20, 45). Schiino et al. (43) discussed this fact, but failed to identify relevant differences in study design that could explain these different results. Interestingly, both Schiino et al. (43) and Watanabe et al. (44) report metabolite ratios as well as absolute metabolite levels, whereby the significant differences between VD patients and healthy controls almost completely disappear when using the ratio values. Since both studies obtained lowered tCr levels, this may indicate that tCr is not suitable as an internal reference (at least for VD). This could explain the discrepancies with the study by Herminghaus et al. (41), in which only ratios were reported. In addition, the white matter hyperintensity load within the voxels may have an influence, but in an early study no deviations of the metabolites tCho and mI between white matter hyperintensities and normal appearing white matter were found (20). In all MRS studies on VD, patients with AD were also included, with six of the seven studies showing significant

TABLE 5 | Magnetic resonance spectroscopy studies in dementia with Lewy bodies (studies reporting metabolite ratios).

Study	Parameters				Results					
	Field strength TR/TE (ms) technique	Sample	Area Voxel size (mm^3)	Cohort	NAA/ tCr	NAA/ ml	ml/ tCr	tCho/ tCr	Glx/ tCr	Others
Waragai et al. (29)	1.5 T2,000/25 Single-voxel	Baseline: HC (n=289)*	Midline PCC (20x20x20)	DLB	↔	↓a	↔	–	–	–
				PD	↔	↔a	↔	–	–	–
		7 years follow-up: AD (n=21), MCI (n=53), DLB (n=7), PD (n=8)		DLB	↓b	↓	↑	–	–	–
				PD	↔b	↔	↔	–	–	–
Su et al. (31)	3.0 T3,450/35 Multi-voxel	AD (n=35),DLB (n=25),HC (n=34)	PCC	DLB	↓	–	↓	↔	↓	–
			Thalamus		↓	–	↔	↓	↔	–
			Hippocampus		↔	–	↓	↔	↓	–
			Superior temporal cortex		↓c	–	↓	↓	↓	–
			Prefrontal cortex		↓	–	↔	↓	↔	–
			Occipital cortex		↔c	–	↑	↔c	↔	–
			Caudate		↓	–	↓	↓	↓	–
			Corpus callosum		↓	–	↔	↔	↔	–
Delli Pizzi et al. (17)	3.0 T2,000/39 Single-voxel	DLB (n=16), AD (n=16), HC (n=13)	Thalamus (left+right) (15x10x15)	DLB	↓	–	–	↑d	–	tCr/ H2O ↔
Xuan et al. (46)	1.5 T1,500/135 Single-voxel	DLB (n=8),HC (n=8)	Hippocampus (left+right)	DLB	↓	–	–	↔	–	–
Zhang et al. (35)	1.5 T2,000/30 Single-voxel	Baseline: MCI (n=57),Follow-up (after 18–32 months): DLB (n=10), AD (n=27), MCI (n=20)*	Midline frontal lobe (20x20x20)	DLB	↔	–	↔	↔	–	–
			Midline PCC (20x20x20)		↔e	–	↔	↔	–	–
			Midline occipital lobe (20x20x20)		↔	–	↔	↔	–	–
Graff-Radford et al. (47)	1.5 T2,000/30 Single-voxel	DLB (n=34), AD (n=35), HC (n=148)	Midline frontal lobe (20x20x20)	DLB	↔	–	↔	↔	–	–
			Midline PCC (20x20x20)		↔	–	↑	↑	–	–
			Midline occipital lobe (20x20x20)		↓	–	↔	↔	–	–
Kantarci et al. (40)	NA2,000/30 Single-voxel	FTD (n=41),AD (n=121),DLB (n=20),VD (n=8),HC (n=206)	Midline PCC (20x20x20)	DLB	↔f	–	↔g	↑	–	–
Molina et al. (48)	1.5 T1,700/35 Single-voxel	DLB (n=12), HC (n=11)	Left centrum semiovale (WM) (4,840)	DLB	↓	–	↔	↓	↓	–
			Midline parietal region (GM) (5,830)		↔	–	↔	↔	↔	–

AD, Alzheimer's disease; tCho, total choline; tCr, total creatine; DLB, dementia with Lewy bodies; FTD, Frontotemporal dementia; Glx, glutamate-glutamine; GM, gray matter; HC, healthy controls; MCI, mild cognitive impairment; ml, myo-Inositol; NA, Not applicable; NAA, N-acetlyaspartate; PCC, posterior cingulate cortex; PD, Parkinson's disease; TR, repetition time; TE, echo time; VD, vascular dementia; WM, white matter.

↑increased, ↓ decreased and ↔ unchanged metabolite concentrations between DLB and controls.

**Baseline differences were calculated on retrospective grouping according to clinical outcome.*

[a]significantly lower ratios in DLB compared to PD at baseline.

[b]significantly lower ratios in DLB compared to PD after 7 years.

[c]significantly higher ratios in DLB compared to AD [d] in the right thalamus.

[e]significantly lower ratios in MCI converted to AD compared to MCI converted to DLB.

[f]significantly lower ratios in AD and FTD compared to DLB.

[g]significantly lower ratios in DLB compared to FTD.

TABLE 6 | Magnetic resonance spectroscopy studies in dementia with Lewy bodies (studies reporting absolute metabolite levels).

Study	Parameters				Results					
	Field strength TR/TE (ms) technique	Sample	Area Voxel size (mm^3)	Cohort	NAA	mI	tCho	tCr	Glx	Others
Zhong et al. (39)	3.0 T2,000/35 Single-voxel	DLB(n=19), AD (n=21), HC (n=18)	PCC (20x20x20)	DLB	↓	↔	↔	↔	↓	Glu ↓
			Bilateral occipital lobe (20x20x20)		↓a	↔	↔	↓a	↓	Glu ↓a

AD, Alzheimer's disease; tCho, total choline; tCr, total creatine; DLB, dementia with Lewy bodies; Glu, glutamate; Glx, glutamate-glutamine; HC, healthy controls; mI, myo-Inositol; NAA, N-acetlyaspartate; PCC, posterior cingulate cortex; TR, repetition time; TE, echo time.

↑ increased, ↓ decreased and ↔ unchanged metabolite concentrations between AD and controls.

[a]*significantly lower levels in DLB compared to AD.*

TABLE 7 | Magnetic resonance spectroscopy studies in frontotemporal dementias (studies reporting metabolite ratios).

Study	Parameters				Results			
	Field strength TR/TE (ms) technique	Sample	Area Voxel size (mm^3)	Cohort	NAA/tCr	NAA/mI	mI/tCr	tCho/tCr
Chen et al. (49)	3.0 T2,000/30 Single-voxel	MAPT mutation carriers (n=19), HC (N=25)	Midline superior frontal gyrus (20x20x20)	Symptomatic (n=10)	↓	↓	↑	–
				Asymptomatic(n=9)	↓	↓	↔	–
Kantarci et al. (50)	3.0 T2,000/30 Single-voxel	MAPT mutation carriers (n=24), HC (N=24)	Midline PCC (20x20x20)	Symptomatic (n=10)	↓a	↓a	↑	–
				Asymptomatic(n=14)	↔a	↓a	↑	–
Coulthard et al. (51)	1.5 T2,000/30 Single-voxel	FTD (n=7),HC (n=11)	Midline frontal lobe (40x40x20)	FTD	↓	–	↑	–
			Left parietal lobe (40x30x20)		↔	–	↔	–
			Right temporal lobe (40x20x20)		↓	–	↔	–
Mihara et al. (52)	3.0 T6,000/25 Multi-voxel	FTD (n=6),PSP (n=3),CBD (n=1),AD (n=8),HC (n=14)	Midline ACC (20x20x20)	FTD	↓	–	↔	↔
			Midline PCC (20x20x20)		↓	–	↑	↔
			Perieto-occipital WM (left) (20x20x20)		↔	–	↔	↔
			Frontal WM (left) (20x20x20)		↓b	–	↑b	↑
Kantarci et al. (40)	NA2,000/30 Single-voxel	FTD (n=41),AD (n=121),DLB (n=20),VD (n=8),HC (n=206)	Midline PCC (20x20x20)	FTD	↓c	–	↑d	↑
Kizu et al. (53)	1.5 T2,000/135 Multi-voxel	FTD (n=6), AD (n=6),HC (n=5)	PCC (left+right) (18x18x10)	FTD	↓	–	–	↔

ACC, anterior cingulate cortex; AD, Alzheimer's disease; CBD, corticobasal degeneration; tCho, total choline; tCr, total creatine; DLB, dementia with Lewy bodies; FTD, Frontotemporal dementia; HC, healthy controls; mI, myo-Inositol; NA, Not applicable; NAA, N-acetlyaspartate; PCC, posterior cingulate cortex; PSP, progressive supranuclear palsy; TR, repetition time; TE, echo time; VD, vascular dementia; WM, white matter.

↑ increased, ↓ decreased and ↔ unchanged metabolite ratios between FTD and controls.

[a]*significantly lower ratios in symptomatic compared to presymptomatic mutation carriers.*

[b]*significant differences between FTD and AD.*

[c]*significantly lower ratios in FTD compared to DLB.*

TABLE 8 | Magnetic resonance spectroscopy studies in frontotemporal dementias (studies reporting absolute metabolite levels).

Study	Parameters				Results			
	Field strength TR/TE (ms) Technique	Sample	Area Voxel size (mm^3)	Cohort	NAA	mI	tCho	tCr
Chawla et al. (54)	3.0 T1,700/30 Multi-voxel	FTD (n=26), HC (n=10)	Dorsolateral PFC (left+right) (10x9.4x20) Motor cortex (left+right) (10x9.4x20) Parietal cortex (10x9.4x20)	FTD	↓ ↓ ↕	↑ ↕ ↕	↑ ↑ ↕	↓ ↕ ↕

tCho, total choline; tCr, total creatine; FTD, Frontotemporal dementia; HC, healthy controls; mI, myo-Inositol; NAA, N-acetylaspartate; PFC, prefrontal cortex; TR, repetition time; TE, echo time.
↑ increased, ↓ decreased and ↔ unchanged metabolite levels between FTD and controls.

differences between both disorders. Metabolic alterations (NAA, mI, tCho) from the control group were more pronounced in VD in the frontal and parietal lobes (in particular in white matter) and in AD in the hippocampus and PCC (20, 40–44).

In recent years, studies have been conducted in patients with vascular MCI (vMCI), the equivalent of aMCI in AD, which is considered the early form of cognitive impairment due to cerebrovascular disease. Reduced NAA/tCr ratios were reported in three studies, affecting the frontal white matter, PCC, and thalamus. Largely no differences were observed for other metabolites compared to the healthy controls (63–65), indicating early detectable deviations. One limitation is that in the study by Liu et al. (65) significant differences between vMCI and controls were only found when considering metabolite ratios, but not absolute metabolite levels. The other two studies did not report absolute metabolite levels, therefore further studies are needed.

Dementia With Lewy Bodies

DLB is a neurodegenerative disorder and, like Parkinson's disease (PD) and multiple system atrophy, belongs to α-synucleinopathies. The common feature of this heterogeneous group of disorders is the detection of Lewy bodies in various brain regions and the occurrence of parkinsonism, cognitive decline, and visual hallucinations [for review see Hansen et al. (66)]. However, AD-typical amyloid β plaques and tau pathology are also observed in many DLB patients (67–69). In contrast to AD, antipsychotic treatment with neuroleptics is contraindicated due to inducing extrapyramidal symptoms, which emphasizes the importance of early detection of DLB.

A total of nine MRS studies in which DLB patients were examined have been identified. Seven studies also examined patients with AD and one study included AD, FTD, and VD patients (see **Tables 5** and **6**). Overall, the results for DLB are inconsistent, which is evident when looking at the PCC. The PCC was investigated in six studies: Three studies obtained reduced NAA/tCr ratios and three studies found no difference between patients and healthy subjects (31, 35, 39, 40, 47, 54). Metabolic alterations in the occipital lobe were observed in three studies (31, 39, 47), while one study found no differences (35). This study included MCI patients and deviations may not yet be detectable due to the early stage of the disease. Other brain regions affected by metabolite alterations were the thalamus (17, 31) and the hippocampus (31, 46), whereas no differences were found for the frontal lobe in two studies (35, 47). An exception is the study by Su et al. (31), in which, in contrast to the other studies, lowered tCho/tCr and mI/tCr ratios were obtained in several brain regions (PCC, thalamus, hippocampus, temporal cortex, prefrontal cortex, basal ganglia). The authors discussed these contradictory results with possibly decreasing glial cell activation and inflammation (and thus decreasing metabolite levels) within these brain regions over the course of the disease. According to cognitive severity measured with the Mini Mental Status Examination (MMSE), however, DLB patients were more affected in other studies (Su et al.: 20.3/30 points; Delli Pizzi et al.: 17.9/30, Xuan et al.: 17.0/30 points), therefore this assumption is purely speculative and further studies are necessary. Technical

reasons are also conceivable, as the study by Su et al. was the only one using multi-voxel technology.

Significant differences between DLB and AD were detected in the occipital lobe with significantly lower NAA, tCr, and Glu levels in DLB patients in a study by Zhong et al. (39). Significant deviations of NAA/tCr and mI/tCr from AD in the occipital lobe were also found in another study (47), which additionally considered post-mortem autopsy confirmation. The authors explained this approach with the fact that DLB is often accompanied by AD-typical pathology. Interestingly, those DLB patients without histological evidence of AD pathology showed preserved occipital NAA/tCr ratios compared to healthy controls, while patients with mixed DLB/AD tended to have reduced NAA/tCr levels. Nevertheless, it remains questionable whether it is possible to distinguish between DLB and AD by using MRS, as the results are not conclusive for the two most frequently examined brain regions (PCC and occipital lobe) (17, 31, 39, 40).

Two studies used a longitudinal design. Waragai et al. (29) included 289 cognitive healthy controls and performed MRS at baseline and 7 years later, and Zhang et al. (35) performed MRS in 57 MCI patients at baseline and assessed clinical outcome 18–32 months later. In the first study, no differences in metabolites between DLB and AD, but between DLB and PD (at baseline lower NAA/mI ratio in DLB and after 7 years lower NAA/tCr ratio in DLB in the PCC), have been detected. In the second study, however, it was possible to distinguish MCI patients who converted to AD from those who converted to DLB (lower NAA/tCr ratio in the PCC of AD converters). Significant differences at baseline between individuals who have progressed to DLB and individuals who remained cognitively unaffected were only found in the study by Waragai et al. (reduced NAA/mI ratio in PCC). Therefore, it is doubtful whether early detection of DLB using MRS is possible. A limiting factor is that only a small proportion of the individuals examined have converted to dementia. Although the longitudinal approach is promising, much larger samples must be recruited.

Frontotemporal Dementia

Frontotemporal dementia (FTD) is a neurodegenerative disorder that is classified into different variants according to its predominant clinical symptoms: the behavioral subtype, primary progressive aphasia (semantic and nonfluent agrammatic variant) and FTD with motor neuron disease. Other diseases related to FTD are corticobasal degeneration (CBD) and progressive supranuclear palsy (PSP) [for review see Finger (2016) (70)]. Typically, FTD occurs earlier than other common dementias with the highest incidence rate between 45 and 64 years (71).

Although FTD is the second most common early-onset neurodegenerative dementia, only seven, mostly small sample size MRS studies have been identified in the literature search (see **Tables 7** and **8**).

The most consistent results were found in the frontal lobe and PCC, which were investigated in four studies each, and all showed decreased NAA/tCr (or NAA levels) and increased mI/tCr ratios (or mI levels) (40, 49–52, 54, 71). The same pattern of metabolic differences was found in the temporal lobe, motor cortex, and ACC, but these brain regions were only investigated in one study each (51, 52, 54). Three studies investigated the parietal lobe, where no metabolic differences in FTD patients were observed compared to healthy controls (51, 52, 54). Thus, metabolic alterations seem to occur particular in brain regions predominantly affected by FTD (frontal and temporal lobes).

More frequently than other common dementias, FTD shows a dominant inheritance pattern (10–23 % of the patients), with mutations in the *MAPT* gene (microtubule associated protein tau) being found in several affected families [for review see Gossye et al. (72)]. In two studies, asymptomatic and symptomatic *MAPT* mutation carriers were investigated, providing insights into early metabolic changes in the brains of affected individuals. Significant differences in metabolites for both symptomatic and asymptomatic mutation carriers compared to non-carriers were found in the frontal lobe (49) and the PCC (50), indicating early detectable alterations. In addition, three studies compared FTD with other dementias. While significant differences between FTD, DLB, and VD, but not between FTD and AD (40, 53), were shown in the PCC, another study found differences between FTD and AD in the frontal white matter (WM) (52). However, current data are too limited and samples from previous studies are too small to draw conclusions on the value of MRS in distinguishing FTD from other dementias or to detect it at an early stage.

DISCUSSION

Dementias are caused by neurodegenerative processes in the brain and lead to progressive cognitive decline. By far the most common form is AD, followed by VD, DLB, and FTD. Even if no causal treatments are available for these diseases, a reliable diagnosis as early as possible plays a major role in modulating the course of the disease through drug and non-drug therapies and enable patients to create a self-determined future. The establishment of validated biomarkers for AD and non-AD neurodegenerative disorders remains a major challenge (73).

MRS provides a non-invasive, widely available and cost-effective technique to investigate neurometabolites in brain tissue *in vivo*. However, the use of MRS technology in the field of neurodegenerative disorders has been limited primarily to research activities. Among MRS studies in dementia, by far the most were conducted in AD, the results of which were analyzed in a meta-analysis published in 2015 (26). The most robust results with a reduced NAA/tCr and increased mI/tCr and tCho/tCr ratios were obtained in the PCC. The results for the other brain areas analyzed (hippocampus, temporal and parietal lobes) were less clear and, only a consistent reduction in NAA/tCr ratios has been demonstrated.

For this review, 14 studies on AD were identified which have been published since the meta-analysis and largely confirmed the previous results (see **Tables 1** and **2**). Thus, metabolic alterations in AD seem to occur predominantly in those brain regions that are particularly affected by the disease. This is supported by some recent studies showing the frontal and occipital lobes apparently

less affected (35, 39). There is still controversy over the significance of reduced NAA levels. For example, a decreasing number of neurons in the affected tissues or a lowered neuronal energy status are being discussed (8).

There are considerably fewer MRS studies on other common dementias (in the PubMed search seven studies in VD, nine studies in DLB, and seven studies in FTD were identified, which have been published since 2000). Compared to AD, metabolic changes in VD do not seem to be restricted to certain brain regions (**Tables 3** and **4**), and many studies focus on the white matter, which appears to be particularly affected in VD (74). In DLB, metabolite deviations were reported in the occipital lobe, thalamus, and hippocampus (see **Tables 5** and **6**), but metabolic alterations were also found in the PCC. Besides metabolic alterations in the frontal and temporal lobes, the PCC was also affected in FTD (see **Tables 7** and **8**). Although significant metabolite differences between dementias were found in comparative MRS studies [e.g. metabolic alterations in the PCC were more pronounced in AD than in DLB (35, 40)], metabolites acquired in MRS are not dementia-specific and per se do not allow any conclusion on the underlying pathology. Topographic patterns of metabolite alterations across the brain may be helpful in distinguishing dementias, but this needs to be investigated systematically (e.g. by using MRSI technology), as some brain regions were underrepresented in previous MRS studies.

Besides the use of MRS to differentiate dementia, another interesting aspect is the detection of metabolic alterations in early disease stages. This is a particular challenge, as mild cognitive complaints caused by incipient dementia are difficult to distinguish from non-pathological ageing processes (4). Previous studies indicate that metabolic changes can be detected in preclinical (29, 37, 49) and MCI stages (27, 38). However, in order to assess the potential use of MRS for early detection, large-scale, preferably longitudinal studies are necessary.

Despite some consistent findings obtained in previous MRS studies in common dementias, there are numerous limitations restricting the validity of the results and hampering the transfer of MRS technology to clinical application. This will be addressed in the following. The individual studies differ, in part significantly, in terms of their acquisition parameters, which makes a direct comparison difficult. In most studies, single-voxel spectroscopy (SVS) was used, in which only signals from one selected brain region are obtained. Although this enables a more accurate quantification of metabolites, only a limited number of brain regions can be examined in order to keep the scan time reasonable for patients. As a consequence, the focus was on many different brain regions, and replications were lacking. Compared to SVS, magnetic resonance spectroscopic imaging (MRSI) has an advantage, because it allows the acquisition of numerous voxels simultaneously (23). In addition, the voxel size must have a certain volume to achieve a good quality signal to noise ratio. This, however, impairs the acquisition of signals from small anatomical structures such as the hippocampus, especially if it is atrophied (75). Partial volume effects are expected in many MRS studies in dementia, as often voxels were used for MRS acquisition, which included surrounding tissue and cerebral fluid in addition to target structures. The increased use of devices with higher magnetic field strengths (3 T and higher) can partially counteract this problem by enabling smaller voxel sizes. Another advantage is that 3 T scanners provide a better spectral resolution, which allows the quantification of further metabolites in the brain (76).

The problem has already been mentioned that the metabolites detectable with MRS are not disease specific and that alterations have been observed in all dementias. Furthermore, many studies report on metabolite ratios rather than absolute metabolite levels. As an internal reference, total Cr (consisting of phosphocreatine and creatine) is usually used, since it has been shown to be relatively stable in AD (17, 18) and with age (19). However, there are also studies that found fluctuations in tCr levels in dementia (44, 48, 77). In the case of fluctuating tCr levels, relative ratios may lead to artificially altered group differences, as in the study of Watanabe and colleagues (44), where a dissociation between absolute metabolite levels and ratios has occurred. As an alternative to tCr, the unsuppressed tissue water signal can be used as an internal reference as it is subject to few pathology associated fluctuations (78). Also the authors of the meta-analysis in AD recommend the preferred use of absolute metabolite levels (26).

A general problem of almost all MRS studies in dementia is the small sample size and the classification of patients, which is mostly based on clinical criteria. Only five studies used additional tests to increase diagnostic certainty: in the study by Waragai et al. (29), CSF biomarkers (Aβ40, Aβ42, and phospho-Tau) and ^{123}I-MIBG myocardial scintigraphy were used to confirm the clinical diagnosis in those participants who had progressed to MCI or dementia during the 7-year follow-up period. Murray and colleagues (36) performed post-mortem histopathological examinations to verify the clinical diagnosis of AD. And the presence of genetic origins was demonstrated in three further studies by the detection of disease-causing mutations [autosomal-dominant AD (37) and *MAPT* mutations (50, 63)]. The vast majority of studies did not use complementary biomarkers and the diagnosis relied exclusively on clinical criteria, which may have contributed to the heterogeneity of the study results. In order to make a reliable diagnosis, extensive and invasive diagnostic tests or post-mortem confirmation by autopsy are necessary, which would probably go beyond the scope of what is feasible for many research projects. This is a dilemma, because reliable diagnosis without valid biomarkers will continue to be a difficulty in these studies. Furthermore, effect sizes are often not reported and some studies do not provide group mean values, which also limits the ability to assess and compare between studies. And finally, correction for multiple statistical tests performed within a study is usually omitted, but this entails the risk of alpha error accumulation.

These numerous limitations make ^{1}H-MRS currently not suitable for diagnostics and classification of dementia in clinical routine. New technologies, such as MEGA-PRESS spectroscopy, which facilitate the quantification of metabolites (e.g. GABA and GSH) that cannot be differentiated with conventional methods (79, 80), high speed magnetic resonance spectroscopic imaging (25), and 3D magnetic resonance

spectroscopic imaging (81) may help to overcome the obstacles mentioned above. This requires large-scale, multi-center studies, which are conducted under standardized conditions (7). Longitudinal studies with a sufficiently long observation period are also necessary to assess early metabolite alterations and changes over time in patients with dementia.

CONCLUSIONS

Proton magnetic resonance spectroscopy (^{1}H-MRS) is a cost-effective, non-invasive and widely available technique for *in vivo* measurements of the biochemical milieu in brain tissue. MRS studies on dementia have been conducted in particular for AD, whereas studies on VD, DLB, and FTD are relatively rare. Alterations of several metabolic markers have been identified in all common dementias, which are already detectable in preclinical and early stages of the disease. The most consistent findings have been obtained for AD, where a decrease in NAA and an increase in mI and tCho levels in the posterior cingulate cortex were demonstrated in numerous studies and confirmed in a meta-analysis. Further brain regions and the other dementias have been less intensively researched and there are numerous inconsistencies in the results. In addition, the detected metabolic alterations are not disease specific. The heterogeneity of the studies conducted so far as well as methodological limitations lead to insufficient interpretation and comparability of the results. Large-scale, multi-center, cross-dementia MRS studies under standardized conditions and the use of new technologies are needed to overcome existing barriers in order to evaluate the potential benefits for dementia diagnosis and treatment.

AUTHOR CONTRIBUTIONS

All authors contributed to the article and approved the submitted version.

ACKNOWLEDGMENTS

The authors thank Bente Flier and Annette Pomberg for proofreading the manuscript. We acknowledge the financial support of the Open Access Publication Fund of the Martin-Luther-University Halle-Wittenberg.

REFERENCES

1. Prince M, Guerchet M, Prina M. *The Global Impact of Dementia 2013–2050*. Alzheimer's Disease International: London (2013). [cited 2019 Nov 18].
2. Cunningham EL, McGuinness B, Herron B, Passmore AP. Dementia. *Ulster Med J* (2015) 84(2):79–87.
3. Petersen RC. Mild cognitive impairment as a diagnostic entity. *J Intern Med* (2004) 256(3):183–94. doi: 10.1111/j.1365-2796.2004.01388.x
4. Petersen RC. Clinical practice. Mild cognitive impairment. *N Engl J Med* (2011) 364(23):2227–34. doi: 10.1056/NEJMcp0910237
5. Høilund-Carlsen PF, Barrio JR, Gjedde A, Werner TJ, Alavi A. Circular Inference in Dementia Diagnostics. *J Alzheimers Dis* (2018) 63(1):69–73. doi: 10.3233/JAD-180050
6. Ulmer S, Backens M, Ahlhelm FJ. Basic Principles and Clinical Applications of Magnetic Resonance Spectroscopy in Neuroradiology. *J Comput Assist Tomogr* (2016) 40(1):1–13. doi: 10.1097/RCT.0000000000000322
7. Oz G, Alger JR, Barker PB, Bartha R, Bizzi A, Boesch C, et al. Clinical proton MR spectroscopy in central nervous system disorders. *Radiology* (2014) 270 (3):658–79. doi: 10.1148/radiol.13130531
8. Moffett JR, Ross B, Arun P, Madhavarao CN. Namboodiri AMA. N-Acetylaspartate in the CNS: from neurodiagnostics to neurobiology. *Prog Neurobiol* (2007) 81(2):89–131. doi: 10.1016/j.pneurobio.2006.12.003
9. Francis JS, Wojtas I, Markov V, Gray SJ, McCown TJ, Samulski RJ, et al. N-acetylaspartate Supports the Energetic Demands of Developmental Myelination via Oligodendroglial Aspartoacylase. *Neurobiol Dis* (2016) 96:323–34. doi: 10.1016/j.nbd.2016.10.001
10. Ariyannur PS, Moffett JR, Manickam P, Pattabiraman N, Arun P, Nitta A, et al. Methamphetamine-induced neuronal protein NAT8L is the NAA biosynthetic enzyme: implications for specialized acetyl coenzyme A metabolism in the CNS. *Brain Res* (2010) 1335:1–13. doi: 10.1016/j.brainres.2010.04.008
11. Nitta A, Noike H, Sumi K, Miyanishi H, Tanaka T, Takaoka K, et al. *Nicotinic Acetylcholine Receptor Signaling in Neuroprotection: Shati/Nat8l and N-acetylaspartate (NAA) Have Important Roles in Regulating Nicotinic Acetylcholine Receptors in Neuronal and Psychiatric Diseases in Animal Models and Humans*. Singapore: Springer (2018). doi: 10.1007/978-981-10-8488-1_6
12. Klein J. Membrane breakdown in acute and chronic neurodegeneration: focus on choline-containing phospholipids. *J Neural Transm (Vienna)* (2000) 107 (8-9):1027–63. doi: 10.1007/s007020070051
13. Walter A, Korth U, Hilgert M, Hartmann J, Weichel O, Hilgert M, et al. Glycerophosphocholine is elevated in cerebrospinal fluid of Alzheimer patients. *Neurobiol Aging* (2004) 25(10):1299–303. doi: 10.1016/j.neurobiolaging.2004.02.016
14. Granger MW, Liu H, Fowler CF, Blanchard AP, Taylor MW, Sherman SPM, et al. Distinct disruptions in Land's cycle remodeling of glycerophosphocholines in murine cortex mark symptomatic onset and progression in two Alzheimer's disease mouse models. *J Neurochem* (2019) 149(4):499–517. doi: 10.1111/jnc.14560
15. Bizzarri M, Fuso A, Dinicola S, Cucina A, Bevilacqua A. Pharmacodynamics and pharmacokinetics of inositol(s) in health and disease. *Expert Opin Drug Metab Toxicol* (2016) 12(10):1181–96. doi: 10.1080/17425255.2016.1206887
16. Marques EP, Wyse ATS. Creatine as a Neuroprotector: an Actor that Can Play Many Parts. *Neurotox Res* (2019) 36(2):411–23. doi: 10.1007/s12640-019-00053-7
17. Delli Pizzi S, Franciotti R, Taylor J-P, Thomas A, Tartaro A, Onofrj M, et al. Thalamic Involvement in Fluctuating Cognition in Dementia with Lewy Bodies: Magnetic Resonance Evidences. *Cereb Cortex* (2015) 25(10):3682–9. doi: 10.1093/cercor/bhu220
18. Kantarci K. Proton MRS in mild cognitive impairment. *J Magn Reson Imaging* (2013) 37(4):770–7. doi: 10.1002/jmri.23800
19. Christiansen P, Toft P, Larsson HB, Stubgaard M, Henriksen O. The concentration of N-acetyl aspartate, creatine + phosphocreatine, and choline in different parts of the brain in adulthood and senium. *Magn Reson Imaging* (1993) 11(6):799–806. doi: 10.1016/0730-725x(93)90197-l
20. Schuff N, Capizzano AA, Du AT, Amend DL, O'Neill J, Norman D, et al. Different patterns of N-acetylaspartate loss in subcortical ischemic vascular dementia and AD. *Neurology* (2003) 61(3):358–64. doi: 10.1212/01.WNL.0000078942.63360.22
21. Barker PB, Hearshen DO, Boska MD. Single-voxel proton MRS of the human brain at 1.5T and 3.0T. *Magn Reson Med* (2001) 45(5):765–9. doi: 10.1002/mrm.1104
22. Sonnewald U, Schousboe A. Introduction to the Glutamate-Glutamine Cycle. *Adv Neurobiol* (2016) 13:1–7. doi: 10.1007/978-3-319-45096-4_1

23. Bertholdo D, Watcharakorn A, Castillo M. Brain proton magnetic resonance spectroscopy: introduction and overview. *Neuroimaging Clin N Am* (2013) 23 (3):359–80. doi: 10.1016/j.nic.2012.10.002
24. Hajek M, Dezortova M. Introduction to clinical in vivo MR spectroscopy. *Eur J Radiol* (2008) 67(2):185–93. doi: 10.1016/j.ejrad.2008.03.002
25. Posse S, Otazo R, Dager SR, Alger J. MR spectroscopic imaging: principles and recent advances. *J Magn Reson Imaging* (2013) 37(6):1301–25. doi: 10.1002/jmri.23945
26. Wang H, Tan L, Wang H-F, Liu Y, Yin R-H, Wang W-Y, et al. Magnetic Resonance Spectroscopy in Alzheimer's Disease: Systematic Review and Meta-Analysis. *J Alzheimers Dis* (2015) 46(4):1049–70. doi: 10.3233/JAD-143225
27. Mitolo M, Stanzani-Maserati M, Capellari S, Testa C, Rucci P, Poda R, et al. Predicting conversion from mild cognitive impairment to Alzheimer's disease using brain 1H-MRS and volumetric changes: A two- year retrospective follow-up study. *NeuroImage Clin* (2019) 23:101843. doi: 10.1016/j.nicl.2019.101843
28. Huang D, Liu D, Yin J, Qian T, Shrestha S, Ni H. Glutamate-glutamine and GABA in brain of normal aged and patients with cognitive impairment. *Eur Radiol* (2017) 27(7):2698–705. doi: 10.1007/s00330-016-4669-8
29. Waragai M, Moriya M, Nojo T. Decreased N-Acetyl Aspartate/Myo-Inositol Ratio in the Posterior Cingulate Cortex Shown by Magnetic Resonance Spectroscopy May Be One of the Risk Markers of Preclinical Alzheimer's Disease: A 7-Year Follow-Up Study. *J Alzheimers Dis* (2017) 60(4):1411–27. doi: 10.3233/JAD-170450
30. Fayed N, Modrego PJ, García-Martí G, Sanz-Requena R, Marti-Bonmatí L. Magnetic resonance spectroscopy and brain volumetry in mild cognitive impairment. A prospective study. *Magn Reson Imaging* (2017) 38:27–32. doi: 10.1016/j.mri.2016.12.010
31. Su L, Blamire AM, Watson R, He J, Hayes L, O'Brien JT. Whole-brain patterns of 1H-magnetic resonance spectroscopy imaging in Alzheimer's disease and dementia with Lewy bodies. *Transl Psychiatry* (2016) 6(8):e877–. doi: 10.1038/tp.2016.140
32. Guo Z, Liu X, Hou H, Wei F, Chen X, Shen Y, et al. (1)H-MRS asymmetry changes in the anterior and posterior cingulate gyrus in patients with mild cognitive impairment and mild Alzheimer's disease. *Compr Psychiatry* (2016) 69:179–85. doi: 10.1016/j.comppsych.2016.06.001
33. Mandal PK, Saharan S, Tripathi M, Murari G. Brain glutathione levels–a novel biomarker for mild cognitive impairment and Alzheimer's disease. *Biol Psychiatry* (2015) 78(10):702–10. doi: 10.1016/j.biopsych.2015.04.005
34. Bai X, Edden RAE, Gao F, Wang G, Wu L, Zhao B, et al. Decreased γ-aminobutyric acid levels in the parietal region of patients with Alzheimer's disease. *J Magn Reson Imaging* (2015) 41(5):1326–31. doi: 10.1002/jmri.24665
35. Zhang B, Ferman TJ, Boeve BF, Smith GE, Maroney-Smith M, Spychalla AJ, et al. MRS in mild cognitive impairment: early differentiation of dementia with Lewy bodies and Alzheimer's disease. *J Neuroimaging* (2015) 25(2):269–74. doi: 10.1111/jon.12138
36. Murray ME, Przybelski SA, Lesnick TG, Liesinger AM, Spychalla A, Zhang B, et al. Early Alzheimer's disease neuropathology detected by proton MR spectroscopy. *J Neurosci* (2014) 34(49):16247–55. doi: 10.1523/JNEUROSCI.2027-14.2014
37. Joe E, Medina LD, Ringman JM, O'Neill J. 1H MRS spectroscopy in preclinical autosomal dominant Alzheimer disease. *Brain Imaging Behav* (2019) 13 (4):925–32. doi: 10.1007/s11682-018-9913-1
38. Glodzik L, Sollberger M, Gass A, Gokhale A, Rusinek H, Babb JS, et al. Global N-acetylaspartate in normal subjects, mild cognitive impairment and Alzheimer's disease patients. *J Alzheimers Dis* (2015) 43(3):939–47. doi: 10.3233/JAD-140609
39. Zhong X, Shi H, Shen Z, Hou LE, Luo X, Chen X, et al. 1H-proton magnetic resonance spectroscopy differentiates dementia with Lewy bodies from Alzheimer's disease. *J Alzheimers Dis* (2014) 40(4):953–66. doi: 10.3233/JAD-131517
40. Kantarci K, Petersen RC, Boeve BF, Knopman DS, Tang-Wai DF, O'Brien PC, et al. 1H MR spectroscopy in common dementias. *Neurology* (2004) 63 (8):1393–8. doi: 10.1212/01.wnl.0000141849.21256.ac
41. Herminghaus S, Frölich L, Gorriz C, Pilatus U, Dierks T, Wittsack H-J, et al. Brain metabolism in Alzheimer disease and vascular dementia assessed by in vivo proton magnetic resonance spectroscopy. *Psychiatry Res: Neuroimaging* (2003) 123(3):183–90. doi: 10.1016/S0925-4927(03)00071-4
42. Waldman ADB, Rai GS, McConnell JR, Chaudry M, Grant D. Clinical brain proton magnetic resonance spectroscopy for management of Alzheimer's and sub-cortical ischemic vascular dementia in older people. *Arch Gerontol Geriatr* (2002) 35(2):137–42. doi: 10.1016/S0167-4943(02)00014-6
43. Shiino A, Watanabe T, Shirakashi Y, Kotani E, Yoshimura M, Morikawa S, et al. The profile of hippocampal metabolites differs between Alzheimer's disease and subcortical ischemic vascular dementia, as measured by proton magnetic resonance spectroscopy. *J Cereb Blood Flow Metab* (2012) 32 (5):805–15. doi: 10.1038/jcbfm.2012.9
44. Watanabe T, Shiino A, Akiguchi I. Absolute quantification in proton magnetic resonance spectroscopy is superior to relative ratio to discriminate Alzheimer's disease from Binswanger's disease. *Dement Geriatr Cognit Disord* (2008) 26(1):89–100. doi: 10.1159/000144044
45. Capizzano AA, Schuff N, Amend DL, Tanabe JL, Norman D, Maudsley AA, et al. Subcortical Ischemic Vascular Dementia: Assessment with Quantitative MR Imaging and 1H MR Spectroscopy. *AJNR Am J Neuroradiol* (2000) 21 (4):621–30.
46. Xuan X, Ding M, Gong X. Proton magnetic resonance spectroscopy detects a relative decrease of N-acetylaspartate in the hippocampus of patients with dementia with Lewy bodies. *J Neuroimaging* (2008) 18(2):137–41. doi: 10.1111/j.1552-6569.2007.00203.x
47. Graff-Radford J, Boeve BF, Murray ME, Ferman TJ, Tosakulwong N, Lesnick TG, et al. Regional proton magnetic resonance spectroscopy patterns in dementia with Lewy bodies. *Neurobiol Aging* (2014) 35(6):1483–90. doi: 10.1016/j.neurobiolaging.2014.01.001
48. Molina JA, García-Segura JM, Benito-León J, Gómez-Escalonilla C, del Ser T, Martínez V, et al. Proton magnetic resonance spectroscopy in dementia with Lewy bodies. *Eur Neurol* (2002) 48(3):158–63. doi: 10.1159/000065520
49. Chen Q, Boeve BF, Tosakulwong N, Lesnick T, Brushaber D, Dheel C, et al. Frontal lobe 1H MR spectroscopy in asymptomatic and symptomatic MAPT mutation carriers. *Neurology* (2019) 93(8):e758–65. doi: 10.1212/WNL.0000000000007961
50. Kantarci K, Boeve BF, Wszolek ZK, Rademakers R, Whitwell JL, Baker MC, et al. MRS in presymptomatic MAPT mutation carriers: a potential biomarker for tau-mediated pathology. *Neurology* (2010) 75(9):771–8. doi: 10.1212/WNL.0b013e3181f073c7
51. Coulthard E, Firbank M, English P, Welch J, Birchall D, O'Brien J, et al. Proton magnetic resonance spectroscopy in frontotemporal dementia. *J Neurol* (2006) 253(7):861–8. doi: 10.1007/s00415-006-0045-y
52. Mihara M, Hattori N, Abe K, Sakoda S, Sawada T. Magnetic resonance spectroscopic study of Alzheimer's disease and frontotemporal dementia/Pick complex. *Neuroreport* (2006) 17(4):413–6. doi: 10.1097/01.wnr.0000203353.52622.05
53. Kizu O, Yamada K, Ito H, Nishimura T. Posterior cingulate metabolic changes in frontotemporal lobar degeneration detected by magnetic resonance spectroscopy. *Neuroradiology* (2004) 46(4):277–81. doi: 10.1007/s00234-004-1167-5
54. Chawla S, Wang S, Moore P, Woo JH, Elman L, McCluskey LF, et al. Quantitative proton magnetic resonance spectroscopy detects abnormalities in dorsolateral prefrontal cortex and motor cortex of patients with frontotemporal lobar degeneration. *J Neurol* (2010) 257(1):114–21. doi: 10.1007/s00415-009-5283-3
55. Ballard C, Gauthier S, Corbett A, Brayne C, Aarsland D, Jones E. Alzheimer's disease. *Lancet* (2011) 377(9770):1019–31. doi: 10.1016/S0140-6736(10)61349-9
56. Hane FT, Robinson M, Lee BY, Bai O, Leonenko Z, Albert MS. Recent Progress in Alzheimer's Disease Research, Part 3: Diagnosis and Treatment. *J Alzheimers Dis* (2017) 57(3):645–65. doi: 10.3233/JAD-160907
57. Schneider LS, Mangialasche F, Andreasen N, Feldman H, Giacobini E, Jones R, et al. Clinical trials and late-stage drug development for Alzheimer's disease: an appraisal from 1984 to 2014. *J Intern Med* (2014) 275(3):251–83. doi: 10.1111/joim.12191
58. Jack CR, Bennett DA, Blennow K, Carrillo MC, Dunn B, Haeberlein SB, et al. NIA-AA Research Framework: Toward a biological definition of Alzheimer's disease. *Alzheimers Dement* (2018) 14(4):535–62. doi: 10.1016/j.jalz.2018.02.018

59. Zhu X, Schuff N, Kornak J, Soher B, Yaffe K, Kramer JH, et al. Effects of Alzheimer disease on fronto-parietal brain N-acetyl aspartate and myo-inositol using magnetic resonance spectroscopic imaging. *Alzheimer Dis Assoc Disord* (2006) 20(2):77–85. doi: 10.1097/01.wad.0000213809.12553.fc
60. Rae CD, Williams SR. Glutathione in the human brain: Review of its roles and measurement by magnetic resonance spectroscopy. *Anal Biochem* (2017) 529:127–43. doi: 10.1016/j.ab.2016.12.022
61. Chiang GC, Mao X, Kang G, Chang E, Pandya S, Vallabhajosula S, et al. Relationships among Cortical Glutathione Levels, Brain Amyloidosis, and Memory in Healthy Older Adults Investigated In Vivo with 1H-MRS and Pittsburgh Compound-B PET. *AJNR Am J Neuroradiol* (2017) 38(6):1130–7. doi: 10.3174/ajnr.A5143
62. O'Brien JT, Thomas A. Vascular dementia. *Lancet* (2015) 386(10004):1698–706. doi: 10.1016/S0140-6736(15)00463-8
63. Chen S-Q, Cai Q, Shen Y-Y, Xu C-X, Zhou H, Zhao Z. Hydrogen Proton Magnetic Resonance Spectroscopy in Multidomain Amnestic Mild Cognitive Impairment and Vascular Cognitive Impairment Without Dementia. *Am J Alzheimers Dis Other Demen* (2016) 31(5):422–9. doi: 10.1177/1533317515628052
64. Zhu X, Cao L, Hu X, Dong Y, Wang H, Liu F, et al. Brain metabolism assessed via proton magnetic resonance spectroscopy in patients with amnestic or vascular mild cognitive impairment. *Clin Neurol Neurosurg* (2015) 130:80–5. doi: 10.1016/j.clineuro.2014.12.005
65. Liu Y-Y, Yang Z-X, Shen Z-W, Xiao Y-Y, Cheng X-F, Chen W, et al. Magnetic Resonance Spectroscopy Study of Amnestic Mild Cognitive Impairment and Vascular Cognitive Impairment With No Dementia. *Am J Alzheimers Dis Other Demen* (2014) 29(5):474–81. doi: 10.1177/1533317513495106
66. Hansen D, Ling H, Lashley T, Holton JL, Warner TT. Review: Clinical, neuropathological and genetic features of Lewy body dementias. *Neuropathol Appl Neurobiol* (2019) 45(7):635–54. doi: 10.1111/nan.12554
67. Jellinger KA, Attems J. Prevalence and impact of vascular and Alzheimer pathologies in Lewy body disease. *Acta Neuropathol* (2008) 115(4):427–36. doi: 10.1007/s00401-008-0347-5
68. Gomperts SN, Rentz DM, Moran E, Becker JA, Locascio JJ, Klunk WE, et al. Imaging amyloid deposition in Lewy body diseases. *Neurology* (2008) 71 (12):903–10. doi: 10.1212/01.wnl.0000326146.60732.d6
69. Irwin DJ, Grossman M, Weintraub D, Hurtig HI, Duda JE, Xie SX, et al. Neuropathological and genetic correlates of survival and dementia onset in synucleinopathies: a retrospective analysis. *Lancet Neurol* (2017) 16(1):55–65. doi: 10.1016/S1474-4422(16)30291-5
70. Finger EC. Frontotemporal Dementias. *Continuum (Minneap Minn)* (2016) 22(2 Dementia):464–89. doi: 10.1212/CON.0000000000000300
71. Knopman DS, Roberts RO. Estimating the number of persons with frontotemporal lobar degeneration in the US population. *J Mol Neurosci* (2011) 45(3):330–5. doi: 10.1007/s12031-011-9538-y
72. Gossye H, van Broeckhoven C, Engelborghs S. The Use of Biomarkers and Genetic Screening to Diagnose Frontotemporal Dementia: Evidence and Clinical Implications. *Front Neurosci* (2019) 13:757. doi: 10.3389/fnins.2019.00757
73. Ehrenberg AJ, Khatun A, Coomans E, Betts MJ, Capraro F, Thijssen EH, et al. Relevance of biomarkers across different neurodegenerative. *Alzheimers Res Ther* (2020) 12(1):56. doi: 10.1186/s13195-020-00601-w
74. Kalaria RN. The pathology and pathophysiology of vascular dementia. *Neuropharmacology* (2018) 134(Pt B):226–39. doi: 10.1016/j.neuropharm.2017.12.030
75. Mato Abad V, Quirós A, García-Álvarez R, Loureiro JP, Alvarez-Linera J, Frank A, et al. The partial volume effect in the quantification of 1H magnetic resonance spectroscopy in Alzheimer's disease and aging. *J Alzheimers Dis* (2014) 42(3):801–11. doi: 10.3233/JAD-140582
76. Jissendi Tchofo P, Balériaux D. Brain (1)H-MR spectroscopy in clinical neuroimaging at 3T. *J Neuroradiol* (2009) 36(1):24–40. doi: 10.1016/j.neurad.2008.04.001
77. Schuff N, Ezekiel F, Gamst AC, Amend DL, Capizzano AA, Maudsley AA, et al. Region and tissue differences of metabolites in normally aged brain using multislice 1H magnetic resonance spectroscopic imaging. *Magn Reson Med* (2001) 45(5):899–907. doi: 10.1002/mrm.1119
78. Barker PB, Bonekamp D, Riedy G, Smith M. Quantitation of NAA in the brain by magnetic resonance spectroscopy. *Adv Exp Med Biol* (2006) 576:183–97; discussion 361–3. doi: 10.1007/0-387-30172-0_13
79. Mullins PG, McGonigle DJ, O'Gorman RL, Puts NAJ, Vidyasagar R, Evans CJ, et al. Current practice in the use of MEGA-PRESS spectroscopy for the detection of GABA. *Neuroimage* (2014) 86:43–52. doi: 10.1016/j.neuroimage.2012.12.004
80. Sanaei Nezhad F, Anton A, Parkes LM, Deakin B, Williams SR. Quantification of glutathione in the human brain by MR spectroscopy at 3 Tesla: Comparison of PRESS and MEGA-PRESS. *Magn Reson Med* (2016) 78(4):1257–66. doi: 10.1002/mrm.26532
81. Bogner W, Hess AT, Gagoski B, Tisdall MD, van der Kouwe AJW, Trattnig S, et al. Real-time motion- and B0-correction for LASER-localized spiral-accelerated 3D-MRSI of the brain at 3T. *Neuroimage* (2014) 88:22–31. doi: 10.1016/j.neuroimage.2013.09.034

Conflict of Interest: The authors declare that the research was conducted in the absence of any commercial or financial relationships that could be construed as a potential conflict of interest.

frontiers in Psychiatry

ORIGINAL RESEARCH
published: 13 August 2020
doi: 10.3389/fpsyt.2020.00793

Regional Cerebral Associations Between Psychometric Tests and Imaging Biomarkers in Alzheimer's Disease

Dennis M. Hedderich[1,2], René Drost[3], Oliver Goldhardt[3], Marion Ortner[3], Felix Müller-Sarnowski[3], Janine Diehl-Schmid[3], Claus Zimmer[1], Hans Förstl[3], Igor Yakushev[2,4], Thomas Jahn[3] and Timo Grimmer[3]*

[1] Department of Neuroradiology, Klinikum rechts der Isar, School of Medicine, Technical University of Munich, Munich, Germany, [2] TUM-NIC Neuroimaging Center, Klinikum rechts der Isar, School of Medicine, Technical University of Munich, Munich, Germany, [3] Department of Psychiatry and Psychotherapy, Klinikum rechts der Isar, School of Medicine, Technical University of Munich, Munich, Germany, [4] Department of Nuclear Medicine, Klinikum rechts der Isar, School of Medicine, Technical University of Munich, Munich, Germany

OPEN ACCESS

Edited by:
Sven Haller,
Rive Droite SA, Switzerland

Reviewed by:
Stephen F. Carter,
University of Cambridge,
United Kingdom
Paul Gerson Unschuld,
University of Zurich, Switzerland

***Correspondence:**
Dennis M. Hedderich
dennis.hedderich@tum.de

Specialty section:
This article was submitted to Neuroimaging and Stimulation, a section of the journal Frontiers in Psychiatry

Received: 14 January 2020
Accepted: 23 July 2020
Published: 13 August 2020

Citation:
Hedderich DM, Drost R, Goldhardt O, Ortner M, Müller-Sarnowski F, Diehl-Schmid J, Zimmer C, Förstl H, Yakushev I, Jahn T and Grimmer T (2020) Regional Cerebral Associations Between Psychometric Tests and Imaging Biomarkers in Alzheimer's Disease. Front. Psychiatry 11:793. doi: 10.3389/fpsyt.2020.00793

Recently, imaging biomarkers have gained importance for the characterization of patients with Alzheimer's disease; however, the relationship between regional biomarker expression and cognitive function remains unclear. In our study, we investigated associations between scores on CERAD neuropsychological assessment battery (CERAD-NAB) subtests with regional glucose metabolism, cortical thickness and amyloid deposition in patients with early Alzheimer's disease (AD) using [18F]-fluorodeoxyglucose (FDG), structural MRI, and 11C-Pittsburgh Compound B (PiB) positron emission tomography (PET), respectively. A total of 76 patients (mean age 68.4 ± 8.5 years, 57.9% male) with early AD (median global clinical dementia rating (CDR) score = 0.5, range: 0.5–2.0) were studied. Associations were investigated by correlation and multiple regression analyses. Scores on cognitive subtests were most closely predicted by regional glucose metabolism with explained variance up to a corrected R^2 of 0.518, followed by cortical thickness and amyloid deposition. Prediction of cognitive subtest performance was increased up to a corrected R^2 of 0.622 for Word List—Delayed Recall, when biomarker information from multiple regions and multiple modalities were included. For verbal, visuoconstructive and mnestic domains the closest associations with FDG-PET imaging were found in the left lateral temporal lobe, right parietal lobe, and posterior cingulate cortex, respectively. Decreased cortical thickness in parietal regions was most predictive of impaired subtest performance. Remarkably, cerebral amyloid deposition significantly predicted cognitive function in about half of the subtests but with smaller extent of variance explained (corrected $R^2 \leq 0.220$). We conclude that brain metabolism and atrophy affect cognitive performance in a regionally distinct way.

Significant predictions of cognitive function by PiB-PET in half of CERAD-NAB subtests suggest functional relevance even in symptomatic patients with AD, challenging the concept of plateauing cortical amyloid deposition early in the disease course. Our results underscore the complex spatial relationship between different imaging biomarkers.

Keywords: Alzheimer's disease, magnetic resonance imaging, positron-emission-tomography, biomarkers, cognitive function

INTRODUCTION

Alzheimer's disease (AD) is the most common cause for dementia and its prevalence continues to rise in ageing societies (1). Histologically, AD is characterized by pathological β-amyloid plaques and neurofibrillary tau deposits (2–4). *In vivo* characterization of corresponding imaging biomarkers have been strengthened in a currently published research framework (5).

Another hallmark of AD is decline in different cognitive domains, which is typically assessed by standardized neuropsychological testing (6). One of the most widely used procedures is the neuropsychological assessment battery (NAB) of the Consortium to Establish a Registry for Alzheimer's Disease (CERAD) (7). This neuropsychological assessment covers both general cognitive ability—as determined by the short tests incorporated in the Mini-Mental State examination (MMSE)—and certain cognitive domains such as verbal and non-verbal episodic memory, visuoconstructive capacities, semantic fluency, and executive functions (6, 8).

Imaging techniques are able to provide valuable biomarkers for diagnosis and staging of AD. These are localized or generalized cortical amyloid deposition on Pittsburgh Compound B positron emission tomography (PiB-PET), characteristic glucose hypometabolism on [18F]-fluorodeoxyglucose-PET or cortical thinning derived from magnetic resonance imaging (MRI) (5). In previous studies, the associations between single biomarkers and measures of cognitive decline have been investigated in patients across the spectrum of AD either globally or locally (9–11). Since imaging biomarkers represent distinct aspects of AD and evolve differently during the course of disease, it makes sense to study the three imaging biomarkers amyloid deposition, glucose metabolism, and cortical thickness together (12). However, the relationship between these biomarkers and cognitive function in a single cohort of early AD patients remains unknown.

The present study aims to fill this knowledge gap by examining the regional associations of these three cerebral imaging biomarkers with age-adjusted cognitive function in the same, well-characterized, and relatively large cohort of early AD patients, i.e. patients with prodromal and mild stages of AD (13), using a three-step approach: First, correlation analyses were performed in order to get an overview of the relationship between cortical biomarkers and cognitive function. In a second step, we aimed at identifying the single most predictive cortical brain region for each cognitive subtest performance. Third, we examined which set of cortical brain regions led to the highest predictive power regarding different aspects of cognitive function for the three imaging biomarkers both separately and together. We hypothesized that associations would be closest for glucose metabolism and loosest for amyloid deposition. Furthermore, we hypothesized an increase in predictive power for regression models with biomarker information from multiple ROIs and multiple modalities.

MATERIALS AND METHODS

Participants

All participants were referred to the Center for Cognitive Disorders (Department of Psychiatry and Psychotherapy, Klinikum rechts der Isar, Technical University of Munich) for the evaluation of a cognitive disorder and a possibly underlying neurodegenerative disease. Inclusion criteria were: Fulfillment of National Institute on Aging-Alzheimer's Association (NIA-AA) criteria for probable Alzheimer's disease dementia (14), very mild to moderate clinical dementia severity, and characteristic findings on FDG-PET (hypometabolism of the temporoparietal junction and the posterior cingulate cortex with relative sparing of the primary somatosensory and somatomotor cortices) (15). Exclusion criteria were: (1) fulfillment of diagnostic criteria for dementia with proven underlying non-AD pathology (e.g. Normal Pressure Hydrocephalus, presence of vascular dementia according to the NINDS-AIREN criteria) (16), (2) pathological findings on MRI such as advanced leukoencephalopathy, strategic infarctions, intracranial aneurysms, or arteriovenous malformations, or (3) possible alternative causes for neurocognitive impairment such as antidepressant or antipsychotic medication, derangement of blood electrolytes, or drug abuse. Amyloid imaging by [^{11}C] PiB PET was used as a research add-on.

All patients provided written informed consent regarding the scientific evaluation of their data. The study protocol was approved by the German radiation protection authorities and the ethics committee of the School of Medicine of the Technical University of Munich, Munich, Germany (reference number 1285/05).

Clinical and Cognitive Assessment

All tests were performed by trained experts, neuropsychological testing and brain MRI were performed within 60 days for every participant. Clinical Dementia Rating scale (CDR) global score served to clinically grade the severity of dementia (0 = no impairment, 0.5 = very mild dementia, 1 = mild dementia, 2 = moderate dementia, 3 = severe dementia) and the sum of subscores (CDR SOB) indicating the grade of impairment in six categories (memory, orientation, judgment and problem solving, community

affairs, home and hobbies, personal care) were calculated (8, 17). Mini-Mental State examination (MMSE) was used to capture global cognitive deficits (18). All participants underwent neuropsychological testing using the full neuropsychological assessment battery by the Consortium to Establish a Registry for Alzheimer's Disease (CERAD-NAB) (7). Raw values of CERAD-NAB subtests of study participants were transformed to z-scores adjusting for age, sex, and years of education using CERAD-Plus 1.0 for Microsoft Excel (available at: https://www.memoryclinic.ch/de/main-navigation/neuropsychologen/cerad-plus/auswertungprogramme/cerad-plus-10-excel/). Normative values within this software package were derived from a reference cohort consisting of 617 healthy control participants between 53 and 92 years of age as described by Berres et al. (19).

MRI Data Acquisition and Analysis

All patients underwent structural magnetic resonance imaging on a 1.5 Tesla Siemens Magnetom Symphony platform (Siemens, Erlangen, Germany) at the time of initial presentation in order to exclude major structural abnormalities and to evaluate atrophy. The imaging protocol comprised a three-dimensional, T1-weighted, gradient echo sequence that was used for further analyses. Imaging parameters were as follows: TR = 1520 ms, TE = 3.93 ms, matrix size = 256 x 256, flip angle = 15°, slice thickness = 1 mm. In addition to visual assessment, scans were normalized to a MNI template using SPM 8, warping parameters were recorded for later normalization of individual FDG-PET and PiB-PET images as previously described (20, 21). Cortical thickness was calculated following the established–reconall pipeline in Freesurfer (Version 5.1.0) (22, 23). Cortical segmentation was checked visually and deemed satisfactory in all cases. Mean cortical thickness values were extracted for 31 cortical regions-of-interest per hemisphere as defined in the Desikan-Killiany-Tourville (DKT) protocol (24). Additionally, a global cortical thickness score per participant was calculated using the following formula: (Mean_cortical_thickness [ROI1] x Surface_Area [ROI1] + Mean_cortical_thickness [ROI2] x Surface_Area [ROI2] + … + Mean_cortical_thickness [ROI62] x Surface_Area [ROI62])/(Surface_Area [ROI1] + Surface_Area [ROI2] + … + Surface_Area [ROI62]).

PET Data Acquisition

Imaging studies (MRI, FDG-PET, and PiB-PET) were performed within 30 days according to the study protocol. All participants were imaged under standard resting condition (eyes closed in dimmed ambient light) using a Siemens ECAT HR+ PET scanner (CTI, Knoxville, TN, USA) (25). Participants were positioned with the head parallel to the canthomeatal line within the gantry. Image data were acquired in 3D mode with a total axial field of view of 15.5 cm. A transmission scan was acquired after completion of the emission scan for attenuation correction. A 3-dimensional attenuation-weighted ordered-subsets expectation maximization iterative reconstruction algorithm (AW OSEM 3D) was applied with four iterations and eight subsets, Gaussian smoothing of 10 mm in full width at half maximum, and a zoom of 1.

PET imaging was started 30 min after injection of about 185 MBq [^{18}F] FDG. A sequence of one frame of 10 min and two frames of 5 min was started and later summed into a single frame. Primarily, an experienced observer for quality control and individual assessment performed visual analysis of all FDG-scans.

For amyloid imaging, patients were injected with about 370 MBq [^{11}C] PiB at rest. Thirty minutes later, patients were placed in the scanner and at 40 min post-injection, three 10-min frames of data acquisition were started and later summed into a single frame (40–70 min).

PET Data Analysis

[^{18}F] FDG and [^{11}C] PiB PET scans were analyzed using SPM 8 (http://www.fil.ion.ucl.ac.uk/spm/) running on MATLAB (Version 12, The MathWorks Inc., Natick, Massachusetts, United States). PET analyses were performed following standard procedures as published previously (26–28). Images were realigned using a least squares approach and a six parameter (rigid body) spatial transformation to account for minimal motion artifacts and spatially normalized to MNI space using the warping parameters from the individual normalization of structural MRI scans. Furthermore, images were smoothed with a 10 mm x 10 mm x 10 mm full width at half maximum (FWHM) Gaussian kernel. After normalization to MNI space, PET imaging data was parcellated to ROIs based on the DKT atlas (24) using the free software tool AMIDE (29). Signal intensities of [^{18}F] FDG and [^{11}C] PiB imaging data were normalized to the pons and the vermis cerebelli, respectively and reported as standardized uptake value ratios (SUVR). In addition to ROI-based analyses, a mean value of global grey matter signal intensity per each individual was calculated.

Statistical Analysis

Mean values of ROI-based cortical thickness and relative signal intensities of FDG-PET and PiB-PET images were extracted for external analyses in IBM SPSS (Version 23 IBM Corp.) Mean values, standard deviation, coefficient of variation, minimum, and maximum values were calculated for demographic and test variables. In order to explore correlations of regional imaging data with neuropsychiatric test results, Pearson correlation analyses were performed to identify the regional pattern of correlation with z-scores of cognitive tests adjusted for sex, age, and years of education. In addition we performed multiple linear regression analyses in order to identify a) the most predictive region and b) the most predictive set of regions associated with cognitive z-scores adjusted for sex, age, and years of education. For multiple linear regression analyses, all 62 brain regions were initially entered followed by stepwise selection of significant variables (in $p<0.05$, out $p>0.10$). In order to account for influences of age and disease severity on the three biomarkers, we added age and CDR-SOB as covariates into the model resulting from the stepwise regression approach described above. The alpha level was set at $\alpha = 0.05$. The Bonferroni method was used as correction for multiple comparisons (Pearson correlation: 62 brain regions, multiple linear regression analyses: three biomarkers).

RESULTS

Sample Characteristics

Clinical and Demographic Information

A total of 76 patients (mean age 68.4 ± 8.5 years, range 50–83 years, 57.9% male) with early AD were included in this study. Mean time of education was 12.6 years ± 2.4 years. Median CDR global was 0.5, range: 0.5–2.0 and median CDR sum of boxes was 3.0, range: 0.5–11.0). Visual reading of PiB-PET showed positive cortical amyloid deposition in all cases. Mean z-scores of CERAD-NAB subtests, adjusted to sex, age, and time of education are given in **Table 1**. In cases of CERAD-NAB subtests with n < 76 participants, the individuals refused to complete the test and the result could not be evaluated.

Variance of Cerebral Biomarkers

In order to describe the variance and dynamic range of cerebral biomarkers, we calculated global and regional means presented as SUVRs, together with standard deviations and coefficients of variation. On a global level, amyloid deposition showed the highest variance (SUVR 1.727 ± 0.336 [a.u.], coefficient of variation: 19.4%), followed by glucose metabolism (SUVR 1.395 ± 0.179 [a.u.], coefficient of variation: 12.8%) and cortical thickness (mean 2.24 ± 0.26 mm, coefficient of variation: 11.5%). ROI-based coefficients of variation ranged from 15.1%–23.9%, 8.2%–17.8%, and 8.9%–20.9% for PiB uptake, FDG uptake, and cortical thickness, respectively. Detailed ROI-based characteristics are given in supplementary **Tables S1**-**S3**.

Correlation Analyses

Correlation of Global Imaging Data With Neuropsychological Test Scores

Global normalized FDG uptake correlated significantly with three CERAD-NAB subtests, explicitly with the MMSE (r = 0.419, p = 0.002), Figures—Recall (r = 0.412, p = 0.002), and Figures—Savings (r = 0.360, p = 0.017). No significant correlations of neuropsychological test scores with global cortical thickness and global, normalized PiB-PET signal intensity were observed.

TABLE 1 | Z-scores of CERAD-NAB subtests.

	n	Mean	SD	Min	Max
Verbal Fluency	75	-1.64	1.01	-3.66	0.29
Mod. Boston Naming Test	75	-1.24	1.47	-4.49	1.35
MMSE	76	-2.99	1.72	-7.21	0.78
Word List—Immediate Recall	75	-2.56	1.48	-6.45	0.92
Word List—Delayed Recall	75	-2.30	1.27	-4.64	0.88
Word List—Savings	74	-2.22	1.92	-5.31	3.52
World List—Discriminability	71	-1.74	1.61	-5.98	1.28
Constructional Praxis	76	-1.04	1.88	-7.65	1.74
Figures—Recall	76	-2.39	1.48	-5.56	1.73
Figures—Savings	75	-1.88	1.26	-3.78	2.60

CERAD-NAB, Consortium to Establish a Registry for Alzheimer's Disease—Neuropsychological Assessment Battery; MMSE, Mini-Mental State Examination; SD, standard deviation; Min, Minimum; Max, Maximum. n indicates number of participants for particular subtest.

Correlation of Neuropsychological Test Scores With Regional Amyloid Deposition

After correction for multiple comparisons, no subtest z-score showed a significant correlation with ROI-based amyloid deposition as measured by [^{11}C] PiB PET. Pearson's r for the correlation between ROI-based amyloid deposition and neuropsychological test scores is visualized in **Figure 1**.

Correlation of Neuropsychological Test Scores With Regional Glucose Metabolism

After correction for multiple comparisons for 62 brain regions, no significant correlations were found between Word List—Delayed Recall, Word List—Savings, and Word List—Discriminability and regional glucose metabolism. Most significant correlations were found for MMSE, with a predominance of left-sided frontotemporal regions. For a graphical overview of Pearson's r coefficients, please see **Figure 2**. Cognitive tasks demanding verbal capacities correlated mostly with left-sided temporal regions. Cognitive tasks including constructional praxis and visuospatial coordination correlated predominantly with right hemispheric, parietal ROIs. For a graphical overview about correlations, irrespective of statistical thresholds between ROIs and z-scores of cognitive tasks, please see **Figure 2**. Detailed correlation coefficients for significant ROIs after Bonferroni correction are given in **Table S4**.

Correlation of Neuropsychological Test Scores With Regional Cortical Thickness

After correction for multiple comparisons for 62 brain regions, no significant correlations were found between Modified Boston Naming Test, Word List—Discriminability, Figures—Recall and Figures Savings and regional cortical thickness. In general, fewer significant correlations with cognitive z-scores were seen for cortical thickness than for glucose metabolism. Most significant correlations overall were found for the parietal lobe on the left and right side. The left-sided inferior parietal lobule correlated with Word List task performance. The fusiform gyrus on the left and right side correlated with constructional praxis tasks. For a graphical overview of Pearson's r coefficients, irrespective of statistical thresholds, please see **Figure 3**. Detailed correlation coefficients for significant ROIs after Bonferroni correction are given in **Table S5**.

Multiple Linear Regression Analyses

Prediction of Neuropsychological Performance by Cortical Amyloid Deposition

Detailed results for regional amyloid deposition predicting CERAD-NAB subtest performance in the single most predictive ROI and the most predictive set of ROIs can be found in **Table 2**. Five out of 10 CERAD-NAB subtests could be predicted by amyloid PiB binding in single ROI. Three predictions remained significant after correction for multiple comparisons: Modified Boston Naming Test, Word List—Immediate Recall, and Word List—Delayed Recall. In the significant linear regression analyses, corrected R^2 ranged from 0.081–0.108 for the single regions.

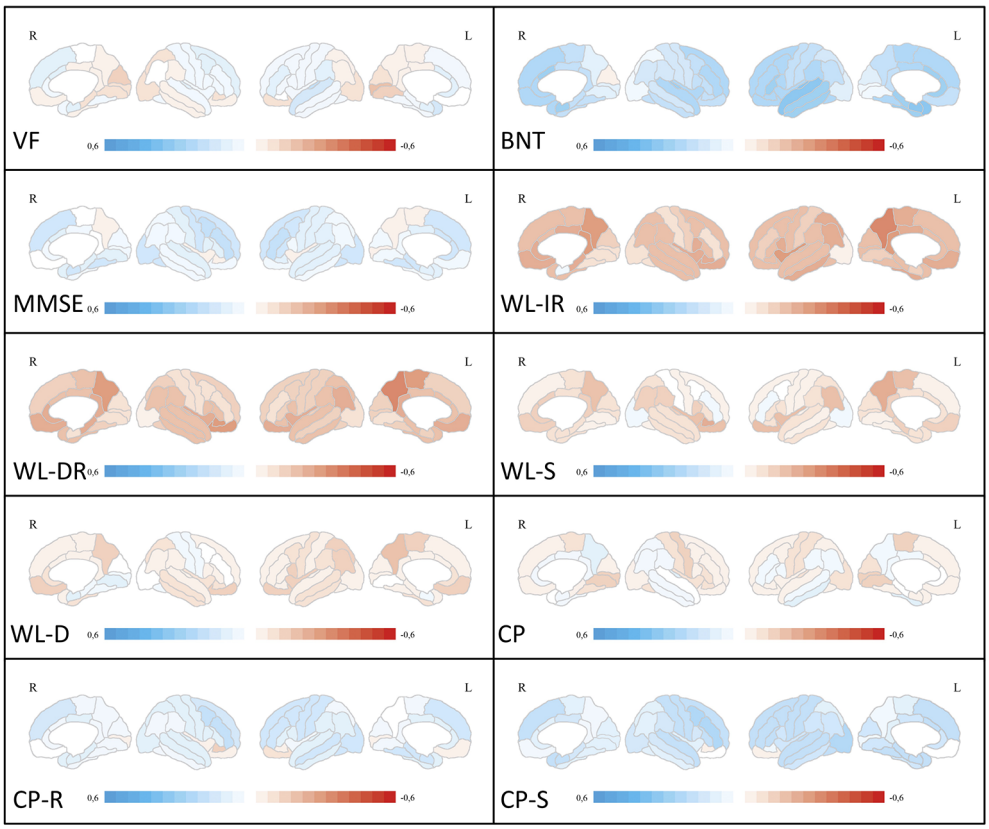

FIGURE 1 | Correlation analyses between ROI-based amyloid deposition and neuropsychological test scores. Medial and lateral projections of the right and left hemisphere are shown. Red color depicts negative correlations (Pearson's r), blue color depicts positive correlations. Maximum Pearson's r is set at -0.6 and 0.6, respectively. Verbal fluency (VF), Boston Naming Test (BNT), Mini-Mental State examination (MMSE), Word List Immediate Recall (WL-IR), Word List Delayed Recall (WL-DR), Word List Savings (WL-S), Word List Discriminability (WL-D), Constructional Practice (CP), Figures Recall (CP-R), Figures Savings (CP-S). ROI, region of interest.

Five out of 10 CERAD-NAB subtests could be predicted by regional amyloid PiB binding in a set of ROIs, namely Modified Boston Naming Test, Word List—Immediate Recall, Word List—Delayed Recall, Word List—Savings and Figures—Savings with corrected R^2 ranging between 0.108–0.220.

Interestingly, regional amyloid deposition predicted CERAD-NAB subtest performance showing both positive and negative β-coefficients and thus both positive and inverse relationships. The five subtests Verbal Fluency, MMSE, Word List—Discriminability, Constructional praxis, and Figures Recall could neither be predicted by a single ROI nor a set of regions.

Prediction of Neuropsychological Performance by Regional Glucose Metabolism

Detailed results for cortical FDG uptake predicting CERAD-NAB subtest performance in the single most predictive ROIs and the most predictive set of ROIs can be found in **Table 3**. Regional glucose metabolism was able to significantly predict performance in every CERAD-NAB subtest based on both a single ROI and a set of ROIs. Corrected R^2 values ranged from 0.083–0.300 for single ROI predictions and from 0.176–0.518 for multiple ROI regression analyses. All β-coefficients were positive in the single ROI analyses and ranged from 0.309–0.556. The single most predictive ROIs were located in the left lateral temporal lobe and the (posterior) cingulate cortex and precuneus. β-coefficients were both positive and negative when using multiple ROIs for the prediction of CERAD-NAB subtest performance.

Prediction of Neuropsychological Performance by Regional Cortical Thickness

Detailed results for regional cortical thickness predicting CERAD-NAB subtest performance in the single most predictive ROIs and the most predictive set of ROIs can be found in **Table 4**. ROI-based measurement of cortical thickness was able to significantly predict performance in every CERAD-NAB subtest, and in all but the Word List—Discriminability after correction for multiple testing, based on both a single ROI and a set of ROIs. Corrected R^2 values ranged from 0.065–0.178 for single ROI and from 0.151–0.520 for multiple ROI regression analyses. All β-coefficients were positive in the single ROI analyses and ranged from 0.279–0.434. Single most predictive ROIs were located in the lateral and medial parietal lobe and the

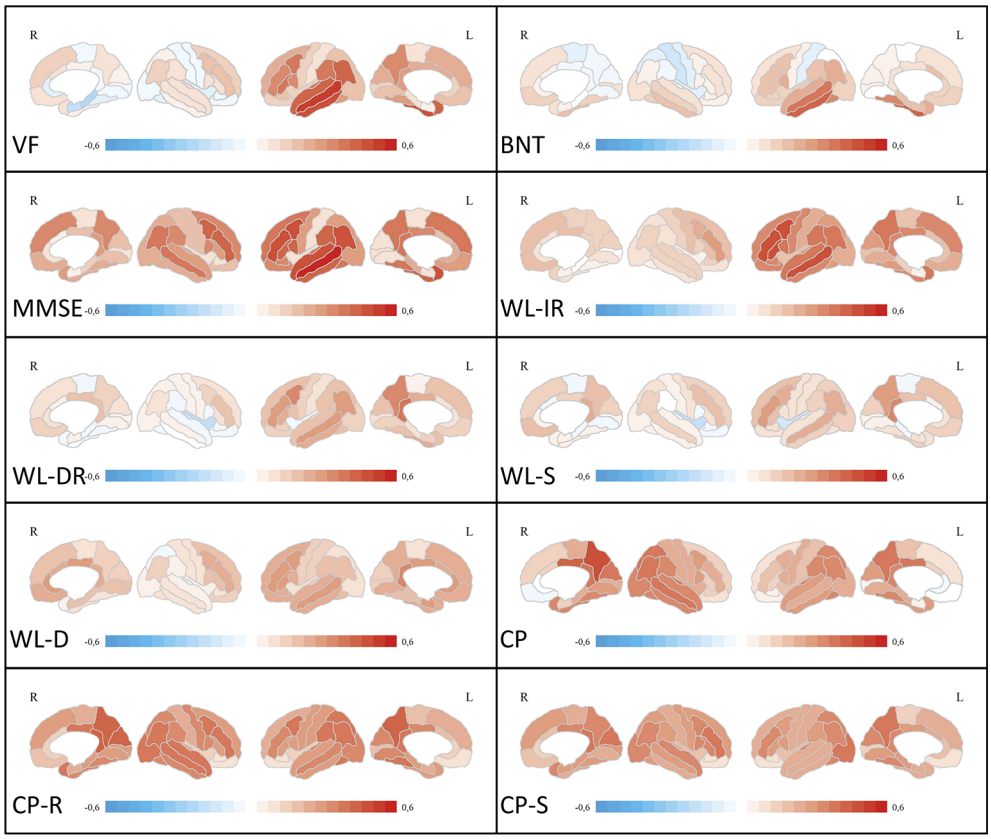

FIGURE 2 | Correlation analyses between ROI-based FDG uptake and neuropsychological test scores. Medial and lateral projections of the right and left hemisphere are shown. Red color depicts positive correlations (Pearson's r), blue color depicts negative correlations. Maximum Pearson's r is set at -0.6 and 0.6, respectively. Verbal fluency (VF), Boston Naming Test (BNT), Mini-Mental State examination (MMSE), Word List Immediate Recall (WL-IR), Word List Delayed Recall (WL-DR), Word List Savings (WL-S), Word List Discriminability (WL-D), Constructional Practice (CP), Figures Recall (CP-R), Figures Savings (CP-S). FDG, [18F]-fluorodeoxyglucose; ROI, region of interest.

inferior temporal lobe. β-coefficients were both positive and negative when using multiple ROIs for the prediction of CERAD-NAB subtest performance.

Prediction of Neuropsychological Performance by Multimodal Biomarker Information

In order to investigate the interplay of the three cerebral imaging biomarkers, we included cortical thickness, amyloid deposition, and glucose metabolism into the same regression model. Interestingly, we observe that for all cognitive tests, biomarkers of different entities from distinct regions are included. Additionally, the variance explained by the multimodal regression model mostly increases substantially compared to unimodal regression models. Detailed results are given in **Table 5**.

Influence of Age and Disease Severity on Multiple Regression Analyses

In order to account for the possible influences of age and disease severity, age and CDR-SOB were forced as covariates into the regression models from *Prediction of Neuropsychological Performance by Cortical Amyloid Deposition* to *Prediction of Neuropsychological Performance by Regional Cortical Thickness*. Detailed results are given in the supplement (**Tables S6**-**S8**). The majority of beta coefficients remained rather stable. For a graphical overview of ROI-based correlations between age, disease-severity and the three imaging biomarkers, please see **Figure S1**.

In the models based on amyloid deposition, age was a significant predictor of performance at Word List—Savings ($p=0.006$). CDR-SOB was a significant predictor of Modified Boston Naming Test performance ($p=0.024$).

In the models based on glucose metabolism, age was a significant predictor of performance at Figures—Recall ($p=0.042$). CDR-SOB was a significant predictor of MMSE performance ($p=0.006$).

In the models based on cortical thickness, age was not a significant predictor of any cognitive subtest. CDR-SOB was a significant predictor of MMSE performance ($p<0.001$) and Figures—Savings ($p=0.033$).

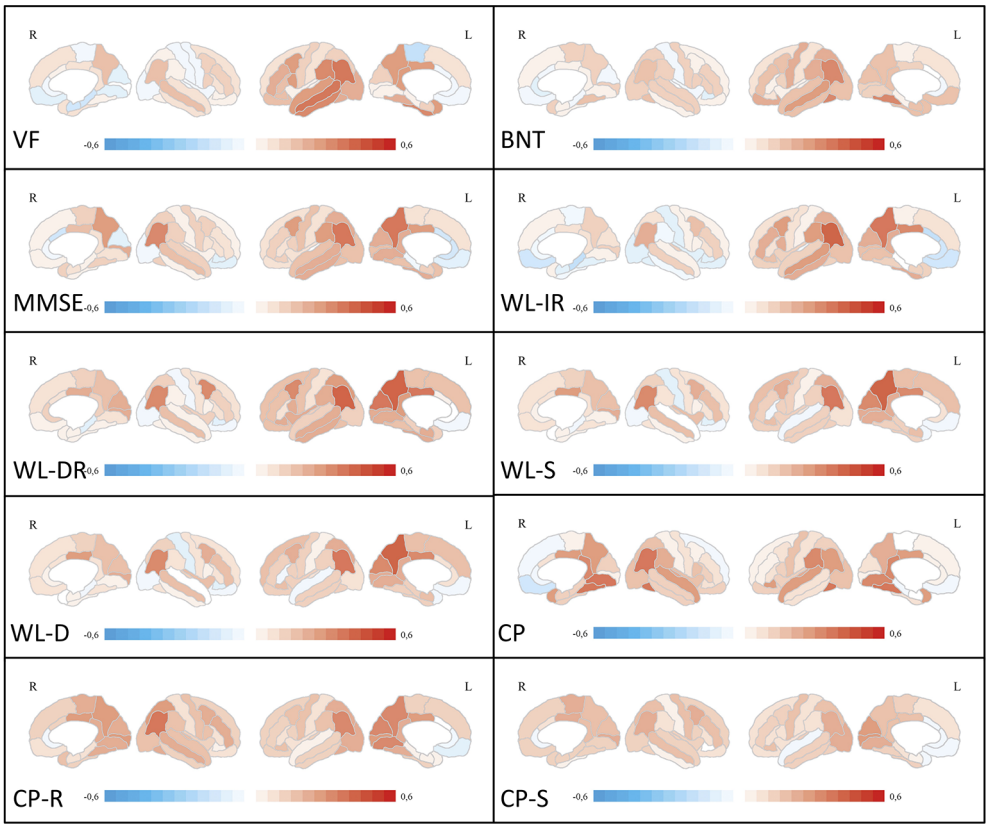

FIGURE 3 | Correlation analyses between ROI-based cortical thickness and neuropsychological test scores. Medial and lateral projections of the right and left hemisphere are shown. Red color depicts positive correlations (Pearson's r), blue color depicts negative correlations. Maximum Pearson's r is set at -0.6 and 0.6, respectively. Verbal fluency (VF), Boston Naming Test (BNT), Mini-Mental State examination (MMSE), Word List Immediate Recall (WL-IR), Word List Delayed Recall (WL-DR), Word List Savings (WL-S), Word List Discriminability (WL-D), Constructional Practice (CP), Figures Recall (CP-R), Figures Savings (CP-S). ROI, region of interest.

DISCUSSION

In this study, we have systematically investigated the relationship between cognitive performance and three cortical imaging biomarkers, namely cortical thickness, glucose metabolism, and amyloid deposition in a single, reasonably sized cohort of well-characterized early AD patients.

We found that on a global level, only glucose metabolism but not cortical atrophy or cortical amyloid deposition was correlated with CERAD-NAB subtest results. Furthermore, regional glucose metabolism was able to explain the highest percentage of variance of neuropsychological test scores, followed by neurodegeneration measured by cortical thickness. Regression analyses of regional amyloid deposition predicting CERAD-NAB subtest performance were significant in 50% of subtests and explained the least percentages of test score variance.

Interestingly, regarding the most significant associations between cerebral ROIs and CERAD-NAB subtest scores, there is very little spatial agreement between cortical thickness and local glucose metabolism. With regard to cortical thickness, the majority of single ROIs with the highest regression coefficients is located in the medial and lateral parietal lobe. In contrast, the highest regression coefficients between glucose metabolism and CERAD-NAB subtest scores can be found both in the lateral temporal lobe and the medial parietal lobe. Also, a lateralization of glucose metabolism is associated with visuoconstructive subtests to the right parietal lobe, whereas subtests that predominantly check verbal domains are associated with glucose metabolism mostly in left temporal ROIs. This is in line with previous studies on the cerebral representation of CERAD subtests (30, 31). In our study, FDG uptake was rather closely associated to the physiological representations of cognitive domains while neuronal injury follows more the general distribution of AD in the inferior temporal lobe and the medial and lateral parietal lobe (3). In any case, there is a clear discrepancy in the spatial patterns of glucose metabolism and cortical thickness predicting cognitive functioning. In the currently proposed research framework both FDG-PET and structural MRI are considered biomarkers of neurodegeneration based on an assumed sequence of hypometabolism and neuron cell loss (5). However, our study suggests that these two modalities do not reflect the same aspects

TABLE 2 | Relationship between cognitive performance and ROI-based amyloid deposition.

CERAD-NAB subtest	Single ROI	β	T	p*	F	Corr. R^2	Set of ROIs	β	T	p*	F	Corr. R^2	p
Verbal Fluency	*No significant ROI*						*No significant ROI*						
Mod. BNT	Left entorhinal cortex	0.346	3.171	0.006	10.057	0.108	Left entorhinal cortex	0.346	3.171	0.006	10.057	0.108	0.002
MMSE	*No significant ROI*						*No significant ROI*						
Word List—Immediate Recall	Left precuneus	-0.305	-2.755	0.021	7.587	0.081	Left precuneus	-0.683	-3,747	0.001	7.352	0.145	0.001
							Right fusiform gyrus	0.466	2.559	0.039			
Word List—Delayed Recall	Left precuneus	-0.322	-2.927	0.015	8.567	0.092	Left precuneus	-0.788	-4.01	<0.001	8.623	0.169	<0.001
							Left caudal middle frontal gyrus	0.551	2.808	0.018			
Word List—Savings	Right inferior frontal gyrus, pars orbitalis	-0.241	-2.14	0.108	4.581	0.046	Right inferior frontal gyrus, pars orbitalis	-0.322	-2.14	0.108	4.581	0.046	0.036
World List—Discriminability	*No significant ROI*						*No significant ROI*						
Constructional Praxis	*No significant ROI*						*No significant ROI*						
Figures—Recall	*No significant ROI*						*No significant ROI*						
Figures—Savings	Right caudal middle frontal gyrus	0.246	2.182	0.096	4.762	0.048	Right caudal middle frontal gyrus	0.801	4.154	<0.001	8.060	0.220	<0.001
							Right lateral orbitofrontal gyrus	-0.904	-4.273	<0.001			
							Left parahippocampal gyrus	0.318	2.115	0.114			

Relationship between regional amyloid deposition as measured by [^{11}C] PiB-PET and cognitive performance as measured by z-scores on CERAD-NAB subtests. Coefficients of determination are given for the single most predictive ROI and a set of most predictive ROIs with regard to CERAD-NAB subtests performance. P-values are Bonferroni corrected (*) for testing three different biomarkers.

β, standardized regression coefficient; CERAD-NAB, Consortium to Establish a Registry for Alzheimer's Disease—Neuropsychological Assessment Battery; Corr., corrected; MMSE, Mini-Mental State Examination; Mod. BNT, Modified Boston Naming Test; PET, Positron emission tomography; PIB, Pittsburgh Compound B; ROI, region of interest.

of neurodegeneration but on the contrary differ quite a lot spatially when predicting cognitive function in AD patients.

We reported significant predictions of cognitive function in half of CERAD-NAB subtests by cortical amyloid deposition in our cohort of early, but symptomatic AD patients. Furthermore, variance in regional amyloid deposition was higher than those of regional glucose metabolism and cortical thickness. This is remarkable because it is challenging concepts that propose a saturated state of amyloid deposition once AD patients become symptomatic (12). In contrary, our study suggests local amyloid burden measured by PiB-PET may at least in part be related to cognitive decline in patients with symptomatic early AD. This association has been shown in healthy older adults before (32, 33) and should encourage further investigation of regional quantification of cortical amyloid burden in the work-up of AD patients.

Interestingly, when forcing age and CDR-SOB (as a measure of disease severity) into the regression model, we found that these factors were significant only for very few cognitive subtests and that beta coefficients of biomarkers remained largely unchanged. The significant association between CDR-SOB and MMSE performance in the FDG-PET and cortical thickness based models stands out in this regard, which can be explained by the obvious association between increasing disease severity and poorer scores at the MMSE. Overall, we conclude that the influence of age and CDR-SOB as confounders to our analysis is rather small.

When including multimodal regional biomarker expression into the regression model, we found that the explained variance increased compared to unimodal regression models and that the remaining variables came from different regions and different biomarkers. This underscores the complex spatial relationship between brain regions and their biomarker expression. Future studies should focus on how regional biomarkers influence each other, e.g. by means of mediation analyses. The same is true for the multiple ROI approach compared to the single ROI approach, underlining the network character of AD pathophysiology.

Strengths of our study include the relatively large and well-characterized patient cohort, which was investigated by structural MRI, FDG-PET, and PiB-PET. Thus, we could study the association between neuropsychological impairments and different aspects of AD, amyloid plaque deposition, neuronal metabolism and neurodegeneration.

Limitations of our study include the cross-sectional character and lack of healthy individuals as controls. On the one hand, the selected ROI-based approach might be considered a limitation since it decreases the resolution and otherwise highly significant focal effects might be canceled out in large ROIs. On the other hand, we obtained identical spatial resolutions for the statistical comparisons for all imaging modalities by choosing a ROI approach. However, the impact of partial volume effects on ROI means due to different original resolutions of the imaging modalities cannot be ruled out and constitute a methodological

TABLE 3 | Relationship between cognitive performance and ROI-based glucose metabolism.

CERAD-NAB subtest	Single ROI	β	T	p*	F	Corr. R^2	Set of ROIs	β	T	p*	F	Corr. R^2	p
Verbal Fluency	Left middle temporal gyrus	0.507	5.056	<0.001	25.566	0.247	Right parahippocampal gyrus	-0.473	5.001	<0.001	19.238	0.422	<0.001
							Left transverse temporal gyrus	0.306	2.956	0.012			
							Left inferior temporal gyrus	0.465	4.582	<0.001			
Mod. BNT	Left inferior temporal gyrus	0.435	4.152	<0.001	17.241	0.178	Left inferior temporal gyrus	0.466	4.504	<0.001	10.082	0.266	<0.001
							Right postcentral gyrus	-0.555	-3.243	0.006			
							Right superior frontal gyrus	0.383	2.218	0.090			
MMSE	Left middle temporal gyrus	0.556	5.762	<0.001	33.195	0.300	Left middle temporal gyrus	0.228	1.751	0.252	14.432	0.518	<0.001
							Left rostral middle frontal gyrus	0.594	3.765	<0.001			
							Left postcentral gyrus	-0.677	-4.946	<0.001			
							Right caudal middle frontal gyrus	0.648	4.070	<0.001			
							Right inferior frontal gyrus pars triangularis	-0.491	-3.139	0.006			
							Left fusiform gyrus	0.297	2.358	0.063			
Word List—Immediate Recall	Left middle temporal gyrus	0.476	4.653	<0.001	21.652	0.216	Left middle temporal gyrus	0.290	2.464	0.048	12.699	0.319	<0.001
							Left rostral middle frontal gyrus	0.647	3.630	0.003			
							Right superior frontal gyrus	-0.444	-2.765	0.021			
Word List—Delayed Recall	Left isthmus of the cingulate gyrus	0.378	3.51	0.003	12.317	0.131	Left isthmus of cingulate gyrus	0.505	4.641	<0.001	12.134	0.229	<0.001
							Right insula	-0.351	-3.223	0.006			
Word List—Savings	Left isthmus of the cingulate gyrus	0.309	2.793	0.021	7.801	0.083	Left isthmus of cingulate gyrus	0.587	5.025	<0.001	8.778	0.384	<0.001
							Right medial orbitofrontal gyrus	0.851	4.870	<0.001			
							Right lateral orbitofrontal gyrus	-0.798	-4.210	<0.001			
							Left insula	-0.426	-3.263	0.006			
							Right lingual gyrus	-0.362	-2.830	0.018			
							Right precentral gyrus	0.282	2.103	0.117			
World List—Discriminability	Left isthmus of the cingulate gyrus	0.333	3.04	0.009	9.245	0.099	Left isthmus of the cingulate gyrus	0.403	3.530	0.003	6.883	0.190	<0.001
							Right transverse temporal gyrus	-0.276	-2.435	0.051			
							Left entorhinal cortex	0.234	2.217	0.09			
Constructional Praxis	Right precuneus	0.464	4.51	<0.001	20.34	0.205	Right precuneus	0.567	5.206	<0.001	12.466	0.314	<0.001
							Right medial orbitofrontal gyrus	-0.402	-3.494	0.003			
							Left inferior temporal gyrus	0.260	2.414	0.054			
Figures—Recall	Right precuneus	0.439	4.205	<0.001	17.68	0.182	Right precuneus	0.439	4.205	<0.001	17.680	0.182	<0.001
Figures—Savings	Right isthmus of the cingulate gyrus	0.393	3.673	0.001	13.489	0.143	Right isthmus of the cingulate gyrus	0.293	2.525	0.042	9.006	0.176	<0.001
							Left occipital complex	0.232	1.995	0.15			

Relationship between regional glucose metabolism as measured by [^{18}F] FDG-PET and cognitive performance as measured by z-scores on CERAD-NAB subtests. Coefficients of determination are given for the single most predictive ROI and a set of most predictive ROIs with regard to CERAD-NAB subtests performance. P-values are Bonferroni corrected (*) for testing three different biomarkers.

β, standardized regression coefficient; CERAD-NAB, Consortium to Establish a Registry for Alzheimer's Disease—Neuropsychological Assessment Battery; Corr., corrected; FDG, [18F]-fluorodeoxyglucose; MMSE, Mini-Mental State Examination; PET, Positron emission tomography; ROI, region of interest.

TABLE 4 | Relationship between cognitive performance and ROI-based cortical thickness.

CERAD-NAB subtest	Single ROI	β	T	p*	F	Corr. R^2	Set of ROIs	β	T	p*	F	Corr. R^2	p
Verbal Fluency	Left inferior parietal lobule	0.377	3.504	<0.001	12.280	0.131	Left inferior parietal lobule	0.335	1.936	0.171	10.907	0.398	<0.001
							Left paracentral gyrus	-0.441	-3.940	<0.001			
							Right lingual gyrus	-0.447	-3.752	<0.001			
							Left superior temporal gyrus	0.316	2.612	0.033			
							Left precuneus	0.371	2.188	0.096			
Mod. BNT	Left fusiform gyrus	0.309	2.795	0.021	7.813	0.083	Left fusiform gyrus	0.480	3.849	<0.001	7.677	0.151	0.001
							Right inferior frontal gyrus. pars orbitalis	-0.328	-2.630	0.03			
MMSE	Left precuneus	0.395	3.701	0.001	13.697	0.145	Left precuneus	0.706	6.033	<0.001	10.067	0.326	<0.001
							Right cuneus	-0.400	-3.411	0.003			
							Right entorhinal cortex	0.259	2.631	0.03			
							Left rostral anterior cingulate cortex	-0.221	-2.187	0.096			
Word List—Immediate Recall	Left inferior parietal lobule	0.413	3.897	<0.001	15.183	0.159	Left parietal inferior lobule	0.598	4.472	<0.001	10.857	0.345	<0.001
							Right supramarginal gyrus	-0.418	-3.234	0.006			
							Left medial orbitofrontal gyrus	-0.284	-2.678	0.027			
							Left posterior cingulate cortex	0.302	2.426	0.054			
Word List—Delayed Recall	Left inferior parietal lobule	0.434	4.148	<0.001	17.205	0.178	Left parietal inferior lobule	0.457	3.434	0.003	13.232	0.449	<0.001
							Right supramarginal gyrus	-0.793	-4.868	<0.001			
							Right parietal inferior lobule	0.723	3.626	<0.001			
							Right lateral occipital complex	-0.476	-3.702	<0.001			
							Right cuneus	0.357	2.930	0.015			
Word List—Savings	Left precuneus	0.390	3.645	0.001	13.285	0.141	Left precuneus	0.629	5.209	<0.001	13.805	0.255	<0.001
							Right postcentral gyrus	-0.423	-3.507	<0.001			
World List—Discriminability	Left posterior cingulate cortex	0.269	2.404	0.057	5.780	0.060	Left posterior cingulate cortex	0.403	3.530	0.057	5.780	0.060	0.019
Constructional Praxis	Right fusiform gyrus	0.407	3.834	<0.001	14.701	0.154	Right fusiform gyrus	0.265	2.086	0.123	14.520	0.520	<0.001
							Right medial orbitofrontal gyrus	-0.357	-3.207	0.006			
							Right posterior cingulate cortex	0.310	2.758	0.021			
							Right superior frontal gyrus	-0.551	-4.099	<0.001			
							Left isthmus of the cingulate gyrus	0.375	3.753	<0.001			
							Right lingual gyrus	0.420	3.361	0.003			
Figures—Recall	Right inferior parietal lobule	0.366	3.382	0.003	11.435	0.122	Right inferior parietal lobule	0.780	4.011	<0.001	9.322	0.182	<0.001
							Right supramarginal gyrus	-0.491	-2.525	0.042			
Figures—Savings	Left cuneus	0.279	2.500	0.045	6.250	0.065	Left cuneus	0.279	2.500	0.045	6.250	0.065	0.015

Relationship between regional cortical thickness as measured by structural MRI and cognitive performance as measured by z-scores on CERAD-NAB subtests. Coefficients of determination are given for the single most predictive ROI and a set of most predictive ROIs with regard to CERAD-NAB subtests performance. P-values are Bonferroni corrected (*) for testing three different biomarkers.

β, standardized regression coefficient; CERAD-NAB, Consortium to Establish a Registry for Alzheimer's Disease—Neuropsychological Assessment Battery; Corr., corrected; MMSE, Mini-Mental State Examination; MRI, Magnetic Resonance Imaging; ROI, region of interest.

TABLE 5 | Relationship between cognitive performance and multimodal ROI-based biomarker information.

CERAD-NAB subtest	Biomarker	ROI	β	T	p	F	Corr. R^2	p
Verbal Fluency	FDG	Left middle temporal gyrus	0.633	6.864	<0.001	14.516	0.422	<0.001
	FDG	Right parahippocampal gyrus	-0.341	-3.773	<0.001			
	CTh	Right inferior frontal gyrus, pars triangularis	0.414	3.291	0.002			
	CTh	Left superior frontal gyrus	-0.287	-2.28	0.026			
Mod. BNT	FDG	Left inferior temporal gyrus	0.410	4.032	<0.001	9.494	0.408	<0.001
	PiB	Left caudal anterior cingulate cortex	0.546	3.619	0.001			
	PiB	Right precuneus	-1.196	-3.632	0.001			
	PiB	Left precuneus	0.895	2.641	0.010			
	FDG	Right insular lobe	-0.300	-2.802	0.007			
	FDG	Left inferior frontal gyrus, pars triangularis	0.237	2.001	0.049			
MMSE	FDG	Left middle temporal gyrus	0.223	1.805	0.076	14.364	0.555	<0.001
	CTh	Left precuneus	0.239	2.997	0.004			
	FDG	Left rostral middle frontal gyrus	0.478	3.443	0.001			
	FDG	Left postcentral gyrus	-0.598	-4.592	<0.001			
	FDG	Right caudal middle frontal gyrus	0.417	3.12	0.003			
	FDG	Right inferior frontal gyrus, pars orbitalis	-0.267	-2.65	0.010			
	FDG	Left fusiform gyrus	0.251	2.117	0.038			
Word List—Immediate Recall	FDG	Left middle temporal gyrus	0.569	6.665	<0.001	15.276	0.491	<0.001
	PiB	Left precuneus	-0.589	-4.655	<0.001			
	CTh	Right parahippocampal gyrus	-0.374	-4.239	<0.001			
	CTh	Right transverse temporal gyrus	0.276	3.156	0.002			
	PiB	Right postcentral gyrus	0.360	2.839	0.006			
Word List—Delayed Recall	CTh	Left inferior parietal lobule	0.520	4.619	<0.001	16.233	0.622	<0.001
	CTh	Right supramarginal gyrus	-1.011	-6.922	<0.001			
	CTh	Right posterior cingulate gyrus	0.387	4.183	<0.001			
	PiB	Right caudal middle frontal gyrus	0.676	4.738	<0.001			
	CTh	Right inferior parietal lobule	0.408	2.577	0.012			
	PiB	Right inferior parietal lobule	-0.565	-3.896	<0.001			
	PiB	Left insular lobe	-0.372	-2.466	0.016			
	CTh	Right caudal middle frontal gyrus	0.247	2.126	0.037			
Word List—Savings	CTh	Left precuneus	0.591	5.291	<0.001	10.97	0.353	<0.001
	CTh	Left postcentral gyrus	-0.407	-3.665	<0.001			
	PiB	Right inferior frontal gyrus, pars orbitalis	-0.674	-3.306	0.002			
	PiB	Right inferior frontal gyrus, pars triangularis	0.529	2.608	0.011			
World List—Discriminability	FDG	Left isthmus of the cingulate gyrus	0.349	3.296	0.002	7.434	0.216	<0.001
	CTh	Left insular lobe	0.523	3.311	0.001			
	CTh	Right superior frontal gyrus	-0.319	-2.022	0.047			
Constructional Praxis	FDG	Right precuneus	0.410	4.436	<0.001	13.189	0.565	<0.001
	CTh	Left fusiform gyrus	0.273	2.279	0.026			
	CTh	Right superior frontal gyrus	-0.879	-5.802	<0.001			
	FDG	Right medial orbitofrontal gyrus	-0.290	-3.231	0.002			
	CTh	Left posterior cingulate cortex	0.340	3.429	0.001			
	CTh	Right superior temporal gyrus	0.390	2.856	0.006			
	CTh	Right inferior frontal gyrus, pars orbitalis	0.319	2.315	0.024			
	CTh	Left entorhinal area	-0.201	-2.159	0.034			
Figures—Recall	FDG	Right precuneus	0.402	3.942	<0.001	12.535	0.235	<0.001
	CTh	Left cuneus	0.253	2.482	0.015			
Figures—Savings	FDG	Right isthmus of the cingulate gyrus	0.368	3.579	0.001	8.296	0.228	<0.001
	CTh	Left cuneus	0.266	2.563	0.013			
	PiB	Left transverse temporal gyrus	0.225	2.176	0.033			

Most predictive set of ROI-based biomarkers across modalities and cognitive performance as measured by z-scores on CERAD-NAB subtests.
β, standardized regression coefficient; CERAD-NAB, Consortium to Establish a Registry for Alzheimer's Disease—Neuropsychological Assessment Battery; Corr., corrected; CTh, Cortical Thickness; FDG, [18F]-fluorodeoxyglucose; MMSE, Mini-Mental State Examination; PiB, Pittsburgh Compound B; ROI, region of interest.

limitation of the current study. Specifically, partial volume effects may be in part the reason for relatively diverging results of glucose metabolism and cortical thickness.

In conclusion, our study shows a tight association between FDG metabolism and physiological representations of neuropsychological capacities, while neurodegeneration could be observed mostly in areas that are generally affected during the course of AD. Moreover, we have shown that cortical amyloid deposition is predictive of cognitive functioning in half of CERAD-NAB subtests. This suggests direct or indirect functional relevance of cortical amyloid deposition in already symptomatic AD patients, which should encourage further investigation of regional amyloid quantification in symptomatic AD patients. Our results emphasize the complex spatial relationships between imaging biomarkers in AD and their different impact on cognitive functioning of early AD patients. Further studies are needed to elucidate the interaction of different biomarkers and their effect on cognitive functioning in early AD patients.

DATA AVAILABILITY STATEMENT

The datasets for this manuscript are not publicly available because: Restrictions regarding data availability were imposed by the local ethics committee. Requests to access the datasets should be directed to TG (t.grimmer@tum.de).

ETHICS STATEMENT

The studies involving human participants were reviewed and approved by Ethics Committee of the School of Medicine of the Technical University of Munich. The patients/participants provided their written informed consent to participate in this study.

AUTHOR CONTRIBUTIONS

RD, TJ, IY, JD-S, and TG designed the experiment. RD, OG, MO, FM-S, and JD-S carried it out. DH, RD, OG, TG, and IY analyzed the data. DH, RD, and TG wrote the manuscript. TJ, IY, HF, JD-S, and CZ edited the manuscript. HF, JD-S, CZ, and TJ supervised the work. All authors discussed the results and reviewed the manuscript.

SUPPLEMENTARY MATERIAL

The Supplementary Material for this article can be found online at: https://www.frontiersin.org/articles/10.3389/fpsyt.2020.00793/full#supplementary-material

REFERENCES

1. Hebert LE, Weuve J, Scherr PA, Evans DA. Alzheimer disease in the United States (2010-2050) estimated using the 2010 census. *Neurology* (2013) 80:1778–83. doi: 10.1212/WNL.0b013e31828726f5
2. Thal DR, Rüb U, Orantes M, Braak H. Phases of Aβ-deposition in the human brain and its relevance for the development of AD. *Neurology* (2002) 58:1791–800. doi: 10.1212/WNL.58.12.1791
3. Braak H, Braak E. Neuropathological stageing of Alzheimer-related changes. *Acta Neuropathol* (1991) 82:239–59. doi: 10.1007/BF00308809
4. Braak H, Braak E. Staging of Alzheimer's disease-related neurofibrillary changes. *Neurobiol Aging* (1995) 16:271–84. doi: 10.1007/s00134-002-1380-9
5. Jack CR, Bennett DA, Blennow K, Carrillo MC, Dunn B, Budd S, et al. NIA-AA research framework: toward a biological definition of Alzheimer ' s disease. *Alzheimer's Dement* (2018) 14:535–62. doi: 10.1016/j.jalz.2018.02.018
6. Fields JA, Ferman TJ, Boeve BF, Smith GE. Neuropsychological assessment of patients with dementing illness. *Nat Rev Neurol* (2011) 7:677–87. doi: 10.1038/nrneurol.2011.173
7. Morris JC, Heyman A, Mohs RC, Hughes JP, van Belle G, Fillenbaum G, et al. The Consortium to Establish a Registry for Alzheimer's Disease (CERAD). Part I. Clinical and neuropsychological assessment of Alzheimer's disease. *Neurology* (1989) 39:1159–65. doi: 10.1212/WNL.39.9.1159
8. Morris JC. The Clinical Dementia Rating (CDR): current version and scoring rules. *Neurology* (1993) 43:2412–4. doi: 10.1212/WNL.43.11.2412-a
9. Schönknecht ODP, Hunt A, Toro P, Guenther T, Henze M, Haberkorn U, et al. Bihemispheric Cerebral FDG PET correlates of cognitive dysfunction as assessed by the CERAD in Alzheimer's disease. *Clin EEG Neurosci* (2011) 42:71–6. doi: 10.1177/155005941104200207
10. Eliassen CF, Reinvang I, Selnes P, Fladby T, Hessen E. Convergent results from neuropsychology and from neuroimaging in patients with mild cognitive impairment. *Dement Geriatr Cognit Disord* (2017) 42:144–54. doi: 10.1159/000455832
11. Farrell ME, Kennedy KM, Rodrigue KM, Wig G, Bischof GN, Rieck JR, et al. Association of longitudinal cognitive decline with amyloid burden in middle-aged and older adults evidence for a dose-response relationship. *JAMA Neurol* (2018) 75235:830–8. doi: 10.1001/jamaneurol.2017.0892
12. Jack CRJ, Knopman DS, Jagust WJ, Petersen RC, Weiner MW, Aisen PS, et al. Tracking pathophysiological processes in Alzheimer's disease: an updated hypothetical model of dynamic biomarkers. *Lancet Neurol* (2013) 12:207–16. doi: 10.1016/S1474-4422(12)70291-0
13. Sperling RA, Aisen PS, Beckett LA, Bennett DA, Craft S, Fagan AM, et al. Toward defining the preclinical stages of Alzheimer's disease: recommendations from the National Institute on Aging-Alzheimer's Association workgroups on diagnostic guidelines for Alzheimer's disease. *Alzheimers Dement* (2011) 7:280–92. doi: 10.1016/j.jalz.2011.03.003
14. McKhann GM, Knopman DS, Chertkow H, Hyman BT, Jack CRJ, Kawas CH, et al. The diagnosis of dementia due to Alzheimer's disease: recommendations from the National Institute on Aging-Alzheimer's Association workgroups on diagnostic guidelines for Alzheimer's disease. *Alzheimers Dement* (2011) 7:263–9. doi: 10.1016/j.jalz.2011.03.005
15. Minoshima S. Imaging Alzheimer's disease: clinical applications. *Neuroimaging Clin N Am* (2003) 13:769–80. doi: 10.1016/S1052-5149(03)00099-6
16. Roman GC, Tatemichi TK, Erkinjuntti T, Cummings JL, Masdeu JC, Garcia JH, et al. Vascular dementia: diagnostic criteria for research studies. Report of the NINDS-AIREN International Workshop. *Neurology* (1993) 43:250–60. doi: 10.1212/WNL.43.2.250
17. Cedarbaum JM, Jaros M, Hernandez C, Coley N, Andrieu S, Grundman M, et al. Rationale for use of the Clinical Dementia Rating Sum of Boxes as a primary outcome measure for Alzheimer's disease clinical trials. *Alzheimers Dement* (2013) 9:S45–55. doi: 10.1016/j.jalz.2011.11.002
18. Folstein MF, Folstein SE, McHugh PR. "Mini-mental state". A practical method for grading the cognitive state of patients for the clinician. *J Psychiatr Res* (1975) 12:189–98. doi: 10.1016/0022-3956(75)90026-6
19. Berres M, Monsch AU, Bernasconi F, Thalmann B, Stahelin HB. Normal ranges of neuropsychological tests for the diagnosis of Alzheimer's disease. *Stud Health Technol Inform* (2000) 77:195–9. doi: 10.3233/978-1-60750-921-9-195.
20. Friston KJ, Frith CD, Liddle PF, Dolan RJ, Lammertsma AA, Frackowiak RS. The relationship between global and local changes in PET scans. *J Cereb Blood Flow Metab* (1990) 10:458–66. doi: 10.1038/jcbfm.1990.88
21. Drzezga A, Grimmer T, Henriksen G, Stangier I, Perneczky R, Diehl-Schmid J, et al. Imaging of amyloid plaques and cerebral glucose metabolism in semantic dementia and Alzheimer's disease. *Neuroimage* (2008) 39:619–33. doi: 10.1016/j.neuroimage.2007.09.020
22. Dale AM, Fischl B, Sereno MI. Cortical surface-based analysis. I. Segmentation and surface reconstruction. *Neuroimage* (1999) 9:179–94. doi: 10.1006/nimg.1998.0395
23. Fischl B, Dale AM. Measuring the thickness of the human cerebral cortex from magnetic resonance images. *Proc Natl Acad Sci* (2000) 97:11050–5. doi: 10.1073/pnas.200033797
24. Klein A, Tourville J. 101 labeled brain images and a consistent human cortical labeling protocol. *Front Neurosci* (2012) 6:171. doi: 10.3389/fnins.2012.00171
25. Diehl J, Grimmer T, Drzezga A, Riemenschneider M, Forstl H, Kurz A. Cerebral metabolic patterns at early stages of frontotemporal dementia and semantic dementia. A PET study. *Neurobiol Aging* (2004) 25:1051–6. doi: 10.1016/j.neurobiolaging.2003.10.007
26. Grimmer T, Tholen S, Yousefi BH, Alexopoulos P, Forschler A, Forstl H, et al. Progression of cerebral amyloid load is associated with the apolipoprotein E epsilon4 genotype in Alzheimer's disease. *Biol Psychiatry* (2010) 68:879–84. doi: 10.1016/j.biopsych.2010.05.013
27. Grimmer T, Riemenschneider M, Forstl H, Henriksen G, Klunk WE, Mathis CA, et al. Beta amyloid in Alzheimer's disease: increased deposition in brain is reflected in reduced concentration in cerebrospinal fluid. *Biol Psychiatry* (2009) 65:927–34. doi: 10.1016/j.biopsych.2009.01.027
28. Grimmer T, Henriksen G, Wester H-J, Forstl H, Klunk WE, Mathis CA, et al. Clinical severity of Alzheimer's disease is associated with PIB uptake in PET. *Neurobiol Aging* (2009) 30:1902–9. doi: 10.1016/j.neurobiolaging.2008.01.016

29. Loening AM, Gambhir SS. AMIDE: a free software tool for multimodality medical image analysis. *Mol Imaging* (2003) 2:131–7. doi: 10.1162/153535003322556877
30. Welsh KA, Hoffman JM, Earl NL, Hanson MW. Neural correlates of dementia: regional brain metabolism (FDG-PET) and the CERAD neuropsychological battery. *Arch Clin Neuropsychol* (1994) 9:395–409. doi: 10.1016/0887-6177(94)90003-5
31. Teipel SJ, Willoch F, Ishii K, Burger K, Drzezga A, Engel R, et al. Resting state glucose utilization and the CERAD cognitive battery in patients with Alzheimer's disease. *Neurobiol Aging* (2006) 27:681–90. doi: 10.1016/j.neurobiolaging.2005.03.015
32. Hedden T, Oh H, Younger AP, Patel TA. Meta-analysis of amyloid-cognition relations in cognitively normal older adults. *Neurology* (2013) 80:1341–8. doi: 10.1212/WNL.0b013e31828ab35d
33. Resnick SM, Sojkova J, Zhou Y, An Y, Ye W, Holt DP, et al. Longitudinal cognitive decline is associated with fibrillar amyloid-beta measured by [11C]PiB. *Neurology* (2010) 74:807–15. doi: 10.1212/WNL.0b013e3181d3e3e9

Conflict of Interest: IY has no related conflicts of interest, outside the submitted work. IY is a consultant for Blue Earth Diagnostics and a lecturer for Piramal and has received grants from the Alzheimer Research Initiative Germany and the German Research Foundation (DFG). TG has no related conflicts of interest. Outside the submitted work, he reported having received consulting fees from Actelion, Biogen, Eli Lilly, Iqvia/Quintiles; MSD; Novartis, Quintiles, Roche Pharma, lecture fees from Biogen, Lilly, Parexel, Roche Pharma, and grants to his institution from Actelion, Novartis and PreDemTech.

The remaining authors declare that the research was conducted in the absence of any commercial or financial relationships that could be construed as a potential conflict of interest.

frontiers in Psychiatry

REVIEW
published: 23 September 2020
doi: 10.3389/fpsyt.2020.567534

Selective Review of Neuroimaging Findings in Youth at Clinical High Risk for Psychosis: On the Path to Biomarkers for Conversion

Justin K. Ellis[1], *Elaine F. Walker*[2] *and David R. Goldsmith*[1]*

[1] Department of Psychiatry and Behavioral Sciences, Emory University School of Medicine, Atlanta, GA, United States,
[2] Department of Psychology, Emory University, Atlanta, GA, United States

First episode psychosis (FEP), and subsequent diagnosis of schizophrenia or schizoaffective disorder, predominantly occurs during late adolescence, is accompanied by a significant decline in function and represents a traumatic experience for patients and families alike. Prior to first episode psychosis, most patients experience a prodromal period of 1–2 years, during which symptoms first appear and then progress. During that time period, subjects are referred to as being at Clinical High Risk (CHR), as a prodromal period can only be designated in hindsight in those who convert. The clinical high-risk period represents a critical window during which interventions may be targeted to slow or prevent conversion to psychosis. However, only one third of subjects at clinical high risk will convert to psychosis and receive a formal diagnosis of a primary psychotic disorder. Therefore, in order for targeted interventions to be developed and applied, predicting who among this population will convert is of critical importance. To date, a variety of neuroimaging modalities have identified numerous differences between CHR subjects and healthy controls. However, complicating attempts at predicting conversion are increasingly recognized co-morbidities, such as major depressive disorder, in a significant number of CHR subjects. The result of this is that phenotypes discovered between CHR subjects and healthy controls are likely non-specific to psychosis and generalized for major mental illness. In this paper, we selectively review evidence for neuroimaging phenotypes in CHR subjects who later converted to psychosis. We then evaluate the recent landscape of machine learning as it relates to neuroimaging phenotypes in predicting conversion to psychosis.

Keywords: schizophrenia, psychosis, clinical high risk, prodrome, neuroimaging, MRI, PET

OPEN ACCESS

Edited by:
Sven Haller,
Rive Droite SA, Switzerland

Reviewed by:
Tsutomu Takahashi,
University of Toyama, Japan
Stefan Borgwardt,
University of Basel, Switzerland

***Correspondence:**
David R. Goldsmith
drgolds@emory.edu

Specialty section:
This article was submitted to Neuroimaging and Stimulation, a section of the journal Frontiers in Psychiatry

Received: *29 May 2020*
Accepted: *31 August 2020*
Published: *23 September 2020*

Citation:
Ellis JK, Walker EF and Goldsmith DR (2020) Selective Review of Neuroimaging Findings in Youth at Clinical High Risk for Psychosis: On the Path to Biomarkers for Conversion. Front. Psychiatry 11:567534. doi: 10.3389/fpsyt.2020.567534

INTRODUCTION

Schizophrenia is a debilitating illness that affects 1% of the global population (1, 2), shortens the lifespan of those afflicted (3), and imposes a substantial financial burden on patients, their families, and society (4, 5). Clinically, it is characterized by positive symptoms, such as hallucinations and delusions, negative symptoms, such as anhedonia and amotivation, and cognitive symptoms, such

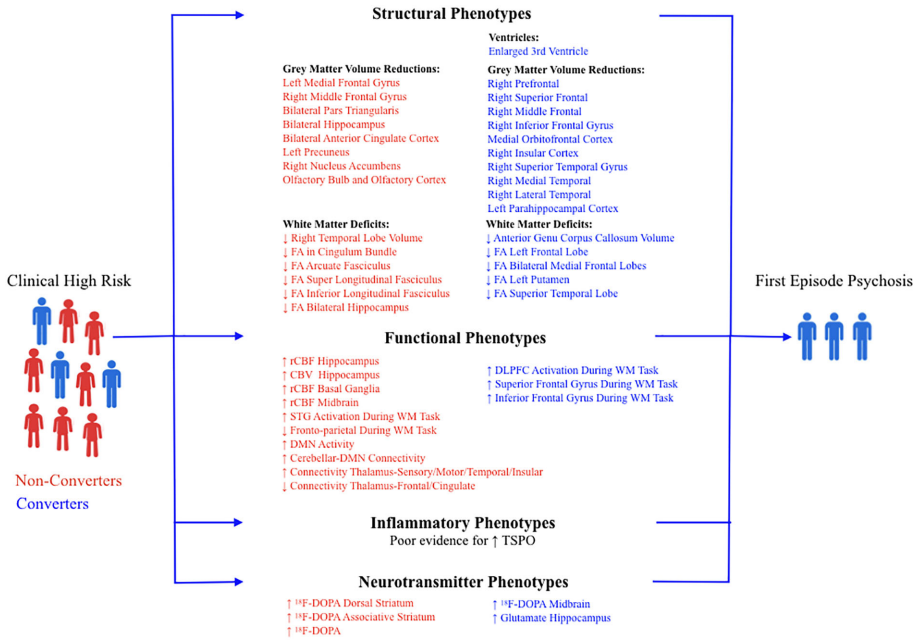

FIGURE 1 | Summary of neuroimaging findings in non-converters (red) and converters (blue) at clinical high risk for psychosis. FA, Fractional Anisotropy; rCBF, Regional Cerebral Blood Flow; CBV, Cerebral Blood Volume; DMN, Default Mode Network; DLPFC, Dorsolateral Prefrontal Cortex; STG, Superior Temporal Gyrus; WM, Working Memory.

as deficits in working memory, executive function, and attention. Despite significant ongoing efforts to understand the pathophysiology of this disease, currently available treatments are generally only successful in ameliorating the positive symptoms. However, it is the negative and cognitive symptom burden that correlate most with overall decline in global functioning and lifespan (6, 7), and no adequate treatments currently exist. Thus, more and more efforts have begun to look at early identification of illness, with the goals of predicting disease onset and severity, and ultimately, prevention of conversion to first episode psychosis.

Diagnosis of schizophrenia usually occurs in late adolescence with the onset of a first psychotic episode. Prior to a first episode of psychosis (FEP), patients experience a prodromal period of 1–2 years, during which symptoms of psychosis first appear in an attenuated form and then progress. Prodromal symptoms are also characterized by social withdrawal, increased isolation, and a global decline in functioning (8–10). During that time period, subjects are referred to as being at Clinical High Risk (CHR), as a prodromal period can only be designated in hindsight in those who convert. 30–35% of clinical high risk subjects will experience a first psychotic episode and be diagnosed with a primary psychotic disorder (11, 12). Of those who do not, approximately 7% will recover, 28% will continue to experience persistent, attenuated psychotic symptoms, and 65% will be diagnosed with another non-psychotic psychiatric disorder (12). The clinical high risk period represents a critical window during which targeted interventions may be developed and applied. Therefore, predicting who among the this population will convert is of critical importance.

For the past 100 years, neuroimaging has taken a distinguished role in providing new insights into the pathophysiology of schizophrenia and is uniquely primed to evaluate the adolescent brain both pre- and post-first psychotic episode. To date, a variety of neuroimaging modalities have identified numerous differences between CHR subjects and healthy controls. However, thus far the majority of studies have been cross-sectional in design, and a significant degree of variation among phenotypes have been reported. Further complicating attempts at predicting conversion is the increasingly recognized co-morbidity of other psychiatric diagnoses among CHR subjects. In one study, 79% of CHR subjects met criteria for comorbid psychiatric diagnoses, including mood, anxiety, and substance use disorders (13). In a follow up report, 60% of CHR subjects were diagnosed with comorbid major depressive disorder, which was associated with more pronounced negative and general symptoms, as well as poorer prognosis (14). Comorbidity, thus far, has not been associated with conversion to psychosis. Nevertheless, it has become quite clear that phenotypes discovered between CHR subjects and healthy controls are likely non-specific to psychosis and generalized for major mental illness. In order to improve prediction algorithms there needs to be a greater focus on longitudinal studies that identify phenotypes present among converters and non-converters.

In this narrative review, we selectively evaluate evidence for neuroimaging phenotypes in CHR subjects who later converted to psychosis. We then evaluate the recent landscape of machine learning and prediction algorithms as they relate to neuroimaging phenotypes in predicting conversion to psychosis.

STRUCTURAL PHENOTYPES

Enlarged Ventricles

The first report of enlarged ventricles in patients with schizophrenia was in 1927 using pneumoencephalography (PEG) to measure ventricular size (15). Despite early concerns due to lack of controls and variation in methodology, this observation is one of the most replicated findings in the literature using both computed tomography (16) and magnetic resonance imaging (17–19). Originally studied in chronic cases, ventricular enlargement has been observed and well replicated in first episode psychosis. In support of this, three meta-analyses have reported ventricular enlargement in FEP patients (20–22). All three found enlargement in the lateral ventricles compared to controls, but two also observed enlargement of the 3rd ventricle (21, 22). The 3rd ventricle was not measured in the third meta-analysis (20).

As ventricular enlargement is such a consistent finding in FEP patients, it is surprising that few studies have investigated ventricular enlargement in the CHR population. To the best of our knowledge, there are only two longitudinal studies evaluating ventricular size in converters versus non-converters, and there are discrepancies in their findings. Ziermans et al. evaluated 43 CHR subjects, 8 of whom converted to psychosis, and found no difference in lateral ventricular volume among converters and non-convertors in post-hoc analysis (23). 3rd ventricular volume was not measured. However, in a much larger study, Cannon et al. evaluated 274 CHR subjects, of whom 35 converted to psychosis (24). They did not observe enlarged lateral ventricles, but did observe expansion of the 3rd ventricle in CHR subjects who converted to psychosis compared to both non-convertors and controls. Furthermore, a shorter prodromal period before conversion was associated with greater expansion of the ventricle.

Although not many studies appear to have looked specifically at ventricular enlargement in CHR subjects, those that did failed to find enlargement in the lateral ventricles at baseline. However, one phenotype that warrants further investigation and replication is enlargement of the 3rd ventricle in CHR subjects at baseline that later convert to psychosis.

Decreased Grey Matter Volume

Reductions in grey matter volume in multiple brain regions have been well established in patients with schizophrenia (25). In FEP, multiple meta-analyses have reported whole brain reductions in grey matter volume (20–22), as well as reductions in hippocampal volume. Specifically, anterior hippocampal volume deficits have been reported in FEP (26), with "anterior" defined as containing the CA1, CA3, CA4, molecular layer, GC/DG, and subiculum/presubiculum subfields. Deceases in grey matter volume are also clinically relevant as they are positively correlated with symptom severity (27). Furthermore, degree of grey matter loss in the cerebellum within the first year of diagnosis has been correlated with worsening of negative symptoms and functional outcome at 5 year follow up (28).

To our knowledge, there is thus far only two reports that examined whole brain grey matter volume in CHR subjects. One reported a reduction in whole brain grey matter volume, (29), but the other did not (30), although the study may have been underpowered. However, multiple subsequent studies in CHR subjects have identified individual brain regions exhibiting grey matter reduction both at baseline compared to controls and post-conversion to psychosis. Two meta-analyses by the same group revealed that subjects who converted to psychosis had baseline reductions in the right inferior frontal gyrus and the right superior temporal gyrus compared to non-converters (31, 32). Although they didn't follow subjects longitudinally, Iwashiro et al. reported bilateral reduction of the pars triangularis within the inferior frontal gyrus in CHR subjects, and the degree of reduction was negatively correlated with severity of positive symptoms (33). Another large study reported reduced grey matter volume in the left parahippocampal cortex in CHR convertors compared to non-convertors (34). Increased grey matter loss in the right superior frontal, middle frontal and medial orbitofrontal regions was reported in CHR subjects who converted compared to both non-convertors and healthy controls (24). Grey matter loss occurred in the absence of treatment with antipsychotics, and reduction was also steeper in convertors who exhibited shorter duration of prodromal symptoms. An adjunct study to the previous report found a positive correlation between severity of prodromal symptoms, especially unusual thought content, and degree of grey matter loss among converters (35). Decrease in the right prefrontal region (36) and the right insular cortex (37) has been observed in convertors compared to non-convertors. Degree of decrease in the prefrontal region was associated with more severe negative symptoms at baseline, and longitudinally, convertors showed greater reduction over time compared to non-convertors. Finally, decreased grey matter in the right medial temporal, lateral temporal and inferior frontal cortex, and cingulate cortex bilaterally was observed at baseline in those who in converted compared to non-convertors (38). Collectively, these studies consistently identify grey matter deficits in the prefrontal cortex cingulate cortex and temporal lobes in CHR subjects who convert to psychosis versus those who do not, indicating that deficits in these regions may be more specific to psychosis than generalized mental illness.

White Matter Deficits

Although grey matter deficits have received much of the focus of investigation, multiple observations of white matter disruption in patients with schizophrenia have been reported (39). Postmortem data has revealed abnormal numbers and morphology of oligodendrocytes (40, 41). Genome wide association studies have also shown an increase in risk related to single nucleotide polymorphisms in oligodendrocyte specific genes (42). Furthermore, rodent models have shown that 2nd trimester insults, especially maternal infection, a known risk factor for schizophrenia (43), can produce a decrease in fractional anisotropy (FA) in fronto-striatal-limbic circuitry similar to that seen in the illness (44). Supporting these discoveries, investigators have characterized white matter abnormalities in the CHR population.

Voxel based morphometry of structural magnetic resonance images has been used to investigate white matter volume in CHR

subjects. In a cross-sectional study, Witthaus et al. reported a reduction in white matter volume in the right superior temporal lobe in CHR subjects compared to controls. This observation was enhanced in a separate cohort of FEP patients but not studied longitudinally in order to compare converters vs non-converters (45). However, imaging of the anterior genu of the corpus callosum revealed a significant reduction in thickness in CHR subjects who later converted to psychosis compared to both controls and CHR subjects who did not convert (46). Furthermore, the authors reported that a Cox regression analysis revealed that mean anterior genu thickness was predictive of transition to psychosis.

Diffusion tensor imaging, which indirectly measures the integrity of white matter tracts based on the diffusion of water molecules, has also been used to evaluate white matter integrity in CHR subjects. Unfortunately, to date, most studies did not follow CHR subjects longitudinally to evaluate baseline differences in converters vs non-converters. Furthermore, the findings are heterogeneous. Reduced fractional anisotropy has been reported both globally (47), as well as in the cingulum bundle (48), in cross sectional studies of CHR subjects at baseline compared to healthy controls. Furthermore, Karlsgodt et al. observed reduced FA in the superior longitudinal fasciculus (SLF) (49) in a similar comparison of CHR subjects to controls, and the SLF was also reported to exhibit increased mean diffusivity, another measure of reduced white matter integrity, in a different study (50). In a longitudinal study of CHR subjects that converted to psychosis, decreased FA was observed in the left frontal lobe (51). Bloemen et al. reported a similar finding; decreased FA in the bilateral medial frontal lobes, as well as the left putamen and the left superior temporal lobe in CHR subjects who converted compared to non-convertors and controls (52). However, not all investigations have yielded positive results. Peters et al. evaluated the uncinate and arcuate fasciculi, the anterior and dorsal cingulate, and subdivisions of the corpus callosum and did not find any differences between CHR subjects who converted to psychosis and those who did not (53).

Overall, decreased thickness in the corpus callosum and decreased FA in the frontal and temporal lobes are the most consistent phenotypes in convertors to psychosis. However, these findings require further replication in larger sample sizes.

FUNCTIONAL PHENOTYPES

Regional Abnormalities

With the development of fMRI, researchers were able to move beyond structural abnormalities and begin inferring changes in cortical activity *via* localized changes in cerebral blood flow and neurovascular coupling, either at rest or during specific cognitive tasks, in relevant brain regions for schizophrenia. One of the earliest and most consistent findings has been hippocampal hyperactivity at baseline in patients with chronic disease (54). The same finding was observed in first episode psychosis, as well as decreased recruitment during a scene processing task compared to controls (55). Interestingly, the degree of recruitment was inversely correlated with baseline activity. The authors attributed these findings to a worsening imbalance in excitation/inhibition as a result of interneuron dysfunction. To evaluate hippocampal activity in CHR subjects, arterial spin labeling (ASL) was used to measure regional cerebral blood flow (rCBF) (56). CHR subjects exhibited increased rCBF in the hippocampus, as well as in the basal ganglia and midbrain. Furthermore, subjects whose symptoms improved and no longer met criteria for CHR exhibited a significant reduction in left hippocampal rCBF. Unfortunately, subjects were not followed for progression to psychosis.

Multimodal imaging has been used to evaluate relationships between hippocampal activity and other neurotransmitters in CHR subjects. GABA concentration in the medial prefrontal cortex (mPFC) was measured using magnetic resonance spectroscopy (MRS), and a positive correlation was detected with hippocampal rCBF in subjects who converted to psychosis compared to non-convertors (57). MRI, fMRI, and MRS were combined to measure grey matter volume, cerebral blood volume (CBV), and glutamate in the hippocampus of CHR subjects, and both elevated glutamate and CBV was observed compared to controls (58). However, only baseline hippocampal atrophy predicted conversion to psychosis.

Deficits in working memory and the dorsolateral prefrontal cortex (DLPFC) have long been reported in patients with schizophrenia (59, 60). To evaluate DLPFC recruitment during working memory tasks, CHR subjects performed an item recognition task at baseline and were then followed for 2 years for conversion (61). CHR subjects performed as well as controls during the task. However, CHR subjects who later converted to psychosis showed a positive association between age and greater activation of the DLPFC, inferior frontal gyrus, frontal eye fields, and superior frontal gyrus, during verbal working memory tasks. The authors speculate that the greater activation may reflect compensatory activity. In CHR subjects who did not convert, several regions were positively associated with age and greater activation, but they were diffusely spread out throughout the temporal, parietal and occipital lobes, and not in the frontal lobes. Control subjects showed a negative association with age and activation of the DLPFC during verbal WM tasks, which was hypothesized to reflect maturation, and thus, greater efficiency of the circuit. In a different working memory task, the superior temporal gyrus (STG) showed reduced activation in controls, greater activation in subjects with FEP, and an intermediate level of activation in CHR subjects (62). The STG also failed to de-couple with the middle frontal gyrus, a finding that was even more pronounced in FEP subjects. Finally, CHR subjects showed decreased activation in fronto-parietal regions during encoding of a working memory task (63), along with increased activation in the STG.

Network Abnormalities

The Default Mode Network (DMN) is an interconnected set of brain regions, consisting of the mPFC, the posterior cingulate cortex, the inferior parietal lobules, the precuneus, and the medial temporal lobes. Functionally, the DMN is thought to be involved in internal mentation, such as thoughts regarding one's

self, thoughts about others, and reflecting on the past. Of particular importance, multiple regions of the DMN exhibit significant grey matter volume loss in patients with schizophrenia. Therefore, it is unsurprising that functional DMN abnormalities have been reported. In patients with schizophrenia, increased activity at rest is routinely observed compared to controls, and the degree of increase correlates to the severity of positive symptoms (64, 65).

CHR subjects also exhibit functional abnormalities in the DMN, although, to date, very few studies have investigated differences between converters and non-converters. In a verbal working memory task, healthy controls exhibited load dependent decreases in DMN activity, whereas CHR subjects maintained inappropriately elevated levels of DMN activity (66). CHR deficits were similar to, but less pronounced than, those seen in FEP subjects. Increased DMN connectivity, between the PCC/Precuneus and vmPFC, in CHR subjects is also associated with poorer clinical insight (67). Furthermore, graph theoretical analysis revealed a progressive reduction in efficiency in the DMN and an increase in network diversity in subjects who converted to psychosis (68), indicating continuing changes in brain networks as psychosis develops. Increased cerebellar-default mode network connectivity was also reported at resting state in CHR subjects (69). Specifically, there was increased connectivity between the right Crus 1 of the cerebellum and bilateral PCC/precuneus and between Lobule IX of the cerebellum and the left superior medial prefrontal cortex. There was also a positive correlation between precuneus connectivity and SIPS and PANSS scores in CHR subjects.

Patients with chronic disease have also been shown to exhibit functional dysconnectivity between the ventrolateral prefrontal cortex (vlPFC) and the amygdala (70). To evaluate this relationship prior to illness onset, CHR subjects were given an emotion activation task, and functional connectivity between the vlPFC and amygdala was evaluated (71). While performing the task, CHR individuals exhibited a proportional increase in activation in the amygdala and decrease in activation of the vlPFC, whereas controls exhibited the opposite pattern.

Another highly reproduced finding in the CHR population is disruptions in thalamocortical connectivity. Thalamocortical connectivity is disrupted at baseline in CHR subjects, and even more so in those who convert to psychosis (72). Specifically, there is hypoconnectivity between the thalamus and the prefrontal cortex, as well as the cerebellum. Furthermore, there is hyperconnectivity between the thalamus and the sensory motor areas. A meta-analysis on thalamocortical connectivity at baseline in CHR subjects found hypoconnectivity between the thalamus and the middle frontal and cingulate regions (73). Hyperconnectivity was found in motor, somatosensory, temporal, occipital, and insular regions. Furthermore, a strong negative correlation was found between hypo and hyperconnectivity, indicating that abnormalities in one are likely influencing abnormalities in the other. Finally, hyperconnectivity in the cerebello-thalamo-cortical circuitry has been reported, which correlated with degree of disorganized symptoms and time to conversion (74). The finding was also observed in patients with chronic schizophrenia.

Together these studies indicate multiple focal and regional abnormalities in functional connectivity in CHR subjects, some of which seem to be specific to conversion to psychosis. Further studies, specifically looking at conversion, are needed to validate some of the more promising phenotypes, such as baseline hippocampal activation and thalamocortical dysconnectivity.

INFLAMMATORY PHENOTYPES

Inflammation has long been associated with the pathophysiology of schizophrenia (75). Winter births and maternal infections (43), genetic risk associated with the major histocompatibility complex (76), and subsequent discovery of the association of complement protein C4A (77) all represent converging evidence for the involvement of inflammation in the disease. Furthermore, in CHR subjects, several lines of evidence indicate increased inflammation prior to first episode psychosis. Increased peripheral cytokines have been associated with both symptom severity and degree of grey matter loss in CHR subjects (24), as well as predicting conversion to psychosis (78), and peripheral TNF-alpha levels have been shown to predict negative symptom severity (79).

Translocator Protein 18D (TSPO) is an outer mitochondrial membrane protein with multiple functions that is found throughout the body. Increased expression in the brain has been linked to injury from any etiology (80), as well as activation of both microglia and astrocytes (81, 82). Thus, investigators have used PET imaging to measure degrees of activation and try to extrapolate levels of inflammation in the brains of patients with schizophrenia. Furthermore, given the hypothesis that grey matter loss may be secondary to hyperactive microglia, it was thought that elevated TSPO might be an indicator of this activity. Early studies in chronic cases reported an increase in TSPO signal in both total grey matter (83) and in the hippocampus (84). Subsequently, investigators began looking at CHR subjects for evidence of microglial activation prior to FEP. Of note, multiple radiotracers have been used to measure TSPO activation in the brain *via* PET imaging. [^{11}C]PK11195 was the first to be widely utilized. However, due to the relative non-specific binding of [^{11}C]PK11195, 2nd generation radiotracers were developed with significantly higher binding affinity; [^{11}C]DAA1106, [^{18}F]FEPPA, and [^{11}C]PBR28. However, due to the rs6971 polymorphism in the TSPO gene, a subject may be a high, medium, or low-affinity binder of the newer radiotracers. Therefore, genotyping of subjects prior to inclusion in a study, which is not always performed, is essential for accurate data interpretation. Complicating matters further, more recent studies using the 2nd generation ligands have failed to show an increase in TSPO in chronic disease (85, 86), and one meta-analysis (87) concluded that there was a decrease in TSPO signal.

Evaluating multiple cortical and subcortical brain regions, no evidence of increased TSPO signal was reported in CHR subjects using [^{11}C]PK11195 as the radioligand (88). Using the ligand [^{18}F]FEPPA in CHR subjects, and controlling for the TSPO

rs6971 polymorphism, no differences were observed in either the DLPFC or the hippocampus (89). Operating under the hypothesis that microglial pruning may be causative in grey matter loss, the same group then attempted to correlate changes in TSPO with grey matter volume reductions in CHR subjects. They found a positive correlation between increased TSPO signal and grey matter volume loss in FEP, but not in CHR subjects (90). Selvaraj et al. used the [^{11}C]PBR28 ligand to investigate the same relationship and also failed to observe an association between cortical grey matter volumes and TSPO signal in CHR subjects (91). They did find a negative association in patients with schizophrenia, suggesting that TSPO may be related to grey matter loss as the disease progresses. One positive finding has been reported. Using [^{11}C]PBR28, TSPO signal was elevated in total grey matter in CHR subjects at baseline compared to controls and was positively correlated with symptom severity (92). Patients with schizophrenia exhibited the same finding. Unfortunately, subjects were not followed longitudinally to evaluate signal changes in those who converted.

Beyond measuring TSPO signal levels in isolation, other groups have combined PET imaging with magnetic resonance spectroscopy (MRS) in order to examine the relationship between TSPO and other molecules. A negative correlation was reported between glutathione levels, an anti-oxidant, and TSPO using [^{18}F]FEPPA, in the medial prefrontal cortex (mPFC) of healthy volunteers (93). However, this association was not present in CHR subjects, suggesting an abnormal redox status in this population. No differences were seen in TSPO or glutathione levels between groups in direct comparisons. Also in the medial mPFC, a region highly implicated in the disease, GABA levels were negatively associated with TSPO signal in CHR subjects (94). Finally, PET imaging was used to measure dopamine release in the prefrontal cortex (PFC) during a stress task in CHR subjects. Subjects with lower stress induced PFC dopamine release exhibited higher TSPO increase in the hippocampus (95).

Although the findings involving TSPO signal and schizophrenia have been heterogeneous and controversial, no studies have yet examined TSPO signal between CHR subjects that converted to psychosis and those that did not. Given the growing evidence for the involvement of inflammation, it may be prudent to perform these experiments before closing the door on this modality.

NEUROTRANSMITTER SPECIFIC PHENOTYPES

Positron Emission Tomography (PET) is a common imaging modality that has been used to study the dynamics of neurotransmitter synthesis and release in patients with schizophrenia. Using radiotracers, such as 3,4-dihydroxy-6-[^{18}F]fluoro-L-phenylalanine (^{18}F-DOPA), researchers have been able to establish that aberrations in neurotransmitter systems, such as the dopaminergic system, are common in patients with chronic disease (96). Abnormalities have been found in presynaptic dopamine synthesis (97, 98), dopamine release following amphetamine administration (99, 100), and in occupancy of D2 receptors (101, 102). PET is now being used to examine neurotransmitter systems in the CHR population to investigate if similar abnormalities are present prior to FEP.

Increased ^{18}F-DOPA uptake was reported in the striatum, specifically the associative subdivision, of CHR subjects (103), indicating increased dopamine synthesis capacity, a finding that was replicated in a second cohort (104). Clinical follow up of the first cohort revealed that CHR subjects with the highest level of striatal dopamine synthesis converted to psychosis (105), and that progression towards psychosis was associated with increasing levels of dopamine (106). Other groups have also found increased fluorodopa uptake in the associative striatum in CHR subjects (107). Increased ^{18}F-DOPA uptake has been reported in the midbrain region in CHR subjects who converted compared to non-convertors (108). ^{1}H-MRS was used to measure hippocampal glutamate activity and was combined with ^{18}F-DOPA dopamine synthesis capacity in the evaluation of CHR subjects (109). Striatal dopamine synthesis capacity predicted worsening psychotic symptoms at clinical follow up, but not transition to psychosis, and was not significantly related to hippocampal glutamate concentration.

Recently, investigators have begun combining fMRI with PET imaging in order to correlate activation of implicated brain regions with neurotransmitter dysfunction. When given a verbal encoding and recognition task, CHR subjects showed a positive correlation between medial temporal lobe activation and striatal dopamine synthesis during encoding but not recognition (110). When given the Salience Attribution Test, CHR subjects were more likely to attribute motivational salience to irrelevant stimuli, and dopamine synthesis capacity was negatively correlated with hippocampal responses to irrelevant stimuli (111). Magnetic Resonance Spectroscopy (MRS) was used measure baseline hippocampal glutamate levels in CHR subjects, and higher levels were recorded in subjects who converted to psychosis (112). Higher levels were also associated with a poor functional outcome.

MACHINE LEARNING AND PREDICTION ALGORITHMS

The first part of this review summarized neural imaging phenotypes observed in CHR subjects, with an emphasis on subjects that converted to first episode psychosis compared to subjects who did not. The second part of this review will discuss the significant efforts that have been made using machine learning approaches to translate those observations into clinically relevant classification and prediction algorithms. As discussed in previous sections, a significant number of neuroimaging phenotypes have been discovered that differentiate CHR subjects who converted from those who did not. However, most of those studies evaluated average differences at the group level, which do not allow for inference or prediction at the individual level. With advances in computational methods, the field could move forward from traditional neuroimaging

analytic approaches to more sophisticated methodology that would employ neuroimaging data to make clinically relevant diagnoses and predictions. Machine learning, an application of artificial intelligence, allows for multivariate analyses and pattern recognition, which then allows for inference at the individual level. There are multiple machine learning methods, but the most common type applied to neuroimaging data in psychiatry has been the support vector machine (SVM). An SVM is a form of supervised learning, which learns by being trained on an initial dataset of known outcome and is then validated by applying it to another independent data set of known outcome [for further review of SVM and neuroimaging datasets see Orru et al., Neurosci Biobehav Rev, 2012, ref (113)]. In the realm of CHR subjects and psychosis, SVM has been used both in the classification and diagnosis of CHR subjects, as well as prediction of conversion to psychosis.

Machine Learning and Clinical Phenotypes

The first attempts at creating and validating risk calculators for conversion to psychosis were based solely on clinical symptomatology. From these early studies (11, 114), several high risk symptoms were able to be identified, such as high unusual thought content score, social impairment, and genetic risk for schizophrenia plus recent functional decline, and were part of one of the 1st psychosis risk calculators (115). The calculator achieved a C-index, similar to AUC but applicable to censored data, of 0.71, with a sensitivity and specificity of 66.7 and 72.1%, respectively, which indicates fair predictive accuracy. Risk calculators using similar variables were also created in China (116) and the UK (117) with equivalent results. However, the early risk calculators were based on inferences at the group level, making the applicability to the individual unclear. The first study to apply machine learning and SVM to clinical variables to predict individual transition to psychosis came from the PACE clinic in Australia. Four hundred sixteen subjects were included, and the accuracy of individual prediction was 64.6% with reported sensitivity and specificity of 68.6 and 60.6%, respectively (118). For an excellent table summarizing studies of clinical predictors of conversion to psychosis, see Worthington et al., Biol Psych, 2020, ref (119).

These early pioneering studies were useful in identifying which symptoms represent the greatest risk for conversion and showing the applicability of using machine learning to make predictions at the individual level. However, one inescapable conclusion from these studies is that while progress has been made in using machine learning to expand the predictive capabilities of risk calculators, clinical and demographic variables alone cannot predict individualized risk for conversion with a high enough accuracy to be clinically relevant. As discussed below, a combination of modalities and phenotypes will likely be necessary.

Machine Learning and Neuroimaging Phenotypes

Building upon the neuroimaging phenotypes between in CHR subjects, investigators have built machine learning algorithms to classify CHR subjects based on neuroimaging scans using structural and functional data sets. For example, Bendfeldt et al., evaluated fMRI data during a verbal working memory task from 19 CHR subjects and 19 controls and were able to separate CHR subjects from Controls with a balanced accuracy of 76.2% (sensitivity 89.5% and specificity 63.2%) (120). However, their algorithm could not correctly classify CHR from FEP or FEP from controls, likely due to small sample size. Another fMRI study of 34 CHR subjects and 37 controls focused on regional homogeneity, which summarizes functional connectivity between a given region and its local neighboring regions, and was able to classify CHR subjects with a sensitivity and specificity of 88 and 91%, respectively (121). In doing so, they noted that CHR subjects exhibited significant decreases in regional homogeneity in the left inferior temporal gyrus and increases in the right inferior frontal gyrus and right putamen compared with the controls. Of importance, Salvador et al. attempted to use structural MRI and a wide range of machine learning methods, as well as multiple structural metrics, to classify schizophrenia subjects versus controls (122). However, the largest balanced accuracy did not exceed 75%. Furthermore, their sample size of 128 patients with schizophrenia and 127 controls was considerably larger than the two previous studies. These results imply that, like clinical predictors, neuroimaging datasets alone may not be enough to achieve a level of accuracy necessary to be clinically relevant. One way investigators have sought to increase classification accuracy is by applying machine learning to multimodal datasets. For example, Valli et al. utilized machine learning to classify CHR subjects from controls by combining univariate and multivariate analyses to look at structural MRI and functional MRI during a verbal memory task (123). SVM applied to the structural MRI datasets identified CHR subjects from Controls with an accuracy of 72% (sensitivity and specificity of 68 and 76%, respectively). They also identified univariate differences at the group level in the fMRI data in the left middle frontal and precentral gyri, supramarginal gyrus, and insula as well as the right medial frontal gyrus. Finally, Lei et al. used SVM to analyze structural MRI datasets of both grey and white matter and rs-fMRI to classify schizophrenia vs controls and obtained an accuracy of 90.83% (124). The study utilized a multi-site design, which resulted in 295 patients and 452 controls at 5 different sites. Of note, they analyzed the datasets collected at each site separately because the SVM algorithm created for each dataset did not perform well when applied to the datasets at the other sites, a phenomenon that will be further discussed below.

Two other studies used machine learning to discover new phenotypes in the classification of CHR subjects. Chung et al. trained a machine learning algorithm on grey matter volumes in healthy subjects and correlated those measurements to subjects' chronological age to create a "brain age" (125). They then applied their algorithm to structural MRI scans from 275 CHR subjects. The difference between the estimated brain age and the chronological age was termed the "brain age gap". Overall, CHR subjects exhibited a brain age gap of 0.64[2.16] years.

Younger CHR subjects (12–17 years) who later converted exhibited a brain age gap of 1.59 years. Furthermore, the top 25 (out of 92) brain regions studied aligned with areas of significance to schizophrenia. A similar study used cognitive measures to create an algorithm to predict "neurocognitive age" relative to chronological age, and found that CHR subjects have delayed neurocognitive maturation of approximately 4.3 years compared to controls (126). However, this did not differ in converters vs non-converters. These studies show how machine learning can be used to generate new phenotypes that may aid in both classification and prediction.

Only a few studies to date have used machine learning algorithms to predict conversion to psychosis among CHR subjects. In 2012, Koutsouleris et al. trained an SVM algorithm on structural MRI datasets among 37 CHR subjects (16 of whom converted) and 22 volunteers (127). A balanced accuracy of 84.2% was achieved in classifying converters vs non-converters (sensitivity 81%, specificity 87.5%). A follow up study by the same group validated their previous findings in 73 CHR subjects from two different sites (128). This time, the accuracy of prediction was 80% (sensitivity 76%, specificity 85%). They also used their algorithm to stratify subjects at baseline into high, intermediate, and low risk, and the high-risk group had a transition rate of 88% and the low risk group had a transition rate of 8%.

One complication in predicting conversion to psychosis is that there are potentially multiple pathophysiological routes. As a result, being able to predict functional outcome, regardless of presence or absence of psychosis, may be just as valuable. Several investigators have used machine learning to explore this avenue. Kambietz-Ilankovic et al. used structural MRI at baseline and the Global Assessment of Functioning (GAF) scale at clinical follow up to predict functional outcome in 27 CHR subjects (129). Classifying outcome as "good" or "poor" achieved an accuracy of 82%. In a similar vein, de Wit et al. looked at predicting resilience as a primary outcome in 64 CHR subjects (130). They, as well, used sMRI at baseline and the GAF score at 6 year clinical follow up as an indicator of resilience. However, they used support vector regression analyses, allowing for predictions along a continuous, instead of binary, scale. The highest correlation, 0.42, was found between long term functioning and subcortical volumes. Finally, a report by the PRONIA consortium combined clinical variables with structural MRI datasets to predict 1 year social and role-functioning outcome in 116 CHR subjects (131). The accuracy of prediction using clinical variables was 76.9%, using structural MRI variables was 76.2%, and in combined models was 82.7%. These results show definitively how combining multi-model datasets increases accuracy of prediction and will be necessary moving forward.

To summarize, the application of machine learning to neuroimaging datasets has allowed for new paradigms to be created in the classification and outcome prediction of CHR subjects. However, it is clear that a single modality, whether clinical, imaging, or other, will likely not provide enough information to allow for more accurate predictions. A combination of clinical variables and neuroimaging data improves prediction accuracy compared to either modality alone. Continued application and testing of different modalities in different combinations will be essential.

DISCUSSION AND CONCLUSION

The prodromal period in schizophrenia, during which time clinically high-risk subjects experiencing attenuated symptoms may present for care, represents a critical window for identification, stratification of risk, and implementation of appropriate therapies. Although the illness carries a strong genetic risk, the leading theory surrounding development of schizophrenia is the "two hit" phenomena, whereby environmental stressors act upon genetic predisposition to initiate progression to first episode psychosis. This implies that development of illness may not be inevitable, and that prevention of conversion is not an unreasonable goal. For this to occur, however, progress needs to continue in several areas. There must be continued identification of biomarkers in longitudinal studies that follow CHR subjects through conversion. Only then will it be possible to segregate abnormalities at baseline into genetic or clinical risk. Biomarkers that identify clinical risk need to continue to be combined and administered in prospective studies that assess their predictive power. The underlying mechanisms driving development of the biomarker will then need to be elucidated in preclinical or *in vitro* models of disease. Only once the predictive framework is established, and mechanisms understood, will new therapeutic models and targets emerge for testing in clinical trials.

Neuroimaging has been successful in identifying multiple indicators of pathology in CHR subjects; some that represent generalized mental illness and are present in both converters and non-converters, and some that represent risk for psychosis and are present only in converters (see **Figure 1**). Structural MRI studies have identified multiple phenotypes in CHR subjects that convert to psychosis. Although enlarged lateral ventricles are well replicated in both first episode psychosis and chronic disease, only 3rd ventricular expansion has been reported and replicated in CHR convertors vs non-convertors. As enlarged lateral ventricles are thought to be secondary to decreased grey matter volume, an enlarged 3rd ventricle may represent earlier deficits in subcortical thalamic regions, or even the temporal lobes. However, although decreased thalamic volume has been reported in chronic disease, a recent study found no difference in thalamic volume in CHR subjects compared with controls (132). Furthermore, a longitudinal analysis of neuroimaging data from CHR subjects who later developed psychosis concluded that ventricular expansion was linked in time to progressive grey matter loss and not to structural changes in subcortical regions (133). Reductions in grey matter volume have been consistently reported in the frontal (superior frontal, prefrontal, middle frontal, medial orbitofrontal, inferior frontal gyri, and insular cortex) and temporal lobes (lateral temporal, medial temporal, and parahippocampal cortex) in CHR subjects that convert. Very interestingly, the degree and timing of grey matter loss may

depend on age of symptom onset. In a recent report, Chung et al. evaluated baseline MRI parameters of converters and non-converters and observed that younger CHR subjects (12–17 years old) that converted to psychosis exhibited decreased grey matter volume at baseline and a less steep grey matter decline at first episode psychosis (134). However, older CHR subjects (> 18yrs old) that converted to psychosis did not have decreased grey matter volume at baseline, but exhibited a much steeper rate of volume loss as illness progressed. The first type is more insidious and ultimately debilitating and indicates that there is heterogeneity in the progression of grey matter loss among CHR subjects that convert.

Two other structural phenotypes warrant further exploration in CHR subjects, cerebral asymmetry and olfactory bulb volume loss. Reduced cerebral asymmetry is a common observation in established schizophrenia (135), and is more pronounced in the language areas of the temporal lobes and the pars triangularis and pars orbitalis in the inferior frontal gyrus. In healthy people, this asymmetry is thought to be related to maturation of language regions and the establishment of language dominance in one side of the brain. For example, verbal fluency is correlated with the degree of lateralization, and it's been well established that patients with schizophrenia have decreased verbal fluency (136). CHR subjects appear to have reduced cerebral asymmetry, similar to schizophrenia, compared with controls (137). However, this warrants further exploration in subjects who convert. Abnormalities in the olfactory system have been reported in CHR subjects (138). Bilateral reductions in olfactory bulb volume in males, as well as reduced left olfactory grey matter volume, were observed in subjects at baseline. Furthermore, left olfactory bulb volume correlated with negative symptom severity. However, these phenotypes have not been compared between converters and non-converters.

White matter abnormalities are also present in CHR subjects, and they mostly overlap with implicated regions of grey matter reduction, i.e. the frontal and temporal lobes. Deficits reported are either reduced volume or reduced structural integrity as measured by diffusion tensor imaging. Of particular interest is that subjects who converted exhibited decreased thickness in the anterior genu of the corpus callosum, implying that its inclusion in prediction algorithms may improve accuracy.

Functional imaging has revealed several highly replicable findings in CHR subjects who convert to psychosis. Hippocampal hyperactivity and reduced recruitment during relevant cognitive tasks have been reported multiple times using different modalities including rCBF, CBV, and measurement of glutamate. Elevated activity is thought to result from an imbalance in excitation/inhibition secondary to interneuron dysfunction and may be responsible for the mesolimbic hyperdopaminergic state seen in patients, as evidenced by preclinical models. Functional dysconnectivity has been reported between multiple brain regions in CHR subjects at baseline, including increased activation in the amygdala and decreased activation in the ventrolateral prefrontal cortex during emotion labeling tasks and inappropriate activation of the superior temporal gyrus and lack of decoupling with middle frontal gyrus during verbal working memory tasks. Increased activation of the default mode network (DMN) at baseline, with decreased suppression during cognitive tasks, has been observed in CHR subjects. Subjects that convert exhibit abnormal thalamocortical connectivity, specifically hypoconnectivity between the thalamus and the prefrontal cortex and cerebellum, and hyperconnectivity between the thalamus and the sensory motor areas.

Inflammation has been strongly implicated in the pathophysiology of schizophrenia, in both FEP and chronic disease. Surprisingly, most studies have failed to find an increase in TSPO signaling in CHR subjects, either using 1st or 2nd generation radioligands. This may be due to the inference of TSPO as a marker for microglial activation, as it is known to be expressed on both microglia and astrocytes. Furthermore, the early evidence for an elevated signal used the 1st generation radioligand, [^{11}C]PK11195, which was later shown to have significant non-specific binding. Given the preponderance of evidence that inflammation is present during both the prodromal period and first episode psychosis, the lack of TSPO abnormalities may reflect more on the method than the pathophysiology. Furthermore, to the best of our knowledge there are no reports comparing TSPO signal between converters and non-converters, and these studies may help determine whether TSPO should be used moving forward or not.

Finally, CHR subjects that convert to psychosis have been shown to exhibit neurotransmitter abnormalities, including increased dopamine synthesis capacity in the dorsal and associative striatum. Higher levels predicted transition to psychosis, as did increased dopamine synthesis capacity in the midbrain. Furthermore, when given a verbal encoding and recognition task, CHR subjects showed a positive correlation between medial temporal lobe activation and striatal dopamine synthesis during encoding but not recognition.

One of the major challenges in using clinical or neuroimaging phenotypes discovered in CHR subjects is applying that knowledge at the individual level to predict conversion. The latest front in the prediction of psychosis is to apply machine learning methods to datasets of those phenotypes. Training algorithms on datasets of known outcome has allowed investigators to begin fine-tuning accuracies of prediction to greater and greater degrees. Seemingly, the greatest progress has come when combining modalities, such as clinical and neuroimaging, implying that heterogeneity within each modality may prevent anyone from being singularly adequate for prediction. One can hypothesize, then, that further combinations of modalities may finally allow for balanced accuracies to cross the 90th percentile. Therefore, along with the known clinical and neuroimaging predictors, adding in peripheral blood phenotypes may aid as well. For example, Perkins et al. looked at peripheral blood analytes, specifically 15 analytes reflecting markers of inflammation, oxidative stress, hormones and metabolism, and were able to distinguish CHR converters from non-converters, with an area under the ROC curve of 0.88 (78). Furthermore, CHR subjects were found to

have higher blood cortisol levels compared to controls, which moderately correlated with symptom severity, with higher baseline cortisol in those who converted (139).

Multiple challenges exist when using machine learning to create prediction algorithms. One major challenge is the small sample sizes of CHR populations, especially considering the low conversion rate. In order to attain large enough sample sizes, multi-site studies are necessary. However, multi-site studies incur their own challenges, most significant of which is inter-site variability in data collection and processing. Multiple strategies have been implemented to try to overcome this variability. One such strategy is the leave-one-out strategy, whereby an algorithm is trained on datasets from all sites but one, which is then used to validate the algorithm. Another is strategy is the healthy traveler design, in which healthy volunteers physically travel to each site in the study for scanner and software calibration. Furthermore, data must be collected on the same model equipment and must be processed using the same software. Software updates must be implemented at the same time across sites. Finally, overfitting of the model, due to small sample sizes, may explain some of the difficulties in validating external datasets and may also explain why accuracies appear to decrease with increasing sample size. It has been suggested that limiting the number of predictors compared to the number of converters may assist in solving this problem (119). One example of a large multi-site consortium trying to overcome these issues is the PSYSCAN Consortium (140). They have developed a protocol which aims to use multimodal methodologies (clinical, cognitive, genetics, blood, and imaging) and machine learning to create algorithms that predict conversion.

In conclusion, neuroimaging has significantly contributed to our understanding of developing abnormalities in the clinically high-risk population for psychosis. Further longitudinal research, in order to identify differences between converters and non-converters, large multi-site studies, the combination of multi-modal predictors, and machine learning algorithms that allow for prediction at the individual level will be necessary to identify the pre-conversion changes that are most clinically relevant and build more accurate prediction algorithms.

AUTHOR CONTRIBUTIONS

DG and JE equally contributed to the literature review, synthesis, and writing of the manuscript. All authors contributed to the article and approved the submitted version.

FUNDING

This review has been supported by the National Institute of Mental Health (K23 MH114037 to DG. JE is supported by an R25 MH101079).

REFERENCES

1. Kooyman I, Dean K, Harvey S, Walsh E. Outcomes of public concern in schizophrenia. *Br J Psychiatry Suppl* (2007) 50:s29–36. doi: 10.1192/bjp.191.50.s29
2. Murray CJ, Lopez AD. Alternative projections of mortality and disability by cause 1990-2020: Global Burden of Disease Study. *Lancet* (1997) 349 (9064):1498–504. doi: 10.1016/S0140-6736(96)07492-2
3. Laursen TM, Nordentoft M, Mortensen PB. Excess early mortality in schizophrenia. *Annu Rev Clin Psychol* (2014) 10:425–48. doi: 10.1146/annurev-clinpsy-032813-153657
4. Goeree R, Farahati F, Burke N, Blackhouse G, O'Reilly D, Pyne J, et al. The economic burden of schizophrenia in Canada in 2004. *Curr Med Res Opin* (2005) 21(12):2017–28. doi: 10.1185/030079905X75087
5. McEvoy JP. The costs of schizophrenia. *J Clin Psychiatry* (2007) 68 Suppl 14:4–7.
6. Fervaha G, Foussias G, Agid O, Remington G. Motivational and neurocognitive deficits are central to the prediction of longitudinal functional outcome in schizophrenia. *Acta Psychiatr Scand* (2014) 130 (4):290–9. doi: 10.1111/acps.12289
7. Harvey PD. Assessment of everyday functioning in schizophrenia: implications for treatments aimed at negative symptoms. *Schizophr Res* (2013) 150(2-3):353–5. doi: 10.1016/j.schres.2013.04.022
8. Addington J, Liu L, Buchy L, Cadenhead KS, Cannon TD, Cornblatt BA, et al. North American Prodrome Longitudinal Study (NAPLS 2): The Prodromal Symptoms. *J Nerv Ment Dis* (2015) 203(5):328–35. doi: 10.1097/NMD.0000000000000290
9. Piskulic D, Addington J, Cadenhead KS, Cannon TD, Cornblatt BA, Heinssen R, et al. Negative symptoms in individuals at clinical high risk of psychosis. *Psychiatry Res* (2012) 196(2-3):220–4. doi: 10.1016/j.psychres.2012.02.018
10. Tarbox SI, Addington J, Cadenhead KS, Cannon TD, Cornblatt BA, Perkins DO, et al. Functional development in clinical high risk youth: prediction of schizophrenia versus other psychotic disorders. *Psychiatry Res* (2014) 215 (1):52–60. doi: 10.1016/j.psychres.2013.10.006
11. Cannon TD, Cadenhead K, Cornblatt B, Woods SW, Addington J, Walker E, et al. Prediction of psychosis in youth at high clinical risk: a multisite longitudinal study in North America. *Arch Gen Psychiatry* (2008) 65(1):28–37. doi: 10.1001/archgenpsychiatry.2007.3
12. Lin A, Wood SJ, Nelson B, Beavan A, McGorry P, Yung AR. Outcomes of nontransitioned cases in a sample at ultra-high risk for psychosis. *Am J Psychiatry* (2015) 172(3):249–58. doi: 10.1176/appi.ajp.2014.13030418
13. Addington J, Piskulic D, Liu L, Cadenhead KS, Cannon TD, Cornblatt BA, et al. Comorbid diagnoses for youth at clinical high risk of psychosis. *Schizophr Res* (2017) 190:90–5. doi: 10.1016/j.schres.2017.03.043
14. Kline ER, Seidman LJ, Cornblatt BA, Woodberry KA, Bryant C, Bearden CE, et al. Depression and clinical high-risk states: Baseline presentation of depressed vs. non-depressed participants in the NAPLS-2 cohort. *Schizophr Res* (2018) 192:357–63. doi: 10.1016/j.schres.2017.05.032
15. Jacobi W, Winkler H. Encephalographische studien an chronisch schizophrenen. *Arch Psychiatr Nervenkr* (1927) 81:299–332. doi: 10.1007/BF01825649
16. Weinberger DR, Torrey EF, Neophytides AN, Wyatt RJ. Lateral cerebral ventricular enlargement in chronic schizophrenia. *Arch Gen Psychiatry* (1979) 36(7):735–9. doi: 10.1001/archpsyc.1979.01780070013001
17. Fusar-Poli P, Smieskova R, Kempton MJ, Ho BC, Andreasen NC, Borgwardt S. Progressive brain changes in schizophrenia related to antipsychotic treatment? A meta-analysis of longitudinal MRI studies. *Neurosci Biobehav Rev* (2013) 37 (8):1680–91. doi: 10.1016/j.neubiorev.2013.06.001
18. Olabi B, Ellison-Wright I, McIntosh AM, Wood SJ, Bullmore E, Lawrie SM. Are there progressive brain changes in schizophrenia? A meta-analysis of structural magnetic resonance imaging studies. *Biol Psychiatry* (2011) 70 (1):88–96. doi: 10.1016/j.biopsych.2011.01.032
19. Kempton MJ, Stahl D, Williams SC, DeLisi LE. Progressive lateral ventricular enlargement in schizophrenia: a meta-analysis of longitudinal MRI studies. *Schizophr Res* (2010) 120(1-3):54–62. doi: 10.1016/j.schres.2010.03.036
20. De Peri L, Crescini A, Deste G, Fusar-Poli P, Sacchetti E, Vita A. Brain structural abnormalities at the onset of schizophrenia and bipolar disorder: a meta-analysis of controlled magnetic resonance imaging studies. *Curr Pharm Des* (2012) 18(4):486–94. doi: 10.2174/138161212799316253

21. Steen RG, Mull C, McClure R, Hamer RM, Lieberman JA. Brain volume in first-episode schizophrenia: systematic review and meta-analysis of magnetic resonance imaging studies. *Br J Psychiatry* (2006) 188:510–8. doi: 10.1192/bjp.188.6.510
22. Vita A, De Peri L, Silenzi C, Dieci M. Brain morphology in first-episode schizophrenia: a meta-analysis of quantitative magnetic resonance imaging studies. *Schizophr Res* (2006) 82(1):75–88. doi: 10.1016/j.schres.2005.11.004
23. Ziermans TB, Schothorst PF, Schnack HG, Koolschijn PC, Kahn RS, van Engeland H, et al. Progressive structural brain changes during development of psychosis. *Schizophr Bull* (2012) 38(3):519–30. doi: 10.1093/schbul/sbq113
24. Cannon TD, Chung Y, He G, Sun D, Jacobson A, van Erp TGM, et al. Progressive reduction in cortical thickness as psychosis develops: a multisite longitudinal neuroimaging study of youth at elevated clinical risk. *Biol Psychiatry* (2015) 77(2):147–57. doi: 10.1016/j.biopsych.2014.05.023
25. van Erp TGM, Walton E, Hibar DP, Schmaal L, Jiang W, Glahn DC, et al. Cortical Brain Abnormalities in 4474 Individuals With Schizophrenia and 5098 Control Subjects via the Enhancing Neuro Imaging Genetics Through Meta Analysis (ENIGMA) Consortium. *Biol Psychiatry* (2018) 84(9):644–54. doi: 10.1016/j.biopsych.2018.04.023
26. McHugo M, Talati P, Woodward ND, Armstrong K, Blackford JU, Heckers S. Regionally specific volume deficits along the hippocampal long axis in early and chronic psychosis. *NeuroImage Clin* (2018) 20:1106–14. doi: 10.1016/j.nicl.2018.10.021
27. Clementz BA, Sweeney JA, Hamm JP, Ivleva EI, Ethridge LE, Pearlson GD, et al. Identification of Distinct Psychosis Biotypes Using Brain-Based Biomarkers [published correction appears. *Am J Psychiatry* (2016) 173 (4):373–84. doi: 10.1176/appi.ajp.2015.14091200
28. Cahn W, van Haren NE, Hulshoff Pol HE, Schnack HG, Caspers E, Laponder DA, et al. Brain volume changes in the first year of illness and 5-year outcome of schizophrenia. *Br J Psychiatry* (2006) 189:381–2. doi: 10.1192/bjp.bp.105.015701
29. Velakoulis D, Wood SJ, Wong MT, McGorry PD, Yung A, Phillips L, et al. Hippocampal and amygdala volumes according to psychosis stage and diagnosis: a magnetic resonance imaging study of chronic schizophrenia, first-episode psychosis, and ultra-high-risk individuals. *Arch Gen Psychiatry* (2006) 63(2):139–49. doi: 10.1001/archpsyc.63.2.139
30. Ziermans TB, Durston S, Sprong M, Nederveen H, van Haren NE, Schnack HG, et al. No evidence for structural brain changes in young adolescents at ultra high risk for psychosis. *Schizophr Res* (2009) 112(1-3):1–6. doi: 10.1016/j.schres.2009.04.013
31. Fusar-Poli P, Borgwardt S, Crescini A, Deste G, Kempton MJ, Lawrie S, et al. Neuroanatomy of vulnerability to psychosis: a voxel-based meta-analysis. *Neurosci Biobehav Rev* (2011) 35(5):1175–85. doi: 10.1016/j.neubiorev.2010.12.005
32. Fusar-Poli P, Radua J, McGuire P, Borgwardt S. Neuroanatomical maps of psychosis onset: voxel-wise meta-analysis of antipsychotic-naive VBM studies. *Schizophr Bull* (2012) 38(6):1297–307. doi: 10.1093/schbul/sbr134
33. Iwashiro N, Suga M, Takano Y, Inoue H, Natsubori T, Satomura Y, et al. Localized gray matter volume reductions in the pars triangularis of the inferior frontal gyrus in individuals at clinical high-risk for psychosis and first episode for schizophrenia. *Schizophr Res* (2012) 137(1-3):124–31. doi: 10.1016/j.schres.2012.02.024
34. Mechelli A, Riecher-Rössler A, Meisenzahl EM, Tognin S, Wood SJ, Borgwardt SJ, et al. Neuroanatomical abnormalities that predate the onset of psychosis: a multicenter study. *Arch Gen Psychiatry* (2011) 68(5):489–95. doi: 10.1001/archgenpsychiatry.2011.42
35. Chung Y, Jacobson A, He G, van Erp TGM, McEwen S, Addington J, et al. Prodromal Symptom Severity Predicts Accelerated Gray Matter Reduction and Third Ventricle Expansion Among Clinically High Risk Youth Developing Psychotic Disorders. *Mol Neuropsychiatry* (2015) 1(1):13–22. doi: 10.1159/000371887
36. Sun D, Phillips L, Velakoulis D, Yung A, McGorry PD, Wood SJ, et al. Progressive brain structural changes mapped as psychosis develops in 'at risk' individuals. *Schizophr Res* (2009) 108(1-3):85–92. doi: 10.1016/j.schres.2008.11.026
37. Takahashi T, Wood SJ, Yung AR, Phillips LJ, Soulsby B, McGorry PD, et al. Insular cortex gray matter changes in individuals at ultra-high-risk of developing psychosis. *Schizophr Res* (2009) 111(1-3):94–102. doi: 10.1016/j.schres.2009.03.024
38. Pantelis C, Velakoulis D, McGorry PD, Wood SJ, Suckling J, Phillips LJ, et al. Neuroanatomical abnormalities before and after onset of psychosis: a cross-sectional and longitudinal MRI comparison. *Lancet* (2003) 361(9354):281–8. doi: 10.1016/S0140-6736(03)12323-9
39. Davis KL, Stewart DG, Friedman JI, Buchsbaum M, Harvey PD, Hof PR, et al. White matter changes in schizophrenia: evidence for myelin-related dysfunction. *Arch Gen Psychiatry* (2003) 60(5):443–56. doi: 10.1001/archpsyc.60.5.443
40. Hof PR, Haroutunian V, Friedrich VLJr, Byne W, Buitron C, Perl DP, et al. Loss and altered spatial distribution of oligodendrocytes in the superior frontal gyrus in schizophrenia. *Biol Psychiatry* (2003) 53(12):1075–85. doi: 10.1016/s0006-3223(03)00237-3
41. Vikhreva OV, Rakhmanova VI, Orlovskaya DD, Uranova NA. Ultrastructural alterations of oligodendrocytes in prefrontal white matter in schizophrenia: A post-mortem morphometric study. *Schizophr Res* (2016) 177(1-3):28–36. doi: 10.1016/j.schres.2016.04.023
42. Hakak Y, Walker JR, Li C, Wong WH, Davis KL, Buxbaum JD, et al. Genome-wide expression analysis reveals dysregulation of myelination-related genes in chronic schizophrenia. *Proc Natl Acad Sci U S A* (2001) 98(8):4746–51. doi: 10.1073/pnas.081071198
43. Davies C, Segre G, Estradé A, Radua J, Micheli AD, Provenzani U, et al. Prenatal and perinatal risk and protective factors for psychosis: a systematic review and meta-analysis. *Lancet Psychiatry* (2020) 7(5):399–410. doi: 10.1016/S2215-0366(20)30057-2
44. Li Q, Cheung C, Wei R, Cheung V, Hui ES, You Y, et al. Voxel-based analysis of postnatal white matter microstructure in mice exposed to immune challenge in early or late pregnancy. *Neuroimage* (2010) 52(1):1–8. doi: 10.1016/j.neuroimage.2010.04.015
45. Witthaus H, Brüne M, Kaufmann C, Bohner G, Ozgürdal S, Gudlowski Y, et al. White matter abnormalities in subjects at ultra high-risk for schizophrenia and first-episode schizophrenic patients. *Schizophr Res* (2008) 102(1-3):141–9. doi: 10.1016/j.schres.2008.03.022
46. Walterfang M, Yung A, Wood AG, Reutens DC, Phillips L, Wood SJ, et al. Corpus callosum shape alterations in individuals prior to the onset of psychosis. *Schizophr Res* (2008) 103(1-3):1–10. doi: 10.1016/j.schres.2008.04.042
47. Krakauer K, Ebdrup BH, Glenthøj BY, Raghava JM, Nordholm D, Randers L, et al. Patterns of white matter microstructure in individuals at ultra-high-risk for psychosis: associations to level of functioning and clinical symptoms. *Psychol Med* (2017) 47(15):2689–707. doi: 10.1017/S0033291717001210
48. Fitzsimmons J, Rosa P, Sydnor VJ, Reid BE, Makris N, Goldstein JM, et al. Cingulum bundle abnormalities and risk for schizophrenia. *Schizophr Res* (2020) 215:385–91. doi: 10.1016/j.schres.2019.08.017
49. Karlsgodt KH, Niendam TA, Bearden CE, Cannon TD. White matter integrity and prediction of social and role functioning in subjects at ultra-high risk for psychosis. *Biol Psychiatry* (2009) 66(6):562–9. doi: 10.1016/j.biopsych.2009.03.013
50. von Hohenberg CC, Pasternak O, Kubicki M, Ballinger T, Vu MA, Swisher T, et al. White matter microstructure in individuals at clinical high risk of psychosis: a whole-brain diffusion tensor imaging study. *Schizophr Bull* (2014) 40(4):895–903. doi: 10.1093/schbul/sbt079
51. Carletti F, Woolley JB, Bhattacharyya S, Perez-Iglesias R, Fusar Poli P, Valmaggia L, et al. Alterations in white matter evident before the onset of psychosis. *Schizophr Bull* (2012) 38(6):1170–9. doi: 10.1093/schbul/sbs053
52. Bloemen OJ, de Koning MB, Schmitz N, Nieman DH, Becker HE, de Haan L, et al. White-matter markers for psychosis in a prospective ultra-high-risk cohort. *Psychol Med* (2010) 40(8):1297–304. doi: 10.1017/S0033291709991711
53. Peters BD, Dingemans PM, Dekker N, Blaas J, Akkerman E, van Amelsvoort TA, et al. White matter connectivity and psychosis in ultra-high-risk subjects: a diffusion tensor fiber tracking study. *Psychiatry Res* (2010) 181 (1):44–50. doi: 10.1016/j.pscychresns.2009.10.008
54. Tregellas JR. Neuroimaging biomarkers for early drug development in schizophrenia. *Biol Psychiatry* (2014) 76(2):111–9. doi: 10.1016/j.biopsych.2013.08.025

55. McHugo M, Talati P, Armstrong K, Vandekar SN, Blackford JU, Woodward ND, et al. Hyperactivity and Reduced Activation of Anterior Hippocampus in Early Psychosis [published correction appears in Am J Psychiatry. 2019 Dec 1;176(12):1051] [published correction appears in Am J Psychiatry. 2019 Dec 1;176(12):1056]. *Am J Psychiatry* (2019) 176(12):1030–8. doi: 10.1176/appi.ajp.2019.19020151
56. Allen P, Chaddock CA, Egerton A, Howes OD, Bonoldi I, Zelaya F, et al. Resting Hyperperfusion of the Hippocampus, Midbrain, and Basal Ganglia in People at High Risk for Psychosis. *Am J Psychiatry* (2016) 173(4):392–9. doi: 10.1176/appi.ajp.2015.15040485
57. Modinos G, Şimşek F, Azis M, Bossong M, Bonoldi I, Samson C, et al. Prefrontal GABA levels, hippocampal resting perfusion and the risk of psychosis [published correction appears in Neuropsychopharmacology. 2018 Oct 2;:]. *Neuropsychopharmacology* (2018) 43(13):2652–9. doi: 10.1038/s41386-017-0004-6
58. Provenzano FA, Guo J, Wall MM, Feng X, Sigmon HC, Brucato G, et al. Hippocampal Pathology in Clinical High-Risk Patients and the Onset of Schizophrenia. *Biol Psychiatry* (2020) 87(3):234–42. doi: 10.1016/j.biopsych.2019.09.022
59. Callicott JH, Ramsey NF, Tallent K, Bertolino A, Knable MB, Coppola R, et al. Functional magnetic resonance imaging brain mapping in psychiatry: methodological issues illustrated in a study of working memory in schizophrenia. *Neuropsychopharmacology* (1998) 18(3):186–96. doi: 10.1016/S0893-133X(97)00096-1
60. Kraguljac NV, Srivastava A, Lahti AC. Memory deficits in schizophrenia: a selective review of functional magnetic resonance imaging (FMRI) studies. *Behav Sci (Basel)* (2013) 3(3):330–47. doi: 10.3390/bs3030330
61. Karlsgodt KH, van Erp TG, Bearden CE, Cannon TD. Altered relationships between age and functional brain activation in adolescents at clinical high risk for psychosis. *Psychiatry Res* (2014) 221(1):21–9. doi: 10.1016/j.pscychresns.2013.08.004
62. Crossley NA, Mechelli A, Fusar-Poli P, Broome MR, Matthiasson P, Johns LC, et al. Superior temporal lobe dysfunction and frontotemporal dysconnectivity in subjects at risk of psychosis and in first-episode psychosis. *Hum Brain Mapp* (2009) 30(12):4129–37. doi: 10.1002/hbm.20834
63. Choi JS, Park JY, Jung MH, Jang JH, Kang DH, Jung WH, et al. Phase-specific brain change of spatial working memory processing in genetic and ultra-high risk groups of schizophrenia. *Schizophr Bull* (2012) 38(6):1189–99. doi: 10.1093/schbul/sbr038
64. Hu ML, Zong XF, Mann JJ, Zheng JJ, Liao YH, Li ZC, et al. A Review of the Functional and Anatomical Default Mode Network in Schizophrenia. *Neurosci Bull* (2017) 33(1):73–84. doi: 10.1007/s12264-016-0090-1
65. Garrity AG, Pearlson GD, McKiernan K, Lloyd D, Kiehl KA, Calhoun VD. Aberrant "default mode" functional connectivity in schizophrenia. *Am J Psychiatry* (2007) 164(3):450–7. doi: 10.1176/ajp.2007.164.3.450
66. Fryer SL, Woods SW, Kiehl KA, Calhoun VD, Pearlson GD, Roach BJ, et al. Deficient Suppression of Default Mode Regions during Working Memory in Individuals with Early Psychosis and at Clinical High-Risk for Psychosis. *Front Psychiatry* (2013) 4:92:92. doi: 10.3389/fpsyt.2013.00092
67. Clark SV, Mittal VA, Bernard JA, Ahmadi A, King TZ, Turner JA. Stronger default mode network connectivity is associated with poorer clinical insight in youth at ultra high-risk for psychotic disorders. *Schizophr Res* (2018) 193:244–50. doi: 10.1016/j.schres.2017.06.043
68. Cao H, Chung Y, McEwen SC, Bearden CE, Addington J, Goodyear B, et al. Progressive reconfiguration of resting-state brain networks as psychosis develops: Preliminary results from the North American Prodrome Longitudinal Study (NAPLS) consortium. *Schizophr Res* (2019), S0920–9964(19)30024-6. doi: 10.1016/j.schres.2019.01.017
69. Wang H, Guo W, Liu F, Wang G, Lyu H, Wu R, et al. Patients with first-episode, drug-naive schizophrenia and subjects at ultra-high risk of psychosis shared increased cerebellar-default mode network connectivity at rest. *Sci Rep* (2016) 6:26124. doi: 10.1038/srep26124
70. Fakra E, Salgado-Pineda P, Delaveau P, Hariri AR, Blin O. Neural bases of different cognitive strategies for facial affect processing in schizophrenia. *Schizophr Res* (2008) 100(1-3):191–205. doi: 10.1016/j.schres.2007.11.040
71. Gee DG, Karlsgodt KH, van Erp TG, Bearden CE, Lieberman MD, Belger A, et al. Altered age-related trajectories of amygdala-prefrontal circuitry in adolescents at clinical high risk for psychosis: a preliminary study. *Schizophr Res* (2012) 134(1):1–9. doi: 10.1016/j.schres.2011.10.005
72. Anticevic A, Haut K, Murray JD, Repovs G, Yang GJ, Diehl C, et al. Association of Thalamic Dysconnectivity and Conversion to Psychosis in Youth and Young Adults at Elevated Clinical Risk. *JAMA Psychiatry* (2015) 72(9):882–91. doi: 10.1001/jamapsychiatry.2015.0566
73. Ramsay IS. An Activation Likelihood Estimate Meta-analysis of Thalamocortical Dysconnectivity in Psychosis. *Biol Psychiatry Cognit Neurosci Neuroimaging* (2019) 4(10):859–69. doi: 10.1016/j.bpsc.2019.04.007
74. Cao H, Chén OY, Chung Y, Forsyth JK, McEwen SC, Gee DG, et al. Cerebello-thalamo-cortical hyperconnectivity as a state-independent functional neural signature for psychosis prediction and characterization. *Nat Commun* (2018) 9(1):3836. doi: 10.1038/s41467-018-06350-7
75. Miller BJ, Goldsmith DR. Towards an Immunophenotype of Schizophrenia: Progress, Potential Mechanisms, and Future Directions. *Neuropsychopharmacology* (2017) 42(1):299–317. doi: 10.1038/npp.2016.211
76. Schizophrenia Working Group of the Psychiatric Genomics Consortium. Biological insights from 108 schizophrenia-associated genetic loci. *Nature* (2014) 511(7510):421–7. doi: 10.1038/nature13595
77. Sekar A, Bialas AR, de Rivera H, Davis A, Hammond TR, Kamitaki N, et al. Schizophrenia risk from complex variation of complement component 4. *Nature* (2016) 530(7589):177–83. doi: 10.1038/nature16549
78. Perkins DO, Jeffries CD, Addington J, Bearden CE, Cadenhead KS, Cannon TD, et al. Towards a psychosis risk blood diagnostic for persons experiencing high-risk symptoms: preliminary results from the NAPLS project. *Schizophr Bull* (2015) 41(2):419–28. doi: 10.1093/schbul/sbu099
79. Goldsmith DR, Haroon E, Miller AH, Addington J, Bearden CE, Cadenhead KS, et al. Association of baseline inflammatory markers and the development of negative symptoms in individuals at clinical high risk for psychosis. *Brain Behav Immun* (2019) 76:268–74. doi: 10.1016/j.bbi.2018.11.315
80. Venneti S, Lopresti BJ, Wiley CA. The peripheral benzodiazepine receptor (Translocator protein 18kDa) in microglia: from pathology to imaging. *Prog Neurobiol* (2006) 80(6):308–22. doi: 10.1016/j.pneurobio.2006.10.002
81. Chen MK, Guilarte TR. Translocator protein 18 kDa (TSPO): molecular sensor of brain injury and repair. *Pharmacol Ther* (2008) 118(1):1–17. doi: 10.1016/j.pharmthera.2007.12.004
82. Guilarte TR. TSPO in diverse CNS pathologies and psychiatric disease: A critical review and a way forward. *Pharmacol Ther* (2019) 194:44–58. doi: 10.1016/j.pharmthera.2018.09.003
83. van Berckel BN, Bossong MG, Boellaard R, Kloet R, Schuitemaker A, Caspers E, et al. Microglia activation in recent-onset schizophrenia: a quantitative (R)-[11C]PK11195 positron emission tomography study. *Biol Psychiatry* (2008) 64(9):820–2. doi: 10.1016/j.biopsych.2008.04.025
84. Doorduin J, de Vries EF, Willemsen AT, de Groot JC, Dierckx RA, Klein HC. Neuroinflammation in schizophrenia-related psychosis: a PET study. *J Nucl Med* (2009) 50(11):1801–7. doi: 10.2967/jnumed.109.066647
85. Kenk M, Selvanathan T, Rao N, Suridjan I, Rusjan P, Remington G, et al. Imaging neuroinflammation in gray and white matter in schizophrenia: an in-vivo PET study with [18F]-FEPPA. *Schizophr Bull* (2015) 41(1):85–93. doi: 10.1093/schbul/sbu157
86. Takano A, Arakawa R, Ito H, Tateno A, Takahashi H, Matsumoto R, et al. Peripheral benzodiazepine receptors in patients with chronic schizophrenia: a PET study with [11C]DAA1106. *Int J Neuropsychopharmacol* (2010) 13(7):943–50. doi: 10.1017/S1461145710000313
87. Plavén-Sigray P, Matheson GJ, Collste K, Ashok AH, Coughlin JM, Howes OD, et al. Positron Emission Tomography Studies of the Glial Cell Marker Translocator Protein in Patients With Psychosis: A Meta-analysis Using Individual Participant Data. *Biol Psychiatry* (2018) 84(6):433–42. doi: 10.1016/j.biopsych.2018.02.1171
88. Di Biase MA, Zalesky A, O'keefe G, Laskaris EL, Baune BT, Weickert CS, et al. PET imaging of putative microglial activation in individuals at ultra-high risk for psychosis, recently diagnosed and chronically ill with schizophrenia. *Transl Psychiatry* (2017) 7(8):e1225. doi: 10.1038/tp.2017.193
89. Hafizi S, Da Silva T, Gerritsen C, Kiang M, Bagby RM, Prce I, et al. Imaging Microglial Activation in Individuals at Clinical High Risk for Psychosis: an In Vivo PET Study with [^{18}F]FEPPA. *Neuropsychopharmacology* (2017) 42(13):2474–81. doi: 10.1038/npp.2017.111

90. Hafizi S, Guma E, Koppel A, Silva TD, Kiang M, Houle S, et al. TSPO expression and brain structure in the psychosis spectrum. *Brain Behav Immun* (2018) 74:79–85. doi: 10.1016/j.bbi.2018.06.009
91. Selvaraj S, Bloomfield PS, Cao B, Veronese M, Turkheimer F, Howes OD. Brain TSPO imaging and gray matter volume in schizophrenia patients and in people at ultra high risk of psychosis: An [^{11}C]PBR28 study. *Schizophr Res* (2018) 195:206–14. doi: 10.1016/j.schres.2017.08.063
92. Bloomfield PS, Selvaraj S, Veronese M, Rizzo G, Bertoldo A, Owen DR, et al. Microglial Activity in People at Ultra High Risk of Psychosis and in Schizophrenia: An [(11)C]PBR28 PET Brain Imaging Study [published correction appears in Am J Psychiatry. 2017 Apr 1;174(4):402]. *Am J Psychiatry* (2016) 173(1):44–52. doi: 10.1176/appi.ajp.2015.14101358
93. Hafizi S, Da Silva T, Meyer JH, Kiang M, Houle S, Remington G, et al. Interaction between TSPO-a neuroimmune marker-and redox status in clinical high risk for psychosis: a PET-MRS study. *Neuropsychopharmacology* (2018) 43 (8):1700–5. doi: 10.1038/s41386-018-0061-5
94. Da Silva T, Hafizi S, Rusjan PM, Houle S, Wilson AA, Prce I, et al. GABA levels and TSPO expression in people at clinical high risk for psychosis and healthy volunteers: a PET-MRS study. *J Psychiatry Neurosci* (2019) 44 (2):111–9. doi: 10.1503/jpn.170201
95. Schifani C, Hafizi S, Tseng HH, Gerritsen C, Kenk M, Wilson AA, et al. Preliminary data indicating a connection between stress-induced prefrontal dopamine release and hippocampal TSPO expression in the psychosis spectrum. *Schizophr Res* (2019) 213:80–6. doi: 10.1016/j.schres.2018.10.008
96. Howes OD, Kambeitz J, Kim E, Stahl D, Slifstein M, Abi-Dargham A, et al. The nature of dopamine dysfunction in schizophrenia and what this means for treatment. *Arch Gen Psychiatry* (2012) 69(8):776–86. doi: 10.1001/archgenpsychiatry.2012.169
97. Hietala J, Syvälahti E, Vuorio K, Räkköläinen V, Bergman J, Haaparanta M, et al. Presynaptic dopamine function in striatum of neuroleptic-naive schizophrenic patients. *Lancet* (1995) 346(8983):1130–1. doi: 10.1016/s0140-6736(95)91801-9
98. Lindström LH, Gefvert O, Hagberg G, Lundberg T, Bergström M, Hartvig P, et al. Increased dopamine synthesis rate in medial prefrontal cortex and striatum in schizophrenia indicated by L-(beta-11C) DOPA and PET. *Biol Psychiatry* (1999) 46(5):681–8. doi: 10.1016/s0006-3223(99)00109-2
99. Abi-Dargham A, Gil R, Krystal J, Baldwin RM, Seibyl JP, Bowers M, et al. Increased striatal dopamine transmission in schizophrenia: confirmation in a second cohort. *Am J Psychiatry* (1998) 155(6):761–7. doi: 10.1176/ajp.155.6.761
100. Laruelle M, Abi-Dargham A, van Dyck CH, Gil R, D'Souza CD, Erdos J, et al. Single photon emission computerized tomography imaging of amphetamine-induced dopamine release in drug-free schizophrenic subjects. *Proc Natl Acad Sci U S A* (1996) 93(17):9235–40. doi: 10.1073/pnas.93.17.9235
101. Abi-Dargham A, Rodenhiser J, Printz D, Zea-Ponce Y, Gil R, Kegeles LS, et al. Increased baseline occupancy of D2 receptors by dopamine in schizophrenia. *Proc Natl Acad Sci U S A* (2000) 97(14):8104–9. doi: 10.1073/pnas.97.14.8104
102. Kegeles LS, Abi-Dargham A, Frankle WG, Gil R, Cooper TB, Slifstein M, et al. Increased synaptic dopamine function in associative regions of the striatum in schizophrenia. *Arch Gen Psychiatry* (2010) 67(3):231–9. doi: 10.1001/archgenpsychiatry.2010.10
103. Howes OD, Montgomery AJ, Asselin MC, Murray RM, Valli I, Tabraham P, et al. Elevated striatal dopamine function linked to prodromal signs of schizophrenia. *Arch Gen Psychiatry* (2009) 66(1):13–20. doi: 10.1001/archgenpsychiatry.2008.514
104. Egerton A, Chaddock CA, Winton-Brown TT, Bloomfield M, Bhattacharyya S, Allen P, et al. Presynaptic striatal dopamine dysfunction in people at ultra-high risk for psychosis: findings in a second cohort. *Biol Psychiatry* (2013) 74 (2):106–12. doi: 10.1016/j.biopsych.2012.11.017
105. Howes OD, Bose SK, Turkheimer F, Valli I, Egerton A, Valmaggia LR, et al. Dopamine synthesis capacity before onset of psychosis: a prospective [18F]-DOPA PET imaging study. *Am J Psychiatry* (2011) 168(12):1311–7. doi: 10.1176/appi.ajp.2011.11010160
106. Howes O, Bose S, Turkheimer F, Valli I, Egerton A, Stahl D, et al. Progressive increase in striatal dopamine synthesis capacity as patients develop psychosis: a PET study. *Mol Psychiatry* (2011) 16(9):885–6. doi: 10.1038/mp.2011.20
107. Fusar-Poli P, Howes OD, Allen P, Broome M, Valli I, Asselin MC, et al. Abnormal frontostriatal interactions in people with prodromal signs of psychosis: a multimodal imaging study. *Arch Gen Psychiatry* (2010) 67 (7):683–91. doi: 10.1001/archgenpsychiatry.2010.77
108. Allen P, Luigjes J, Howes OD, Egerton A, Hirao K, Valli I, et al. Transition to psychosis associated with prefrontal and subcortical dysfunction in ultra high-risk individuals. *Schizophr Bull* (2012) 38(6):1268–76. doi: 10.1093/schbul/sbr194
109. Howes OD, Bonoldi I, McCutcheon RA, Azis M, Antoniades M, Bossong M, et al. Glutamatergic and dopaminergic function and the relationship to outcome in people at clinical high risk of psychosis: a multi-modal PET-magnetic resonance brain imaging study. *Neuropsychopharmacology* (2020) 45(4):641–8. doi: 10.1038/s41386-019-0541-2
110. Allen P, Chaddock CA, Howes OD, Egerton A, Seal ML, Fusar-Poli P, et al. Abnormal relationship between medial temporal lobe and subcortical dopamine function in people with an ultra high risk for psychosis. *Schizophr Bull* (2012) 38(5):1040–9. doi: 10.1093/schbul/sbr017
111. Roiser JP, Howes OD, Chaddock CA, Joyce EM, McGuire P. Neural and behavioral correlates of aberrant salience in individuals at risk for psychosis [published correction appears in Schizophr Bull. 2016 Sep;42(5):1303]. *Schizophr Bull* (2013) 39(6):1328–36. doi: 10.1093/schbul/sbs147
112. Bossong MG, Antoniades M, Azis M, Samson C, Quinn B, Bonoldi I, et al. Association of Hippocampal Glutamate Levels With Adverse Outcomes in Individuals at Clinical High Risk for Psychosis. *JAMA Psychiatry* (2019) 76 (2):199–207. doi: 10.1001/jamapsychiatry.2018.3252
113. Orrù G, Pettersson-Yeo W, Marquand AF, Sartori G, Mechelli A. Using Support Vector Machine to identify imaging biomarkers of neurological and psychiatric disease: a critical review. *Neurosci Biobehav Rev* (2012) 36 (4):1140–52. doi: 10.1016/j.neubiorev.2012.01.004
114. Thompson A, Nelson B, Yung A. Predictive validity of clinical variables in the "at risk" for psychosis population: international comparison with results from the North American Prodrome Longitudinal Study. *Schizophr Res* (2011) 126(1-3):51–7. doi: 10.1016/j.schres.2010.09.024
115. Cannon TD, Yu C, Addington J, Bearden CE, Cadenhead KS, Cornblatt BA, et al. An Individualized Risk Calculator for Research in Prodromal Psychosis. *Am J Psychiatry* (2016) 173(10):980–8. doi: 10.1176/appi.ajp.2016.15070890
116. Zhang T, Xu L, Tang Y, Li H, Tang X, Cui H, et al. Prediction of psychosis in prodrome: development and validation of a simple, personalized risk calculator. *Psychol Med* (2019) 49(12):1990–8. doi: 10.1017/S0033291718002738
117. Fusar-Poli P, Rutigliano G, Stahl D, Davies C, Bonoldi I, Reilly T, et al. Development and Validation of a Clinically Based Risk Calculator for the Transdiagnostic Prediction of Psychosis [published correction appears in JAMA Psychiatry. 2018 Jul 1;75(7):759]. *JAMA Psychiatry* (2017) 74(5):493–500. doi: 10.1001/jamapsychiatry.2017.0284
118. Mechelli A, Lin A, Wood S, McGorry P, Amminger P, Tognin S, et al. Using clinical information to make individualized prognostic predictions in people at ultra high risk for psychosis. *Schizophr Res* (2017) 184:32–8. doi: 10.1016/j.schres.2016.11.047
119. Worthington MA, Cao H, Cannon TD. Discovery and Validation of Prediction Algorithms for Psychosis in Youths at Clinical High Risk. *Biol Psychiatry Cognit Neurosci Neuroimaging* (2020) 5(8):738–47. doi: 10.1016/j.bpsc.2019.10.006
120. Bendfeldt K, Smieskova R, Koutsouleris N, Klöppel S, Schmidt A, Walter A, et al. Classifying individuals at high-risk for psychosis based on functional brain activity during working memory processing. *NeuroImage Clin* (2015) 9:555–63. doi: 10.1016/j.nicl.2015.09.015
121. Wang S, Wang G, Lv H, Wu R, Zhao J, Guo W. Abnormal regional homogeneity as potential imaging biomarker for psychosis risk syndrome: a resting-state fMRI study and support vector machine analysis. *Sci Rep* (2016) 6:27619. doi: 10.1038/srep27619
122. Salvador R, Radua J, Canales-Rodríguez EJ, Solanes A, Sarró S, Goikolea JM, et al. Evaluation of machine learning algorithms and structural features for optimal MRI-based diagnostic prediction in psychosis. *PloS One* (2017) 12 (4):e0175683. doi: 10.1371/journal.pone.0175683
123. Valli I, Marquand AF, Mechelli A, Raffin M, Allen P, Seal ML, et al. Identifying Individuals at High Risk of Psychosis: Predictive Utility of

Support Vector Machine using Structural and Functional MRI Data. *Front Psychiatry* (2016) 7:52:52. doi: 10.3389/fpsyt.2016.00052
124. Lei D, Pinaya WHL, Young J, van Amelsvoort T, Marcelis M, Donohoe G, et al. Integrating machining learning and multimodal neuroimaging to detect schizophrenia at the level of the individual. *Hum Brain Mapp* (2020) 41(5):1119–35. doi: 10.1002/hbm.24863
125. Chung Y, Addington J, Bearden CE, Cadenhead KS, Cornblatt BA, Mathalon DH, et al. Use of Machine Learning to Determine Deviance in Neuroanatomical Maturity Associated With Future Psychosis in Youths at Clinically High Risk. *JAMA Psychiatry* (2018) 75(9):960–8. doi: 10.1001/jamapsychiatry.2018.1543
126. Kambeitz-Ilankovic L, Haas SS, Meisenzahl E, Dwyer DB, Weiske J, Peters H, et al. Neurocognitive and neuroanatomical maturation in the clinical high-risk states for psychosis: A pattern recognition study. *NeuroImage Clin* (2019) 21:101624. doi: 10.1016/j.nicl.2018.101624
127. Koutsouleris N, Borgwardt S, Meisenzahl EM, Bottlender R, Möller HJ, Riecher-Rössler A. Disease prediction in the at-risk mental state for psychosis using neuroanatomical biomarkers: results from the FePsy study. *Schizophr Bull* (2012) 38(6):1234–46. doi: 10.1093/schbul/sbr145
128. Koutsouleris N, Riecher-Rössler A, Meisenzahl EM, Smieskova R, Studerus E, Kambeitz-Ilankovic L, et al. Detecting the psychosis prodrome across high-risk populations using neuroanatomical biomarkers. *Schizophr Bull* (2015) 41 (2):471–82. doi: 10.1093/schbul/sbu078
129. Kambeitz-Ilankovic L, Meisenzahl EM, Cabral C, von Saldern S, Kambeitz J, Falkai P, et al. Prediction of outcome in the psychosis prodrome using neuroanatomical pattern classification. *Schizophr Res* (2016) 173(3):159–65. doi: 10.1016/j.schres.2015.03.005
130. de Wit S, Ziermans TB, Nieuwenhuis M, Schothorst PF, van Engeland H, Kahn RS, et al. Individual prediction of long-term outcome in adolescents at ultra-high risk for psychosis: Applying machine learning techniques to brain imaging data. *Hum Brain Mapp* (2017) 38(2):704–14. doi: 10.1002/hbm.23410
131. Koutsouleris N, Kambeitz-Ilankovic L, Ruhrmann S, Rosen M, Ruef A, Dwyer DB, et al. Prediction Models of Functional Outcomes for Individuals in the Clinical High-Risk State for Psychosis or With Recent-Onset Depression: A Multimodal, Multisite Machine Learning Analysis [published correction appears in JAMA Psychiatry. 2019 May 1;76(5):550]. *JAMA Psychiatry* (2018) 75(11):1156–72. doi: 10.1001/jamapsychiatry.2018.2165
132. Takahashi T, Tsugawa S, Nakajima S, Plitman E, Chakravarty MM, Masuda F, et al. Thalamic and striato-pallidal volumes in schizophrenia patients and individuals at risk for psychosis: A multi-atlas segmentation study [published online ahead of print, 2020 May 21]. *Schizophr Res* (2020), S0920–9964(20) 30223-1. doi: 10.1016/j.schres.2020.04.016
133. Chung Y, Haut KM, He G, van Erp TGM, McEwen S, Addington J, et al. Ventricular enlargement and progressive reduction of cortical gray matter are linked in prodromal youth who develop psychosis. *Schizophr Res* (2017) 189:169–74. doi: 10.1016/j.schres.2017.02.014
134. Chung Y, Allswede D, Addington J, Bearden CE, Cadenhead KS, Cornblatt BA, et al. Cortical abnormalities in youth at clinical high-risk for psychosis: Findings from the NAPLS2 cohort. *NeuroImage Clin* (2019) 23:101862. doi: 10.1016/j.nicl.2019.101862
135. Dollfus S, Razafimandimby A, Delamillieure P, Brazo P, Joliot M, Mazoyer B, et al. Atypical hemispheric specialization for language in right-handed schizophrenia patients. *Biol Psychiatry* (2005) 57(9):1020–8. doi: 10.1016/j.biopsych.2005.01.009
136. Goldberg TE, Aloia MS, Gourovitch ML, Missar D, Pickar D, Weinberger DR. Cognitive substrates of thought disorder, I: the semantic system. *Am J Psychiatry* (1998) 155(12):1671–6. doi: 10.1176/ajp.155.12.1671
137. Damme KSF, Vargas T, Calhoun V, Turner J, Mittal VA. Global and Specific Cortical Volume Asymmetries in Individuals With Psychosis Risk Syndrome and Schizophrenia: A Mixed Cross-sectional and Longitudinal Perspective. *Schizophr Bull* (2020) 46(3):713–21. doi: 10.1093/schbul/sbz096
138. Turetsky BI, Moberg PJ, Quarmley M, Dress E, Calkins ME, Ruparel K, et al. Structural anomalies of the peripheral olfactory system in psychosis high-risk subjects. *Schizophr Res* (2018) 195:197–205. doi: 10.1016/j.schres.2017.09.015
139. Walker EF, Trotman HD, Pearce BD, Addington J, Cadenhead KS, Cornblatt BA, et al. Cortisol levels and risk for psychosis: initial findings from the North American prodrome longitudinal study. *Biol Psychiatry* (2013) 74(6):410–7. doi: 10.1016/j.biopsych.2013.02.016
140. Tognin S, van Hell HH, Merritt K, Winter-van Rossum I, Bossong MG, Kempton MJ, et al. Towards Precision Medicine in Psychosis: Benefits and Challenges of Multimodal Multicenter Studies-PSYSCAN: Translating Neuroimaging Findings From Research into Clinical Practice. *Schizophr Bull* (2020) 46(2):432–41. doi: 10.1093/schbul/sbz067

Conflict of Interest: The authors declare that the research was conducted in the absence of any commercial or financial relationships that could be construed as a potential conflict of interest.

frontiers in Psychiatry

ORIGINAL RESEARCH
published: 21 October 2020
doi: 10.3389/fpsyt.2020.568982

DSM-5 Attenuated Psychosis Syndrome in Adolescents Hospitalized With Non-psychotic Psychiatric Disorders

*Gonzalo Salazar de Pablo[1,2], Daniel Guinart[3,4], Barbara A. Cornblatt[3,4,5], Andrea M. Auther[3,4], Ricardo E. Carrión[3,4,5], Maren Carbon[3], Sara Jiménez-Fernández[6,7], Ditte L. Vernal[8], Susanne Walitza[9], Miriam Gerstenberg[9], Riccardo Saba[10], Nella Lo Cascio[11], Martina Brandizzi[12], Celso Arango[2], Carmen Moreno[2], Anna Van Meter[3,4,5], Paolo Fusar-Poli[1,13,14] and Christoph U. Correll[3,4,5,15]**

[1] Early Psychosis: Interventions and Clinical-Detection (EPIC) Lab, Department of Psychosis Studies, Institute of Psychiatry, Psychology & Neuroscience, King's College London, London, United Kingdom, [2] Department of Child and Adolescent Psychiatry, Centro de Investigación Biomédica en Red de Salud Mental, General Universitario Gregorio Marañón School of Medicine, Institute of Psychiatry and Mental Health, Hospital Instituto de Investigación Sanitaria Gregorio Marañón (IiSGM), Universidad Complutense, Madrid, Spain, [3] Department of Psychiatry, The Zucker Hillside Hospital, Northwell Health, Glen Oaks, NY, United States, [4] Department of Psychiatry and Molecular Medicine, Donald and Barbara Zucker School of Medicine at Hofstra/Northwell, Hempstead, NY, United States, [5] Institute for Behavioral Science, The Feinstein Institutes for Medical Research, Manhasset, NY, United States, [6] Child and Adolescent Mental Health Unit, Jaén Medical Center, Jaén, Spain, [7] Department of Psychiatry, University of Granada, Granada, Spain, [8] Research Unit for Child- and Adolescent Psychiatry, Aalborg University Hospital, Aalborg, Denmark, [9] Psychiatric University Hospital Zurich, Department of Child and Adolescent Psychiatry and Psychotherapy, Zurich, Switzerland, [10] Department of Mental Health, Rome, Italy, [11] Prevention and Early Intervention Service, Department of Mental Health, Rome, Italy, [12] Local Health Agency Rome 1, Santo Spirito in Sassia Hospital, Department of Mental Health, Inpatient Psychiatric Unit, Rome, Italy, [13] Department of Brain and Behavioral Sciences, University of Pavia, Pavia, Italy, [14] Outreach and Support in South London Service, South London and Maudsley National Health Service Foundation Trust, London, United Kingdom, [15] Department of Child and Adolescent Psychiatry, Charité Universitätsmedizin, Berlin, Germany

OPEN ACCESS

Edited by:
Alessio Squassina, University of Cagliari, Italy

Reviewed by:
George Foussias, Center for Addiction and Mental Health (CAMH), Canada
Arthur D. P. Mak, The Chinese University of Hong Kong, China

***Correspondence:**
Christoph U. Correll
ccorrell@northwell.edu

Specialty section:
This article was submitted to Neuroimaging and Stimulation, a section of the journal Frontiers in Psychiatry

Received: *02 June 2020*
Accepted: *14 September 2020*
Published: *21 October 2020*

Citation:
Salazar de Pablo G, Guinart D, Cornblatt BA, Auther AM, Carrión RE, Carbon M, Jiménez-Fernández S, Vernal DL, Walitza S, Gerstenberg M, Saba R, Lo Cascio N, Brandizzi M, Arango C, Moreno C, Van Meter A, Fusar-Poli P and Correll CU (2020) DSM-5 Attenuated Psychosis Syndrome in Adolescents Hospitalized With Non-psychotic Psychiatric Disorders. Front. Psychiatry 11:568982. doi: 10.3389/fpsyt.2020.568982

Introduction: Although attenuated psychotic symptoms often occur for the first time during adolescence, studies focusing on adolescents are scarce. Attenuated psychotic symptoms form the criteria to identify individuals at increased clinical risk of developing psychosis. The study of individuals with these symptoms has led to the release of the DSM-5 diagnosis of Attenuated Psychosis Syndrome (APS) as a condition for further research. We aimed to characterize and compare hospitalized adolescents with DSM-5-APS diagnosis vs. hospitalized adolescents without a DSM-5-APS diagnosis.

Methods: Interviewing help-seeking, hospitalized adolescents (aged 12–18 years) and their caregivers independently with established research instruments, we (1) evaluated the presence of APS among non-psychotic adolescents, (2) characterized and compared APS and non-APS individuals regarding sociodemographic, illness and intervention characteristics, (3) correlated psychopathology with levels of functioning and severity of illness and (4) investigated the influence of individual clinical, functional and comorbidity variables on the likelihood of participants to be diagnosed with APS.

Results: Among 248 consecutively recruited adolescents (age=15.4 ± 1.5 years, females = 69.6%) with non-psychotic psychiatric disorders, 65 (26.2%) fulfilled APS criteria and 183 (73.8%) did not fulfill them. Adolescents with APS had higher number

of psychiatric disorders than non-APS adolescents (3.5 vs. 2.4, $p < 0.001$; Cohen's d = 0.77), particularly, disruptive behavior disorders (Cramer's V = 0.16), personality disorder traits (Cramer's V = 0.26), anxiety disorders (Cramer's V = 0.15), and eating disorders (Cramer's V = 0.16). Adolescents with APS scored higher on positive (Cohen's d = 1.5), negative (Cohen's d = 0.55), disorganized (Cohen's d = 0.51), and general symptoms (Cohen's d = 0.84), and were more severely ill (Cohen's d = 1.0) and functionally impaired (Cohen's d = 0.31). Negative symptoms were associated with lower functional levels (Pearson $\rho = -0.17$ to -0.20; $p = 0.014$ to 0.031). Global illness severity was associated with higher positive, negative, and general symptoms (Pearson $\rho = 0.22$ to 0.46; $p = 0.04$ to $p < 0.001$). APS status was independently associated with perceptual abnormalities (OR = 2.0; 95% CI = 1.6–2.5, $p < 0.001$), number of psychiatric diagnoses (OR = 1.5; 95% CI = 1.2–2.0, $p = 0.002$), and impaired stress tolerance (OR = 1.4; 95% CI = 1.1–1.7, $p = 0.002$) ($r^2 = 0.315$, $p < 0.001$).

Conclusions: A considerable number of adolescents hospitalized with non-psychotic psychiatric disorders meet DSM-5-APS criteria. These help-seeking adolescents have more comorbid disorders and more severe symptoms, functional impairment, and severity of illness than non-APS adolescents. Thus, they warrant high intensity clinical care.

Keywords: Attenuated Psychosis Syndrome (APS), adolescence, epidemiology, risk, psychosis, prevention

INTRODUCTION

Psychotic disorders, such as schizophrenia, are usually preceded by a clinical high-risk for psychosis (CHR-P) state (1), which is characterized by subtle symptoms, functional impairment and help-seeking behavior (2–4), as well as non-psychotic comorbidity (5, 6). The CHR-P state, which includes individuals at ultra-high risk for psychosis and/or those with basic symptoms, has allowed preventive efforts to be implemented (7, 8). This area of clinical research has grown until it has become one of the most established preventive approaches in psychiatry (7, 8).

The achievements and challenges of the CHR-P paradigm have been recently appraised by an umbrella review (9). In brief, three CHR-P subgroups have been established: attenuated psychotic symptoms; brief limited and intermittent psychotic symptoms (BLIPS) and genetic risk and deterioration (GRD) syndrome (9, 10). There are substantial diagnostic (11), prognostic (10, 12), clinical (13), and therapeutic (14) differences across these three subgroups. For example, psychosis risk is higher in the BLIPS group (38%) than in the attenuated psychotic symptoms group (24%) and higher in both groups than in the GRD group (8%) at >48 months follow-up (10).

Although most research and clinical studies have evaluated the three groups together (15–17), the most common group by far is the attenuated psychotic symptoms group, which includes 85% of CHR-P individuals (10). Psychosis-risk syndromes, including attenuated psychotic symptoms, are usually characterized using semi-structured interviews as the Structured Interview for Psychosis-Risk Syndromes (SIPS) (18, 19) or the Comprehensive Assessment of At-Risk Mental States (CAARMS) (1), which have comparable prognostic accuracy (20). In the SIPS, the characterization used is Attenuated Positive Symptoms Syndrome (APSS). Seven years ago, the DSM-5 introduced the Attenuated Psychosis Syndrome (APS) diagnosis in the research appendix, listed in both section II and section III (21) (**Figure 1**). This diagnosis is defined by the presence of delusions, hallucinations, or disorganized speech in attenuated form, but with sufficient severity and frequency to warrant clinical attention (23, 24) (**Figure 1**). The diagnostic, prognostic, and therapeutic characteristics of this diagnosis have been recently appraised by a systematic review and meta-analysis (21). This review concluded that DSM-5-APS criteria have received substantial concurrent and prognostic validation, mostly driven by research in adult populations (21). A previous study looking at the agreement between CAARMS and DSM-5-APS criteria found that the agreement was only moderate (kappa 0.59) (25). Meanwhile, as findings from other studies point out (26, 27), SIPS and DSM criteria for APS are more similar (**Figure 1**).

While most reports to date on APS are based on cohorts that also include adults (25, 28–30), APS features often occur for the first time in adolescence (31, 32). Broadly speaking, studies that focus on DSM-5-APS in adolescents are scarce (21, 22), and there are few studies on APS in adolescents in clinical care and hospital settings.

To our knowledge, only a few efforts have been made (22, 33, 34) to characterize APS, excluding other ultra-high risk criteria, and advance knowledge specifically in children and adolescents, comparing them to other help-seeking individuals. Among them, 22 APS individuals were compared to other treatment-seeking individuals and healthy controls regarding clinical and cognitive features (34), finding that APS was associated with impaired

Criteria	DSM-5-APS Section III (American Psychiatric Association, 2013)	DSM-5-APS Section II (American Psychiatric Association, 2013)	APSS SIPS (Miller et al., 1999;Miller et al., 2003;McGlashan T, 2010)
Severity	A. At least one of the following symptoms is present in attenuated form, with relatively intact reality testing, and is of sufficient severity or frequency to warrant clinical attention: 1. Delusions 2. Hallucinations 3. Disorganized speech	Examples of presentations that can be specified using this designation include APS. This syndrome is defined by psychotic-like symptoms below a threshold for full psychosis (e.g., they are less severe and more transient, and insight is relatively maintained)	SOPS-positive symptom scales P1. unusual thought content, P2. suspiciousness, P3. grandiose ideas, P4. perceptual abnormalities, P5. disorganized communication, with at least one of these symptoms rated 3, 4, or 5 indicating clinically significant disturbance below a psychotic level of intensity
Frequency	B. Symptom(s) must have been present at least once per week for the past month	Not specified	Symptoms ever been present at an average frequency of at least once/week over a month
New onset and worsening	C. Symptom(s) must have begun or worsened in the past year	Not specified	Begin within the past year, or any currently rate one or more scale points higher compared to 12 months ago; rated only symptoms that occurred over the past month
Distress/disability	D. Symptom(s) is sufficiently distressing and disabling to the individual to warrant clinical attention	Symptoms cause clinically significant distress or impairment in social, occupational, or other important areas of functioning.	Attenuated positive symptoms sufficiently distressing and disabling to the patient to warrant clinical attention
Differential diagnosis	E. Symptom(s) is not better explained by another mental disorder, including a depressive or bipolar disorder with psychotic features, and is not attributable to the physiological effects of a substance or another medical condition	Symptoms do not meet the full criteria for any of the disorders in the schizophrenia spectrum and other psychotic disorders diagnostic class	Symptoms ever not been explained better by another DSM disorder

FIGURE 1 | DSM-5-APS Attenuated Psychosis Syndrome diagnostic criteria compared with SIPS operationalization [adapted from (Gerstenberg et al. (22); Salazar De Pablo et al. (21)]. APS, Attenuated Psychosis Syndrome; APSS, Attenuated Positive Symptoms Syndrome; SIPS, Structured Interview for Psychosis-Risk Syndromes.

neurocognition. Also, APS was associated with self-reported internalizing problems and thought problems in a study with 7 APS adolescents (33). One further study without a comparison group found that an older age of APS presentation in adolescents (comparing 9–14 years vs. 15–18 years) was associated with better social and role functioning and fewer depressive symptoms (35).

There is little evidence on how many help-seeking adolescents accessing inpatient care meet APS criteria. Our preliminary data from the Adolescent Mood Disorder and Psychosis Study (AMDPS) clinical study compared the first 21 APS and 68 non-APS adolescents who were recruited and found that APS was present in 23.6% of psychiatrically hospitalized adolescents, who suffered from a broad range of psychiatric symptoms and disorders (22).

Although specific knowledge for APS is limited, CHR-P individuals show impairments in work, educational and social functioning as well as poor quality of life (9, 36). Furthermore, psychopathology can adversely influence functioning (37). Negative symptoms have been associated with functioning, both daily (38), work related (39) and real-world functioning (40). Among CHR-P individuals, the severity of attenuated positive and negative symptoms has been associated with some outcomes [e.g., transition to psychosis (9, 21)] but not with others [e.g., cannabis use (9)]. Our preliminary results showed that poorer functioning in adolescents with APS was associated with more severe attenuated positive, negative, and general symptoms (22).

In the CHR-P field, the influence of sociodemographic and clinical variables on diagnostic and treatment outcomes has been widely studied, particularly regarding the transition to psychosis (41–45). Unusual thought content and suspiciousness have been found to predict conversion to psychosis along with decline in social functioning, lower verbal learning and memory performance (46). However, there is no convincing evidence of the association between any variable and the onset of psychotic disorders according to a meta-analysis, and only attenuated positive psychotic symptoms and global functioning show suggestive evidence (47). The influence of demographic and clinical variables on the presence of APS, particularly in adolescents, is even less known. In the first 89 individuals recruited into AMDPS, lowest GAF score in the past year, and social isolation were independently associated with APS (22).

The current study analyzes the final sample of this cohort of hospitalized adolescents to (1) assess how many non-psychotic, help-seeking adolescents accessing inpatient care meet APS criteria, (2) describe and compare both groups regarding sociodemographic, illness and intervention characteristics, (3) correlate attenuated positive, negative, general and disorganized symptoms with the level of functioning and severity of illness, and (4) investigate the influence of individual clinical, functional and comorbidity variables, selected empirically, on the likelihood of participants to be diagnosed with APS.

Based on prior literature, we hypothesized that (1) a significant number of adolescents with non-psychotic psychiatric disorders would fulfill APS criteria, (2) APS individuals would report significant comorbidity, clinical burden and functional impairment that would exceed those of non-APS individuals, (3) severity of negative symptoms would be significantly associated with the level of functioning and severity of illness, and (4)

APS status would be associated with specific attenuated positive symptoms and other clinical variables.

MATERIALS AND METHODS

Design and Setting

AMDPS was registered at ClinicalTrials.gov (NCT01383915).

Participants were recruited consecutively into AMDPS between September 2009 and July 2017 from the Adolescent Child and Adolescent Inpatient Unit of The Zucker Hillside Hospital, New York, USA (48, 49). AMDPS is an ongoing, prospective study that aims to assess predictors of the development of bipolar disorder and psychotic disorders in hospitalized adolescents. Analyses for this study are restricted to baseline data. The protocol was approved by the Institutional Review Board of the North Shore-Long Island Jewish Health System in accordance with the Helsinki Declaration of 1975 and the UNESCO Universal Declaration on human rights. Written informed consent was obtained from subjects aged 18 or the guardians/legal representatives of minors, obtaining written assent from the minors.

Participants

Inclusion criteria for AMDPS study were: (1) age 12–18 years; (2) hospitalized at the adolescent inpatient unit of The Zucker Hillside Hospital, a self-standing psychiatric hospital; (3) admission chart diagnosis of any bipolar-spectrum disorder, cyclothymia, major depressive disorder, depressive disorder not otherwise specified (NOS), dysthymia or mood disorder NOS, schizophrenia, schizoaffective disorder, schizophreniform disorder or psychotic disorder NOS, re-evaluated by research interview, using the Structured Clinical Interview for DSM Disorders (SCID) (50), supplemented for missing pediatric diagnoses by the Schedule for Affective Disorders and Schizophrenia for School-Age Children-Present and Lifetime version (K-SADS-PL) (51); (4) subject and guardian/caregiver (if subject<18) willing and able to provide written, informed consent/assent. Exclusion criteria were: (1) an estimated premorbid IQ<70; (2) DSM-5 clinical criteria for autism spectrum disorders or pervasive developmental disorder and (3) history of any neurological or medical condition known to affect the brain.

For the purpose of this study, we also excluded patients: (1) with a psychotic disorder according to DSM-5 criteria; (2) in whom the Structured Interview for Psychosis-Risk Syndromes, version 4.0 (52) was not completed (**Figure 2**).

Psychiatric diagnoses were established in diagnostic research consensus conferences based on in-person independent interview assessments of the adolescents and caregivers whenever possible. The interviews were typically conducted a few days after hospital admission. In consensus conferences, both assessments were integrated assuming that symptoms are more likely forgotten or hidden than invented or exaggerated. Also, SIPS items were discussed one by one for both interviews to reach to the correct value, and every psychiatric primary or comorbid diagnosis, including APS, was discussed among all the attendees and confirmed by the study lead (CUC). In order to conduct AMDPS assessments, experienced clinicians had to be certified by the study PI (CUC) after having gone through a structured training program, which involved observing several assessments, followed by conducting several assessments in front of one of the certified trainers, and presenting their ratings as part of a diagnostic consensus conference led by the study PI. All raters continually took part in the diagnostic consensus conference, during which all interview ratings were discussed and finalized as part of a group consensus, which served to assure validity of the ratings, facilitate interrater reliability via consensual rating, and avoid rater drift after completion of the initial training and certification.

Diagnostic Assessments

The Structured Interview for Psychosis-Risk Syndromes (SIPS) (18, 19) is a semi-structured interview used to diagnose psychosis-risk syndromes in the last month. We used SIPS Version 4.0 (53). It includes four primary sections according to the symptoms evaluated: attenuated positive symptoms, negative symptoms, disorganized symptoms, and general symptoms. As part of the SIPS, the Scale of Prodromal Symptoms (SOPS) is used to determine whether participants meet research criteria for APSS. SIPS/SOPS psychometric instruments and DSM-5 criteria were both used to diagnose DSM-5-APS in a precise way.

Clinical and Functional Assessments

Additional rating scales were administered to both adolescents and their caregivers, including the Clinical Global Impression–Severity scale (CGI-S; range = 1–7) to assess the overall severity of illness (54) and Global Assessment of Functioning (GAF) scale (55) to assess global functioning. Social and role functioning were assessed as well, using the Global Functioning: Social (GF: Social) and the Global Functioning: Role (GF: Role) (56, 57) scales. Insight was assessed using the Scale to Assess Unawareness of Mental Disorder (SUMD) (58), using three general awareness items: mental disorder, social consequences of mental disorder, and achieved effect of medication. Suicidality was assessed as the % of individuals who reported suicidal ideation lifetime and those with a history of at least one suicide attempt prior to admission.

Data Analysis

We used descriptive statistics to characterize the study population, including diagnosis according to DSM-5 criteria, demographic variables, clinical characteristics and treatment characteristics. Between-group comparisons of categorical variables were performed using χ^2-test or Fisher's exact test, whenever at least one cell contained $\leq$5 patients. For comparisons of continuous variables, we used *t*-test. The following effect sizes were calculated: (a) Cramer's V for χ^2 (59), which was interpreted as follows: 0.1=small; 0.3=moderate; 0.5=large effect size; and (b) Cohen's d (60) for *t*-test, which was interpreted as follows: 0.2=small; 0.5=moderate; 0.8=large effect size, using effect size calculator for *t*-test (61). We correlated attenuated positive, negative, general and disorganized symptoms with the level of functioning and severity of illness using Pearson's correlation. We finally conducted a multivariable, backward logistic regression analysis, entering into the model

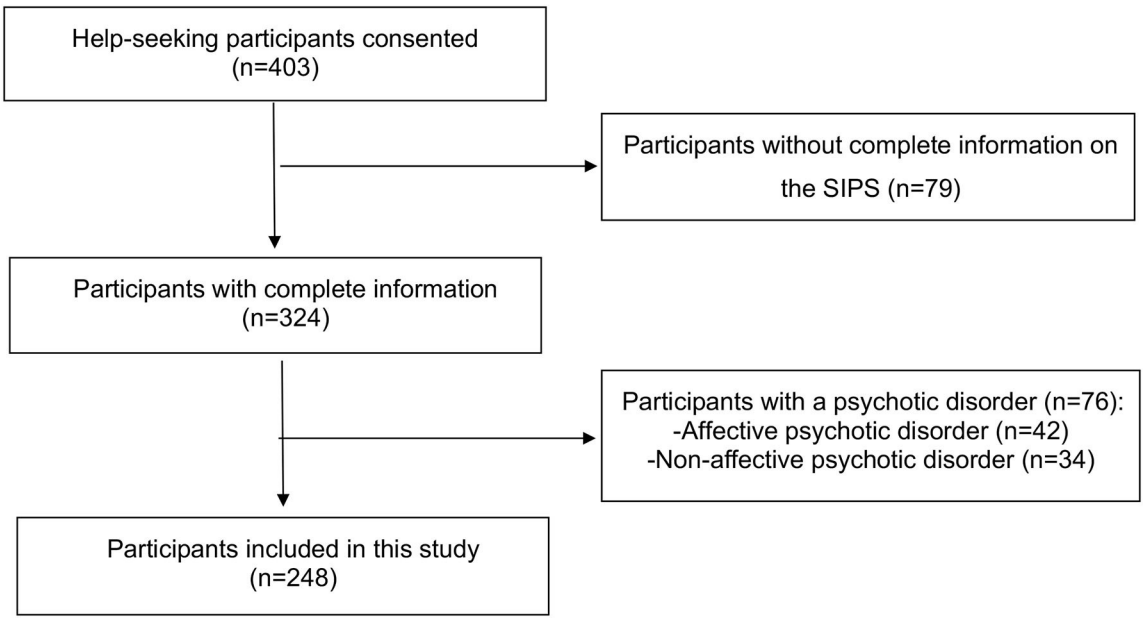

FIGURE 2 | Flowchart outlining selection of study population. SIPS, Structured Interview for Psychosis-Risk Syndromes.

variables that were significantly different ($p < 0.05$) between APS vs. non-APS groups in univariate analyses with data in >67% of subjects. For DSM-5 diagnoses, we entered into the multivariable model broad diagnostic categories (e.g., anxiety disorders), instead of single diagnoses (e.g., panic disorder), that were significantly different between the APS and non-APS group, in order to maximize power for the analyses. For the SIPS psychopathology symptoms, we included only individual items and not subscale sum scores to identify potentially clinically relevant symptoms that can guide clinical identification of APS status. The percent variance explained by the significant variables retained in the final multivariable logistic regression model was expressed as r^2. Significance level was set at alpha=0.05, and all tests were two-tailed. Statistical analyses were performed with SPSS 21 for Windows software (IBM) (62).

RESULTS

Demographic, Comorbidity and Treatment Characteristics

Altogether, 403 help-seeking adolescents and their guardians/legal representatives were consented into AMDPS. Of those, 79 (16.9%) were excluded from this study due to incomplete information on the SIPS, and of the remaining 324 patients, 76 (23.5%) had a psychotic disorder and were therefore also excluded. Finally, 248 hospitalized adolescents with non-psychotic psychiatric disorders were included in this study. Of those, 65 (26.2%) fulfilled DSM-5-APS criteria and 183 (83.8%) did not fulfill APS criteria (**Figure 2**). Agreement was 100% between DSM-5 clinical criteria and the SIPS.

Table 1 shows the demographic, illness and baseline treatment characteristics of the sample at the time of the interview. The average age of participants was 15.4 years (SD=1.5). Most participants were female (69.4%) and white (54.6%). There were no significant differences between the two groups in any of the demographic characteristics (**Table 1**).

APS individuals had a higher number of comorbid disorders (3.5 vs. 2.4, $p < 0.001$; Cohen's d = 0.77) compared to non-APS individuals. The most frequent in the total sample (APS plus non-APS) were depressive disorders (77.0%), particularly major depressive disorder (55.2%), followed by anxiety disorders (42.7%), and disruptive behavior disorders (39.1%). The following disorders were significantly more common in individuals with APS vs. non-APS: disruptive behavior disorders ($p = 0.011$; Cramer's V = 0.16), including oppositional defiant disorder ($p = 0.03$; Cramer's V = 0.14), and conduct disorder ($p = 0.049$; Cramer's V = 0.12); bipolar disorders ($p = 0.002$, Cramer's V = 0.20), including other specified bipolar and related disorders ($p = 0.005$; Cramer's V = 0.18)—also known as bipolar disorder NOS as defined by the COBY study criteria (63)–; personality disorder traits ($p < 0.001$; Cramer's V = 0.26), including borderline personality disorder traits ($p = 0.002$; Cramer's V = 0.20) and other personality disorder traits ($p < 0.001$; Cramer's V = 0.27); anxiety disorders ($p = 0.016$; Cramer's V = 0.15), including panic disorder ($p = 0.031$; Cramer's V = 0.14), generalized anxiety disorder ($p = 0.011$; Cramer's V = 0.16) and specific phobia ($p = 0.005$; Cramer's V = 0.18); and eating disorders ($p = 0.012$; Cramer's V = 0.16). The two groups did not differ in comorbid depressive disorders, substance use

TABLE 1 | Demographic, comorbidity and treatment characteristics.

	Total ($n = 248$)	APS ($n = 65$)	Non-APS ($n = 183$)	*P*-value	Effect size
Demographic characteristics					
Sex, male, *n* (%)	76 (30.6)	16 (24.6)	60 (32.8)	0.22	0.078
Age (years) mean ± SD	15.4 ± 1.5	15.5 ± 1.3	15.4 ± 1.5	0.63	0.070
Race/ethnicity, *n*, (%)[a]				0.60	0.11
White	124 (54.6)	32 (55.2)	92 (54.4)		
Black or African American	41 (18.1)	13 (22.4)	28 (16.6)		
Other	31 (13.7)	8 (13.8)	23 (13.6)		
Asian or Pacific Islander	28 (12.3)	5 (8.6)	23 (13.6)		
Indian American	3 (1.3)	0 (0.0)	3 (1.8)		
Estimated IQ, mean ± SD	108.4 ± 18.9	107.2 ± 17.8	108.8 ± 19.3	0.56	0.088
Lifetime consensus diagnoses, *n* (%)					
Number of psychiatric diagnoses	2.6 ± 1.5	3.5 ± 1.5	2.4 ± 1.4	**<0.001**	**0.77**
Depressive disorders	191 (77.0)	52 (80.0)	139 (76.0)	0.51	0.042
Major depressive disorder	137 (55.2)	42 (64.6)	95 (51.9)	0.077	0.11
Other specified depressive disorder	53 (21.4)	10 (15.4)	43 (23.5)	0.170	0.087
Persistent depressive disorder	18 (7.3)	5 (7.7)	13 (7.1)	0.87	0.010
Disruptive, impulse-control and conduct disorders	97 (39.1)	34 (52.3)	63 (34.4)	**0.011**	**0.16**
Attention-deficit/hyperactivity disorder	58 (23.4)	13 (20.0)	45 (24.6)	0.45	0.048
Oppositional defiant disorder	40 (16.1)	16 (24.6)	24 (13.1)	**0.03**	**0.14**
Conduct disorder	26 (10.5)	11 (16.9)	15 (8.2)	**0.049**	**0.12**
Disruptive behavior disorder not otherwise specified	11 (4.4)	4 (6.2)	7 (3.8)	0.43	0.050
Bipolar disorders	57 (23.0)	24 (36.9)	33 (18.0)	**0.002**	**0.20**
Other specified bipolar and related disorder	41 (16.5)	18 (27.7)	23 (12.6)	**0.005**	**0.18**
Bipolar I disorder	12 (4.8)	6 (9.2)	6 (3.3)	0.055	0.12
Bipolar II disorder	8 (3.2)	3 (4.6)	5 (2.7)	0.46	0.047
Personality disorder traits	48 (19.4)	24 (36.9)	24 (13.1)	**<0.001**	**0.26**
Borderline personality disorder traits	42 (16.9)	19 (29.2)	23 (12.6)	**0.002**	**0.20**
Other personality disorder traits	13 (5.2)	10 (15.4)	3 (1.6)	**<0.001**	**0.27**
Substance use disorders	39 (15.7)	13 (20.0)	26 (14.2)	0.27	0.070
Cannabis use disorder	31 (12.5)	9 (13.8)	22 (12.0)	0.70	0.024
Alcohol use disorder	14 (5.6)	6 (9.2)	8 (4.4)	0.14	0.093
Others	6 (2.4)	2 (3.1)	4 (2.2)	0.67	0.026
Trauma- and stressor-related disorders	38 (15.3)	8 (12.3)	30 (16.4)	0.43	0.050
Posttraumatic stress disorder	20 (8.1)	7 (10.8)	13 (7.1)	0.35	0.059
Adjustment disorder	19 (7.7)	2 (3.1)	17 (9.3)	0.11	0.10
Anxiety disorders	106 (42.7)	36 (55.4)	70 (38.3)	**0.016**	**0.15**
Panic disorder	63 (25.4)	23 (35.4)	40 (21.9)	**0.031**	**0.14**
Generalized anxiety disorder	37 (14.9)	16 (24.6)	21 (11.5)	**0.011**	**0.16**
Social phobia	24 (9.7)	10 (15.4)	14 (7.7)	0.07	0.11
Others	20 (8.1)	5 (7.7)	15 (8.2)	0.90	0.008
Obsessive-compulsive disorder	13 (5.2)	6 (9.2)	7 (3.8)	0.093	0.11
Specific phobia	9 (3.6)	6 (9.2)	3 (1.6)	**0.005**	**0.18**
Other diagnostic categories					
Eating disorders	20 (8.1)	10 (15.4)	10 (5.5)	**0.012**	**0.16**
Enuresis (not due to a general medical condition)	9 (3.6)	3 (4.6)	6 (3.3)	0.62	0.031
Treatment characteristics at time of the interview *n* (%)[b]					
Antipsychotics[c]	118 (53.6)	37 (66.1)	81 (49.4)	**0.031**	**0.15**
Antidepressants[d]	112 (50.9)	24 (42.9)	88 (53.7)	0.16	0.094
Mood stabilizers[e]	55 (25.0)	14 (25.0)	41 (25.0)	1.0	0.000

(Continued)

TABLE 1 | Continued

	Total ($n = 248$)	APS ($n = 65$)	Non-APS ($n = 183$)	*P*-value	Effect size
Lithium	41 (18.6)	9 (16.1)	32 (19.5)	0.57	0.038
Anxiolytics[f]	23 (10.5)	7 (12.5)	16 (9.8)	0.56	0.039
Others[h]	21 (9.5)	7 (12.5)	14 (8.5)	0.38	0.059
Antiepileptic drugs	18 (8.2)	6 (10.7)	12 (7.3)	0.42	0.054
ADHD medication[g]	4 (1.8)	0 (0.0)	4 (2.4)	0.24	0.080
Two or more drugs	91 (41.4)	22 (39.3)	69 (42.1)	0.71	0.025
Three or more drugs	25 (11.4)	7 (12.5)	18 (11.0)	0.76	0.021

ADHD, Attention Deficit Hyperactivity Disorder; APS, Attenuated Psychosis Syndrome.
[a]*Information available for 227 individuals.*
[b]*Information available for 220 individuals.*
[c]*Antipsychotics: aripiprazole, molindone, quetiapine, risperidone, lurasidone, ziprasidone, olanzapine, haloperidol, chlorpromazine, clozapine.*
[d]*Antidepressants: amitriptyline, nortriptyline, bupropion, citalopram, escitalopram, duloxetine, fluoxetine, paroxetine, sertraline, venlafaxine, mirtazapine.*
[e]*Mood stabilizers: lamotrigine, lithium, valproic acid.*
[f]*Anxiolytics/tranquilizers: clonazepam, lorazepam, hydroxyzine, buspirone.*
[g]*Anti-ADHD medications: atomoxetine, lisdexamphetamine, methylphenidate, modafinil, clonidine, guanfacine.*
[h]*Others: zolpidem, melatonin, propranolol, diphenhydramine, amlodipine.*
Bold values indicate $p < 0.05$ for between-groups analysis.

disorders, trauma and stressor-related disorders or enuresis (all $p > 0.05$).

Overall, the most used psychotropic medications at the time of the interview were antipsychotics (53.6%; $p = 0.031$), followed by antidepressants (50.9%; $p = 0.16$), and mood stabilizers (25.0%; $p = 1.0$). Antipsychotics, which were more common in the APS group ($p = 0.031$; Cramer's V = 0.15), were the only medication class that was significantly different between the groups. The use of multiple medications (use of two or more drugs or use of three or more drugs) was equally frequent in both groups ($p = 0.71$ to 0.76).

Severity of Symptoms and Symptom Domains

Total attenuated positive ($p < 0.001$; Cohen's d = 1.5), negative ($p < 0.001$; Cohen's d = 0.55), disorganized ($p < 0.001$; Cohen's d = 0.51), and general ($p < 0.001$; Cohen's d = 0.84) symptom scores were significantly higher in APS individuals vs. non-APS hospitalized adolescents. All group-defining SIPS attenuated positive symptoms (unusual thought content, suspiciousness, grandiosity, perceptual abnormalities and disorganized communication) were significantly more severe in the APS group (Cohen's d = 0.39 to 1.3), with the largest effect size for perceptual abnormalities (Cohen's d = 1.3) (**Table 2**). Additionally, the following symptoms were more severe in the APS vs. non-APS group: social anhedonia ($p < 0.001$; Cohen's d = 0.57), avolition ($p = 0.002$; Cohen's d = 0.51), experiences of emotions and self ($p < 0.001$; Cohen's d = 0.54), bizarre thinking ($p < 0.001$; Cohen's d = 0.60), trouble with focus and attention ($p = 0.001$; Cohen's d = 0.53), sleep disturbances ($p = 0.002$; Cohen's d = 0.38), dysphoric mood ($p = 0.004$; Cohen's d = 0.34) and impaired stress tolerance ($p < 0.001$; Cohen's d = 0.63).

Illness Severity, Functional Level, Illness Insight and Suicidality

Overall illness severity (CGI-S) was higher in the APS group ($p<0.001$) and the effect size was large (Cohen's d = 1.0). The mean current GAF score was 23.0 ± 11.9 in the APS group and 28.1 ± 17.9 in the non-APS group ($p = 0.012$; Cohen's d = 0.31). Scores for the highest functioning in the past year ($p = 0.002$; Cohen's d = 0.52) and lowest functioning in the past year ($p = 0.002$; Cohen's d = 0.38) were lower in the APS group as well (i.e., poorer functioning in the APS group). Unlike current role functioning, which did not differ significantly between the groups ($p = 0.35$), current social functioning was better in the non-APS group ($p = 0.003$; d = 0.66). Both groups did not differ regarding awareness of mental disorder or social consequences, suicidal ideation or suicidal attempts (all $p > 0.05$) (**Table 3**).

Correlation Between Symptom Domains and Functioning (GAF)–Severity of Illness (CGI-S)

Total negative symptoms were significantly correlated with lower current functioning (Pearson $\rho = -0.17$; $p = 0.031$), lower lowest functioning in the past year (Pearson $\rho = -0.20$; $p = 0.014$) and lower highest functioning reached in the past year (Pearson $\rho = -0.19$; $p = 0.022$). Functioning was not significantly correlated with attenuated positive symptoms, disorganized symptoms or general symptoms. The severity of illness was associated with more severe SIPS positive, negative, disorganized and general symptoms (Pearson $\rho = 0.22$ to 0.46; $p = 0.04$ to $p < 0.001$) (**Table 4**).

Multivariable Logistic Regression Analysis

Independent correlates of APS in the final model were perceptual abnormalities (OR = 2.0; 95% CI = 1.6–2.5, $p < 0.001$), number of psychiatric diagnoses (OR = 1.5; 95% CI = 1.2–2.0, $p = 0.002$),

TABLE 2 | Severity of structured interview of prodromal syndromes (SIPS) assessed symptoms and symptom domains.

	Total ($n = 248$)	APS ($n = 65$)	Non-APS ($n = 183$)	*P*-value	Effect size
Structured interview of prodromal syndromes mean± SD					
Positive symptoms					
Total positive symptom score	3.2 ± 4.1	7.4 ± 4.6	1.9 ± 3.3	**<0.001**	**1.5**
Highest positive symptom score	1.8 ± 1.8	3.5 ± 1.3	1.2 ± 1.6	**<0.001**	**1.5**
P1 unusual thought content	0.73 ± 1.4	1.6 ± 1.6	0.41 ± 1.1	**<0.001**	**0.95**
P2 suspiciousness	0.84 ± 1.3	1.8 ± 1.6	0.48 ± 0.93	**<0.001**	**1.2**
P3 grandiosity	0.54 ± 1.2	0.89 ± 1.5	0.41 ± 1.1	**0.024**	**0.39**
P4 perceptual abnormalities/hallucinations	0.99 ± 1.7	2.3 ± 1.9	0.47 ± 1.2	**<0.001**	**1.3**
P5 disorganized communication	0.29 ± 0.86	0.63 ± 1.1	0.16 ± 0.68	**<0.001**	**0.58**
Negative symptoms					
Total negative symptom score	8.0 ± 6.22	10.4 ± 6.7	7.1 ± 5.8	**<0.001**	**0.55**
Highest negative symptom score	3.4 ± 1.83	3.8 ± 1.6	3.2 ± 1.9	**0.012**	**0.33**
N1 social anhedonia	1.5± 1.79	2.2 ± 1.9	1.2 ± 1.7	**<0.001**	**0.57**
N2 avolition	2.1 ± 2.0	2.9 ± 1.7	1.9 ± 2.0	**0.002**	**0.51**
N3 expression of emotions	0.88 ± 1.5	1.2 ± 1.6	0.75 ± 1.4	0.061	0.31
N4 experience of emotions and self	0.87 ± 1.7	1.6 ± 2.3	0.65 ± 1.4	**<0.001**	**0.54**
N5 ideational richness	0.20 ± 0.65	0.18 ± 0.18	0.21 ± 0.75	0.88	0.050
N6 occupational functioning	2.4 ± 2.1	2.5 ± 2.4	2.3 ± 2.0	0.31	0.11
Disorganized symptoms					
Total disorganized symptom score	3.1 ± 3.2	4.3 ± 3.7	2.7 ± 2.9	**<0.001**	**0.51**
Highest disorganized symptom score	2.2 ± 1.9	2.9 ± 1.7	2.03 ± 1.9	**0.003**	**0.47**
D1 odd behavior or appearance	0.16 ± 0.94	0.14 ± 1.4	0.17 ± 0.71	0.297	−0.03
D2 bizarre thinking	0.18 ± 0.7	0.48 ± 1.1	0.08 ± 0.4	**<0.001**	**0.60**
D3 trouble with focus and attention	1.9 ± 1.8	2.6 ± 1.7	1.66 ± 1.81	**0.001**	**0.53**
D4 impairment in personal hygiene	0.76 ± 1.7	0.86 ± 2.1	0.73 ± 1.54	0.45	0.08
General symptoms					
Total general symptom score	8.4 ± 4.5	11.0 ± 3.5	7.5 ± 4.4	**<0.001**	**0.84**
Highest general symptom score	4.3 ± 1.7	5.0 ± 1.1	4.1 ± 1.8	**<0.001**	**0.55**
G1 sleep disturbance	2.3 ± 1.9	2.8 ± 2.0	2.1 ± 1.8	**0.002**	**0.38**
G2 dysphoric mood	4.0 ± 2.1	4.5 ± 2.3	3.8 ± 2.0	**0.004**	**0.34**
G3 motor disturbance	0.14 ± 0.80	0.17 ± 1.4	0.13 ± 0.52	0.73	0.05
G4 impaired stress tolerance	1.9 ± 2.1	2.9 ± 2.3	1.6 ± 1.9	**<0.001**	**0.63**

Bold values indicate p < 0.05 for between-groups analysis.

and impaired stress tolerance (OR = 1.4; 95%CI = 1.1–1.7, $p = 0.002$). The model including these three variables explained 31.5% of the variance ($r^2 = 0.315$, $p < 0.001$) (**Table 5**).

DISCUSSION

To our knowledge, this study is one of the very few and the largest to date to characterize and describe sociodemographic, illness and intervention characteristics in adolescents with APS vs. non-APS. Additionally, this study focused on help-seeking adolescents who had been admitted into an inpatient unit.

According to our results, 26.2% of the adolescents without a psychotic disorder diagnosis fulfilled APS criteria, a somewhat lower prevalence compared to a previous study including mostly adolescent outpatients (33%) (64, 65), but still a clinically significant and higher prevalence than the one found in non-help-seeking adolescents with disruptive behaviors (13%) (33). In the general population, a 7.2% meta-analytical prevalence of psychotic experiences was estimated in children and adults (66). In the Philadelphia Neurodevelopmental Cohort study, 15.5% of the 8–21 year old individuals reported significant psychotic symptoms and another 9.8% reported milder symptoms (67).

APS individuals had a higher number and distribution of comorbid conditions than non-APS individuals (Cohen's d = 0.77), particularly consisting of depressive disorders (5), anxiety disorders (5), and disruptive behavior disorders (68). This finding is clinically relevant because APS status has been associated with hospital treatment for mood and conduct disorders (33). Personality disorder traits, bipolar disorders, disruptive behavior disorders, eating disorders and anxiety disorders, were more frequent in the APS group than the non-APS group, although effect sizes were small. This result supports evidence of the association between APS (21, 22) as well as CHR-P (9, 69) with other comorbid mental disorders.

TABLE 3 | Illness severity, functional level, illness insight and suicidality.

	Total ($n = 248$)	APS ($n = 65$)	Non-APS ($n = 183$)	*P*-value	Effect size
Characteristics					
Illness severity: clinical global impressions-severity scale (CGI-S) mean ± SD[a]					
Overall severity of illness	4.2 ± 1.03	4.8 ± 0.94	3.9 ± 0.9	**<0.001**	**1.0**
Functional level: global assessment of functioning-scale (GAF) mean ± SD[b]					
Current GAF	26.8 ± 16.7	23.0 ± 11.9	28.1 ± 17.9	**0.012**	**0.31**
Highest GAF of past year	57.7 ± 14.7	52.2 ± 16.6	59.7 ± 13.5	**0.002**	**0.52**
Lowest GAF of past year	23.1 ± 15.0	18.9 ± 10.2	24.5 ± 16.0	**0.002**	**0.38**
Global functioning: role scale mean ± SD[c]					
Current role functioning	5.9 ± 1.8	5.7 ± 1.7	6.1 ± 1.9	0.35	0.20
Global functioning: social scale mean ± SD[c]					
Current social functioning	6.5 ± 1.7	5.8 ± 1.5	6.9 ± 1.7	**0.003**	**0.66**
Scale to assess unawareness of mental disorder mean ± SD[d]					
Awareness of mental disorder	2.2 ± 1.7	2.2 ± 1.6	2.2 ± 1.7	0.98	0.006
Awareness of the effect of medication	2.1 ± 1.5	2.2 ± 1.5	2.0 ± 1.5	0.45	0.14
Awareness of the social consequences	1.9 ± 1.5	1.9 ± 1.4	1.9 ± 1.5	0.99	0.0
Suicidality, *n* (%)[e]					
Suicidal ideation	131 (61.8)	38 (73.1)	93 (58.1)	0.29	0.067
Suicide attempts	21 (10.0)	8 (15.3)	13 (8.2)	0.19	0.082

[a]*Data available for 86 patients.*
[b]*Data available for 225 patients.*
[c]*Data available for 88 patients.*
[d]*Data available for 168 patients.*
[e]*Data available for 212 patients.*
Bold values indicate $p < 0.05$ for between-groups analysis.

TABLE 4 | Correlation between Structured Interview of Prodromal Syndromes (SIPS) symptom domains and functioning as well as severity of illness.

	Current GAF		Lowest GAF past year		Highest GAF past year		Severity of illness CGI-S	
	Pearson's Rho	*p*-value	Pearson's Rho	*p*-value	Pearson's Rho	*p*-value	Pearson's Rho	*p*-value
Total SIPS positive symptom score	−0.034	0.66	−0.045	0.57	0.0005	0.95	0.46	**<0.001**
Total SIPS negative symptom score	−0.17	**0.031**	−0.20	**0.014**	−0.19	**0.022**	0.39	**<0.001**
Total SIPS disorganized symptom score	−0.04	0.58	−0.06	0.46	−0.043	0.61	0.22	**0.04**
Total SIPS general symptom score	0.095	0.21	0.082	0.3	0.017	0.36	0.45	**<0.001**

CGI-S, Clinical Global Impression–Severity scale; GAF, Global Assessment of Functioning; SIPS, Structured Interview for Psychosis-Risk Syndromes.
Bold values indicate $p < 0.05$ for between-groups analysis.

TABLE 5 | Results of the multivariable, backward elimination logistic regression analysis of variables distinguishing APS vs. non-APS at $p < 0.05$ in univariate analyses.

	B	SE	Wald	Sig	OR	95.0% C.I.	
						Lower	Upper
SIPS P4 perceptual abnormalities/hallucinations	0.69	0.11	38.9	**<0.001**	2.0	1.6	2.5
SIPS G4 impaired stress tolerance	0.31	0.10	9.8	**0.002**	1.4	1.1	1.7
Number of psychiatric diagnoses	0.42	0.14	9.5	**0.002**	1.5	1.2	2.0

($r^2 = 0.315$, $p < 0.001$).
Bold values indicate $p < 0.05$ for between-groups analysis.

Thus, comorbidity should not rule out APS, but, if anything, increase the diagnostic suspicion. On the other hand, it is also possible for APS status to be a byproduct of overlapping disease processes and expressions of non-psychotic disorders, lowering the true risk for developing a psychotic disorder in the future (22, 28, 70).

Regarding psychopharmacological treatment, as previously reported (22), a high percentage of our non-psychotic APS

sample received atypical antipsychotics (66.1%), which was also high in the non-psychotic non-APS individuals (49.4%). This finding is worrying because no consistent meta-analytical evidence supports the use of atypical antipsychotic drugs in delaying or preventing transition to psychosis over other interventions (71, 72). However, it is also true that rates of antipsychotics were high in other diagnostic groups in this sample, including bipolar-spectrum disorders (49), which supports that atypical antipsychotic use is likely related to the reason for admission to the psychiatric unit and not only to efforts to treat attenuated psychotic symptoms or to prevent full-blown psychosis. Nevertheless, the widespread use of antipsychotics in adolescents for non-psychotic, predominantly depressive disorders is concerning due to the established adverse effects risks that atypical antipsychotics have in youth (73–77).

APS status was associated with a significantly higher severity of attenuated psychotic symptoms according to the SIPS. Effect sizes for these differences were moderate to large (Cohen's $d = 0.51$ to 1.5). Regarding individual items, differences were found in 13/19 items. Effect sizes were large for unusual thought content, suspiciousness and perceptual abnormalities (Cohen's $d = 1.0$ to 1.3), medium for disorganized communication, social anhedonia, avolition, experience of emotions and self, bizarre thinking, trouble with focus and attention and impaired stress tolerance (Cohen's $d = 0.50$ to 0.63), and small for grandiosity, sleep disturbances and dysphoric mood (Cohen's $d = 0.34$ to 0.39).

This greater severity in psychopathology also translated into greater illness severity (Cohen's $d = 1.0$) and poorer functioning (Cohen's $d = 0.31$ to 0.52), as found before (9, 22, 78, 79), including social functioning (Cohen's $d = 0.66$), but not role functioning. However, a previous study using the same instruments found that both social and role functioning were significantly more impaired in CHR-P individuals compared to controls from as early as age 12, which was our lower age limit (80). However, controls in that study were healthy, while in our sample, we compared hospitalized adolescents with vs. without APS who were likely admitted for symptoms related to other psychiatric disorders, which can explain the difficulties in role functioning as well as social and general functioning. The fact that all adolescents (APS and non-APS) reached stringent US criteria for inpatient care resulted in the low functioning scores found in both groups. Nevertheless, our results support previous evidence that APS status is associated with marked functional impairment (21, 81, 82). This finding is particularly relevant because functional impairment can be helpful to differentiate youth meeting CHR-P from other help-seeking individuals (83).

Interestingly, while illness severity was associated with overall psychopathology, including more severe SIPS total positive, negative, disorganized and general symptoms (Pearson $\rho = -0.22$ to -0.46), functioning (current, lowest and highest) was only and weakly (Pearson $\rho = -0.17$ to -0.20) correlated with total negative symptoms, but not with attenuated positive, disorganized and general symptoms. Negative symptoms have been associated with functioning (38–40), not only in schizophrenia, but also in other psychotic individuals, and non-psychotic depressed patients (84). This association was found to be greater with negative than attenuated positive symptoms (85), in line with our results. In contrast, trauma has been found to be correlated with the severity of attenuated positive symptoms but not with negative symptoms in CHR-P individuals (86); yet, CHR-P individuals' negative symptoms may impact the transition to psychosis even more than attenuated positive symptoms (87), although this has not been found consistently (53).

According to our results, perceptual abnormalities (OR=2.0), number of psychiatric diagnoses (OR=1.5), and impaired stress tolerance (OR=1.4) were independently associated with APS status. Among perceptual abnormalities, auditory perceptual abnormalities have been associated with a higher risk of psychosis, while visual perceptual abnormalities have been associated with a lower risk (88). While the number of psychiatric diagnoses was independently associated with APS status in our study, and while APS has previously been associated with comorbid mental disorders, the impact of the different comorbid conditions may vary (21, 22). The most common comorbid conditions in our sample, anxiety and depressive diagnoses, have been associated with impaired global functioning, as well as higher suicidality or self-harm behaviors, but not with transition to psychosis (5). Implications of the presence of other comorbid conditions in APS and their relevance for true risk for conversion to psychosis need further study, particularly in adolescents. Our results further support previous evidence that impaired stress tolerance is a core CHR-P feature, which is associated with more severe psychopathology (89). The presence of impaired stress tolerance has been also suggested to have therapeutic implications in CHR-P (90).

We also found that APS was associated with functioning in univariate analyses, but not in multivariable analyses, supporting that lower functioning is related to other features, including the presence and duration of attenuated positive symptoms (21, 91) and impaired stress tolerance (89). A model including disorganized communication, suspiciousness, verbal memory deficits, and decline in social functioning was found to predict conversion to psychosis (53). Due to having introduced the Global Functioning scales later into the study, they were only available in a subset of patients and could not be entered into the backward elimination logistic regression model. However, APS was associated with significantly lower levels of social functioning. Clinicians should thus monitor functioning, especially social functioning in adolescents with APS.

Finally, our results stress that in adolescent inpatients, DSM-5 APS is associated with higher severity of overall illness, lower functioning and impaired stress tolerance, requiring a higher intensity of clinical care compared to non-APS adolescents admitted into an inpatient unit. This result is supported by prior findings showing that youth with APS have complex medical histories and frequent comorbidities that require therapeutic attention (22, 28, 70). Research about effective treatments for DSM-5-APS has been limited (21), and evidence from studies analyzing CHR-P individuals—from which knowledge could arguably be applied to APS individuals—does not support one treatment over another (72). At the moment, at least needs-based interventions should be offered (9). Perceptual abnormalities and impaired stress tolerance may be targets of needs-based interventions in adolescents aiming to improve quality of life

and aiming to reduce burden for them and their families. Still, prospective studies are needed to inform and develop guidelines regarding youth fulfilling APS criteria.

Strengths and Limitations

The current study has several strengths and limitations that must be taken into consideration when interpreting its results. First, some symptom assessments were based on retrospective recall, which may be prone to recall bias. However, all SIPS symptoms were rated for presence in the last month. Second, the comparison group, including non-psychotic adolescents who fulfilled criteria for inpatient care in the US health care system, was otherwise heterogeneous and functionally impaired. The results should thus be interpreted in the context of help-seeking APS and non-APS samples in need of inpatient care. Third, data were not available to determine to what degree adolescents with APS sought help specifically for APS-related symptomology. Fourth, we did not collect some potentially relevant information, including the reason for the use of psychotropic medications or dosage, which could have relevant implications. Similarly, verbal memory deficits and other cognitive measures, which are relevant according to previous research, were not included in the current analysis. Fifth, we could not retrieve the data for the total number of patients fulfilling our inclusion criteria within our study timeframe outside of this study. Thus, we could not report the participation rate. Sixth, we did not test for interrater reliability of interviewers for all scales used in this study. However, using the same training, certification and ongoing recalibration system via mandatory presence and presentation of all rating scale scores for all interviewers as part of the regular diagnostic consensus conference (led by the study PI CUC) the interrater reliability of the BPSS-FP indices ranged from intraclass-correlations of 0.93–0.98 (92). Seventh, since the Clinical Global Impressions of Severity Scale and social and role function scales were introduced later into the study, data were not available in a sufficiently large number of patients to enter this variable into the multivariable regression analysis; Eighth, the final model obtained from the multivariable regression analysis was not validated, which may have led to overfitting, thus requiring replication and limiting its generalizability and consequently its implementation in clinical practice. Finally, the cross-sectional design precludes any analysis of the predictive value of APS.

Nevertheless, despite these limitations, the study has several strengths. First, this is the largest study to date to comprehensively describe and characterize DSM-5-APS in adolescents. Second, we used structured and validated assessments that were carried out independently and face-to-face for both adolescents and their parents or caregivers to obtain as precise information as possible. These assessments were led by experienced and internally certified Master or MD level clinicians and psychologists. Third, we focused on individuals with a wide variety of psychopathology and treatment characteristics, both in the DSM-5-APS group and in the non-APS comparison group, increasing clinical value vs. comparisons with healthy control subjects. Finally, focusing on APS individuals allowed us to obtain results from a more homogeneous high-risk sample.

CONCLUSIONS

Approximately one in four adolescents hospitalized with non-psychotic disorders meet DSM-5-APS criteria. These help-seeking adolescents have more comorbid psychiatric disorders as well as more severe symptoms, functional impairment and global severity of illness. Thus, they warrant high intensity clinical care. To what degree APS in adolescents with existing and emerging non-psychotic mental disorders is predictive of future transition to a psychotic disorder and what the predictors are for such transition requires further prospective study.

DATA AVAILABILITY STATEMENT

Datasets generated for this study are included in the article. Additional data might be shared upon request from the first or corresponding author.

ETHICS STATEMENT

The studies involving human participants were reviewed and approved by Institutional Review Board of the North Shore-Long Island Jewish Health System; Ethical Committee of Human Experimentation in the USA. Written informed consent to participate in this study was provided by the participants' legal guardian/next of kin.

AUTHOR CONTRIBUTIONS

GS had full access to all of the data in the study and takes responsibility for the integrity of the data and the accuracy of the data analysis. CC: study concept and design. GS, DG, BC, AA, RC, MC, SJ-F, DV, SW, MG, RS, NL, MB, and CC: acquisition of data. GS and CC: statistical analysis, drafting of the manuscript, administrative, technical, and material support. All authors critical revision of the manuscript for important intellectual content and interpretation of data.

FUNDING

This study was partially funded by a grant from the John and Maxine Bendheim Foundation (PI: CC). GS is supported by the Alicia Koplowitz Foundation. CM and CA have received support by the Spanish Ministry of Science and Innovation. Instituto de Salud Carlos III (PI17/02227), co-financed by ERDF Funds from the European Commission, A way of making Europe, CIBERSAM. Madrid Regional Government (B2017/BMD-3740 AGES-CM-2), European Union Structural Funds. European Union Seventh Framework Program under grant agreements FP7-4-HEALTH-2009-2.2.1-2-241909 (Project EU-GEI), FP7- HEALTH-2013-2.2.1-2-603196 (Project PSYSCAN) and FP7- HEALTH-2013-2.2.1-2-602478 (Project METSY); and European Union H2020 Program under the Innovative Medicines Initiative 2 Joint Undertaking (grant agreement No. 115916, Project PRISM, and grant agreement No. 777394, Project AIMS-2-TRIALS), Fundación Familia Alonso, Fundación Alicia Koplowitz and Fundación Mutua Madrileña.

REFERENCES

1. Yung AR, Yuen HP, Mcgorry PD, Phillips LJ, Kelly D, Dell'olio M, et al. Mapping the onset of psychosis: the comprehensive assessment of at-risk mental states. *Aust N Z J Psychiatry*. (2005) 39:964–71. doi: 10.1080/j.1440-1614.2005.01714.x
2. Fusar-Poli P, Borgwardt S, Bechdolf A, Addington J, Riecher-Rossler A, Schultze-Lutter F, et al. The psychosis high-risk state a comprehensive state-of-the-art review. *JAMA Psychiatry*. (2013) 70:107–20. doi: 10.1001/jamapsychiatry.2013.269
3. Falkenberg I, Valmaggia L, Byrnes M, Frascarelli M, Jones C, Rocchetti M, et al. Why are help-seeking subjects at ultra-high risk for psychosis help-seeking? *Psychiatry Res.* (2015) 228:808–15. doi: 10.1016/j.psychres.2015.05.018
4. Fusar-Poli P, Rocchetti M, Sardella A, Avila A, Brandizzi M, Caverzasi E, et al. Disorder, not just state of risk: meta-analysis of functioning and quality of life in people at high risk of psychosis. *British J Psychiatry*. (2015) 207:198–206. doi: 10.1192/bjp.bp.114.157115
5. Fusar-Poli P, Nelson B, Valmaggia L, Yung AR, Mcguire PK. Comorbid depressive and anxiety disorders in 509 individuals with an at-risk mental state: impact on psychopathology and transition to psychosis. *Schizophr Bull.* (2014) 40:120–31. doi: 10.1093/schbul/sbs136
6. Boldrini T, Tanzilli A, Pontillo M, Chirumbolo A, Vicari S, Lingiardi V. Comorbid personality disorders in individuals with an at-risk mental state for psychosis: a meta-analytic review. *Front Psychiatry*. (2019) 10:429. doi: 10.3389/fpsyt.2019.00429
7. Fusar-Poli P, Mcgorry PD, Kane JM. Improving outcomes of first-episode psychosis: an overview. *World Psychiatry*. (2017) 16:251–65. doi: 10.1002/wps.20446
8. Correll CU, Galling B, Pawar A, Krivko A, Bonetto C, Ruggeri M, et al. Comparison of early intervention services vs treatment as usual for early-phase psychosis: a systematic review, meta-analysis, and meta-regression. *JAMA Psychiatry*. (2018) 75:555–65. doi: 10.1001/jamapsychiatry.2018.0623
9. Fusar-Poli P, Salazar De Pablo G, Correll C, Meyer-Lindenberg A, Millan M, Borgwardt S, et al. Prevention of psychosis: advances in detection, prognosis and intervention. *Jama Psychiatry*. (2020) 77:755–65. doi: 10.1001/jamapsychiatry.2019.4779
10. Fusar-Poli P, Cappucciati M, Borgwardt S, Woods SW, Addington J, Nelson B, et al. Heterogeneity of psychosis risk within individuals at clinical high risk: a meta-analytical stratification. *JAMA Psychiatry*. (2016) 73:113–20. doi: 10.1001/jamapsychiatry.2015.2324
11. Fusar-Poli P, Cappucciati M, De Micheli A, Rutigliano G, Bonoldi I, Tognin S, et al. Diagnostic and prognostic significance of brief limited intermittent psychotic symptoms (BLIPS) in individuals at ultra high risk. *Schizophr Bull.* (2017) 43:48–56. doi: 10.1093/schbul/sbw151
12. Nelson B, Yuen K, Yung AR. Ultra high risk (UHR) for psychosis criteria: are there different levels of risk for transition to psychosis? *Schizophr Res.* (2011) 125:62–8. doi: 10.1016/j.schres.2010.10.017
13. Fusar-Poli P, De Micheli A, Chalambrides M, Singh A, Augusto C, Mcguire P. Unmet needs for treatment in 102 individuals with brief and limited intermittent psychotic symptoms (BLIPS): implications for current clinical recommendations. *Epidemiol Psychiatr Sci.* (2019) 29:e67. doi: 10.1017/S2045796019000635
14. Minichino A, Rutigliano G, Merlino S, Davies C, Oliver D, De Micheli A, et al. Unmet needs in patients with brief psychotic disorders: too ill for clinical high risk services and not ill enough for first episode services. *Eur Psychiatry*. (2019) 57:26–32. doi: 10.1016/j.eurpsy.2018.12.006
15. Spada G, Molteni S, Pistone C, Chiappedi M, Mcguire P, Fusar-Poli P, et al. Identifying children and adolescents at ultra high risk of psychosis in Italian neuropsychiatry services: a feasibility study. *Eur Child Adolesc Psychiatry*. (2016) 25:91–106. doi: 10.1007/s00787-015-0710-8
16. Millman ZB, Pitts SC, Thompson E, Kline ER, Demro C, Weintraub MJ, et al. Perceived social stress and symptom severity among help-seeking adolescents with versus without clinical high-risk for psychosis. *Schizophr Res.* (2018) 192:364–70. doi: 10.1016/j.schres.2017.06.002
17. D'angelo EJ, Morelli N, Lincoln SH, Graber K, Tembulkar S, Gaudet A, et al. Social impairment and social language deficits in children and adolescents with and at risk for psychosis. *Schizophr Res.* (2019) 204:304–10. doi: 10.1016/j.schres.2018.07.028
18. Miller T, Mcglashan T, Woods S, Stein K, Driesen N, Corcoran C, et al. Symptom assessment in schizophrenic prodromal states. *Psychiatr Q Winter.* (1999) 70:273–87. doi: 10.1023/A:1022034115078
19. Miller T, Mcglashan T, Rosen J, Cadenhead K, Cannon T, Ventura J, et al. Prodromal assessment with the structured interview for prodromal syndromes and the scale of prodromal symptoms: predictive validity, interrater reliability, and training to reliability. *Schizophr Bull.* (2003) 29:703–15. doi: 10.1093/oxfordjournals.schbul.a007040
20. Fusar-Poli P, Cappucciati M, Rutigliano G, Schultze-Lutter F, Bonoldi I, Borgwardt S, et al. At risk or not at risk? A meta-analysis of the prognostic accuracy of psychometric interviews for psychosis prediction. *World Psychiatry*. (2015) 14:322–32. doi: 10.1002/wps.20250
21. Salazar De Pablo G, Catalan A, Fusar-Poli P. Clinical validity of DSM-5 attenuated psychosis syndrome: advances in diagnosis, prognosis, and treatment. *JAMA Psychiatry*. (2019) 77:311–20. doi: 10.1001/jamapsychiatry.2019.3561
22. Gerstenberg M, Hauser M, Al-Jadiri A, Sheridan EM, Kishimoto T, Borenstein Y, et al. Frequency and correlates of DSM-5 attenuated psychosis syndrome in a sample of adolescent inpatients with nonpsychotic psychiatric disorders. *J Clin Psychiatry.* (2015) 76:1449–58. doi: 10.4088/JCP.14m09435
23. American Psychiatric Association. *Diagnostic and Statistical Manual of Mental Disorders*. Washington, DC: American Psychiatric Association. (2013). doi: 10.1176/appi.books.9780890425596
24. Tsuang MT, Van Os J, Tandon R, Barch DM, Bustillo J, Gaebel W, et al. Attenuated psychosis syndrome in DSM-5. *Schizophr Res.* (2013) 150:31–5. doi: 10.1016/j.schres.2013.05.004
25. Fusar-Poli P, De Micheli A, Cappucciati M, Rutigliano G, Davies C, Ramella-Cravaro V, et al. Diagnostic and prognostic significance of DSM-5 attenuated psychosis syndrome in services for individuals at ultra high risk for psychosis. *Schizophr Bull.* (2018) 44:264–75. doi: 10.1093/schbul/sbx055
26. Cakmak S, Karaytug MO, Bal U, Tamam L, Tasdemir A. Retrospective evaluation of risk determinants in prodromal period with a group of schizophrenia patients. *Cukurova Med J.* (2016) 41:437–46. doi: 10.17826/cukmedj.234960
27. Zoghbi AW, Bernanke JA, Gleichman J, Masucci MD, Corcoran CM, Califano A, et al. Schizotypal personality disorder in individuals with the Attenuated Psychosis Syndrome: frequent co-occurrence without an increased risk for conversion to threshold psychosis. *J Psychiatr Res.* (2019) 114:88–92. doi: 10.1016/j.jpsychires.2019.04.018
28. Gerstenberg M, Theodoridou A, Traber-Walker N, Franscini M, Wotruba D, Metzler S, et al. Adolescents and adults at clinical high-risk for psychosis: age-related differences in attenuated positive symptoms syndrome prevalence and entanglement with basic symptoms. *Psychol Med.* (2016) 46:1069–78. doi: 10.1017/S0033291715002627
29. Brucato G, Masucci MD, Arndt LY, Ben-David S, Colibazzi T, Corcoran CM, et al. Baseline demographics, clinical features and predictors of conversion among 200 individuals in a longitudinal prospective psychosis-risk cohort. *Psychol Med.* (2017) 47:1923–35. doi: 10.1017/S0033291717000319
30. Lu Y, Marshall C, Cadenhead KS, Cannon TD, Cornblatt BA, Mcglashan TH, et al. Perceptual abnormalities in clinical high risk youth and the role of trauma, cannabis use and anxiety. *Psychiatry Res.* (2017) 258:462–8. doi: 10.1016/j.psychres.2017.08.045
31. Arango C. Attenuated psychotic symptoms syndrome: how it may affect child and adolescent psychiatry. *Eur Child Adolesc Psychiatry*. (2011) 20:67–70. doi: 10.1007/s00787-010-0144-2
32. Ziermans TB, Schothorst PF, Sprong M, Van Engeland H. Transition and remission in adolescents at ultra-high risk for psychosis. *Schizophr Res.* (2011) 126:58–64. doi: 10.1016/j.schres.2010.10.022
33. Manninen M, Lindgren M, Therman S, Huttunen M, Ebeling H, Moilanen I, et al. Clinical high-risk state does not predict later psychosis in a delinquent adolescent population. *Early Interv Psychiatry.* (2014) 8:87–90. doi: 10.1111/eip.12045
34. Koren D, Scheyer R, Stern Y, Adres M, Reznik N, Apter A, et al. Metacognition strengthens the association between neurocognition and attenuated psychosis syndrome: preliminary evidence from a pilot study

among treatment-seeking versus healthy adolescents. *Schizophr Res.* (2019) 210:207–14. doi: 10.1016/j.schres.2018.12.036
35. Ribolsi M, Lin A, Wardenaar KJ, Pontillo M, Mazzone L, Vicari S, et al. Clinical presentation of attenuated psychosis syndrome in children and adolescents: is there an age effect? *Psychiatry Res.* (2017) 252:169–74. doi: 10.1016/j.psychres.2017.02.050
36. Carrion RE, Mclaughlin D, Goldberg TE, Auther AM, Olsen RH, Olvet DM, et al. Prediction of functional outcome in individuals at clinical high risk for psychosis. *JAMA Psychiatry.* (2013) 70:1133–42. doi: 10.1001/jamapsychiatry.2013.1909
37. Asher L, Zammit S, Sullivan S, Dorrington S, Heron J, Lewis G. The relationship between psychotic symptoms and social functioning in a non-clinical population of 12 year olds. *Schizophr Res.* (2013) 150:404–9. doi: 10.1016/j.schres.2013.08.031
38. Ventura J, Subotnik KL, Gitlin MJ, Gretchen-Doorly D, Ered A, Villa KF, et al. Negative symptoms and functioning during the first year after a recent onset of schizophrenia and 8 years later. *Schizophr Res.* (2015) 161:407–13. doi: 10.1016/j.schres.2014.10.043
39. Erickson M, Jaafari N, Lysaker P. Insight and negative symptoms as predictors of functioning in a work setting in patients with schizophrenia. *Psychiatry Res.* (2011) 189:161–5. doi: 10.1016/j.psychres.2011.06.019
40. Rocca P, Montemagni C, Zappia S, Piterà R, Sigaudo M, Bogetto F. Negative symptoms and everyday functioning in schizophrenia: a cross-sectional study in a real world-setting. *Psychiatry Res.* (2014) 218:284–9. doi: 10.1016/j.psychres.2014.04.018
41. Perkins DO, Jeffries CD, Cornblatt BA, Woods SW, Addington J, Bearden CE, et al. Severity of thought disorder predicts psychosis in persons at clinical high-risk. *Schizophr Res.* (2015) 169:169–77. doi: 10.1016/j.schres.2015.09.008
42. Ciarleglio AJ, Brucato G, Masucci MD, Altschuler R, Colibazzi T, Corcoran CM, et al. A predictive model for conversion to psychosis in clinical high-risk patients. *Psychol Med.* (2019) 49:1128–37. doi: 10.1017/S003329171800171X
43. Fusar-Poli P, Davies C, Rutigliano G, Stahl D, Bonoldi I, Mcguire P. Transdiagnostic individualized clinically based risk calculator for the detection of individuals at risk and the prediction of psychosis: model refinement including nonlinear effects of age. *Front Psychiatry.* (2019) 10:313. doi: 10.3389/fpsyt.2019.00313
44. Fusar-Poli P, Werbeloff N, Rutigliano G, Oliver D, Davies C, Stahl D, et al. Transdiagnostic risk calculator for the automatic detection of individuals at risk and the prediction of psychosis: second replication in an Independent National Health Service Trust. *Schizophr Bull.* (2019) 45:562–70. doi: 10.1093/schbul/sby070
45. Malda A, Boonstra N, Barf H, De Jong S, Aleman A, Addington J, et al. Individualized prediction of transition to psychosis in 1,676 individuals at clinical high risk: development and validation of a multivariable prediction model based on individual patient data meta-analysis. *Front Psychiatry.* (2019) 10:345. doi: 10.3389/fpsyt.2019.00345
46. Cannon TD, Yu C, Addington J, Bearden CE, Cadenhead KS, Cornblatt BA, et al. An individualized risk calculator for research in prodromal psychosis. *Am J Psychiatry.* (2016) 173:980–8. doi: 10.1176/appi.ajp.2016.15070890
47. Oliver D, Reilly TJ, Baccaredda Boy O, Petros N, Davies C, Borgwardt S, et al. What causes the onset of psychosis in individuals at clinical high risk? A meta-analysis of risk and protective factors. *Schizophr Bull.* (2019) 46:110–20. doi: 10.1093/schbul/sbz039
48. Lo Cascio N, Saba R, Hauser M, Vernal DL, Al-Jadiri A, Borenstein Y, et al. Attenuated psychotic and basic symptom characteristics in adolescents with ultra-high risk criteria for psychosis, other non-psychotic psychiatric disorders and early-onset psychosis. *Eur Child Adolesc Psychiatry.* (2016) 25:1091–102. doi: 10.1007/s00787-016-0832-7
49. Salazar De Pablo G, Guinart D, Cornblatt B, Auther A, Carrión R, Carbon M, et al. Demographic and clinical characteristics, including subsyndromal symptoms across bipolar-spectrum disorders in adolescents. *JCAP.* (2020) 30:222–234. doi: 10.1089/cap.2019.0138
50. First M, Williams J, Karg R, Spitzer R. *Structured Clinical Interview for DSM-5—Research Version (SCID-5 for DSM-5, Research Version; SCID-5-RV).* Arlington, VA: American Psychiatric Association. (2015).
51. Kaufman J, Birmaher B, Brent D, Rao U, Flynn C, Moreci P, et al. Schedule for affective disorders and schizophrenia for school-age children-present and lifetime version (K-SADS-PL): initial reliability and validity data. *J Am Acad Child Adolesc Psychiatry.* (1997) 36:980–8. doi: 10.1097/00004583-199707000-00021
52. Mcglashan TWB, Woods S. *The Psychosis-Risk Syndrome: Handbook for Diagnosis and Follow-Up*: Oxford: Oxford University. (2010).
53. Cornblatt BA, Carrion RE, Auther A, Mclaughlin D, Olsen RH, John M, et al. Psychosis prevention: a modified clinical high risk perspective from the recognition and prevention (RAP) program. *Am J Psychiatry.* (2015) 172:986–94. doi: 10.1176/appi.ajp.2015.13121686
54. Busner J, Targum SD. The clinical global impressions scale: applying a research tool in clinical practice. *Psychiatry.* (2007) 4:28–37.
55. Piersma HL, Boes JL. The GAF and psychiatric outcome: a descriptive report. *Community Ment Health J.* (1997) 33:35–41. doi: 10.1023/A:1022413110345
56. Cornblatt BA, Auther AM, Niendam T, Smith CW, Zinberg J, Bearden CE, et al. Preliminary findings for two new measures of social and role functioning in the prodromal phase of schizophrenia. *Schizophr Bull.* (2007) 33:688–702. doi: 10.1093/schbul/sbm029
57. Carrión RE, Auther AM, Mclaughlin D, Olsen R, Addington J, Bearden CE, et al. The global functioning: social and role scales-further validation in a large sample of adolescents and young adults at clinical high risk for psychosis. *Schizophr Bull.* (2019) 45:763–72. doi: 10.1093/schbul/sby126
58. Agrawal S, Bhat RS, Kuruvilla K. Validity of the scale to assess unawareness of mental disorder. *Am J Psychiatry.* (1994) 151:1843–4. doi: 10.1176/ajp.151.12.1843
59. Cramér H. *Mathematical Methods of Statistics.* Princeton: Princeton University Press. (1946).
60. Cohen J. *Statistical Power Analysis for the Behavioral Sciences.* New York, NY: Routledge Academic. (1988).
61. Daniel T, Kostic B. *Effect Size Calculator for t Tests.* (2019). Retrieved from: https://drive.google.com/drive/folders/1n9aCsq5j4dQ6m_sv62ohDI69aol3rW6Q?usp=sharing.
62. Ibm Corp. *IBM SPSS Statistics for Macintosh, Version 21.0.* Armonk, NY: IBM Corp. (2012).
63. Birmaher B, Axelson D, Strober M, Gill MK, Valeri S, Chiappetta L, et al. Clinical course of children and adolescents with bipolar spectrum disorders. *Arch Gen Psychiatry.* (2006) 63:175–83. doi: 10.1001/archpsyc.63.2.175
64. Lindgren M, Manninen M, Laajasalo T, Mustonen U, Kalska H, Suvisaari J, et al. The relationship between psychotic-like symptoms and neurocognitive performance in a general adolescent psychiatric sample. *Schizophr Res.* (2010) 123:77–85. doi: 10.1016/j.schres.2010.07.025
65. Lindgren M, Manninen M, Kalska H, Mustonen U, Laajasalo T, Moilanen K, et al. Predicting psychosis in a general adolescent psychiatric sample. *Schizophr Res.* (2014) 158:1–6. doi: 10.1016/j.schres.2014.06.028
66. Linscott RJ, Van Os J. An updated and conservative systematic review and meta-analysis of epidemiological evidence on psychotic experiences in children and adults: on the pathway from proneness to persistence to dimensional expression across mental disorders. *Psychol Med.* (2013) 43:1133–49. doi: 10.1017/S0033291712001626
67. Gur RC, Calkins ME, Satterthwaite TD, Ruparel K, Bilker WB, Moore TM, et al. Neurocognitive growth charting in psychosis spectrum youths. *JAMA Psychiatry.* (2014) 71:366–74. doi: 10.1001/jamapsychiatry.2013.4190
68. Simeonova DI, Lee FJ, Walker EF. Longitudinal investigation of the relationship between family history of psychosis and affective disorders and Child Behavior Checklist ratings in clinical high-risk adolescents. *Schizophr Res.* (2015) 166:24–30. doi: 10.1016/j.schres.2015.04.027
69. Addington J, Piskulic D, Liu L, Lockwood J, Cadenhead KS, Cannon TD, et al. Comorbid diagnoses for youth at clinical high risk of psychosis. *Schizophr Res.* (2017) 190:90–5. doi: 10.1016/j.schres.2017.03.043
70. Schimmelmann BG, Michel C, Martz-Irngartinger A, Linder C, Schultze-Lutter F. Age matters in the prevalence and clinical significance of ultra-high-risk for psychosis symptoms and criteria in the general population: findings from the BEAR and BEARS-kid studies. *World Psychiatry.* (2015) 14:189–97. doi: 10.1002/wps.20216
71. Stafford MR, Jackson H, Mayo-Wilson E, Morrison AP, Kendall T. Early interventions to prevent psychosis: systematic review and meta-analysis. *Bmj-British Med J.* (2013) 346:f185. doi: 10.1136/bmj.f185
72. Davies C, Cipriani A, Ioannidis JPA, Radua J, Stahl D, Provenzani U, et al. Lack of evidence to favor specific preventive interventions in psychosis: a network meta-analysis. *World Psychiatry.* (2018) 17:196–209. doi: 10.1002/wps.20526

73. De Hert M, Dobbelaere M, Sheridan EM, Cohen D, Correll CU. Metabolic and endocrine adverse effects of second-generation antipsychotics in children and adolescents: a systematic review of randomized, placebo controlled trials and guidelines for clinical practice. *Eur Psychiatry.* (2011) 26:144–58. doi: 10.1016/j.eurpsy.2010.09.011
74. Carbon M, Kapoor S, Sheridan E, Al-Jadiri A, Azzo S, Sarkaria T, et al. Neuromotor adverse effects in 342 youth during 12 weeks of naturalistic treatment with 5 second-generation antipsychotics. *J Am Acad Child Adolesc Psychiatry.* (2015) 54:718–27.e713. doi: 10.1016/j.jaac.2015.06.015
75. Al-Dhaher Z, Kapoor S, Saito E, Krakower S, David L, Ake T, et al. Activating and tranquilizing effects of first-time treatment with aripiprazole, olanzapine, quetiapine, and risperidone in youth. *J Child Adolesc Psychopharmacol.* (2016) 26:458–70. doi: 10.1089/cap.2015.0141
76. Galling B, Roldán A, Nielsen RE, Nielsen J, Gerhard T, Carbon M, et al. Type 2 diabetes mellitus in youth exposed to antipsychotics: a systematic review and meta-analysis. *JAMA Psychiatry.* (2016) 73:247–59. doi: 10.1001/jamapsychiatry.2015.2923
77. Solmi M, Fornaro M, Ostinelli E, Zangani C, Croatto G, Monaco F, et al. Safety of 80 antidepressants, antipsychotics, anti-attention-deficit/hyperactivity medications and mood stabilizers in children and adolescents with psychiatric disorders: a large scale systematic meta-review of 78 adverse effects. *World Psychiatry.* (2020) 19:214–32. doi: 10.1002/wps.20765
78. Rapado-Castro M, Mcgorry PD, Yung A, Calvo A, Nelson B. Sources of clinical distress in young people at ultra high risk of psychosis. *Schizophr Res.* (2015) 165:15–21. doi: 10.1016/j.schres.2015.03.022
79. Dolz M, Tor J, Portoles L, Pardo M, Munoz-Samons D, Rodriguez-Pascual M, et al. Children and adolescents at risk for psychosis: transition and baseline characteristics. *Early Interv Psychiatry.* (2018) 12:187–187.
80. Velthorst E, Zinberg J, Addington J, Cadenhead KS, Cannon TD, Carrion RE, et al. Potentially important periods of change in the development of social and role functioning in youth at clinical high risk for psychosis. *Dev Psychopathol.* (2018) 30:39–47. doi: 10.1017/S0954579417000451
81. Kelleher I, Murtagh A, Molloy C, Roddy S, Clarke MC, Harley M, et al. Identification and characterization of prodromal risk syndromes in young adolescents in the community: a population-based clinical interview study. *Schizophr Bull.* (2012) 38:239–46. doi: 10.1093/schbul/sbr164
82. Gaudiano BA, Zimmerman M. Prevalence of attenuated psychotic symptoms and their relationship with DSM-IV diagnoses in a general psychiatric outpatient clinic. *J Clin Psychiatry.* (2013) 74:149–55. doi: 10.4088/JCP.12m07788
83. Lo Cascio N, Curto M, Pasqualetti P, Lindau JF, Girardi N, Saba R, et al. Impairment in Social Functioning differentiates youth meeting Ultra-High Risk for psychosis criteria from other mental health help-seekers: a validation of the Italian version of the Global Functioning: social and global functioning: role scales. *Psychiatry Res.* (2017) 253:296–302. doi: 10.1016/j.psychres.2017.04.008
84. Herbener ES, Harrow M. Are negative symptoms associated with functioning deficits in both schizophrenia and nonschizophrenia patients? A 10-year longitudinal analysis. *Schizophr Bull.* (2004) 30:813–25. doi: 10.1093/oxfordjournals.schbul.a007134
85. Rabinowitz J, Levine SZ, Garibaldi G, Bugarski-Kirola D, Berardo CG, Kapur S. Negative symptoms have greater impact on functioning than positive symptoms in schizophrenia: analysis of CATIE data. *Schizophr Res.* (2012) 137:147–50. doi: 10.1016/j.schres.2012.01.015
86. Kline E, Millman ZB, Denenny D, Wilson C, Thompson E, Demro C, et al. Trauma and psychosis symptoms in a sample of help-seeking youth. *Schizophr Res.* (2016) 175:174–9. doi: 10.1016/j.schres.2016.04.006
87. Valmaggia LR, Stahl D, Yung AR, Nelson B, Fusar-Poli P, Mcgorry PD, et al. Negative psychotic symptoms and impaired role functioning predict transition outcomes in the at-risk mental state: a latent class cluster analysis study. *Psychol Med.* (2013) 43:2311–25. doi: 10.1017/S0033291713000251
88. Lehembre-Shiah E, Leong W, Brucato G, Abi-Dargham A, Lieberman JA, Horga G, et al. Distinct relationships between visual and auditory perceptual abnormalities and conversion to psychosis in a clinical high-risk population. *JAMA Psychiatry.* (2017) 74:104–6. doi: 10.1001/jamapsychiatry.2016.3055
89. Devylder JE, Ben-David S, Schobel SA, Kimhy D, Malaspina D, Corcoran CM. Temporal association of stress sensitivity and symptoms in individuals at clinical high risk for psychosis. *Psychol Med.* (2013) 43:259–68. doi: 10.1017/S0033291712001262
90. Mcausland L, Addington J. Biofeedback to treat anxiety in young people at clinical high risk for developing psychosis. *Early Interv Psychiatry.* (2018) 12:694–701. doi: 10.1111/eip.12368
91. Carrion RE, Demmin D, Auther AM, Mclaughlin D, Olsen R, Lencz T, et al. Duration of attenuated positive and negative symptoms in individuals at clinical high risk: associations with risk of conversion to psychosis and functional outcome. *J Psychiatr Res.* (2016) 81:95–101. doi: 10.1016/j.jpsychires.2016.06.021
92. Correll CU, Olvet DM, Auther AM, Hauser M, Kishimoto T, Carrión RE, et al. The Bipolar Prodrome Symptom Interview and Scale-Prospective (BPSS-P): description and validation in a psychiatric sample and healthy controls. *Bipolar Disord.* (2014) 16:505–22. doi: 10.1111/bdi.12209

Conflict of Interest: DG has been a consultant for and/or has received speaker honoraria from Otsuka America and Janssen Pharmaceuticals. DV has received speaking fees from Lundbeck. SW has received in the last 5 years royalties from Thieme Hogrefe, Kohlhammer, Springer, Beltz. Outside professional activities and interests are declared under the link of the University of Zurich https://www.uzh.ch/prof/apps/interessenbindungen/client/. CA has been a consultant to or has received honoraria or grants from Acadia, Ambrosseti, Gedeon Richter, Janssen Cilag, Lundbeck, Otsuka, Roche, Sage, Servier, Shire, Schering Plow, Sumitomo Dainippon Pharma, Sunovion and Takeda. CM has acted as consultant or participated in DMC for Janssen, Servier, Lundbeck, Nuvelution, Angelini and Otsuka. PF-P has received grants and personal fees from Lundbeck and personal fees from Menarini. CC has been a consultant and/or advisor to or has received honoraria from: Acadia, Alkermes, Allergan, Angelini, Axsome, Gedeon Richter, Gerson Lehrman Group, IntraCellular Therapies, Janssen/J&J, LB Pharma, Lundbeck, MedAvante-ProPhase, Medscape, Neurocrine, Noven, Otsuka, Pfizer, Recordati, Rovi, Sumitomo Dainippon, Sunovion, Supernus, Takeda, and Teva. He has provided expert testimony for Bristol-Myers Squibb, Janssen, and Otsuka. He served on a Data Safety Monitoring Board for Lundbeck, Rovi, Supernus, and Teva. He received royalties from UpToDate and grant support from Janssen and Takeda. He is also a shareholder of LB Pharm.

The remaining authors declare that the research was conducted in the absence of any commercial or financial relationships that could be construed as a potential conflict of interest.

frontiers in Psychiatry

ORIGINAL RESEARCH
published: 17 November 2020
doi: 10.3389/fpsyt.2020.552037

Personality Factors' Impact on the Structural Integrity of Mentalizing Network in Old Age: A Combined PET-MRI Study

Panteleimon Giannakopoulos[1,2]*, *Cristelle Rodriguez*[1,2], *Marie-Louise Montandon*[1,2,3], *Valentina Garibotto*[4,5], *Sven Haller*[5,6,7] and *François R. Herrmann*[3]

[1] Department of Psychiatry, University of Geneva, Geneva, Switzerland, [2] Medical Direction, Geneva University Hospitals, Geneva, Switzerland, [3] Department of Readaptation and Geriatrics, Geneva University Hospitals and University of Geneva, Geneva, Switzerland, [4] Division of Nuclear Medicine and Molecular Imaging, Diagnostic Department, Geneva University Hospitals, Geneva, Switzerland, [5] Faculty of Medicine of the University of Geneva, Geneva, Switzerland, [6] CIRD - Centre d'Imagerie Rive Droite, Geneva, Switzerland, [7] Department of Surgical Sciences, Radiology, Uppsala University, Uppsala, Sweden

OPEN ACCESS

Edited by:
Bartosz Zurowski, University Medical Center Schleswig-Holstein, Germany

Reviewed by:
Sara L. Weisenbach, Stony Brook Medicine, United States
Jie Lu, Capital Medical University, China
Zan Wang, Southeast University, China

***Correspondence:**
Panteleimon Giannakopoulos panteleimon.giannakopoulos@unige.ch

Specialty section:
This article was submitted to Neuroimaging and Stimulation, a section of the journal Frontiers in Psychiatry

Received: *20 April 2020*
Accepted: *16 October 2020*
Published: *17 November 2020*

Citation:
Giannakopoulos P, Rodriguez C, Montandon M-L, Garibotto V, Haller S and Herrmann FR (2020) Personality Factors' Impact on the Structural Integrity of Mentalizing Network in Old Age: A Combined PET-MRI Study. Front. Psychiatry 11:552037. doi: 10.3389/fpsyt.2020.552037

The mentalizing network (MN) treats social interactions based on our understanding of other people's intentions and includes the medial prefrontal cortex (mPFC), temporoparietal junction (TPJ), posterior cingulate cortex (PCC), precuneus (PC), and amygdala. Not all elders are equally affected by the aging-related decrease of mentalizing abilities. Personality has recently emerged as a strong determinant of functional connectivity in MN areas. However, its impact on volumetric changes across the MN in brain aging is still unknown. To address this issue, we explored the determinants of volume decrease in MN components including amyloid burden, personality, and APOE genotyping in a previously established cohort of 130 healthy elders with a mean follow-up of 54 months. Personality was assessed with the Neuroticism Extraversion Openness Personality Inventory-Revised. Regression models corrected for multiple comparisons were used to identify predictors of volume loss including time, age, sex, personality, amyloid load, presence of APOE epsilon 4 allele, and cognitive evolution. In cases with higher Agreeableness scores, there were lower volume losses in PCC, PC, and amygdala bilaterally. This was also the case for the right mPFC in elders displaying lower Agreeableness and Conscientiousness. In multiple regression models, the effect of Agreeableness was still observed in left PC and right amygdala and that of Conscientiousness was still observed in right mPFC volume loss (26.3% of variability, significant age and sex). Several Agreeableness (Modesty) and Conscientiousness (order, dutifulness, achievement striving, and self-discipline) facets were positively related to increased volume loss in cortical components of the MN. In conclusion, these data challenge the beneficial role of higher levels of Agreeableness and Conscientiousness in old age, showing that they are associated with an increased rate of volume loss within the MN.

Keywords: amyloid load, cohort studies, mentalizing, personality, structural MRI

INTRODUCTION

Mentalizing is the term used to qualify brain ability to treat social interactions that rely on our understanding of other people's intentions, beliefs, traits, and other high-level characteristics [for a review, see (1)]. Early behavioral research showed that such social inferences are mostly made implicitly without any cognitive control (2). Later event-related potential and functional magnetic resonance imaging (MRI) contributions have started to uncover the key brain regions supporting our ability to "think about other's mental states," giving rise to what has become known as the mentalizing network. The main components of this network are the medial prefrontal cortex (mPFC), temporoparietal junction (TPJ), posterior cingulate cortex (PCC), and precuneus (PC) and less commonly the amygdala [for reviews, see (3–7)]. Although the exact role of its area in the construction of social cognition is not yet elucidated, the most widely accepted hypothesis is that social inferences are hierarchically arranged with amygdala providing valenced information, TPJ interpretation of behaviors, PCC and PC imagery and imagination processes needing to infer the metal states of another, and mPFC final interpretations in terms of intentions and traits (1, 5, 8).

Personality patterns affect activation of the mentalizing network. For instance, avoidant traits were associated with higher task-related activation of mPFC, amygdala, and cingulate cortex, whereas the inverse was true in persons with high levels of Neuroticism (9). In the same line, extraversion was negatively associated with PC functional connectivity (10). In addition, personality has recently emerged as a strong determinant of functional connectivity in DMN that includes most of the key areas of the mentalizing network. In particular, high level of openness to experience but also mind wandering were positively related to DMN functional connectivity (11–14). In contrast, both positive and negative associations were reported between this variable and Agreeableness facets. In particular, the connectivity between PCC and PC decreased in cases with high honesty facet (15).

Old age is known to affect theory of mind performances related to both mentalizing during person perception and in virtual settings in the absence of neurodegenerative disorders (4, 16, 17). Lower activity in mPFC and PC has been reported across a variety of social cognitive tasks in healthy elders (18, 19). Importantly, the mentalizing network key nodes are parts of the default mode network (DMN) that displays well-known age-related disturbances of its structural and functional connectivity [for a review, see (20)]. A recent study postulated that AD risk was associated with DMN gray matter volume loss in elderly controls over 60 years of age (21). Not only functional but also volumetric changes in the mentalizing network may affect its performances in old age. Surprisingly, in contrast to functional MRI observations, the aging-related volumetric changes across the mentalizing network and their determinants have been rarely investigated in longitudinal settings. Only two cross-sectional contributions reported aging-related volume loss in mPFC, PC, and PCC and pointed to an increased rate of 1-year atrophy that partly matched the frontotemporal pattern of changes in healthy aging (22, 23).

Whether or not personality factors accelerate or prevent age-related changes in mentalizing network is still unknown. We report here the data from a longitudinal analysis exploring the determinants of volume decrease in mentalizing network components including amyloid burden, personality, and APOE genotyping in a previously established cohort of 130 healthy elders with a mean follow-up of 54 months. Based on the previously cited observations on the relationship between personality factors and mentalizing network connectivity, we hypothesized that Openness to experience and Agreeableness, two of the five personality factors identified by the Big-Five/Five-Factor model (24), may decrease the aging-related volume loss in mentalizing network.

METHODS

Population

The selection of cases among participants of a still ongoing cohort study was described in detail in our recent contribution focusing on the effect of personality in memory-related areas (22). Briefly, all of the cases were recruited via advertisements in local newspapers and media. Exclusion criteria included psychiatric or neurologic disorders; sustained head injury; history of major medical disorders (neoplasm or cardiac illness); alcohol or drug abuse; regular use of neuroleptics, antidepressants; or psychostimulants; and contraindications to PET or MRI scans. To control for the confounding effect of vascular pathology on MRI findings, individuals with subtle cardiovascular symptoms, hypertension (non-treated), and a history of stroke or transient ischemic episodes were also excluded from the present study. The initial cohort included 526 elderly white non-Latinos of mixed European descent individuals living in Geneva and Lausanne catchment area. Due to the need for an excellent French knowledge (in order to participate in detailed neuropsychological testing), the vast majority of the participants were Swiss (or born in French-speaking European countries, 92%). Cases with three neurocognitive assessments at baseline, 18 months, and 54 months; structural brain MRI at baseline and 54 months post-inclusion; brain amyloid PET at follow-up; and APOE status were considered. The sample 54 months post-inclusion included 397 cases (25–28). As a sub-project of this cohort study, the NEO-PI-R assessment was administrated randomly at inclusion in 130 elderly controls (**Table 1**).

Personality Assessment

Personality features and dimensions were assessed at baseline using the French version of the NEO-PI-R (24). Participants completed the 240-item self-report version of the NEO-PI-R questionnaire using a five-point Likert agreement scale. The NEO-PI-R assesses 30 facets, 6 for each of the five personality factors (Neuroticism, Extraversion, Openness, Agreeableness, and Conscientiousness). Neuroticism is the tendency to feel negative emotions including anxiety, hostility, and anger; Extraversion encapsulates the proneness toward positive emotions and feelings such as warmth and enthusiasm;

TABLE 1 | Clinical, demographic, and PET data according to the amyloid status in the present series.

	PET amyloid			*P*-values
	Negative	**Positive**	**Total**	
N	84	46	130	
Female	60 (71.4%)	22 (47.8%)	82 (63.1%)	0.013
Age at Amy PET	79.5 ± 4.4	78.8 ± 3.6	79.3 ± 4.1	0.336
Education (year)				0.065
<9	16 (19.0%)	2 (4.3%)	18 (13.8%)	
9–12	40 (47.6%)	24 (52.2%)	64 (49.2%)	
>12	28 (33.3%)	20 (43.5%)	48 (36.9%)	
APOE4 positive	8 (9.5%)	16 (34.8%)	24 (18.5%)	0.001
MMSE at baseline	28.4 ± 1.3	28.8 ± 1.0	28.6 ± 1.2	0.089
Change in cognition	−0.2 ± 3.5	−2.3 ± 4.0	−0.9 ± 3.8	0.004
Neuroticism (N)	79.9 ± 17.5	75.6 ± 20.7	78.4 ± 18.7	0.234
Extraversion €	99.4 ± 15.0	100.7 ± 15.6	99.8 ± 15.2	0.647
Openness (O)	113.5 ± 16.6	109.3 ± 17.2	112.0 ± 16.9	0.181
Agreeableness (A)	132.8 ± 16.8	125.3 ± 18.5	130.2 ± 17.7	0.025
Conscientiousness ©	115.2 ± 16.3	111.3 ± 16.1	113.8 ± 16.3	0.196
Mean SUVr	0.6 ± 0.1	0.7 ± 0.1	0.6 ± 0.1	< 0.001

Openness, the personal inclination to experience and the appreciation of new situations and thoughts with a curious, imaginative, and creative attitude, is defined along six facets that cover imagination (or fantasy), sense of aesthetics, emotions, and feelings, but also proactive behaviors and actions to explore and experiment beyond habits and routines, as well as intellectual curiosity, and the disposition to negotiate and discuss social, political, and religious values; Agreeableness is characterized by trustful, cooperative, and altruistic tendencies; and, finally, Consciousness is the predisposition to be reliable, resolute, and well-organized, and unwilling to deviate from rules and moral principles.

Neuropsychological Assessment

At baseline, all individuals were evaluated with a neuropsychological battery described in detail previously (27, 29–31). All individuals were also evaluated with the Clinical Dementia Rating scale (CDR) (32). According to the criteria of Petersen et al. (33), participants with a CDR of 0.5 but no dementia and a score exceeding 1.5 standard deviations below the age-appropriate mean in any of the cognitive tests were classified as MCI and were excluded. Participants with neither dementia nor MCI were classified as cognitively healthy controls and underwent two additional cognitive assessments after a mean period of 18 and 54 months.

In the absence of consensus, the definition of groups within the normal range on the basis of neuropsychological criteria should avoid to include a priori hypotheses on the cognitive fate of cases with unstable cognitive performances. Among them, some cases progress at the first follow-up and remain stable or even improve their performance at the second follow-up. Others are stable at the first follow-up and progress later on (but may improve or remain stable at later time points). To resolve this difficult question, we calculated the number of tests with improved minus the number of tests with decreased performances resulting in a final continuous cognitive score for each time point. Change in cognition between inclusion and last follow-up was defined as the sum of the continuous cognitive scores at two follow-ups. This new approach makes it possible to avoid a priori hypotheses regarding the longitudinal evolution of cognition in our cases. Cognitive trajectories were defined after summing the number of cognitive tests at follow-up with performances at least 0.5 standard deviation (SD) higher or lower compared with the first evaluation (*Z* scores). Change in cognition between inclusion and last follow-up was defined as the sum of the continuous cognitive scores at two follow-ups as previously described (25, 30).

Amyloid PET Imaging

One hundred twenty-two 18F-Florbetapir (Amyvid) and 8 18F-Flutemetanol PET (Vizamyl) data were acquired on two PET scans (Siemens BiographTM mCT scanner and GE Healthcare Discovery PET/CT 710 scanner) of varying resolution and following different platform-specific acquisition protocols. The 18F-Florbetapir images were acquired 50–70 min after injection, and the 18F-Flutemetanol PET images were acquired 90 to 120 min after injection. PET images were reconstructed using the parameters recommended by the ADNI protocol aimed at increasing data uniformity across the multicenter acquisitions (22).

Amyloid positivity was visually assessed following standardized procedures approved by the European Medicinal Agency. Moreover, all scans were intensity normalized using the thalamus-pons as target region as described by Lilja et al. (34), and cortical standard uptake value ratios (SUVRs) were then calculated.

MR Imaging

At baseline, imaging data were acquired on a 3-T MRI scanner (TRIO SIEMENS Medical Systems, Erlangen, Germany). The structural high-resolution T1-weighted anatomical scan was performed with the following fundamental parameters: 256 × 256 matrix, 176 slices, 1 mm isotropic, TR = 2.27 ms. Due to change of MR equipment, follow-up imaging was performed on a 3-T MR750w scanner (GE Healthcare, Milwaukee, Wisconsin) including a high-resolution anatomical 3DT1 sequence (254 × 254 matrix, 178 slices, 1 mm isotropic, TR = 7.24 ms). At both acquisition times, additional sequences (T2w imaging, susceptibility-weighted imaging, and diffusion tensor imaging) were used and analyzed by an experienced neuroradiologist to exclude incidental brain lesions. The average interval between baseline and follow-up imaging was 4.5 ± 0.6 years.

Automatic MR volumetry of both baseline and follow-up MRI was performed with the Combinostics cNeuro software package, using the standard processing parameters as described in the software package (https://www.cneuro.com). Our analysis included both the most frequently cited areas of the mentalizing network (mPFC, TPJ, PC, and PCC) and angular gyrus and amygdala. In order to examine the specificity of our findings,

we also analyzed the personality impact on the volume of three control areas (caudate nuclei, fusiform gyrus, and cerebellum). Volume loss was calculated as follows: (volume follow-up – volume baseline)/(volume baseline × time in years).

APOE Status

Whole blood samples were collected at baseline for all subjects for APOE genotyping. Standard DNA extraction was performed using either 9-ml EDTA tubes (Sarstedt, Germany) or Oragene Saliva DNA Kit (DNA Genotek, Inc., Ottawa, ON, Canada), which were stored at −20°C. APOE genotyping was done on the LightCycler (Roche Diagnostics, Basel, Switzerland) as described previously (35). Subjects were divided according to their APOE epsilon 4 allele status (4/3 vs. 3/3, 3/2 carriers).

Statistics

Amyloid-positive and -negative cases were compared in respect to their clinical data with Fisher exact test, unpaired *t*-test, and Mann–Whitney *U*-test. Mixed effects linear regression models were used to identify predictors of the brain volume (dependent variable) including time, sex, age, personality factors (and facets), mean SUVR, APOE genotyping, and continuous cognitive score. The significance level was set at $p < 0.05$ but was corrected for multivariable testing by using the Benjamini–Hochberg method (36). All statistics were performed with the STATA statistical software, Version 16.1 (StataCorp, College Station, Texas, 2019).

RESULTS

Descriptive Data

Men were overrepresented among amyloid-positive cases. Amyloid positivity was associated with significantly higher frequency of APOE epsilon 4 genotype, lower scores of Agreeableness, and increased mean SUVR (**Table 1**). The association between amyloid positivity and gender or lower Agreeableness did not survive after correction for multiple comparisons. Importantly, no case evolved to MCI during the follow-up period. To decrease the level of inter-individual variability, the mean SUVR (instead of binary amyloid classification) was used in further statistical analyses (37, 38).

NEO-PI Factors

In univariate models, cases with lower Agreeableness scores displayed higher volumes at follow-up in PCC, PC, and amygdala bilaterally. This was also the case for right mPFC in elders displaying lower Agreeableness and Conscientiousness (**Table 2**). The percentage of variability in volume loss explained by agreeableness scores was of 26.3% (left and right amygdala), 24.4% (left PC), 16.7% (left PCC), 27.4% (right mPFC), 24.4% (right PC), and 13.8% (right PCC). This percentage was of 10.1% for the association between lower Conscientiousness and right mPFC volume loss. When correction for multiple comparisons was applied, the associations persisted in all of the abovementioned areas, except the right mPFC for Agreeableness.

In multiple regression models, the negative association between Agreeableness and brain volume was still observed in left PC (38.4% of variability, significant sex variable) and left (35.6% of variability, significant sex and APOE 4 genotype variables) and right amygdala (30.4% of variability, significant sex, APOE4, mean SUVr, and change of continuous cognitive score). This was also the case for the negative association between Conscientiousness and right mPFC volume (26.3% of variability, significant age and sex). Interestingly, a significant association emerged in multivariate models between higher Conscientiousness and increased brain volume loss in bilateral PCC and left PC (**Table 2**). After correction for multiple comparisons, the significance was preserved for the association between higher Agreeableness scores and increased volume loss in left PC. This was also the case for the association between higher Conscientiousness scores and increased volume loss in right mPFC. There were no associations between NEO-PI factors and brain volume changes in all of the control areas.

NEO-PI Facets

The NEO-PI facets of Agreeableness and Conscientiousness have also been considered in regression models. We retained only the associations that survived in multiple regression models and after correction for multiple comparisons (**Tables 3**, **4**). Among agreeableness facets, higher modesty scores were associated with increased volume loss in left PC and right mPFC. Conscientiousness facets had also a negative association with brain volumes within the mentalizing network. In the left hemisphere, higher-order scores (C2) were related to decreased PCC volume at follow-up. In the right hemisphere, the same facet scores were negatively related to PC and PCC volumes. Self-discipline scores were negatively related to PCC volumes. Most importantly, order, dutifulness, achievement striving, and self-discipline scores were all negatively related to mPFC volume at follow-up. In all of the control areas, no association was found between NEO-PI personality facets and volume loss.

DISCUSSION

The present findings reveal that higher levels of Agreeableness and Conscientiousness have a negative impact on the structural integrity of the mentalizing network. This observation concerned not only the factors but also the corresponding facets (modesty for Agreeableness and order, dutifulness, achievement striving, and self-discipline for Conscientiousness). The impact of these personality factors was mainly present in mPFC, PC, and PCC, the three main cortical components of the mentalizing network as well as in amygdala but not in TPJ. Pointing to the specificity of our findings, such associations were not found in control areas (caudate, fusiform gyrus, and cerebellum) and did not concern the other personality factors.

Early cross-sectional data on the association between NEO-PI factors (and facets) and MRI volumes in brain aging revealed discrepant findings. Lower Openness scores were related to a widespread decrease of gray matter volumes whereas higher Neuroticism and scores were associated with decreased volumes in frontal and temporal cortices. Extraversion and Agreeableness scores display positive associations with superior, medial, and orbitofrontal cortex volumes, whereas the effect of Conscientiousness is more ambiguous (36–38). In a recent

TABLE 2 | Association between mentalizing network component volume by side and personality dimensions assessed with univariate and multiple mixed linear regression, adjusted for time, sex, APOE4, amyloid1 load, and change in cognition.

		Left side						Right side					
		Univariate			Multiple			Univariate			Multiple		
Brain region	**Personality dimensions**	**Coeff (95% CI)**	***p***	**BH**	**Coeff (95% CI)**	***p***	**BH**	**Coeff (95% CI)**	***p***	**BH**	**Coeff (95% CI)**	***p***	**BH**
Medial prefrontal cortex (mPFC)	Neuroticism	−0.002 (−0.006, 0.001)	0.246		−0.002 (−0.006, 0.001)	0.139		−0.001 (−0.005, 0.002)	0.469		−0.002 (−0.005, 0.002)	0.380	
	Extraversion	0.002 (−0.003, 0.006)	0.433		0.002 (−0.003, 0.006)	0.435		0.001 (−0.004, 0.005)	0.757		−0.000 (−0.005, 0.004)	0.834	
	Openness	0.004 (0.000, 0.008)	0.039		0.004 (0.000, 0.008)	0.032		0.001 (−0.003, 0.005)	0.733		−0.001 (−0.004, 0.003)	0.800	
	Agreeableness	−0.000 (−0.004, 0.003)	0.871		0.002 (−0.001, 0.006)	0.200		−0.005 (−0.008, −0.001)	0.012		−0.004 (−0.007, 0.000)	0.068	
	Conscientiousness	0.001 (−0.003, 0.005)	0.647		−0.000 (−0.004, 0.004)	0.955		−0.005 (−0.009, −0.002)	0.005	*	−0.006 (−0.010, −0.003)	0.001	*
Posterior cingulate cortex (PCC)	Neuroticism	−0.001 (−0.009, 0.008)	0.835		−0.001 (−0.009, 0.006)	0.740		0.002 (−0.006, 0.010)	0.677		0.001 (−0.006, 0.008)	0.764	
	Extraversion	0.008 (−0.002, 0.018)	0.119		0.006 (−0.003, 0.016)	0.171		0.004 (−0.006, 0.014)	0.430		0.002 (−0.008, 0.011)	0.750	
	Openness	0.009 (−0.000, 0.018)	0.054		0.007 (−0.001, 0.015)	0.087		0.006 (−0.003, 0.015)	0.163		0.006 (−0.003, 0.014)	0.187	
	Agreeableness	−0.014 (−0.023, −0.006)	0.000	*	−0.008 (−0.016, 0.000)	0.061		−0.012 (−0.020, −0.004)	0.004	*	−0.005 (−0.014, 0.003)	0.195	
	Conscientiousness	−0.007 (−0.017, 0.002)	0.132		−0.011 (−0.018, −0.003)	0.009		−0.006 (−0.015, 0.003)	0.213		−0.009 (−0.017, −0.001)	0.022	
Precuneus	Neuroticism	−0.011 (−0.027, 0.006)	0.200		−0.010 (−0.024, 0.004)	0.154		−0.008 (−0.025, 0.009)	0.364		−0.008 (−0.022, 0.006)	0.253	
	Extraversion	0.007 (−0.013, 0.028)	0.474		0.003 (−0.015, 0.021)	0.740		0.012 (−0.009, 0.033)	0.253		0.011 (−0.007, 0.029)	0.236	
	Openness	−0.005 (−0.024, 0.013)	0.561		−0.005 (−0.021, 0.010)	0.502		−0.001 (−0.020, 0.018)	0.894		−0.001 (−0.018, 0.015)	0.880	
	Agreeableness	−0.035 (−0.050, −0.020)	0.000	*	−0.022 (−0.037, −0.007)	0.005		−0.030 (−0.047, −0.013)	0.000	*	−0.014 (−0.030, 0.002)	0.095	
	Conscientiousness	−0.008 (−0.026, 0.011)	0.411		−0.015 (−0.030, −0.000)	0.050		−0.006 (−0.025, 0.014)	0.571		−0.014 (−0.030, 0.002)	0.089	
Temporoparietal junction (TPJ)	Neuroticism	−0.012 (−0.027, 0.003)	0.106		−0.013 (−0.026, 0.000)	0.057		−0.006 (−0.023, 0.012)	0.527		−0.006 (−0.023, 0.010)	0.458	
	Extraversion	0.017 (−0.001, 0.035)	0.069		0.012 (−0.005, 0.030)	0.161		0.019 (−0.002, 0.040)	0.075		0.017 (−0.004, 0.039)	0.110	
	Openness	0.006 (−0.011, 0.022)	0.496		0.004 (−0.011, 0.020)	0.582		0.006 (−0.013, 0.025)	0.542		0.003 (−0.016, 0.023)	0.747	
	Agreeableness	−0.012 (−0.027, 0.004)	0.140		0.001 (−0.014, 0.017)	0.859		−0.009 (−0.028, 0.009)	0.319		0.002 (−0.017, 0.021)	0.844	
	Conscientiousness	−0.000 (−0.017, 0.017)	0.963		−0.005 (−0.020, 0.011)	0.556		0.001 (−0.019, 0.021)	0.947		−0.003 (−0.023, 0.016)	0.730	
Amygdala	Neuroticism	−0.001 (−0.002, 0.001)	0.300		−0.001 (−0.002, 0.000)	0.169		0.000 (−0.001, 0.002)	0.765		0.000 (−0.001, 0.001)	0.847	
	Extraversion	0.001 (−0.001, 0.003)	0.185		0.000 (−0.001, 0.002)	0.665		0.001 (−0.000, 0.003)	0.137		0.001 (−0.001, 0.002)	0.467	
	Openness	0.002 (0.000, 0.003)	0.046		0.001 (−0.000, 0.002)	0.143		0.001 (−0.001, 0.003)	0.199		0.000 (−0.001, 0.002)	0.916	
	Agreeableness	−0.003 (−0.004, −0.002)	0.000	*	−0.002 (−0.003, −0.000)	0.014		−0.003 (−0.004, −0.001)	0.000	*	−0.002 (−0.003, −0.000)	0.011	
	Conscientiousness	0.000 (−0.002, 0.002)	0.779		−0.000 (−0.002, 0.001)	0.755		0.000 (−0.001, 0.002)	0.597		0.000 (−0.001, 0.002)	0.858	
Caudate	Neuroticism	−0.000 (−0.005, 0.005)	0.916		−0.000 (−0.005, 0.005)	0.979		−0.000 (−0.005, 0.005)	0.948		0.000 (−0.005, 0.005)	0.942	
	Extraversion	0.004 (−0.002, 0.010)	0.168		0.002 (−0.004, 0.008)	0.471		0.005 (−0.001, 0.011)	0.119		0.003 (−0.003, 0.009)	0.404	
	Openness	0.003 (−0.002, 0.008)	0.258		0.002 (−0.003, 0.007)	0.412		0.005 (−0.000, 0.010)	0.074		0.003 (−0.002, 0.009)	0.208	
	Agreeableness	−0.004 (−0.009, 0.001)	0.140		−0.001 (−0.006, 0.004)	0.676		−0.002 (−0.007, 0.003)	0.519		0.001 (−0.005, 0.006)	0.773	
	Conscientiousness	−0.002 (−0.008, 0.003)	0.392		−0.003 (−0.008, 0.002)	0.210		−0.003 (−0.009, 0.002)	0.222		−0.004 (−0.009, 0.001)	0.113	
Fusiform gyrus	Neuroticism	−0.010 (−0.021, 0.002)	0.111		−0.009 (−0.019, 0.001)	0.080		−0.007 (−0.020, 0.006)	0.287		−0.006 (−0.017, 0.006)	0.330	
	Extraversion	0.004 (−0.011, 0.018)	0.616		0.001 (−0.012, 0.015)	0.863		0.001 (−0.015, 0.017)	0.892		−0.002 (−0.017, 0.013)	0.799	
	Openness	0.009 (−0.004, 0.022)	0.184		0.008 (−0.004, 0.020)	0.175		0.007 (−0.007, 0.021)	0.344		0.006 (−0.008, 0.019)	0.405	
	Agreeableness	−0.007 (−0.020, 0.005)	0.239		0.005 (−0.006, 0.017)	0.370		−0.015 (−0.029, −0.002)	0.026		−0.004 (−0.017, 0.010)	0.585	
	Conscientiousness	−0.003 (−0.016, 0.011)	0.709		−0.008 (−0.020, 0.003)	0.171		−0.003 (−0.018, 0.011)	0.648		−0.009 (−0.022, 0.004)	0.182	
Cerebellum	Neuroticism	−0.036 (−0.107, 0.034)	0.314		−0.033 (−0.097, 0.030)	0.303		−0.031 (−0.108, 0.045)	0.424		−0.027 (−0.095, 0.042)	0.447	
	Extraversion	0.021 (−0.067, 0.109)	0.643		−0.004 (−0.086, 0.079)	0.933		0.018 (−0.077, 0.113)	0.710		−0.013 (−0.102, 0.076)	0.779	
	Openness	−0.016 (−0.095, 0.064)	0.697		−0.035 (−0.108, 0.038)	0.350		−0.021 (−0.107, 0.064)	0.625		−0.044 (−0.123, 0.034)	0.270	
	Agreeableness	−0.054 (−0.129, 0.020)	0.154		0.015 (−0.059, 0.088)	0.699		−0.065 (−0.145, 0.015)	0.112		0.008 (−0.072, 0.087)	0.852	
	Conscientiousness	−0.001 (−0.084, 0.081)	0.972		−0.024 (−0.097, 0.049)	0.523		−0.007 (−0.096, 0.082)	0.874		−0.030 (−0.109, 0.048)	0.448	

p values are uncorrected. The Benjamini–Hochberg threshold is p = 0.005 for the univariate and p = 0.001 for the multivariable analysis.

**Indicates significant values according to Benjamini-Hochberg correction.*

TABLE 3 | Association between mentalizing network component volume by side and facets of Agreeableness assessed with multiple mixed linear regression, adjusted for time, sex, APOE4, amyloid load, and change in cognition.

		Left side			Right side		
Brain region	**Facets**	**Coeff (95% CI)**	***p***	**BH**	**Coeff (95% CI)**	***p***	**BH**
Medial prefrontal cortex (mPFC)	Trust	0.014 (−0.002, 0.030)	0.096		−0.001 (−0.018, 0.016)	0.906	
	Straightforwardness/morality	0.006 (−0.007, 0.020)	0.363		−0.011 (−0.025, 0.003)	0.134	
	Altruism	0.004 (−0.016, 0.024)	0.709		−0.014 (−0.034, 0.006)	0.168	
	Compliance/cooperation	0.005 (−0.012, 0.022)	0.572		−0.005 (−0.023, 0.012)	0.547	
	Modesty	−0.001 (−0.015, 0.013)	0.871		−0.020 (−0.034, −0.007)	0.003	*
	Tendermindedness/sympathy	0.024 (0.006, 0.043)	0.011		−0.009 (−0.029, 0.011)	0.379	
Posterior cingulate cortex (PCC)	Trust	−0.006 (−0.043, 0.030)	0.742		−0.011 (−0.048, 0.025)	0.547	
	Straightforwardness/morality	−0.017 (−0.047, 0.012)	0.250		−0.020 (−0.050, 0.010)	0.191	
	Altruism	−0.055 (−0.096, −0.013)	0.010		−0.035 (−0.078, 0.007)	0.101	
	Compliance/cooperation	−0.024 (−0.060, 0.012)	0.199		−0.004 (−0.041, 0.033)	0.838	
	Modesty	−0.023 (−0.053, 0.006)	0.120		−0.010 (−0.040, 0.019)	0.496	
	Tendermindedness/sympathy	−0.028 (−0.071, 0.014)	0.190		−0.025 (−0.068, 0.017)	0.244	
Precuneus	Trust	−0.047 (−0.115, 0.022)	0.184		−0.014 (−0.085, 0.057)	0.703	
	Straightforwardness/morality	−0.044 (−0.100, 0.012)	0.124		−0.038 (−0.096, 0.020)	0.202	
	Altruism	−0.089 (−0.168, −0.010)	0.026		−0.062 (−0.145, 0.022)	0.151	
	Compliance/cooperation	−0.025 (−0.094, 0.044)	0.476		−0.019 (−0.090, 0.053)	0.606	
	Modesty	−0.100 (−0.151, −0.049)	< 0.001	*	−0.062 (−0.119, −0.006)	0.030	
	Tendermindedness/sympathy	−0.078 (−0.158, 0.002)	0.055		−0.047 (−0.130, 0.036)	0.268	
Amygdala	Trust	−0.005 (−0.011, 0.002)	0.149		−0.006 (−0.012, 0.000)	0.056	
	Straightforwardness/morality	−0.004 (−0.009, 0.001)	0.102		−0.007 (−0.012, −0.002)	0.011	
	Altruism	−0.005 (−0.013, 0.002)	0.166		−0.004 (−0.011, 0.004)	0.345	
	Compliance/cooperation	−0.008 (−0.014, −0.002)	0.007		−0.006 (−0.012, 0.000)	0.058	
	Modesty	−0.004 (−0.009, 0.001)	0.146		−0.004 (−0.009, 0.001)	0.145	
	Tendermindedness/sympathy	−0.006 (−0.013, 0.001)	0.096		−0.006 (−0.013, 0.001)	0.110	

p values are uncorrected. The Benjamini–Hochberg threshold is p = 0.005.
**Indicates significant values according to Benjamini-Hochberg correction.*

longitudinal study, we reported that lower Agreeableness and higher Openness are associated with better preservation of the areas early affected by Alzheimer disease pathology such as mesial temporal lobe and hippocampus (25). In particular and unlike functional imaging data on DMN and our own observations in AD-related areas (11–14, 25), Openness to experience scores were unrelated to the rate of volume loss in mentalizing network. Taken together, these observations did not support a global effect of personality factors (and facets) on brain aging processes but rather suggests that they have differential impact on brain integrity depending on the circuits studied.

The clinical significance of the present findings merits further development. Traditionally, high Agreeableness in adult lifespan is thought to be a positive trait of personality being associated with increased subjective well-being (39), better outcome in mental health treatments (40), less disengagement coping (41), and less sexual aggressive behavior (42). In old age, higher Agreeableness levels have been instead associated with poorer executive performance and neurocognitive functions (43–45) and medically unexplained symptoms (46). The role of higher levels of Conscientiousness in old age is equally ambiguous. They were associated with more positive attitudes toward own aging (47), increased well-being (48), and more favorable biomedical markers of health status (49) but also increased late-onset suicide attempts (50), decreased benefit of mental demands at workplace (51), and increased exposure to mental health problems (52). Unlike Neuroticism, high levels of Agreeableness and Conscientiousness were frequently considered as positive characteristics in the course of adult life. Agreeable persons are more prone to establish interpersonal relationships without aggressiveness searching for social approval adopting a majoritarian viewpoint. In old age, this kind of social adaption to other's willingness may be much less imperative. Conscientiousness corresponds to the individual ability to regulate impulsiveness and adopt a stable and rational communication style. Individuals with a high level of conscientiousness may formulate long-range goals, being able to work consistently to achieve them. In adult life, they may be seen as responsible and reliable persons. However, when work is less present in daily life, they may be seen as compulsive perfectionists, boring, or with rigid defense mechanisms. The present findings indicate that higher levels of Agreeableness and Conscientiousness may

TABLE 4 | Association between mentalizing network component volume by side and facets of Conscientiousness assessed with multiple mixed linear regression, adjusted for time, sex, APOE4, amyloid load, and change in cognition.

		Left side			Right side		
Brain region	**Facets**	**Coeff (95% CI)**	***p***	**BH**	**Coeff (95% CI)**	***p***	**BH**
Medial prefrontal cortex (mPFC)	Competence	0.006 (−0.012, 0.024)	0.506		−0.007 (−0.026, 0.012)	0.472	
	Order	−0.005 (−0.019, 0.010)	0.553		−0.020 (−0.034, −0.005)	0.007	*
	Dutifulness	−0.002 (−0.019, 0.016)	0.868		−0.025 (−0.042, −0.008)	0.003	*
	Achievement striving	0.004 (−0.017, 0.025)	0.728		−0.038 (−0.058, −0.019)	0.000	*
	Self–discipline	−0.004 (−0.018, 0.010)	0.554		−0.023 (−0.036, −0.010)	0.001	*
	Deliberation	0.005 (−0.015, 0.025)	0.623		−0.017 (−0.037, 0.003)	0.093	
Posterior cingulate cortex (PCC)	Competence	−0.031 (−0.070, 0.008)	0.123		−0.035 (−0.074, 0.004)	0.075	
	Order	−0.048 (−0.078, −0.017)	0.002		−0.043 (−0.074, −0.012)	0.007	*
	Dutifulness	−0.026 (−0.064, 0.012)	0.185		−0.012 (−0.050, 0.026)	0.538	
	Achievement striving	−0.027 (−0.073, 0.019)	0.256		−0.011 (−0.058, 0.035)	0.635	
	Self–discipline	−0.041 (−0.069, −0.013)	0.004		−0.043 (−0.071, −0.015)	0.003	*
	Deliberation	−0.033 (−0.075, 0.010)	0.136		−0.023 (−0.066, 0.020)	0.301	
Precuneus	Competence	0.007 (−0.068, 0.083)	0.855		−0.037 (−0.115, 0.040)	0.342	
	Order	−0.078 (−0.136, −0.020)	0.009		−0.083 (−0.143, −0.023)	0.007	*
	Dutifulness	−0.013 (−0.085, 0.059)	0.721		−0.000 (−0.076, 0.075)	0.990	
	Achievement striving	−0.071 (−0.157, 0.015)	0.107		−0.044 (−0.134, 0.046)	0.334	
	Self–discipline	−0.068 (−0.121, −0.014)	0.014		−0.056 (−0.113, 0.001)	0.054	
	Deliberation	−0.066 (−0.146, 0.014)	0.108		−0.027 (−0.112, 0.057)	0.528	
Amygdala	Competence	0.004 (−0.003, 0.011)	0.282		0.002 (−0.005, 0.009)	0.516	
	Order	−0.002 (−0.008, 0.003)	0.430		−0.000 (−0.006, 0.006)	0.974	
	Dutifulness	−0.002 (−0.008, 0.005)	0.626		0.001 (−0.006, 0.008)	0.742	
	Achievement striving	0.001 (−0.007, 0.009)	0.898		0.004 (−0.004, 0.012)	0.275	
	Self-discipline	−0.002 (−0.007, 0.003)	0.475		−0.002 (−0.007, 0.003)	0.444	
	Deliberation	−0.001 (−0.009, 0.006)	0.774		−0.000 (−0.008, 0.007)	0.912	

p values are uncorrected. The Benjamini–Hochberg threshold is p = 0.005 (left side) and p = 0.008 (right side).
**Indicates significant values according to Benjamini-Hochberg correction.*

be detrimental for the structural integrity of the mentalizing network since they are associated with increasing rate of atrophy of some of its main components. In our series, higher agreeableness was also related to amyloid positivity, further supporting the idea that, unlike young age, it may represent a factor associated with brain vulnerability in old age (25).

Some strengths of the present work should be discussed. Volume loss in old age is a multifactorial phenomenon that is determined by demographic parameters (age, gender), genetic predisposal (in particular APOE epsilon 4 genotype), and progressive formation of aging-related pathologies such as vascular lesions and amyloid accumulation. Moreover, the variability of cognitive trajectories in elderly persons is an additional confounder that correlates with brain volume changes over time in elderly individuals. In a community-based cohort with careful exclusion of significant vascular burden, psychiatric and neurological conditions, and drug abuse, we had the opportunity to control for the relative contribution of all of the previously mentioned factors. The second issue concerns the obvious risk of multiple comparison biases when assessing the relationship between NEO-PI personality factors (and facets) and volumes of various brain areas. To limit this risk, we first formulated a priori hypotheses focusing on the mentalizing network. In addition, the association between personality and MRI measures was studied using a stringent criterion for multiple comparisons to exclude false-positive results. This is particularly important in respect to the numerous personality facets that have been taken into account. Four main limitations should be considered when interpreting these observations. First, baseline and follow-up MRI were acquired on two different scanners, due to the longitudinal study design. One could speculate that this change could confound the estimated volumes. The change of MR scanners is a known problem in a clinical setting. We carefully matched the MR sequences between both scanners and used software with compensation algorithms. Most importantly, our regression models aim to explore the association between personality factors (and facets) and brain volume changes. They are thus not affected by MRI scan changes as could be the cases when assessing group differences. Second, our cases show no or very mild vascular pathology and relatively high level of education. Although necessary for controlling the confounding effect of this variable, this way to proceed decreases the representativeness of our sample. Third, the combination

of all significant predictors allows for explaining < 40% of the volume loss variability in the areas studied. Although substantial in the light of the marked heterogeneity of normal aging and relatively small sample size, this percentage indicates the presence of additional predictors that have been not taken into account in our analysis. Finally, this study focuses on volumetric changes and did not include a functional MRI component. We cannot thus comment on the association between personality and patterns of functional activation within the mentalizing network in old age.

In conclusion, we report here a specific association between lower levels of Agreeableness and Conscientiousness and better preservation of the volume of mentalizing network components in old age. In the light of these findings, one could speculate that ToM performances may be more resistant in the subsample of cognitively preserved elders with such NEO-PI profile. Although research on the association between personality factors and mentalizing is still in its infancy, some first data point to the idea that at least some components of Agreeableness may be negatively associated with this main human ability (15). Future studies in larger community-based cohorts including *ad hoc* theory of mind activation paradigms tasks, as well as *in vivo* assessment of tau pathology and brain metabolism, are warranted to further explore the role of personality in age-related changes of the mentalizing network.

DATA AVAILABILITY STATEMENT

The original contributions presented in the study are publicly available. This data can be found at: https://doi.org/10.5061/dryad.3tx95x6dp.

ETHICS STATEMENT

The studies involving human participants were reviewed and approved by Commission cantonale d'éthique de la recherche CCER. The patients/participants provided their written informed consent to participate in this study.

AUTHOR CONTRIBUTIONS

PG and FH contributed to the study design and wrote the paper. CR and VG were involved in participant recruitment, follow-up, and data acquisition. M-LM, SH, FH, and PG performed and analyzed the data. All authors read and approved the final manuscript.

FUNDING

This project was supported by the Association Suisse pour la Recherche sur Alzheimer, the Schmidheiny Foundation, and the Swiss National Foundation (Grant No. 320030-169390).

REFERENCES

1. Van Overwalle F, Vandekerckhove M. Implicit and explicit social mentalizing: dual processes driven by a shared neural network. *Front Hum Neurosci.* (2013) 7:560. doi: 10.3389/fnhum.2013.00560
2. Winter L, Uleman JS. When are social judgments made? Evidence for the spontaneousness of trait inferences. *J Pers Soc Psychol.* (1984) 47:237–52. doi: 10.1037/0022-3514.47.2.237
3. Ames DL, Fiske ST. Outcome dependency alters the neural substrates of impression formation. *Neuroimage.* (2013) 83:599–608. doi: 10.1016/j.neuroimage.2013.07.001
4. Cassidy BS, Gutchess AH. Neural responses to appearance-behavior congruity. *Soc Cogn.* (2015) 33:211–26. doi: 10.1521/soco.2015.33.3.1
5. Mar RA. The neural bases of social cognition and story comprehension. *Annu Rev Psychol.* (2011) 62:103–34. doi: 10.1146/annurev-psych-120709-145406
6. Prounis GS, Ophir AG. One cranium, two brains not yet introduced: distinct but complementary views of the social brain. *Neurosci Biobehav Rev.* (2020) 108:231–45. doi: 10.1016/j.neubiorev.2019.11.011
7. Stanley DA. Getting to know you: general and specific neural computations for learning about people. *Soc Cogn Affect Neurosci.* (2016) 11:525–36. doi: 10.1093/scan/nsv145
8. Bachmann J, Munzert J, Krüger B. Neural underpinnings of the perception of emotional states derived from biological human motion: a review of neuroimaging research. *Front Psychol.* (2018) 9:1763. doi: 10.3389/fpsyg.2018.01763
9. Schneider-Hassloff H, Straube B, Nuscheler B, Wemken G, Kircher T. Adult attachment style modulates neural responses in a mentalizing task. *Neuroscience.* (2015) 303:462–73. doi: 10.1016/j.neuroscience.2015.06.062
10. Zou L, Su L, Qi R, Zheng S, Wang L. Relationship between extraversion personality and gray matter volume and functional connectivity density in healthy young adults: an fMRI study. *Psychiatr Res Neuroimag.* (2018) 281:19–23. doi: 10.1016/j.pscychresns.2018.08.018
11. Beaty RE, Chen Q, Christensen AP, Qiu J, Silvia PJ, Schacter DL. Brain networks of the imaginative mind: dynamic functional connectivity of default and cognitive control networks relates to openness to experience. *Hum Brain Mapp.* (2018) 39:811–21. doi: 10.1002/hbm.23884
12. Beaty RE, Kaufman SB, Benedek M, Jung RE, Kenett YN, Jauk E, et al. Personality and complex brain networks: the role of openness to experience in default network efficiency. *Hum Brain Mapp.* (2016) 37:773–9. doi: 10.1002/hbm.23065
13. Godwin CA, Hunter MA, Bezdek MA, Lieberman G, Elkin-Frankston S, Romero VL, et al. Functional connectivity within and between intrinsic brain networks correlates with trait mind wandering. *Neuropsychologia.* (2017) 103:140–53. doi: 10.1016/j.neuropsychologia.2017.07.006
14. Simon SS, Varangis E, Stern Y. Associations between personality and whole-brain functional connectivity at rest: evidence across the adult lifespan. *Brain Behav.* (2020) 10:e01515. doi: 10.1002/brb3.1515
15. Allen TA, Rueter AR, Abram SV, Brown JS, DeYoung CG. Personality and neural correlates of mentalizing ability. *Eur J Pers.* (2017) 31:599–613. doi: 10.1002/per.2133
16. Grainger SA, Rakunathan V, Adams AG, Canty AL, Henry JD. An assessment of age differences in theory of mind using the virtual assessment of mentalizing ability. *Neuropsychol Dev Cogn B Aging Neuropsychol Cogn.* (2020) 9:1–11. doi: 10.1080/13825585.2020.1713290
17. Ziaei M, Burianová H, von Hippel W, Ebner NC, Phillips LH, Henry JD. The impact of aging on the neural networks involved in gaze and emotional processing. *Neurobiol Aging.* (2016) 48:182–94. doi: 10.1016/j.neurobiolaging.2016.08.026
18. Moran JM, Jolly E, Mitchell JP. Social-cognitive deficits in normal aging. *J Neurosci.* (2012) 32:5553–61. doi: 10.1523/JNEUROSCI.5511-11.2012
19. Suzuki A, Ueno M, Ishikawa K, Kobayashi A, Okubo M, Nakai T. Age-related differences in the activation of the mentalizing- and reward-related brain regions during the learning of others' true trustworthiness. *Neurobiol Aging.* (2019) 73:1–8. doi: 10.1016/j.neurobiolaging.2018.09.002
20. Mevel K, Chételat G, Eustache F, Desgranges B. The default mode network in healthy aging and Alzheimer's disease. *Int J Alzheimers Dis.* (2011) 2011:535816. doi: 10.4061/2011/535816

21. Cherbuin N, Shaw ME, Walsh E, Sachdev P, Anstey KJ. Validated Alzheimer's disease risk index (ANU-ADRI) is associated with smaller volumes in the default mode network in the early 60s. *Brain Imaging Behav.* (2019) 13:65–74. doi: 10.1007/s11682-017-9789-5
22. Fjell AM, McEvoy L, Holland D, Dale AM, Walhovd KB. Brain changes in older adults at very low risk for Alzheimer's disease. *J Neurosci.* (2013) 33:8237–42. doi: 10.1523/JNEUROSCI.5506-12.2013
23. Goto M, Abe O, Aoki S, Takao H, Hayashi N, Miyati T, et al. Database of normal Japanese gray matter volumes in the default mode network. *J Magn Reson Imaging.* (2014) 39:132–42. doi: 10.1002/jmri.24139
24. Costa T, Mccrae RR. Normal personality assessment in clinical practice: the NEO personality inventory. *Psychol Assessment.* (1992) 4:5–13. doi: 10.1037/1040-3590.4.1.5
25. Giannakopoulos P, Rodriguez C, Montandon ML, Garibotto V, Haller S, Herrmann FR. Less agreeable, better preserved? A PET amyloid and MRI study in a community-based cohort. *Neurobiol Aging.* (2020) 89:24–31. doi: 10.1016/j.neurobiolaging.2020.02.004
26. van der Thiel M, Rodriguez C, Giannakopoulos P, Burke MX, Lebel RM, Gninenko N, et al. Brain perfusion measurements using multidelay arterial spin-labeling are systematically biased by the number of delays. *AJNR Am J Neuroradiol.* (2018) 39:1432–8. doi: 10.3174/ajnr.A5717
27. Xekardaki A, Rodriguez C, Montandon ML, Toma S, Tombeur E, Herrmann FR, et al. Arterial spin labeling may contribute to the prediction of cognitive deterioration in healthy elderly individuals. *Radiology.* (2015) 274:490–9. doi: 10.1148/radiol.14140680
28. Zanchi D, Giannakopoulos P, Borgwardt S, Rodriguez C, Haller S. Hippocampal and amygdala gray matter loss in elderly controls with subtle cognitive decline. *Front Aging Neurosci.* (2017) 9:50. doi: 10.3389/fnagi.2017.00050
29. Haller S, Montandon ML, Rodriguez C, Ackermann M, Herrmann FR, Giannakopoulos P. APOE*E4 is associated with gray matter loss in the posterior cingulate cortex in healthy elderly controls subsequently developing subtle cognitive decline. *AJNR Am J Neuroradiol.* (2017) 38:1335–42. doi: 10.3174/ajnr.A5184
30. Herrmann FR, Rodriguez C, Haller S, Garibotto V, Montandon ML, Giannakopoulos P. Gray matter densities in limbic areas and APOE4 independently predict cognitive decline in normal brain aging. *Front Aging Neurosci.* (2019) 11:157. doi: 10.3389/fnagi.2019.00157
31. Zanchi D, Montandon ML, Sinanaj I, Rodriguez C, Depoorter A, Herrmann FR, et al. Decreased fronto-parietal and increased default mode network activation is associated with subtle cognitive deficits in elderly controls. *Neurosignals.* (2017) 25:127–38. doi: 10.1159/000486152
32. Hughes CP, Berg L, Danziger WL, Coben LA, Martin RL. A new clinical scale for the staging of dementia. *Br J Psychiatr.* (1982) 140:566–72. doi: 10.1192/bjp.140.6.566
33. Petersen RC, Doody R, Kurz A, Mohs RC, Morris JC, Rabins PV, et al. Current concepts in mild cognitive impairment. *Arch Neurol.* (2001) 58:1985–92. doi: 10.1001/archneur.58.12.1985
34. Lilja J, Leuzy A, Chiotis K, Savitcheva I, Sörensen J, Nordberg A. Spatial normalization of [(18)F]flutemetamol PET images utilizing an adaptive principal components template. *J Nucl Med.* (2018) 60:285–91. doi: 10.2967/jnumed.118.207811
35. Nauck M, Hoffmann MM, Wieland H, Marz W. Evaluation of the apo E genotyping kit on the lightcycler. *Clin Chem.* (2000) 46:722–4. doi: 10.1093/clinchem/46.5.722
36. Green GH, Diggle PJ. On the operational characteristics of the Benjamini and Hochberg false discovery rate procedure. *Stat Appl Genet Mol Biol.* (2007) 6:1302. doi: 10.2202/1544-6115.1302
37. Bullich S, Seibyl J, Catafau AM, Jovalekic A, Koglin N, Barthel H, et al. Optimized classification of (18)F-Florbetaben PET scans as positive and negative using an SUVR quantitative approach and comparison to visual assessment. *Neuroimage Clin.* (2017) 15:325–32. doi: 10.1016/j.nicl.2017.04.025
38. Mountz JM, Laymon CM, Cohen AD, Zhang Z, Price JC, Boudhar S, et al. Comparison of qualitative and quantitative imaging characteristics of [11C]PiB and [18F]flutemetamol in normal control and Alzheimer's subjects. *Neuroimage Clin.* (2015) 9:592–8. doi: 10.1016/j.nicl.2015.10.007
39. Strickhouser JE, Zell E, Krizan Z. Does personality predict health and well-being? A metasynthesis. *Health Psychol.* (2017) 36:797–810. doi: 10.1037/hea0000475
40. Bucher MA, Suzuki T, Samuel DB. A meta-analytic review of personality traits and their associations with mental health treatment outcomes. *Clin Psychol Rev.* (2019) 70:51–63. doi: 10.1016/j.cpr.2019.04.002
41. Carver CS, Connor-Smith J. Personality and coping. *Annu Rev Psychol.* (2010) 61:679–704. doi: 10.1146/annurev.psych.093008.100352
42. Allen MS, Walter EE. Health-related lifestyle factors and sexual dysfunction: a meta-analysis of population-based research. *J Sex Med.* (2018) 15:458–75. doi: 10.1016/j.jsxm.2018.02.008
43. Davey A, Siegler IC, Martin P, Costa PT, Poon LW. Personality structure among centenarians: the Georgia centenarian study. *Exp Aging Res.* (2015) 41:361–85. doi: 10.1080/0361073X.2015.1053752
44. Maldonato NM, Sperandeo R, Dell'Orco S, Cozzolino P, Fusco ML, Iorio VS, et al. The relationship between personality and neurocognition among the American elderly: an epidemiologic study. *Clin Pract Epidemiol Ment Health.* (2017) 13:233–45. doi: 10.2174/1745017901713010233
45. Ouanes S, Castelao E, von Gunten A, Vidal PM, Preisig M, Popp J.Ouanes S, et al. Personality, cortisol, and cognition in non-demented elderly subjects: results from a population-based study. *Front Aging Neurosci.* (2017) 9:63. doi: 10.3389/fnagi.2017.00063
46. van Dijk SD, Hanssen D, Naarding P, Lucassen P, Comijs H, Oude Voshaar R. Big five personality traits and medically unexplained symptoms in later life. *Eur Psychiatr.* (2016) 38:23–30. doi: 10.1016/j.eurpsy.2016.05.002
47. Kornadt AE, Siebert JS, Wahl HW. The interplay of personality and attitudes toward own aging across two decades of later life. *PLoS ONE.* (2019) 14:e0223622. doi: 10.1371/journal.pone.0223622
48. Kandler C, Kornadt AE, Hagemeyer B, Neyer FJ. Patterns and sources of personality development in old age. *J Pers Soc Psychol.* (2015) 109:175–91. doi: 10.1037/pspp0000028
49. Sutin AR, Stephan Y, Terracciano A. Facets of conscientiousness and objective markers of health status. *Psychol Health.* (2018) 33:1100–15. doi: 10.1080/08870446.2018.1464165
50. Szücs A, Szanto K, Wright AGC, Dombrovski AY. Personality of late- and early-onset elderly suicide attempters. *Int J Geriatr Psychiatr.* (2020) 35:384–95. doi: 10.1002/gps.5254
51. Hussenoeder FS, Conrad I, Roehr S, Glaesmer H, Hinz A, Enzenbach C, et al. The association between mental demands at the workplace and cognitive functioning: the role of the big five personality traits. *Aging Ment Health.* (2019) 24:1–7. doi: 10.1080/13607863.2019.1617244
52. Farahani MN, Kormi-Nouri R, De Raad B. The relations between conscientiousness and mental health in a North-European and a West-Asian culture. *J Ment Health.* (2019) 28:112–8. doi: 10.1080/09638237.2017.1340597

Conflict of Interest: The authors declare that the research was conducted in the absence of any commercial or financial relationships that could be construed as a potential conflict of interest.

frontiers in Psychiatry

MINI REVIEW
published: 12 January 2021
doi: 10.3389/fpsyt.2020.585769

The Role of Gut Microbiota in the High-Risk Construct of Severe Mental Disorders: A Mini Review

Gabriele Sani[1,2†], *Mirko Manchia*[3,4,5†], *Alessio Simonetti*[6,7], *Delfina Janiri*[1,2,8], *Pasquale Paribello*[3,4], *Federica Pinna*[3,4*] *and Bernardo Carpiniello*[3,4]

[1] Fondazione Policlinico Universitario "Agostino Gemelli" Istituto di ricovero e cura a carattere scientifico (IRCCS), Rome, Italy, [2] Section of Psychiatry, Department of Neuroscience, Università Cattolica del Sacro Cuore, Rome, Italy, [3] Section of Psychiatry, Department of Medical Sciences and Public Health, University of Cagliari, Cagliari, Italy, [4] Unit of Clinical Psychiatry, University Hospital Agency of Cagliari, Cagliari, Italy, [5] Department of Pharmacology, Dalhousie University, Halifax, NS, Canada, [6] Menninger Department of Psychiatry and Behavioral Sciences, Baylor College of Medicine, Houston, TX, United States, [7] Department of Neurology and Psychiatry, Sapienza University of Rome, Rome, Italy, [8] Department of Psychiatry, Icahn School of Medicine at Mount Sinai, New York, NY, United States

Severe mental disorders (SMD) are highly prevalent psychiatric conditions exerting an enormous toll on society. Therefore, prevention of SMD has received enormous attention in the last two decades. Preventative approaches are based on the knowledge and detailed characterization of the developmental stages of SMD and on risk prediction. One relevant biological component, so far neglected in high risk research, is microbiota. The human microbiota consists in the ensemble of microbes, including viruses, bacteria, and eukaryotes, that inhabit several ecological niches of the organism. Due to its demonstrated role in modulating illness and health, as well in influencing behavior, much interest has focused on the characterization of the microbiota inhabiting the gut. Several studies in animal models have shown the early modifications in the gut microbiota might impact on neurodevelopment and the onset of deficits in social behavior corresponding to distinct neurosignaling alterations. However, despite this evidence, only one study investigated the effect of altered microbiome and risk of developing mental disorders in humans, showing that individuals at risk for SMD had significantly different global microbiome composition than healthy controls. We then offer a developmental perspective and provided mechanistic insights on how changes in the microbiota could influence the risk of SMD. We suggest that the analysis of microbiota should be included in the comprehensive assessment generally performed in populations at high risk for SMD as it can inform predictive models and ultimately preventative strategies.

Keywords: microbiome, schizophrenia, depression, genomics, animal models, autism spectrum disorder, Shannon index, alpha diversity

OPEN ACCESS

Edited by:
Sven Haller,
Rive Droite SA, Switzerland

Reviewed by:
Ravinder Nagpal,
Wake Forest School of Medicine, United States
Drozdstoy Stoyanov Stoyanov, Plovdiv Medical University, Bulgaria

***Correspondence:**
Federica Pinna
fedepinna@inwind.it

†These authors have contributed equally to this work

Specialty section:
This article was submitted to Neuroimaging and Stimulation, a section of the journal Frontiers in Psychiatry

Received: *21 July 2020*
Accepted: *15 December 2020*
Published: *12 January 2021*

Citation:
Sani G, Manchia M, Simonetti A, Janiri D, Paribello P, Pinna F and Carpiniello B (2021) The Role of Gut Microbiota in the High-Risk Construct of Severe Mental Disorders: A Mini Review. Front. Psychiatry 11:585769. doi: 10.3389/fpsyt.2020.585769

INTRODUCTION

Severe mental disorders (SMD), including schizophrenia, bipolar disorder and major depressive disorder, are commonly occurring psychiatric conditions exerting an enormous toll on society (1). The 2010 estimate of Gustavsson and co-authors showed that cumulatively direct and indirect costs associated to SMD amount at ∼€140 billion per year in Europe (2). Several factors, other

than the elevated prevalence in the general population, determine the substantial burden of SMD. First, their longitudinal trajectory start during late adolescence-young adulthood with a life-long duration in the vast majority of cases (3, 4). Second, the clinical course of SMD is often chronic with recurrent episodes of psychopathological disturbances and presence of persistent residual symptoms that significantly affect functioning and quality of life. Indeed, SMD represent a major contributor to the total amount of disability-adjusted life-years attributed to communicable and non-communicable diseases at a global level (5). This appears to be mainly determined by the third determinant of burden, i.e., the presence of suboptimal patterns of response to treatments, either pharmacological or non-pharmacological, leading to only a minority of patients achieving psychopathological and functional remission. Finally, SMD are associated with a considerable excess morbidity and mortality (6–8), which cause a significant reduction in life expectancy (on average 10–20 years) compared to the general population (9, 10). In this context, there has been a constant attempt to improve outcomes of SMD. This strategy has mainly focused on prevention, with the most validated paradigm focusing on primary prevention in individuals presenting subtle symptoms and at clinical high risk for SMD (11). Although the early phases of SMD appear to have distinct developmental trajectories for major affective disorders (4) and schizophrenia (3), particularly in the prodromal phases, there is a general consensus that individuals at risk for SMD are those having a genetic liability due to a high familial loading and/or the presence of antecedents such as basic symptoms, cognitive development, affective lability, anxiety, sleep problems, and psychotic-like experiences (11–13).

In this context, risk prediction of SMD is of paramount importance. Several modeling approaches have been developed using clinical (phenotypic) (14), genomic (15, 16), epigenomic (17), or integrated phenotypic-omics datasets (18). However, although the accuracy of prediction in the proposed models appears adequate for clinical purposes (18), and/or feasible in their implementations (14), there is still need of replication and validation of their predictive power in real life clinical settings. One biological component, partly inherited (19), that has been so far neglected in risk prediction of SMD, is the microbiota. The human microbiota consists in the ensemble of microbes, including viruses, bacteria, and eukaryotes, that inhabit several ecological niches of the organism (20, 21). Due to its demonstrated role in modulating illness and health, much interest has focused on the characterization of the microbiota inhabiting the gut (20). In fact, alterations of the gut microbiota have been linked, among the others, to obesity (22), maturation of the immune system (23), and response to drugs (24). Of particular interest is the modulating role that the microbiota acquires in human behavior (25), raising the interest for the investigation of its modifications in SMD. Indeed, several studies have shown substantial alterations, mainly decreased diversity in species within the microbiota, in schizophrenia (26, 27), in bipolar disorder (28), and major depressive disorder (29, 30). For instance, Zhu and coauthors found that, compared to 81 healthy controls, the gut microbiota of 90 medication-free patients with schizophrenia harbored many facultative anaerobes such as *Lactobacillus fermentum*, *Enterococcus faecium*, *Alkaliphilus oremlandii*, and *Cronobacter sakazakii/turicensis*, typically rare in a healthy gut (31). Of note the schizophrenia-associated bacterium *Streptococcus vestibularis*, which contributed to the microbiota metagenomic-based discrimination of patients with schizophrenia from healthy controls, when transplanted to mice gut induced deficits in social behaviors, altering neurotransmitter levels in peripheral tissues of recipient animals (31). In bipolar disorder, Painold and co-authors found that gut microbiota alpha-diversity decreased with increasing illness duration and that Actinobacteria and Coriobacteria were overrepresented in patients compared to healthy controls (HC) (28). Finally, patients with major depressive disorder showed a statistically significant overrepresentation of Bacteroides enterotype 2 compared to controls (32). In addition, a recent systematic review showed that gut dysbiosis and the leaky gut may affect pathways implicated in the neurobiology of major depressive disorder, such immune regulation, oxidative and nitrosative stress, and neuroplasticity (29). However, there is still limited evidence on how microbiota might vary in individuals at risk for SMD compared to healthy controls, as well as to individuals in later stages of SMD. However, there is extensive evidence that the microbiota has a key role in neurodevelopment and can be a modulating factor of the maturity of the central nervous system (CNS) in early developmental stages (33). In this scenario, the aim of this mini review is to present the current evidence on microbiota changes in individuals at high risk for SMD, offering a developmental perspective and providing mechanistic insights on how changes in the gut microbiota make-up could influence the risk of SMD.

GUT MICROBIOTA IN AT RISK MENTAL STATES: A DEVELOPMENTAL PERSPECTIVE

Recent evidence suggests that the shaping of the microbiome occurs in parallel with the growth of CNS and that they have similar critical developmental windows (34). Consequently, the influence of alterations of gut microbiota on brain maturation trajectories, as well as their relationship with an increased risk for mental disorders later in life have been extensively investigated by preclinical studies (35, 36). In fact, alterations in maternal microbiome have been shown to impact offspring's brain maturation and post-natal development of psychopathology. Buffington et al. (37), observed that the offspring of high-fat diet exposed mice showed autism spectrum disorders/schizophrenia-like symptoms, such as reduced social interactions, poor interest in social novelty, and altered sociability compared to the offspring of normal fed mice (37). These behavioral alterations were coupled with a 9-fold reduction of *Lactobacillus reuteri* and a reduced number of cells producing oxytocin in the paraventricular nuclei of the hypothalamus (37). Other studies investigated the effect of altered maternal gut microbiome on the offspring's behavior through the administration of antibiotics during or

immediately before mice pregnancy. A plethora of postnatal aberrant behavior, such as decreased locomotor and explorative activity, low prepulse inhibition, poor social interactions, and anxiety emerged (38, 39). Interestingly, aberrant behavior was completely reversed after fostering the pups by control dams (39). Other factors, such as maternal exposure to stress, can alter the offspring's gut microbiome and affect behavior. Several studies showed that the offspring exposed to perinatal maternal stress showed decreased levels of *Lactobacillus and Bifidobacterium* (40–42). These alterations were associated to increased anxiety and impaired cognitive functions, which started early during development and lasted until adulthood (40–42). Furthermore, gut microbiome composition and behavioral alterations were paired with increased levels of interleukin-1β and decreased brain-derived neurotropic factor (BDNF) in the amygdala (41).

Together with the intrauterine stage, the postnatal period represents a critical moment for both gut microbiota and brain development (34). This developmental stage represents the time when the most dramatic changes in the composition of the intestinal microbiota take place. These are mainly driven by a series of factors, spanning from maternal delivery modalities to genetic diathesis (43–45). Therefore, the interactions between the developing gut microbiota and brain structure and function in this specific developmental phase have undergone extensive investigations. Sudo et al. reported that germ-free (GF) mice, i.e., animals that have never had contact with any microorganism, showed heightened hypothalamic-pituitary-adrenal (HPA) system response to acute restraint stress as compared to mice with a normal gut flora (46). Such phenotype was accompanied by reduced expression of hippocampal and cortical brain-derived neurotrophic factor (BDNF). When GF were administered with a single strain of bacterium, *Bifidobacterium infantis*, stress response normalized (46). However, normalization processes were only possible in GF at early developmental stage, whereas the same procedure in later stages had no effects (46). Another study (47) demonstrated that GF mice showed anxious behavior and increased levels of serotonin in the hippocampus. Even in this case, gut colonization after weaning, which is comparable to adolescence in humans, was uncapable of restoring normal serotonin levels, even though anxiety normalized. Accordingly, in another study (48), post-weaning bacteria colonization was not able to normalize myelin oligodendrocyte glycoprotein levels in GF mice. Cumulatively, these data point toward the existence of specific, and limited, critical periods for the gut microbiota to act on neuronal circuits function and plasticity. The work of Desbonnet et al. (49) further expanded such concept. In their work, post-weaning colonization only partially corrected autism-spectrum-disorder-like behavior in GF mice: self-grooming and social avoidance improved, whereas social cognition did not (49). The authors suggested that the window of opportunity for the microbiota to impact brain circuits might be different for distinct emotional/social behaviors and, eventually, sensory modalities (49). These findings are summarized in **Table 1**.

GUT MICROBIOTA IN AT RISK MENTAL STATES: CLINICAL DATA

Despite the relatively large amount of studies investigating the relationship between gut microbiota composition and neurodevelopmental alterations in mice, only one study investigated the effect of altered microbiome and risk of developing mental disorders in humans (51). Specifically, He et al. (51) investigated alpha-diversity (i.e., the bacterial diversity within a single sample) and beta-diversity (differences in species composition among samples) metrics of gut microbiome in high-risk (HR), ultra-high-risk (UHR) subjects for developing schizophrenia and HC (51). Beta-diversity analysis revealed that UHR and HR had significantly different global microbiome composition than HC. Furthermore, UHR showed greater levels of *Clostridiales, Lactobacillales, Bacteroidales*, higher levels of Acetyl coenzyme A synthesis and greater anterior cingulate choline levels than the both HR and HC. The authors pointed out that the alterations in microbiome overlapped with those identified in schizophrenia and autism-spectrum disorder (52, 53). Additionally, higher levels of choline were interpreted as resultant of altered membrane metabolism due to microglial activation, which is one of the possible mechanisms mediating the effects of an altered gut microbiome on neural development (51). Putative mechanisms of the interplay between microbiota and genetic predisposition in modulating the liability toward the development of a SMD is discussed below. We have summarized clinical evidence in **Table 2**.

MECHANISTIC HYPOTHESES ON THE INFLUENCE OF GUT MICROBIOTA ON AT RISK STATUS FOR SEVERE MENTAL DISORDERS

There is compelling evidence that the products of gut microbiota might influence behavior in mammals through the action of their byproducts on the CNS (25). For instance, metabolic waste products of the gut microbiota such as the short-chain fatty acids (SCFAs) can influence neuromodulation via inhibition of the histone deacetylases (25, 54). In addition, another byproduct such as butyrate helps maintaining the integrity of the blood-brain barrier (25, 55), while acetate appears to exert anorectic effects via preferential accumulation in the hypothalamus (56). Other sets of findings have pointed to the link between gut dysbiosis and increased gut permeability and alterations of mitochondrial function, with significant repercussions at the CNS level (57). This amount of evidence, supported by the clinical and preclinical findings on the impact of gut microbiota on neurodevelopment, has fostered several mechanistic hypotheses (58, 59). While an extensive discussion of these mechanisms is out of the scope of the present mini review, we present a synthesis that we reckon as relevant for the high-risk construct of SMD. An altered neurodevelopment due to maternal gut flora modifications might be the resultant of poor regulation of maternal/fetus inflammatory state mediated by the maternal

TABLE 1 | Summary of findings of the pre-clinical studies and/or postulated biological underpinnings of SMD on gut microbiota.

Animals (gender, age)	Tested hypothesis (SMD)	Preclinical model	Tested biological correlates	Findings/results	References
GF, SOF BALC/C mice (males, 9–17 weeks old)	Microbiome influence on the HPA stress response (N/A)	Acute restraint stress, ether stress	Plasma ACTH, CRT, IL-1β and IL-6 bioactivity*; assessment of fecal microbiota through culture; RT-PCR for CRH, GR, NMDAR gene expression on CTX, HPC, HPT; ELISA for BDNF, NT-3, NGF on HPC and HPT.	Higher ACTH and corticosterone plasma levels in response to restraint stress among GF mice as compared to SPF, but not in response to ether stimulation. Lower BDNF expression among GF in CTX and HPC tissues as compared to SPF. Normalization of the HPA stress response with an early reconstitution of the gut microbiome with Bifidobacterium infantis; an increased stress response was observed with enteropathogenic *Escherichia coli*, but not with a strain devoid of the translocated ITR gene.	(46)
GF, SPF NMRI (males, 8–10 weeks old)	Gut microbiome influence on normal brain development and behavior (N/A)	Open field test, Light-Dark Box test, Elevated Plus Maze test	NA, MHPG, DA, DOPAC, HVA, 5-HT, and 5-HIAA on CTX, HPC, STR tissue assessed through RPHPLC; assessment of the NGFI, BDNF, DR1, DR2, DARPP-32 expression with ISH on AMG, HPC, CTX samples; SNP, PSD-95 assessed through WB on CTX, STR, HPC.	GF showed altered expression of genes involved in second messenger pathway and synaptic potentiation, as well as increased motor activity and lower anxiety behaviors as compared to SPF. Early exposure of GF to gut microbiota resulted in a normalization of GF locomotor activity; adult exposure to gut microbiota failed to normalize GF behaviors. GF presented higher expression of SNP, PSD-95 in the STR as compared to SPF. Higher turnover rates were observed among GF for NA, DA, 5-HT in STR as compared to SPF. GF subjects presented lower BDNF expression in the HPC, AMG, CTX, and lower expression of NGFI-A in the STR, CTX, HPC as compared to SPF.	(35)
GF, CC Swiss Webster (males and females, 6–9 weeks old)	Sex differences in the gut microbiome regulation of the hippocampal serotonergic system (N/A)	Novel-environment stress	Plasma CRT; 5-HIAA, 5-HT, KYNA assessed through HPLC; TNF-α following LPS splenocyte stimulation;	GF presented a lower TNF-α production following LPS stimulation and a higher CRT response to stress as compared to CC regardless of gender; male GF subjects presented lower BDNF, and higher production of 5-HT and 5-HIAA in the HPC as compared to CC, as well as a higher plasma TRP and a decreased KYNA/TRP ratio; GF female had a lower body weight as compared to CC. Gut microbiota recolonization led to a normalization of TRP concentration and of anxiety-like behaviors; no effect was described on the 5-HT and 5-HIAA concentrations in the HPC.	(47)
GF, CC Swiss Webster (males and females, 7–8 weeks old); NIH Swiss strain as stimulus mice in the tests	Gut microbiota influence on social behaviors (Autism)	Sociability and social novelty preference (three chamber test); social transmission of food preference test	N/A	- Social impairment among GF as compared to CC (i.e., more time spent in an empty chamber instead of one shared with another subject); GF did not spend more time analyzing unfamiliar environment over familiar ones, as compared to CC. - A second cohort confirmed social deficits and reduced preference for social novelty among GF; the post-weaning bacterial colonization resulted in the reversal of the observed social aversion but did not affect social cognition impairments. GF spent more time in repetitive self-grooming behaviors and less time in social investigation during the social transmission of food preference test; these behaviors normalized after gut microbiota colonization.	(49)
BALB/C mice VPA-E and CON (VPA-E mice were exposed *in utero* at G11; males and females, 4 weeks old)	The association between altered gut microbiota and autism-like behaviors (Autism)	Social behavior scores (time spent near unfamiliar gender-matched mouse)	Cecal levels of SCFA (i.e., acetic, propionic, butyric, isobutyric and valeric acids); 16S rRNA analysis on cecal samples to investigate the stool bacteria composition	Butyric acid levels were higher among male VPA-E mice as compared to CON. No difference was found for the other SCFA assessed. OTU expression was significantly influenced among VPA-E males; changes observed in the gut microbiota correlated with increased ileal neutrophil infiltration, increased intestinal butyrate level, a reduced level of intestinal serotonin and lower social behaviors score.	(36)

(Continued)

TABLE 1 | Continued

Animals (gender, age)	Tested hypothesis (SMD)	Preclinical model	Tested biological correlates	Findings/results	References
SD rats, PNS-E and CON (PNS rats were exposed to restraint stress during gestational day 14–20; males, 2–4 months old)	The complex interplay between prenatal stress, major physiological systems and gut microbiota composition	Behavioral screening (Open field, elevated plus maze, novel object recognition); acute restraint test	- 1st cohort: colon excision and analyzed for innervation density (confocal fluorescence imaging), and secretomotory function (chambers) - 2nd cohort: 16S rRNA analysis on fecal samples to investigate the stool bacteria composition; tail-bleed plasma corticosterone assessment following acute restraint test, somatic pain sensitivity with the hot plate test and respiratory function (whole body plethysmography) - 3rd cohort: blood pressure, colorectal distension, acute restraint stress	PNS-exposure resulted in a decreased distal colon innervation and an increased secretory response to cathecholaminergic stimulation; PNS-exposed rats presented a lower expression of Lactobacillus and a higher expression of Oscillibacter, Anaerotruncus and Peptococcus. The observed changes in the gut microbiota correlated with respiratory and HPA-axis changes.	(40)
Wistar rats, SST-E and CON (SST-E rats were exposed to an unabsorbable antibiotic starting 1 month before breeding until gestational day 15; male and female, 3–7 weeks old)	The complex interplay between perinatal antibiotic exposure and the offspring mental health	Behavioral screening (open field, social interactions, marble burying, elevated plus maze, prepulse inhibition of the acoustic startle reflex)	Homocysteine and tryptophan levels among untested siblings and dams (preconceptional and post euthanasia levels)	No abnormality was documented in the homocysteine and tryptophan levels between SST-E and CON, ruling out folate deficiency in the SST-E group. SST-E showed decreased social interactions, increased anxiety behaviors (i.e., reduced exploration of the open arm in the elevated plus maze), and altered sensorimotor gating (i.e., reduction in the startle inhibition)	(38)
C57/B16 mice, PNS-E and CON (PNS-E mice were exposed during gestational day 10–16; females, 8–10 weeks old)	The complex interplay between perinatal stress, commensal microbes and anxiety-like behaviors in the female offspring	Behavioral screening (elevated plus maze, novel object recognition test, tail suspension test)	- 1st cohort: euthanized at the 17th gestational day for tissue collection - 2nd cohort: behavioral testing, parturition, microbiome sampling (16S rRNA), tissue collection from offspring (i.e., IL-1β, BDNF in placental, and in both fetal and maternal brain)	Stress exposure influenced the maternal gut microbiota; no significant difference was found in the placental microbiota composition. PNS-E mice presented higher Bacteroides and Firmicutes expression as compared to CON; at the family level, a relative increase of the Bifidobacteriaceae, and RIkenellaceae was described. Prenatal stress exposure resulted in increased anxiety-like behaviors and neophobia. Stress exposure resulted in reduced BDNF placental levels and higher levels of IL-1β in placental and fetal brain tissues; adult PNS-E mice had lower BDNF levels in the amygdala.	(41)
GF and CC Swiss Webster (males and females, 10 weeks old)	Gut microbiota influence on prefrontal cortex myelination	N/A	RNA-sequencing, qRT-PCR within various brain regions to investigate myelin component genes; protein extraction and western blot; transmission electron microscopy on prefrontal cortex samples (gathered from 6 male mice)	Differential expression of 250 genes between GF/colonized-GF and CON (14 out of the 94 upregulated genes in GF were directly involved in myelinization, but none of them were upregulated in the colonized-GF); GF and colonized-GF differed for the expression of 15 genes. qRT-PCR confirmed abnormal expression of five myelin component genes among GF; the increased in mRNA expression was confined to the prefrontal cortex, and the gut colonization resulted in the normalization of the genes expression. Electron microscopy revealed increased myelinization among GF regardless of axonal diameter; normalization of mRNA transcription with colonization did not result in a reduction in the relative myelin protein abundance.	(48)

(Continued)

TABLE 1 | Continued

Animals (gender, age)	Tested hypothesis (SMD)	Preclinical model	Tested biological correlates	Findings/results	References
SPF C57BL/6 mice UAA-E and CON (UUA mice were exposed to an unabsorbable antibiotic *in utero* during gestational day 9–16; males and females, 4 weeks old)	The effects of antibiotic exposure on offspring behaviors	Open field test, social interaction test (three chambers social test), 24 h home cage activity test. Study subjects divided in 3 cohorts: - 1st cohort: exposed to UAA *in utero* and fostered by CON - 2nd cohort: not exposed to UAA *in utero* and fostered by CON - 3rd cohort: not exposed to UAA *in utero* and fostered by CON	16S rRNA analysis on fecal samples to investigate the stool bacteria composition	T-RFLP demonstrated different gut microbiota expression between UAA exposed dams and control dams; different expression of gut microbiota was reported between UAA and CON groups also in the offspring. UAA offspring presented lower body weight, lower activity levels in the dark phase of the 24 h home cage activity test, reduced locomotor activity in the open field test, and reduced rearing behaviors in a novel environment. The 1st and the 2nd cohort presented a similar phenotype at week 4 and differed significantly from the 3rd cohort.	(39)
SPF C57BL/6, GF, ASF (males and females, 6–10 weeks old)	Investigating the role of gut microbiota in microglia maturation process	N/A	16S rRNA analysis on fecal samples to investigate the stool bacteria composition; LMCV challenge through right hemisphere injection; LPS challenge applied intracerebrally and intraperitoneally under anesthesia; RT-PCR on adequately processed FACS-separated microglial cells to analyze gene expression; histology IHC and three-dimensional microglia reconstruction	Different mRNA expression between SPF and GF mice was observed, especially among genes involved in cell activation, in pathogen recognition and host defense regulation. Flow cytometry allowed to recognize a pattern consistent with immature microglia phenotype. GF presented more Iba-1+ microglial cells featuring longer processes, more segments and establishing more physical contacts with adjacent cells as compared to SPF. LPS challenge and LCMV test revealed an abnormal immune response among GF subjects, heralded by differential expression of genes involved in the immune response and prominent morphological anomalies. Antibiotic exposure for 4 weeks, induced similar phenotypic changes in microglial cells among SPF, but with no changes in cell numbers; ASF tri-colonized (*Bacteroides distasonis*, *Lactobacillus salivarius*, Clostridium cluster) presented both increased microglial cell numbers and morphological changes, despite having near-normal biomass, reversible by allowing a more diverse bacterial colonization with SPF co-housing. Intriguingly, a 4-week course of SCFA supplements resulted in the normalization of the microglial phenotype among GF.	(50)

**IL-6 bioactivity assessed through IL-6-dependent B cell hybridoma.*

5-HIAA, 5-Hydroxyindoleacetic acid; 5-HT, 5-Hydroxytryptamine; ACTH, Adrenocorticotropic hormone; AMG, Amygdala; ASF, Altered Schaedler flora; BDNF, Brain Derived Neurotrophic Factor; CC, Conventionally Colonized; CRH, Corticotropic Releasing Hormone; CON, Controls; CRT, Corticosterone; CTX, Cortex; GF, Germ Free; DA, Dopamine; DARPP-32, Dopamine- and cAMP-regulated phosphoprotein Mr 32 kDa; DOPAC, Dihydroxyphenylacetic acid; DR1, Dopamine Receptor 1; DR2, Dopamine Receptor 2; G11, Gestational day 11th; GF, Germ Free; GR, Glucocorticoid Receptor; HPA, Hypothalamic Axis; HPC, Hippocampus; HPLC, High-Performance Liquid Chromatography; HPT, Hypothalamus; HVA, Homovanillic acid; IHC, Immunohistochemistry; ISHT, In Situ Hybridation; ITR, Intimin Receptor; KYNA, Kynurenic acid; LCMV, Lymphocytic Choriomeningitis Virus; LPS, LipoPolySaccharide; MHPG, 3-Methoxy-4-HydroxyPhenylGlycol; N/A, Not Available; NA, noradrenaline; NGFI-A, Nerve Growth Factor-Inducible clone A; NMDAR, N-Methyl- D - Aspartic Acid Receptor subunits (NR-1 and NR-2A); NGF, Nerve Growth Factor; NT-3, Neurotrophin-3; OTU, Operational taxonomic unit; PNS-E, Prenatal stress in utero exposure; PSD – 95, Postsynaptic density protein 95; qRT-PCR, quantitative Real Time Polymerase Chain Reaction; RPHPLC, Reversed-Phase High-Performance Liquid Chromatography; SCFA, Short chain fatty acids; SD, Sprague-Dawley; SMD, Severe Mental Disorder; SNP, Synaptophysin; SPF, Specific Pathogen Free; SST-E, Succinyl Sulfa Thiazole exposed in utero; STR, Striatum; TNF-α, Tumor Necrosis Factor-α; T-RFLP, Terminal Restriction Fragment Length Polymorphism; UAA, Unabsorbable Antibiotic; UAA-E, Unabsorbable Antibiotic exposure in utero; VPA-E, Valproic Acid in utero Exposure; WB, Western Blotting.

TABLE 2 | Summary of findings of the clinical studies on gut microbiota in SMD.

SMD (diagnostic criteria)	Sample size and composition (Age range; gender composition)	Methods	Findings/results	References
AD, PDD (DSM – IV)	AD $n = 10$, PDD-NOS $n = 10$, HC $n = 10$ (4–10 y.o.; 14 M, 16 F)	Cross-sectional study; ADI-R, ADOS, FDO; 16S rDNA and 16S rRNA analysis on fecal samples to investigate the stool bacteria composition, its metabolic activity and an assessment of the organic volatile compounds and free fatty acids composition.	PDD-NOS and HC presented higher *Faecalibacterium* and *Ruminococcus* expression; PDD-NOS and HC presented higher expression of Caloramator, Sarcina, and Clostridium; PDD-NOS and AD presented different composition of Lachnospiraceae as compared with the HC. Different levels of organic volatile compounds and free fatty acid between the three groups.	(52)
HR, UHR (DSM – IV)	HR $n = 81$; UHR $n = 19$; HC $n = 69$ (13–30 y.o.; HR 41 M, 40 F; UHR 15 M, 4 F; HC 37 M, 32 F)	Cross-sectional study; 1H-MRS; APSS, BIPS, GAF-M, GRDS, SIPS, SOPS; HR and UHR were screened for the absence of DSM – IV coded diagnoses; 16S rRNA analysis on fecal samples to investigate the stool bacteria composition.	Increased expression of Clostridiales, *Lactobacillales* and Bacteroidales in UHR compared to the other two groups; increased choline levels on 1H-MRS among UHR subjects compared to the other groups.	(51)
SCZ (ICD-10)	SCZ $n = 64$, HC $n = 53$ (18–65 y.o.; 36 M, 28 F in SCZ; 35 M, 18 F in HC)	Cross-sectional study; 16S rDNA and 16S rRNA analysis on fecal samples to investigate the stool bacteria composition; PICRUSt analysis to probe metabolic pathways; PANSS.	SCZ patients presented higher expression of the Proteobacteria phylum, and at the genus level, a relatively higher expression of Succinivibrio, Megasphaera, Collinsella, Clostridium, Klebsiella, Methanobrevibacter, and a lower of Blautia, Coprococcus, Roseburia as compared to HC; differences in numerous metabolic pathways between HC and SCZ (e.g., fatty acid, vitamin B6).	(53)
GP reported depression (NA)	Subset of the FGFP cohort $n = 1,054$ - GPRD $n = 80$, HC $n = 70$, validated in LLD data sets $n = 1,070$ and in TR-MDD* $n = 7$ group. (FGFP m.a. 50.9, 478 M, 576 F; LLD m.a. 57.9 y.o., 447 M, 616 F; TR-MDD balanced to the FGFP group)	Cross-sectional study; BMI; BSS; GP reported depression, HAM-D; RAND-36; 16S rRNA analysis on fecal samples to investigate the stool bacteria composition.	Butyrate-producing *Faecalibacterium* and *Coprococcus* bacteria were associated with higher QOL. Dialister, *Coprococcus* spp. depletion was observed in depression; microbial synthesis of 3,4-dihydroxyphenylacetic acid appeared positively correlated with mental QOL.	(32)
Bipolar Disorder (DSM-IV)	BD $n = 32$; HC $n = 10$ (BD 20–65 y.o., 18 M, 14 F; HC NA y.o., 4 M, 6 F)	Cross-sectional study; BDI-II; HAM-D; inflammatory markers, serum lipids, KYNA, oxidative stress and anthropometric measures; 16S rRNA analysis on fecal samples to investigate the stool bacteria composition.	BD illness duration was negatively correlated with microbial alpha diversity. Actinobacteria and Coriobacteria were more abundant in BD as compared with HC; Ruminococcaceae and *Faecalibacterium* were more abundant in HC as compared with BD. Certain bacterial clades were more commonly observed with the metabolic and inflammatory patterns observed among BD individuals.	(28)
Schizophrenia (DSM-IV)	90 SCZ, 81 HC, validated in a verification sample 45 SCZ[1] and 45 HC[1] (SCZ 14–53 y.o., 46 M, 44 F; HC 18–64 y.o.,41 M, 40 F)	Cross-sectional; MWAS to characterize gut microbiota; MCCB; PANSS; KYNA and tryptophan blood levels; 16S rRNA analysis to probe mice stool microbiota composition.	Different tryptophan and KYNA blood levels between SCZ and HC; SCZ gut microbiota featured higher expression of facultative anaerobes and oral cavity bacteria as compared with HC. Transplantation of Streptococcus vestibularis in mice resulted in altered neurotransmitter production and social behaviors.	(31)

**TR-MDD: TR-MDD was defined as a diagnosis of either Major Depressive Disorder or Bipolar Type II according to the DSM-IV criteria. 1H-MRS, Proton Magnetic Resonance Spectroscopy; AD, Autism Disorder; ADI-R, Autism Diagnostic Interview-Revised; ADOS, Autistic Diagnostic Observation Schedule; APSS, Attenuated Positive Symptom Syndrome; BIPS, Brief Intermittent Psychotic Syndrome; BDI-II, Beck Depression Inventory; BMI, Body Mass Index; BSS, Bristol stool scale; DSM – IV, Diagnostic and Statistical Manual of Mental Disorders IV edition; F, Female; FDO, Free Direct Observation; FGFP, Flemish Gut Flora Project; GAF-M, General Assessment of Functioning – Modified version; GP, General Practitioner; GPRD, General Practitioner Reported Depression; GRDS, Genetic Risk and Deterioration Syndrome; HAM-D, Hamilton Depression Rating Scale; HC, Healthy Control; KYNA, Kynurenic Acid; LLD, Dutch LifeLines DEEP; M, Male; m.a., mean age; MCCB, MATRICS Consensus Cognitive Battery; MWAS, Metagenome-Wide Association Study; NA, Not Available; n, total size; PANSS, Positive and Negative Syndrome Scale; PDD-NOS, Pervasive Developmental Disorder – Not Otherwise Specified; PICRUSt, Phylogenetic Investigation of Communities by Reconstruction of Unobserved States; QOL, Quality Of Life; RAND-36, RAND-36 health-related quality of life survey; SCZ, Schizophrenia; SMD, Severe Mental Disorder; SIPS, Structured Interview for Prodromal Syndromes; SOPS, Scale of Prodromal Symptoms and fulfilled one of the three subsets; spp, species; TR-MDD, Treatment Resistant Major Depressive Disorder; y.o., years old.*

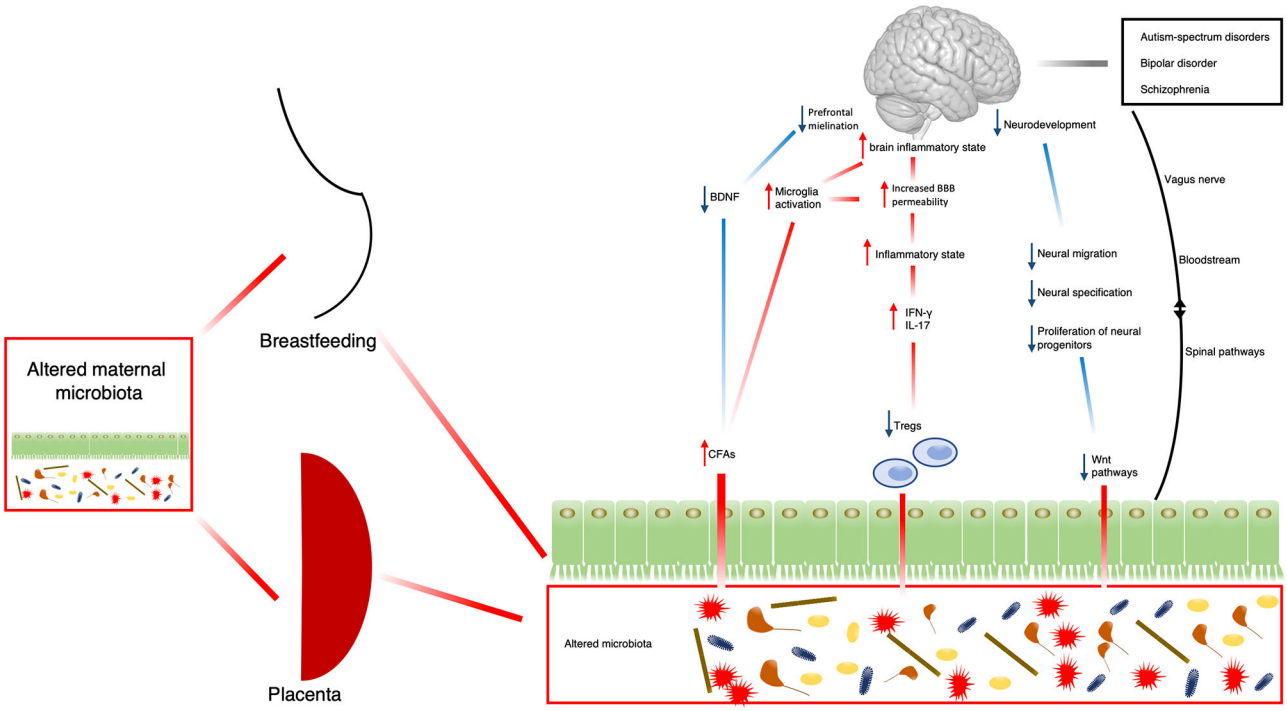

FIGURE 1 | Schematic representation of possible mechanisms by which the microbiota might contribute to the development of SMD. BDNF, brain-derived neurotrophic factor; CFAs, fermentation products; IFN-γ, interferon-γ; IL-17, Interleukin-17; Tregs, regulatory T-cells; Wnt, homologous wingless and Int-1.

gut microbiome (58). Adequate gut microbial colonization in pregnant mice was associated to expression of regulatory T-cells (Tregs). Tregs normalize systemic levels of proinflammatory cytokines, such as IL-17 and interferon-γ (60), thus maintaining correct inflammatory/non-inflammatory balance. The lack of gut microbiota in GF pregnant mice resulted in a decrease of Tregs, with a general imbalance toward maternal and fetal inflammatory state (60). High levels of proinflammatory cytokines have been shown to induce fetal abnormal cortical development and surge of post-natal autism-like behavior (61). Alteration of maternal gut microbiome might also increase levels of fermentation products (CFAs), namely acetate, propionate and butyrate (62). Indeed, CFAs are capable to massively activate microglia, the immune cells of the CNS playing an important role in CNS homeostasis (50). Microglia activity might initiate/exacerbate the inflammatory cascade leading to the massive release of cytokines as well as to associated alterations in the endothelial permeability, including the blood-brain barrier. Such cascade has been shown to predispose to the development of neurodegenerative disorders, including schizophrenia and Parkinson's disease (59, 63).

Another putative mechanism might involve alterations in neurogenesis and specifically the BDNF which is involved in neural growth and cell survival. As previously shown, the gut microbiota is involved in the expression of BDNF (64). Prenatal/postnatal alterations of the gut microbiota can alter BDNF expression, and these changes could alter maturation trajectories of neural circuitry, leading to the development of SMD (65–68). Furthermore, gut microbiota can modify oligodendrocyte products and affect myelination, particularly in the prefrontal cortex, a brain region involved in attention, memory, emotional learning and critically connected to SMD such as ASD (69), schizophrenia (70), major depressive disorder (71), bipolar disorder (72), and substance abuse (73). Specifically, altered myelination has been related to changes in synaptic formation and function, which could lead to the surge of specific cognitive deficits typically seen in schizophrenia, namely deficits in attention, working memory, and executive function (74).

Another interesting, but still under-investigated, mechanism is represented by the effect of the gut microbiome on the Wnt pathways. These are signal transduction pathways mainly involved in human development, cell migration and proliferation and tissue regeneration (75). Wnt pathways are also involved in neural morphogenesis, axon guidance, neurite outgrowth, and synaptic plasticity (76, 77). Alterations in Wnt pathways have been recently related to higher risk to develop SMD, such as schizophrenia or bipolar disorder (78, 79). Of note, GF mice showed poor Wnt pathway activity in intestinal stem cells (80), supporting the speculation of a possible link between alteration of gut microglia, altered neurodevelopment and consequent increased risk for SMD. However, proper investigation of the relationship between gut microbiome alterations and altered Wnt pathways is still underdeveloped and needs further research. All these mechanisms are illustrated in **Figure 1**.

CONCLUSIONS

The findings of our review prompt a series of considerations. First, despite the consensus that microbiota plays a fundamental role in neurodevelopment and substantial changes are detectable in individuals affected by SMD, there is a dearth of studies investigating its modifications during the developmental trajectories of these disorders, particularly in high-risk populations. This could be feasible particularly in consideration that appropriate clinical chemistry and molecular immunology assays to assess for the presence of biological markers of "leaky gut" might be easily implementable in clinical settings (81). Second, only a longitudinal perspective could shed light on the direction of these changes, i.e., whether microbiota modifications precede the onset of psychopathology (of whatever severity) or vice versa. This perspective could be applied, but should not be limited, to the early stages of SMD. Indeed, prospective analysis of microbiota changes are starting to shed light on the longitudinal variation of mood in the course of bipolar disorder (82). Third, this approach can help decrease the confounding associated with the use of drug treatments (if the analyses are performed in pre-diagnostic stages), and at the same time inform on changes that might favor, or be predictive of, response to treatment. In conclusion, we suggest that the analysis of microbiota should be included in the comprehensive assessment generally performed in populations at high risk for SMD as it can inform predictive models and ultimately preventative strategies.

AUTHOR CONTRIBUTIONS

MM and GS drafted the first version of the article. AS, DJ, and PP helped with the search of the literature and contributed to the draft of the manuscript. FP and BC oversaw the project and revised the text critically for important intellectual content. All authors gave final approval of the version to be published and agree to be accountable for all aspects of the work.

FUNDING

This paper was partly funded by Fondo Integrativo per la Ricerca (FIR)-2019 granted to MM, FP, and BC.

ACKNOWLEDGMENTS

The authors wish to thank all patients affected by severe mental illness who make our research possible, and most importantly meaningful.

REFERENCES

1. Rehm J, Shield KD. Global burden of disease and the impact of mental and addictive disorders. *Curr Psychiatr Rep.* (2019) 21:10. doi: 10.1007/s11920-019-0997-0
2. Gustavsson A, Svensson M, Jacobi F, Allgulander C, Alonso J, Beghi E, et al. Cost of disorders of the brain in Europe 2010. *Eur Neuropsychopharmacol.* (2011) 21:718–79. doi: 10.1016/j.euroneuro.2011.08.008
3. Millan MJ, Andrieux A, Bartzokis G, Cadenhead K, Dazzan P, Fusar-Poli P, et al. Altering the course of schizophrenia: progress and perspectives. *Nat Rev Drug Discov.* (2016) 15:485–515. doi: 10.1038/nrd.2016.28
4. Duffy A, Goodday S, Keown-Stoneman C, Grof P. The emergent course of bipolar disorder: observations over two decades from the Canadian high-risk offspring cohort. *Am J Psychiatr.* (2019) 176:720–9. doi: 10.1176/appi.ajp.2018.18040461
5. Hmwe Kyu H, Abate D, Hassen Abate K, Abay SM, Abbafati C, Abbasi N, et al. 2018 Global, regional, and national disability-adjusted life-years (DALYs) for 359 diseases and injuries and healthy life expectancy (HALE) for 195 countries and territories, 1990â€"2017: a systematic analysis for the global burden of disease study 2017. *Lancet.* 392:1859–922. doi: 10.1016/S0140-6736(18)32335-3
6. Harris C, Barraclough B. Excess mortality of mental disorder. *Br J Psychiatr.* (1998) 173:11–53. doi: 10.1192/bjp.173.1.11
7. De Hert M, Correll CU, Bobes J, Cetkovich-Bakmas M, Cohen D, Asai I, et al. Physical illness in patients with severe mental disorders. I Prevalence, impact of medications and disparities in health care. *World Psychiatr.* (2011) 10:52–77. doi: 10.1002/j.2051-5545.2011.tb00014.x
8. Chesney E, Goodwin GM, Fazel S. Risks of all-cause and suicide mortality in mental disorders: a meta-review. *World Psychiatr.* (2014) 13:153–60. doi: 10.1002/wps.20128
9. Druss BG, Zhao L, Von Esenwein S, Morrato EH, Marcus SC. Understanding excess mortality in persons with mental illness: 17-year follow up of a nationally representative US survey. *Med Care.* (2011) 49:599–604. doi: 10.1097/MLR.0b013e31820bf86e
10. Nordentoft M, Wahlbeck K, Hällgren J, Westman J, Ösby U, Alinaghizadeh H, et al. Excess mortality, causes of death and life expectancy in 270,770 patients with recent onset of mental disorders in Denmark, Finland and Sweden. *PLoS ONE.* (2013) 8:e0055176. doi: 10.1371/journal.pone.0055176
11. Fusar-Poli P, Borgwardt S, Bechdolf A, Addington J, Riecher-Rössler A, Schultze-Lutter F, et al. The psychosis high-risk state: A comprehensive state-of-the-art review. *Arch Gen Psychiatr.* (2013) 70:107–20. doi: 10.1001/jamapsychiatry.2013.269
12. Zwicker A, MacKenzie LE, Drobinin V, Howes Vallis E, Patterson VC, Stephens M, et al. Basic symptoms in offspring of parents with mood and psychotic disorders. *BJPsych Open.* (2019) 5:e54. doi: 10.1192/bjo.2019.40
13. Zwicker A, Drobinin V, MacKenzie LE, Howes Vallis E, Patterson VC, Cumby J, et al. Affective lability in offspring of parents with major depressive disorder, bipolar disorder and schizophrenia. *Eur Child Adolesc Psychiatr.* (2020) 29:445–51. doi: 10.1007/s00787-019-01355-z
14. Oliver D, Spada G, Englund A, Chesney E, Radua J, Reichenberg A, et al. Real-world digital implementation of the psychosis polyrisk score (PPS): a pilot feasibility study. *Schizophr Res.* (2020) 226:176–83. doi: 10.1016/j.schres.2020.04.015
15. Docherty AR, Shabalin AA, Adkins DE, Mann F, Krueger RF, BacanuA, et al. Molecular genetic risk for psychosis is associated with psychosis risk symptoms in a population-based UK cohort: findings from generation scotland. *Schizophr Bull.* (2020) 46:1045–52. doi: 10.1093/schbul/sbaa042
16. Musliner KL, Krebs MD, Albiñana C, Vilhjalmsson B, Agerbo E, Zandi PP, et al. Polygenic risk progression to bipolar or psychotic disorders among individuals diagnosed with unipolar depression in early life. *Am J Psychiatr.* (2020) 177:936–43. doi: 10.1176/appi.ajp.2020.19111195
17. Watkeys OJ, Cohen-Woods S, Quidé Y, Cairns MJ, Overs B, Fullerton JM, et al. Derivation of poly-methylomic profile scores for schizophrenia. *Prog Neuro Psychopharmacol Biol Psychiatr.* (2020) 101:109925. doi: 10.1016/j.pnpbp.2020.109925
18. Bhak Y, Jeong H-O, Cho YS, Jeon S, Cho J, Gim JA, et al. Depression and suicide risk prediction models using blood-derived multi-omics data. *Transl Psychiatr.* (2019) 9:262. doi: 10.1038/s41398-019-0595-2
19. Bevins CL, Salzman NH. The potter's wheel: the host's role in sculpting its microbiota. *Cell Mol Life Sci.* (2011) 68:3675. doi: 10.1007/s00018-011-0830-3
20. Almeida A, Mitchell AL, Boland M, Forster SC, Gloor GB, Tarkowska A, et al. A new genomic blueprint of the human gut

microbiota. *Nature.* (2019) 568:499–504. doi: 10.1038/s41586-019-0965-1
21. Proctor LM, Creasy HH, Fettweis JM, Lloyd-Price J, Mahurkar A, Zhou W, et al. The integrative human microbiome project. *Nature.* (2019) 569:641–8. doi: 10.1038/s41586-019-1238-8
22. Scarpellini E, Campanale M, Leone D, Purchiaroni F, Vitale G, Lauritano EC, et al. Gut microbiota and obesity. *Intern Emerg Med.* (2010) 5:53–6. doi: 10.1007/s11739-010-0450-1
23. Mazmanian SK, Liu CH, Tzianabos AO, Kasper DL. An immunomodulatory molecule of symbiotic bacteria directs maturation of the host immune system. *Cell.* (2005) 122:107–18. doi: 10.1016/j.cell.2005.05.007
24. Spanogiannopoulos P, Bess EN, Carmody RN, Turnbaugh PJ. The microbial pharmacists within us: a metagenomic view of xenobiotic metabolism. *Nat Rev Microbiol.* (2016) 14:273. doi: 10.1038/nrmicro.2016.17
25. Johnson KV-A, Foster KR. Why does the microbiome affect behaviour? *Nat Rev Microbiol.* (2018) 16:647–55. doi: 10.1038/s41579-018-0014-3
26. Cuomo A, Maina G, Rosso G, Crescenzi BB, Bolognesi S, Muro A, et al. The microbiome: A new target for research and treatment of schizophrenia and its resistant presentations? A systematic literature search and review. *Front Pharmacol.* (2018) 9:1040. doi: 10.3389/fphar.2018.01040
27. Rodrigues-Amorim D, Rivera-Baltanás T, Regueiro B, Spuch C, de las Heras ME, Vázquez-Noguerol Méndez R, et al. The role of the gut microbiota in schizophrenia: current and future perspectives. *World J Biol Psychiatr.* (2018) 19:571–85. doi: 10.1080/15622975.2018.1433878
28. Painold A, Mörkl S, Kashofer K, Halwachs B, Dalkner N, Bengesser S, et al. A step ahead: exploring the gut microbiota in inpatients with bipolar disorder during a depressive episode. *Bipolar Disord.* (2019) 21:40–9. doi: 10.1111/bdi.12682
29. Slyepchenko A, Maes M, Jacka FN, Köhler CA, Barichello T, McIntyre RS, et al. Gut microbiota, bacterial translocation, and interactions with diet: pathophysiological links between major depressive disorder and non-communicable medical comorbidities. *Psychother Psychosom.* (2017) 86:31–46. doi: 10.1159/000448957
30. Cheung SG, Goldenthal AR, Uhlemann AC, Mann JJ, Miller JM, Sublette ME. Systematic review of gut microbiota and major depression. *Front Psychiatr.* (2019) 10:34. doi: 10.3389/fpsyt.2019.00034
31. Zhu F, Ju Y, Wang W, Wang Q, Guo R, Ma Q, et al. Metagenome-wide association of gut microbiome features for schizophrenia. *Nat Commun.* (2020) 11:1–10. doi: 10.1038/s41467-020-15457-9
32. Valles-Colomer M, Falony G, Darzi Y, Tigchelaar EF, Wang J, Tito RY, et al. The neuroactive potential of the human gut microbiota in quality of life and depression. *Nat Microbiol.* (2019) 4:623–32. doi: 10.1038/s41564-018-0337-x
33. Dinan TG, Borre YE, Cryan JF. Genomics of schizophrenia: time to consider the gut microbiome? *Mol Psychiatr.* (2014) 19:1252–7. doi: 10.1038/mp.2014.93
34. Borre YE, O'Keeffe GW, Clarke G, Stanton C, Dinan TG, Cryan JF. Microbiota and neurodevelopmental windows: implications for brain disorders. *Trends Mol Med.* (2014) 20:509–18. doi: 10.1016/j.molmed.2014.05.002
35. Heijtz RD, Wang S, Anuar F, Qian Y, Björkholm B, Samuelsson A, et al. Normal gut microbiota modulates brain development and behavior. *Proc Natl Acad Sci USA.* (2011) 108:3047–52. doi: 10.1073/pnas.1010529108
36. De Theije CGM, Wopereis H, Ramadan M, van Eijndthoven T, Lambert J, Knol J, et al. Altered gut microbiota and activity in a murine model of autism spectrum disorders. *Brain Behav Immun.* (2014) 37:197–206. doi: 10.1016/j.bbi.2013.12.005
37. Buffington SA, Di Prisco GV, Auchtung TA, Ajami NJ, Petrosino JF, Costa-Mattioli M. Microbial reconstitution reverses maternal diet-induced social and synaptic deficits in offspring. *Cell.* (2016) 165:1762–75. doi: 10.1016/j.cell.2016.06.001
38. Degroote S, Hunting DJ, Baccarelli AA, Takser L. Maternal gut and fetal brain connection: increased anxiety and reduced social interactions in Wistar rat offspring following peri-conceptional antibiotic exposure. *Prog Neuro Psychopharmacol Biol Psychiatr.* (2016) 71:76–82. doi: 10.1016/j.pnpbp.2016.06.010
39. Tochitani S, Ikeno T, Ito T, Sakurai A, Yamauchi T, Matsuzaki H. Administration of non-absorbable antibiotics to pregnant mice to perturb the maternal gut microbiota is associated with alterations in offspring behavior. *PLoS ONE.* (2016) 11:e0138293. doi: 10.1371/journal.pone.0138293
40. Golubeva AV, Crampton S, Desbonnet L, Edge D, O'Sullivan O, Lomasney KW, et al. Prenatal stress-induced alterations in major physiological systems correlate with gut microbiota composition in adulthood. *Psychoneuroendocrinology.* (2015) 60:58–74. doi: 10.1016/j.psyneuen.2015.06.002
41. Gur TL, Shay L, Palkar AV, Fisher S, Varaljay VA, Dowd S, et al. Prenatal stress affects placental cytokines and neurotrophins, commensal microbes, and anxiety-like behavior in adult female offspring. *Brain Behav Immun.* (2017) 64:50–8. doi: 10.1016/j.bbi.2016.12.021
42. Jašarević E, Howard CD, Misic AM, Beiting DP, Bale TL. Stress during pregnancy alters temporal and spatial dynamics of the maternal and offspring microbiome in a sex-specific manner. *Sci Rep.* (2017) 7:44182. doi: 10.1038/srep44182
43. Lozupone CA, Stombaugh JI, Gordon JI, Jansson JK, Knight R. Diversity, stability and resilience of the human gut microbiota. *Nature.* (2012) 489:220–30. doi: 10.1038/nature11550
44. Maynard CL, Elson CO, Hatton RD, Weaver CT. Reciprocal interactions of the intestinal microbiota and immune system. *Nature.* (2012) 489:231–41. doi: 10.1038/nature11551
45. Parfrey LW, Knight R. Spatial and temporal variability of the human microbiota. *Clin Microbiol Infect.* (2012) 18:5–7. doi: 10.1111/j.1469-0691.2012.03861.x
46. Sudo N, Chida Y, Aiba Y, Sonoda J, Oyama N, Yu X, et al. Postnatal microbial colonization programs the hypothalamic–pituitary–adrenal system for stress response in mice. *J Physiol.* (2004) 558:263–75. doi: 10.1113/jphysiol.2004.063388
47. Clarke G, Grenham S, Scully P, Fitzgerald P, Moloney RD, Shanahan F, et al. The microbiome-gut-brain axis during early life regulates the hippocampal serotonergic system in a sex-dependent manner. *Mol Psychiatr.* (2013) 18:666–73. doi: 10.1038/mp.2012.77
48. Hoban AE, Stilling RM, Ryan FJ, Shanahan F, Dinan TG, Claesson MJ, et al. Regulation of prefrontal cortex myelination by the microbiota. *Transl Psychiatr.* (2016) 6:e774. doi: 10.1038/tp.2016.42
49. Desbonnet L, Clarke G, Shanahan F, Dinan TG, Cryan JF. Microbiota is essential for social development in the mouse. *Mol Psychiatr.* (2014) 19:146–8. doi: 10.1038/mp.2013.65
50. Erny D, de Angelis ALH, Jaitin D, Wieghofer P, Staszewski O, David E, et al. Host microbiota constantly control maturation and function of microglia in the CNS. *Nat Neurosci.* (2015) 18:965–77. doi: 10.1038/nn.4030
51. He Y, Kosciolek T, Tang J, Zhou Y, Li Z, Ma X, et al. Gut microbiome and magnetic resonance spectroscopy study of subjects at ultra-high risk for psychosis may support the membrane hypothesis. *Eur Psychiatr.* (2018) 53:37–45. doi: 10.1016/j.eurpsy.2018.05.011
52. de Angelis M, Piccolo M, Vannini L, Siragusa S, De Giacomo A, Serrazzanetti DI, et al. Fecal microbiota and metabolome of children with autism and pervasive developmental disorder not otherwise specified. *PLoS ONE.* (2013) 8:e76993. doi: 10.1371/journal.pone.0076993
53. Shen Y, Xu J, Li Z, Huang Y, Yuan Y, Wang J, et al. Analysis of gut microbiota diversity and auxiliary diagnosis as a biomarker in patients with schizophrenia: a cross-sectional study. *Schizophr Res.* (2018) 197:470–7. doi: 10.1016/j.schres.2018.01.002
54. Koh A, De Vadder F, Kovatcheva-Datchary P, Bäckhed F. From dietary fiber to host physiology: short-chain fatty acids as key bacterial metabolites. *Cell.* (2016) 165:1332–45. doi: 10.1016/j.cell.2016.05.041
55. Braniste V, Al-Asmakh M, Kowal C, Anuar F, Abbaspour A, Tóth M, et al. The gut microbiota influences blood-brain barrier permeability in mice. *Sci Transl Med.* (2014) 6:263ra158. doi: 10.1126/scitranslmed.3009759
56. Frost G, Sleeth ML, Sahuri-Arisoylu M, Lizarbe B, Cerdan S, Brody L, et al. The short-chain fatty acid acetate reduces appetite via a central homeostatic mechanism. *Nat Commun.* (2014) 5:4611. doi: 10.1038/ncomms4611
57. Anderson G, Maes M. Gut dysbiosis dysregulates central and systemic homeostasis via suboptimal mitochondrial function: assessment, treatment and classification implications. *Curr Top Med Chem.* (2020) 20:524–39. doi: 10.2174/1568026620666200131094445
58. Lowry CA, Smith DG, Siebler PH, Schmidt D, Stamper CE, Hassell JE, et al. The microbiota, immunoregulation, and mental health: implications for public health. *Curr Environ Heal Rep.* (2016) 3:270–86. doi: 10.1007/s40572-016-0100-5

59. Warner BB. The contribution of the gut microbiome to neurodevelopment and neuropsychiatric disorders. *Pediatr Res.* (2019) 85:216–24. doi: 10.1038/s41390-018-0191-9
60. Rook GAW, Raison CL, Lowry CA. Microbial 'old friends', immunoregulation and socioeconomic status. *Clin Exp Immunol.* (2014) 177:1–12. doi: 10.1111/cei.12269
61. Choi GB, Yim YS, Wong H, Kim S, Kim H, Kim SV, et al. The maternal interleukin-17a pathway in mice promotes autism-like phenotypes in offspring. *Science.* (2016) 351:933–9. doi: 10.1126/science.aad0314
62. Houser MC, Tansey MG. The gut-brain axis: Is intestinal inflammation a silent driver of Parkinson's disease pathogenesis? *NPJ Park Dis.* (2017) 3:3. doi: 10.1038/s41531-016-0002-0
63. Sampson TR, Debelius JW, Thron T, Janssen S, Shastri GG, Ilhan ZE, et al. Gut microbiota regulate motor deficits and neuroinflammation in a model of Parkinson's disease. *Cell.* (2016) 167:1469–80. doi: 10.1016/j.cell.2016.11.018
64. Lu B, Nagappan G, Lu Y. BDNF synaptic plasticity. cognitive function, and dysfunction. *Handb Exp Pharmacol.* (2015) 220:223–50. doi: 10.1007/978-3-642-45106-5_9
65. Atladóttir HÓ, Thorsen P, Østergaard L, Schendel DE, Lemcke S, Abdallah M, et al. Maternal infection requiring hospitalization during pregnancy autism spectrum disorders. *J Autism Dev Disord.* (2010) 40:1423–30. doi: 10.1007/s10803-010-1006-y
66. Atladóttir HÓ, Henriksen TB, Schendel DE, Parner ET. Autism after infection, febrile episodes, and antibiotic use during pregnancy: an exploratory study. *Pediatrics.* (2012) 130:e1447–54. doi: 10.1542/peds.2012-1107
67. Li M, Chang H, Xiao X. BDNF Val66Met polymorphism and bipolar disorder in European populations: a risk association in case-control, family-based and GWAS studies. *Neurosci Biobehav Rev.* (2016) 68:218–33. doi: 10.1016/j.neubiorev.2016.05.031
68. Di Carlo P, Punzi G, Ursini G. Brain-derived neurotrophic factor and schizophrenia. *Psychiatr Genet.* (2020) 29:200–10. doi: 10.1097/YPG.0000000000000237
69. Karim HT, Wang M, Andreescu C, Tudorascu D, Butters MA, Karp JF, et al. Acute trajectories of neural activation predict remission to pharmacotherapy in late-life depression. *NeuroImage Clin.* (2018) 19:831–9. doi: 10.1016/j.nicl.2018.06.006
70. Zhou Y, Fan L, Qiu C, Jiang T. Prefrontal cortex and the dysconnectivity hypothesis of schizophrenia. *Neurosci Bull.* (2015) 31:207–19. doi: 10.1007/s12264-014-1502-8
71. Janiri D, Moser DA, Doucet GE, Luber MJ, Rasgon A, Lee WH, et al. Shared neural phenotypes for mood and anxiety disorders: a meta-analysis of 226 task-related functional imaging studies. *JAMA Psychiatr.* (2020) 77:172–9. doi: 10.1001/jamapsychiatry.2019.3351
72. Phillips ML, Swartz HA. A critical appraisal of neuroimaging studies of bipolar disorder: toward a new conceptualization of underlying neural circuitry and a road map for future research. *Am J Psychiatr.* (2014) 171:829–43. doi: 10.1176/appi.ajp.2014.13081008
73. Rapinesi C, Del Casale A, Di Pietro S, Ferri VR, Piacentino D, Sani G, et al. Add-on high frequency deep transcranial magnetic stimulation (dTMS) to bilateral prefrontal cortex reduces cocaine craving in patients with cocaine use disorder. *Neurosci Lett.* (2016) 629:43–7. doi: 10.1016/j.neulet.2016.06.049
74. Takahashi N, Sakurai T, Davis KL, Buxbaum JD. Linking oligodendrocyte and myelin dysfunction to neurocircuitry abnormalities in schizophrenia. *Prog Neurobiol.* (2011) 93:13–24. doi: 10.1016/j.pneurobio.2010.09.004
75. Wodarz A, Nusse R. Mechanisms of Wnt signaling in development. *Annu Rev Cell Dev Biol.* (1998) 14:59–88. doi: 10.1146/annurev.cellbio.14.1.59
76. Cotter D, Kerwin R, Al-Sarraji S, Brion JP, Chadwich A, Lovestone S, et al. Abnormalities of Wnt signalling in schizophrenia–evidence for neurodevelopmental abnormality. *Neuroreport.* (1998) 9:1379–83. doi: 10.1097/00001756-199805110-00024
77. Hur EM, Zhou FQ. GSK3 signalling in neural development. *Nat Rev Neurosci.* (2010) 11:539–51. doi: 10.1038/nrn2870
78. Sani G, Napoletano F, Maria Forte A, Kotzalidis G, Panaccione I, Maria Porfiri G, et al. The wnt pathway in mood disorders. *Curr Neuropharmacol.* (2012) 10:239–53. doi: 10.2174/157015912803217279
79. Panaccione I, Napoletano F, Maria Forte A, Kotzalidis G, Del Casale A, Rapinesi C, et al. Neurodevelopment in schizophrenia: the role of the wnt pathways. *Curr Neuropharmacol.* (2013) 11:535–58. doi: 10.2174/1570159X113119990037
80. Moossavi S. Location-specific effect of microbiota and MyD88-dependent signaling on Wnt/β-catenin pathway and intestinal stem cells. *Gut Microbes.* (2014) 5:11–4. doi: 10.4161/gmic.27291
81. Simeonova D, Ivanovska M, Murdjeva M, Carvalho AF, Maes M. Recognizing the leaky gut as a trans-diagnostic target for neuro-immune disorders using clinical chemistry and molecular immunology assays. *Curr Top Med Chem.* (2018) 18:1641–55. doi: 10.2174/1568026618666181115100610
82. Manchia M, Squassina A, Pisanu C, Congiu D, Garzilli M, Guiso B, et al. Investigating the relationship between melatonin levels, melatonin system, microbiota composition and bipolar disorder psychopathology across the different phases of the disease. *Int J Bipolar Disord.* (2019) 7:27. doi: 10.1186/s40345-019-0163-y

Conflict of Interest: The authors declare that the research was conducted in the absence of any commercial or financial relationships that could be construed as a potential conflict of interest.

frontiers in Psychiatry

REVIEW
published: 22 February 2021
doi: 10.3389/fpsyt.2021.565617

Clinical Trials of Cannabidiol for Substance Use Disorders: Outcome Measures, Surrogate Endpoints, and Biomarkers

Alix Morel[1], *Pierre Lebard*[1], *Alexandra Dereux*[1,2,3], *Julien Azuar*[1,2,3], *Frank Questel*[1,2,3], *Frank Bellivier*[1,2,3,4], *Cynthia Marie-Claire*[2,3], *Mélina Fatséas*[5,6,7], *Florence Vorspan*[1,2,3,4]* *and Vanessa Bloch*[2,3,8]

[1] *Département de Psychiatrie et de Médecine Addictologique, Hôpital Lariboisière-Fernand Widal, GHU NORD, Assistance Publique – Hôpitaux de Paris, 200 rue du Fg St Denis, Paris, France,* [2] *INSERM UMRS1144, 4 avenue de l'Observatoire, Paris, France,* [3] *FHU NOR-SUD, Assistance Publique – Hôpitaux de Paris, Paris, France,* [4] *UFR Médecine, Université de Paris, 3 rue Thomas Mann, Paris, France,* [5] *University of Bordeaux, Bordeaux, France,* [6] *CNRS-UMR 5287- Institut de Neurosciences Cognitives et Intégratives d'Aquitaine (INCIA), Bordeaux, France,* [7] *Pôle d'addictologie, CHU de Bordeaux, Hôpital Haut-Lévêque, Avenue de Magellan, Pessac, France,* [8] *Service de Pharmacie, Hôpital Fernand Widal, GHU NORD, Assistance Publique – Hôpitaux de Paris, 200 rue du Fg St Denis, Paris, France*

OPEN ACCESS

Edited by:
Sven Haller,
Rive Droite SA, Switzerland

Reviewed by:
Marilyn A. Huestis,
Thomas Jefferson University, United States
Wolnei Caumo,
Clinical Hospital of Porto Alegre (HCPA), Brazil

****Correspondence:***
Florence Vorspan
florence.vorspan@lrb.aphp.fr

Specialty section:
This article was submitted to Neuroimaging and Stimulation, a section of the journal Frontiers in Psychiatry

Received: *25 May 2020*
Accepted: *21 January 2021*
Published: *22 February 2021*

Citation:
Morel A, Lebard P, Dereux A, Azuar J, Questel F, Bellivier F, Marie-Claire C, Fatséas M, Vorspan F and Bloch V (2021) Clinical Trials of Cannabidiol for Substance Use Disorders: Outcome Measures, Surrogate Endpoints, and Biomarkers. Front. Psychiatry 12:565617. doi: 10.3389/fpsyt.2021.565617

Background: Cannabidiol (CBD) is a cannabinoid of potential interest for the treatment of substance use disorders. Our aim was to review the outcome measures, surrogate endpoints, and biomarkers in published and ongoing randomized clinical trials.

Methods: We conducted a search in PubMed, Web of Science, PMC, PsycINFO, EMBASE, CENTRAL Cochrane Library, "clinicalTrials.gov," "clinicaltrialsregister.eu," and "anzctr.org.au" for published and ongoing studies. Inclusion criteria were randomized clinical trials (RCTs) examining the use of CBD alone or in association with other cannabinoids, in all substance use disorders. The included studies were analyzed in detail and their qualities assessed by a standardized tool (CONSORT 2010). A short description of excluded studies, consisting in controlled short-term or single administration in non-treatment-seeking drug users, is provided.

Findings: The screening retrieved 207 published studies, including only 3 RCTs in cannabis use disorder. Furthermore, 12 excluded studies in cannabis, tobacco, and opioid use disorders are described.

Interpretation: Primary outcomes were validated withdrawal symptoms scales and drug use reduction in the three RCTs. In the short-term or crossover studies, the outcome measures were visual analog scales for subjective states; self-rated scales for withdrawal, craving, anxiety, or psychotomimetic symptoms; and laboratory tasks of drug-induced craving, effort expenditure, attentional bias for substance, impulsivity, or anxiety to serve as surrogate endpoints for treatment efficacy. Of note, ongoing studies

are now adding peripheral biomarkers of the endocannabinoid system status to predict treatment response.

Conclusion: The outcome measures and biomarkers assessed in the ongoing CBD trials for substance use disorders are improving.

Keywords: cannabis, tobacco, opioid, clinical trials, cannabinoids, cannabidiol, efficacy, biomarker

INTRODUCTION

The legalization of "medical marijuana" in several parts of the United States, soon followed by other countries, has produced an exponential increase in research using different active compounds derived from the *Cannabis sativa* plant in various medical conditions including substance use disorders (1).

Among those pharmacological agents, cannabidiol (CBD) may be the one provoking the highest expectations. For the general population, it is a painkiller and anxiolytic compound used either dermally as oil or orally as oil (2) or herbal tea, or smoked in electronic cigarettes (3, 4) for the self-treatment of several conditions associated with chronic pains, insomnia, and various psychological suffering. Compared with tetrahydrocannabinol (THC), CBD is the product of choice for medical cannabis users who do not have an associated recreational use (5).

Pharmacologically speaking, CBD is a CB1-receptor low-affinity agonist (6, 7) with inverse-agonist properties in the presence of THC (8). Targeting the specific CB1-receptor could be of interest in the treatment not only of cannabis use disorder. Indeed, it could be relevant also in depression, anxiety, or substance-related disorders in general for 3 reasons. First, this G-coupled protein is abundant and ubiquitous in the human brain, from the brainstem and cerebellum to the basal ganglia, hippocampus, and neocortex, thus regulating several important brain functions (9). Second, CB1 antagonists can provoke serious mood disorders (10), thus supporting the reverse hypothesis that CB1 agonists, including those with low affinity as CBD, might have antidepressant effects. Third, several genetic variants of *CNR1*, the CB1-coding gene, located on chromosome 6q14–15 (NC_000006.12), have been associated with either addictive (11–15) or mood disorders (16) in case–control studies, highlighting again the potential therapeutic properties of the pharmacological modulation of this target. The published GWAS of lifetime cannabis use and cannabis use disorders (17–19) did not confirm the association. However, the genetic risk conferred by minor alleles in *CNR1* is expected to have a small effect size and to interplay with several risk alleles for various psychiatric disorders. Still, genetic variants of *CNR1*, especially those located in the 3′UTR region, regulating the translation and stability of RNA, are good candidate biomarkers for treatment efficacy of pharmacological agents targeting the CB1-receptor.

Furthermore, CBD has several non-direct CB1-receptor effects, as demonstrated in animal or cellular models. It modulates the conformation of CB1- and CB2-receptor heteromeric complexes (8). It is also a strong agonist of TRPV (vanilloid channel receptors family) located on endothelial cells, including the blood–brain barrier (20), mediating its anti-inflammatory effects along with second messenger pathway activation. CBD inhibits the cellular reuptake of the endocannabinoid anandamide, increasing its activity (21) and also increasing its disposition (22). Lastly, CBD seems to have 5HT1-receptor agonist properties (23) and 5HT3a antagonist properties (24). Because of all those properties, CBD modulates dopamine, serotonin, opioid, and the brain inflammatory systems (25). CBD has shown several effects such as decreasing anxiety and depressive-like symptoms and decreasing pain and biological stress levels in several rodent models (26–28). As those symptoms are known triggers for relapse in substance use disorders (29, 30), those results from the pre-clinical literature suggest that CBD is an interesting candidate to test in human studies.

So far, CBD has demonstrated some anxiolytic properties in human studies (31), but most of this effect was obtained from studies where CBD was compared with THC, the major compound of smoked cannabis. CBD has also anticonvulsant properties (32), now well-established in controlled trials as an adjunctive treatment in child refractory conditions (Lennox–Gastaut and Dravet syndromes), and has a Food and Drug Administration (FDA) and European Medicines Evaluation Agency (EMEA) approval for those indications.

Concerning safety, in human studies, CBD has been safely administrated for several weeks to human subjects. CBD, especially, does not induce psychodysleptic effects or abuse. Indeed, as an add-on treatment of schizophrenia (33), at a dose of 1,000 mg per day during 6 weeks, CBD produced only a slight decrease in positive symptoms compared with placebo, but with acceptable tolerance (the main side effects being nausea in one-third of patients in the active group). CBD does not induce withdrawal symptoms as was shown by a specific trial assessing withdrawal symptoms after 4 weeks of CBD 750 mg twice a day and either blind maintenance or abrupt cessation under placebo (34). In this trial, as in the literature, to the best of our knowledge, no study described any case of CBD use disorder.

Concerning efficacy, CBD has shown some promising properties in pre-clinical studies and some clinical studies in the field of psychiatry and addiction medicine. To help identify the methods currently used to assess the potential therapeutic properties of CBD in substance use disorders and isolate them from the noise of high expectations, we choose to perform a review of both published and ongoing randomized clinical trials in humans. We present the studies with a specific focus on the outcome measures, surrogate endpoints, and biomarkers

developed by the authors to show clinical efficacy or at least to show that CBD could modify targets associated with efficacy in substance use disorders.

METHODS

Search Strategy and Selection Criteria

First, we conducted a review of the published clinical trials through a PubMed data search. Looking for double-blind randomized trials, published before May 2020, we led 10 separate searches. CBD could be assessed alone or in association with other cannabinoids, in (a) alcohol, (b) amphetamine, (c) cannabis, (d) cocaine, (e) hallucinogen, (f) inhalant, (g) opioid, (h) phencyclidine, (i) sedative, and (j) tobacco use disorder.

We used the following terms: "(cannabidiol OR CBD) AND (randomized trial OR randomized study) AND (substance related disorder OR addiction OR use disorder OR use OR abuse OR excessive use OR dependence OR withdrawal)" AND either "(alcohol)," "(amphetamine OR speed OR stimulant)," "(cannabis OR marijuana OR THC)," (cocaine OR crack OR freebase)," "(hallucinogen)," "(inhalant)," "(opioid OR heroin)," "(PCP OR phencyclidine OR angel dust)," "(benzodiazepine OR sedative)," or "(tobacco OR nicotine)." Inclusion criteria for the articles were double-blinded, randomized, placebo, or adequate control, in subjects with a formal diagnosis of substance use disorder, assessing CBD alone or in association with other cannabinoids, and reporting at least one primary outcome regarding substance use disorder.

Exclusion criteria were as follows: studies involving healthy volunteers, single administration, pre-clinical studies, reviews, opinion papers, protocols, open-label studies, case reports, and studies not published in English.

Two authors (AM and PL) independently examined titles and abstracts. Relevant articles were obtained in full text and assessed for inclusion criteria blindly by the two reviewers. Disagreement was resolved *via* discussion to reach consensus.

Detailed data on each included randomized controlled trial, including target population, intervention, treatment dose, frequency and route of administration, treatment duration, control group, outcome measures, surrogate endpoints and biomarkers, adverse events, and study withdrawals, are described. The risk of bias was assessed with the Cochrane risk of bias tool, which includes assessment of indicators of selection bias, performance bias, detection bias, attrition bias, and reporting bias. Furthermore, the CONSORT 2010 (Consolidated Standards of Reporting Trials) statement was used to rate the report made in each article of the study design, analysis, and interpretation.

For the excluded studies consisting in short-term or single-administration, proof-of-concept studies, conducted mostly in non-treatment-seeking drug users, only a shorter presentation of outcome measures, surrogate endpoints, and biomarkers is provided.

Secondly, to ensure that no RCT was missed, we conducted another search with the same key words in Web of Science, PMC, PsycINFO, EMBASE, and CENTRAL Cochrane Library. No further study was added.

Lastly, to identify ongoing or unpublished studies, we searched different online registries: "clinicaltrials.gov," "clinicaltrialsregister.eu," and "anzctr.org.au" websites, using the terms "substance related disorder OR addiction OR use disorder OR use OR abuse OR excessive use OR dependence OR withdrawal" and "cannabidiol OR CBD OR nabiximols OR (THC + CBD)."

RESULTS

The PRISMA flowcharts presenting the selection of studies are shown in **Figure 1**. The initial screening identified 17 published articles presenting studies assessing CBD for alcohol, 2 for amphetamine, 105 for cannabis, 59 for hallucinogen, 6 for inhalant, 8 for opioid, 3 for sedative, and 7 for tobacco use disorder. All the other researches that we conducted retrieved no results. Of those screened studies, we finally retained only 3 studies meeting the inclusion criteria with a classical design of randomization in parallel groups, vs. placebo, for cannabis use disorder, all assessing the efficacy of nabiximol spray (a 1:1 THC/CBD ratio). Their outcome measures, surrogate endpoints, and biomarkers are detailed in **Table 1**.

Although not properly speaking randomized controlled trials of efficacy, 12 other controlled studies are presented: 3 studies of THC–CBD combination on various endpoints in cannabis users and 9 studies assessing the efficacy of CBD alone, mostly as oral tablets, on surrogate endpoints of efficacy for cannabis (4 studies), opioid (1 study), tobacco dependence (3 studies), or multiple substance use (1 study). The main considerations for exclusion are detailed in **Figure 1**.

Outcome Measures, Surrogate Endpoints, and Biomarkers of the Three Randomized Controlled Trials Assessing THC–CBD in Cannabis Use Disorder

Withdrawal Symptoms

Only three trials randomized by group, as well as placebo-controlled, assessed the pharmaceutical preparation nabiximol (1:1 THC/CBD ratio) for cannabis use disorders (30–32). All 3 studies took place in subjects with verified cannabis use disorder criteria during a cessation attempt. The studies lasted between 6 days and 12 weeks, giving way to observe both early withdrawal symptoms and later abstinence maintenance or relapse, but also to quantify cannabis use. The first published study (35), conducted in 6 consecutive days in hospitalized patients, chose to assess the CWS (Cannabis Withdrawal Scale) (38), a self-rated withdrawal scale, as the main outcome.

Drug Use Reduction

In the two other RCTs, the investigators assessed 12-week cannabis use reduction with self-reports collected with the Timeline Followback as their primary outcome (see **Table 1**) and relegate withdrawal symptoms questionnaires as secondary outcome measures. Of note, in those studies, abstinence, defined as a 4-week cannabis cessation, and time-to-relapse were also only secondary outcomes. Furthermore, the 3 studies added

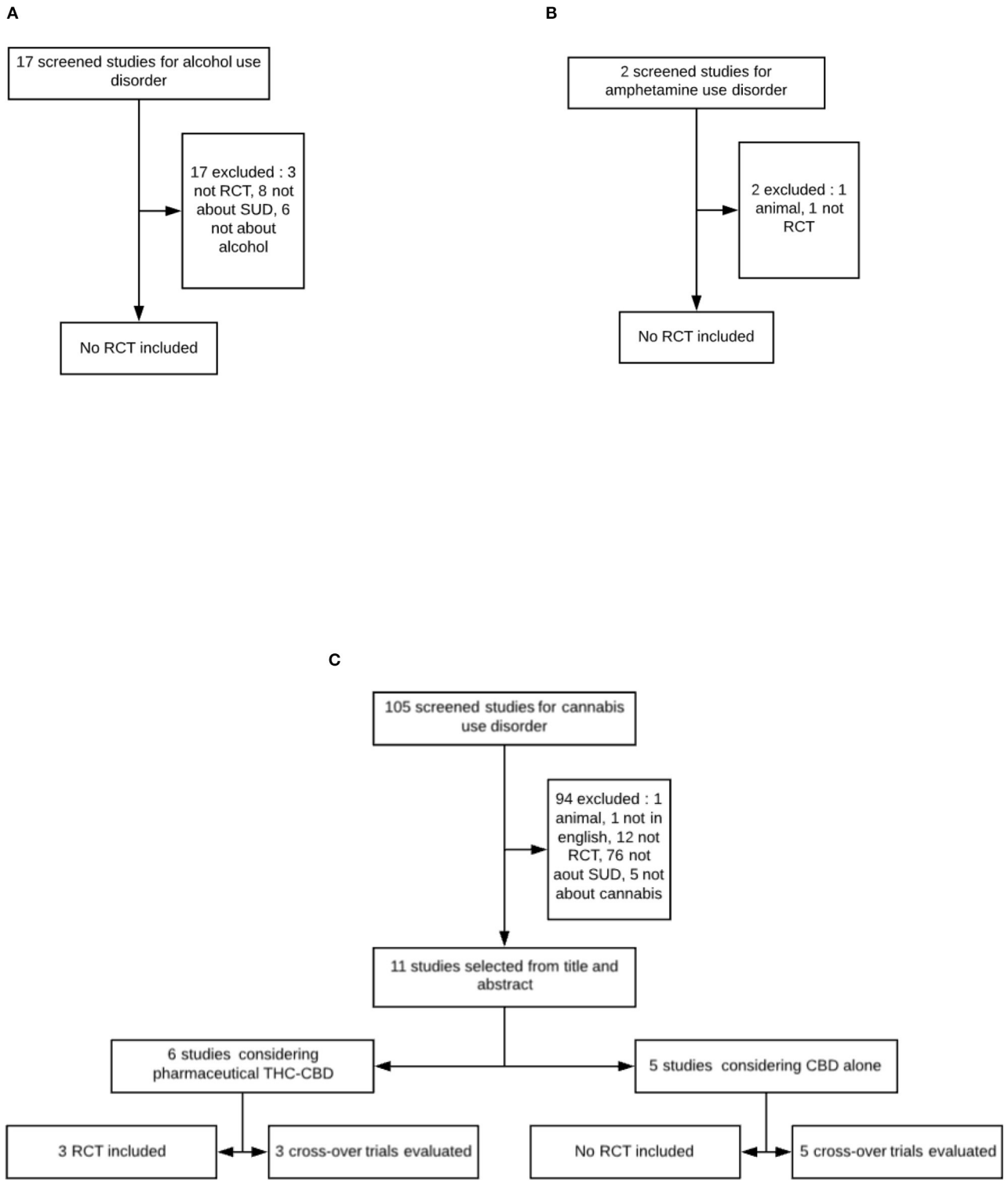

FIGURE 1 | Continued

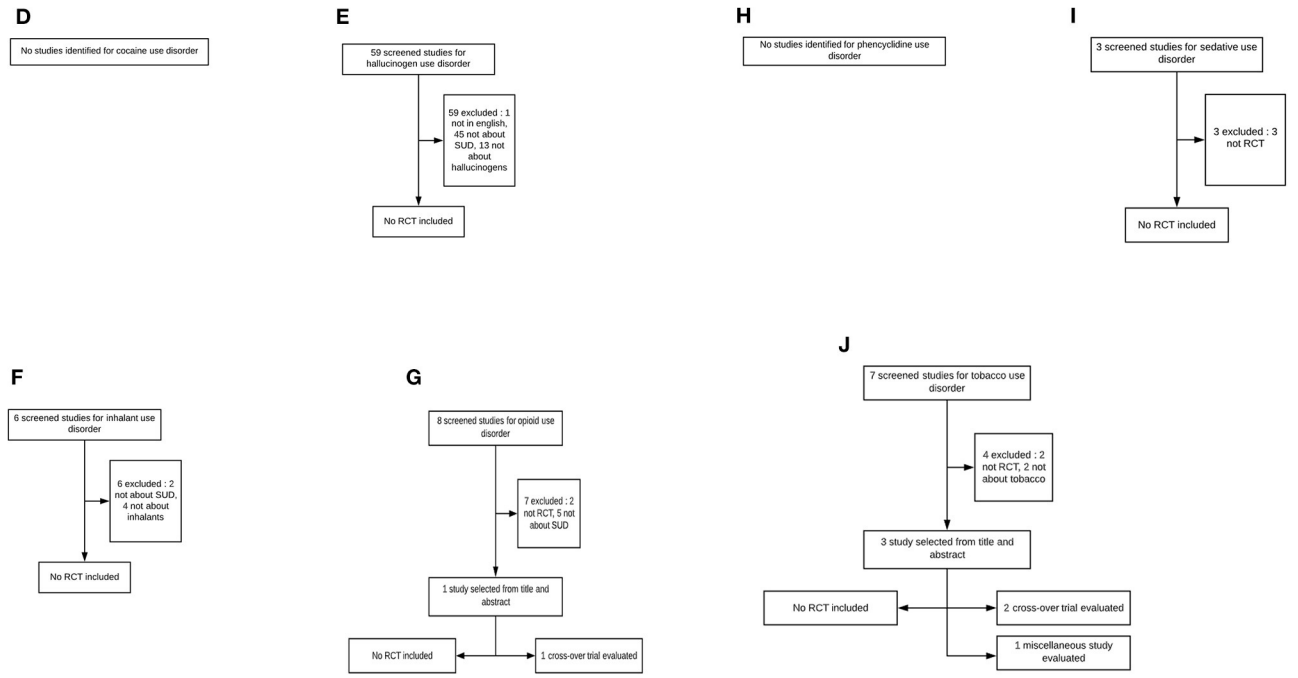

FIGURE 1 | Flowchart of screened, selected, included, and evaluated studies (SUD, substance use disorder; RCT, randomized controlled trial). **(A)** Alcohol use disorder. **(B)** Amphetamine use disorder. **(C)** Cannabis use disorder. **(D)** Cocaine use disorder. **(E)** Hallucinogen use disorder. **(F)** Inhalant use disorder. **(G)** Opioid use disorder. **(H)** Phencyclidine use disorder. **(I)** Sedative use disorder. **(J)** Tobacco use disorder.

urine or plasma cannabis measurement to characterize drug use reduction and act as surrogate endpoint predictors of abstinence. The 3 trials included a validated self-rated craving questionnaire, the Marijuana Craving Questionnaire (MCQ) (39), either complete or short form, as surrogate endpoints for abstinence. None of those 3 studies used biomarkers as a potential predictor of abstinence or cannabis use reduction.

Quality of the Methodology of the Randomized Controlled Trials

Overall, the quality of those 3 studies was good. The detailed risk of bias and quality rating regarding those studies are presented in **Tables 2**, **3**. Analyses were performed in intention-to-treat and missing data were handled by several appropriate methods: multiple imputation (35), maximum likelihood estimation (36), or intention-to-treat restricted to subjects who had received at least one dose of medication (37).

Outcome Measures, Surrogate Endpoints, and Biomarkers of the 12 Excluded Studies

Here, we give a short presentation of the methodology of the 12 pilot controlled studies that are not RCTs enrolling treatment-seeking subjects.

Three Crossover Trials Assessing THC–CBD in Cannabis Use Disorders

Consecutive Administration

Withdrawal Symptoms The study by Trigo et al. (40) used a crossover design in 16 participants with cannabis use disorder to assess withdrawal symptoms during repetitive 5-day cannabis cessation sessions assessing several doses of nabiximol. The primary outcome was assessed by 2 withdrawal scales: the CWS (38) and the Marijuana Withdrawal Scale (MWC) (41). A validated self-rated craving score, the MCQ (39), was used as a secondary outcome measure, as were the side effects or the quotation of feeling "high" with the THC–CBD doses.

Single Administrations Two crossover controlled studies assessing the effect of a single administration of THC–CBD or CBD alone used motivation and anxiety measures as primary endpoints.

Motivation and Reward Expectation One study chose to assess the motivation for rewarded tasks as a primary outcome measure (42). In a double-blinded placebo-controlled experimental study, 17 subjects realized an effort expenditure for rewarded tasks, under 3 conditions: after THC or THC–CBD (vaporized 8 mg THC + 10 mg CBD) or placebo inhalation. The authors measured not only the amount of the effort produced but also the amount of expected reward associated with the effort produced. The authors observed that CBD could attenuate the indifference provoked by THC, expressed in the attenuation of expected reward.

Anxiety Another study (43) reported more classical outcome measures in terms of heart rate and blood pressure and several self-rated visual analog of mood states including good drug effect and high anxiety, but also the repetitive assessment state anxiety part of the Spielberger State–Trait Anxiety Inventory (38). Those

TABLE 1 | Characteristics of the 3 included randomized controlled trials assessing inhaled tetrahydrocannabinol–cannabidiol (THC–CBD) in cannabis use disorder.

Author	Allsop et al. (35), Australia	Trigo et al. (36), Canada	Lintzeris et al. (37), Australia
Number of subjects	P, $n = 24$/N, $n = 27$	P, $n = 20$/N, $n = 20$	P, $n = 73$/N, $n = 64$
Out-/inpatient	Inpatient	Outpatient	Outpatient
Withdrawal	During withdrawal	During withdrawal/follow-up	During withdrawal/follow-up
Treatment	Self-titrated Maximum 86.4 mg THC + 80 mg CBD/day + CBT	Self-titrated Maximum 113.4 mg THC + 105 mg CBD/day + MET/CBT	Self-titrated Maximum 86.4 mg THC + 80 mg CBD/day + CBT
Duration	6 days of treatment, 3 days of washout, 28 days of follow-up	12 weeks	12 weeks
Primary outcome	(Intervention) Withdrawal score	Cannabis use, tolerability	Cannabis use
Secondary outcome	(Intervention) Craving (Follow-up) Time to relapse Use reduction Psychosocial outcome Tolerability	Craving score, withdrawal score	Abstinence, use reduction, withdrawal score, craving score, tolerability
Outcome measures	CWS Urine and plasma drug test	TLFB (7 days) Urine and plasma drug tests MWC MCQ-SF	TLFB (28 days) Urine drug test (placebo group) MWC MCQ
Main results	CWS: N (−66%) > P (+52%), $p = 0.01$ Retention: N > P at day 6	Cannabis use: NSD Tolerability: NSD	P (53/84 d) > N (35/84 d), $p = 0.02$
Secondary results	Time to relapse: NSD Reduction use: NSD Psychosocial: NSD Tolerability: NSD	Withdrawal: NSD Craving: NSD	Abstinence: NSD Withdrawal: NSD Craving: NSD
Quality	CONSORT: 31/32 Biases 1/10	CONSORT: 24/32 Biases 2/10	CONSORT: 30/32 Biases 3/10

MET/CBT, motivational enhancement therapy and cognitive behavior therapy; CBT, cognitive behavior therapy; TLFB, Timeline Followback; MWC, Marijuana Withdrawal Checklist; MCQ, Marijuana Craving Questionnaire; MCQ-SF, Marijuana Craving Questionnaire Short Form; CWS, Cannabis Withdrawal Scale; NSD, non-significant difference; P, placebo; N, nabiximol.

assessments were repeated several times over 10 h after a single intake of either the following: oral THC 5 mg, oral THC 15 mg, oromucosal spray pharmaceutical THC–CBD low dose (5.4 mg THC + 5.0 mg CBD) or high dose (16.2 mg THC + 15.0 mg CBD), oral placebo, or oromucosal spray placebo. The subjects were 9 occasional cannabis users. The adjunction of CBD did not prevent the rise of anxiety associated with THC in the few hours after THC–CBD mixtures.

Outcome Measures, Surrogate Endpoints, and Biomarkers of the Nine Excluded Studies of CBD Alone for Substance Use Disorders

Consecutive Administration

Drug Use Reduction

We identified a pilot study in tobacco dependence (44) with only an indirect comparison design that did not qualify for our inclusion criteria. We thus classified it as "miscellaneous" (see **Figure 1J**). The chosen primary outcome was smoking reduction measured by the declared number of cigarettes smoked in 1 week. Smokers were randomized to receive either *ad libitum* inhaled CBD ($n = 12$) or placebo ($n = 12$) *via* an inhaler delivering 400 μg of CBD at each press. Secondary outcome measures included tobacco craving and self-rated separate visual analog scales of the MRS (Mood Rating Scale) (45) including depression, anxiety, and sedation. The results are presented like those assessments that occurred only once on day 0 and once on day 7. No direct comparison of craving reduction between groups is provided.

Single Administrations

We present here some data from the eight other published articles of interest. They were conducted in heroin-dependent subjects (1 study), in regular cannabis users (4 studies), in dependent tobacco smokers (2 articles), and in subjects with multiple dependencies (1 study). Their primary outcome measures were diverse and are listed below.

Cue-Induced Craving and Anxiety

The only published study assessing CBD effects in 42 subjects with heroin use disorder, currently abstinent (46), was a crossover, placebo-controlled trial examining 3 consecutive days of oral CBD 400 mg per day or CBD 800 mg per day or placebo. The primary outcome measures were repetitive visual analog scales (VASs) of craving and anxiety during cue-induced laboratory sessions, up to 7 days after the

TABLE 2 | Internal and external validity of the 3 THC-CBD trials in cannabis use disorder evaluated by Cochrane risk of bias tool.

	Allsop et al. (35)	Trigo et al. (36)	Lintzeris et al. (37)
Internal validity			
Selection bias			
Random sequence generation	y	y	y
Allocation protected from contamination	y	y	y
Similar baseline characteristics	y	y	y
Detection bias			
PPG calculation	y	y	y
Blinding of outcome assessment	y	y	y
Adequate outcome measurement	y	y	y
Equivalent assessment	y	y	y
Attrition bias			
Incomplete outcome data	y (ITT)	y (ITT)	y (mITT)
Report bias			
No selective reporting	y	y	y
External validity			
Appropriate comparator	y	y	y

PPG, participant per group; y, yes; ITT, intention-to-treat; mITT, modified intention-to-treat.

end of CBD administration. Several secondary outcome measures were also assessed: the Positive and Negative Affect Scores (PANAS) (47) and several cognition tests, mostly consisting in sustained attention tasks, such as a Digit Symbol Substitution Task (DSST), a Digit Span Test–Backward (DSTB), and a Continuous Performance Task (CPT). The investigators added physiological measures, including heart rate, blood pressure, and body temperature and salivary cortisol levels, as biomarkers of cue-induced stress during the exposition task. The authors concluded that both CBD doses reduced craving and anxiety during the tasks of salient drug cue presentation compared with neutral cues. In addition, the drug cue-induced physiological measures of heart rate and salivary cortisol levels were also attenuated. No sedation effects were observed, and there was also no cognitive enhancement.

Psychomimetic Subjective Effect

A study conducted in occasional and regular cannabis users with a single inhalation of either THC 8 mg, CBD 16 mg, THC 8 mg + CBD 16 mg, or placebo (48) chose as primary endpoint a scale designed to assess drug-induced psychotomimetic effects, the Psychotomimetic States Inventory (PSI) (49) along with the validated Brief Psychiatric Rating scale (BPRS) (50). The co-administration of CBD did not attenuate the psychotomimetic effects of THC, and CBD alone reduced PSI scores in light users only. This study included a working memory task using a word list and sustained attention tests as secondary outcome measures, showing again that CBD in co-administration did not attenuate the impairing memory and cognitive effect of THC and that CBD alone had no cognitive enhancement properties.

TABLE 3 | CONSORT quality ratings of the 3 THC-CBD trials in cannabis use disorder.

CONSORT 2010			Allsop et al. (35)	Trigo et al. (36)	Lintzeris et al. (37)
Title and abstract		1a	y	n	y
		1b	y	y	y
Introduction		2a	y	y	y
		2b	y	y	y
Methods	Trial design	3a	y	y	y
		3b	n/a	n/a	n/a
	Participants	4a	y	y	y
		4b	y	n	y
	Interventions	5	y	y	y
	Outcomes	6a	y	n	y
		6b	n/a	n/a	n/a
	Sample size	7a	y	y	y
		7b	n/a	n/a	n/a
Randomization	Sequence generation	8a	y	y	y
		8b	y	y	y
	Allocation concealment mechanism	9	y	n	n
	Implementation	10	n	y	y
	Blinding	11a	y	y	y
		11b	y	y	y
	Statistical methods	12a	y	y	y
		12b	y	y	y
Results	Participant flow	13a	y	n	y
		13b	y	y	y
	Recruitment	14a	y	n	y
		14b	n/a	n/a	n/a
	Baseline data	15	y	y	y
	Numbers analyzed	16	y	n	y
	Outcome measures and estimation	17a	y	y	y
		17b	n/a	n/a	n/a
	Ancillary analyses	18	y	y	y
	Harms	19	y	y	y
Discussion	Limitations	20	y	y	y
	Generalizability	21	y	y	y
	Interpretation	22	y	y	y
Other information	Registration	23	y	y	y
	Protocol	24	n	n	y
	Funding	25	y	y	y
Total/32			31	24	30

n, no; y, yes; n/a, non-applicable.

Attentional Bias and Impulsivity

In order to test what could be surrogate endpoints for CBD efficacy in tobacco use disorder, a British team published

in 2 interesting articles the results of a crossover trial of 1 administration of 800 mg CBD vs. placebo in non-treatment-seeking tobacco smokers during experimental sessions of 24 h abstinence, separated by 1-week washouts (51, 52). In the first report (51), the primary outcome was the attentional bias toward tobacco cues (AB) as a slower response time during a Visual Probe Task (VPT) with both neutral and smoking-related cues. Furthermore, participants had to quote the pleasantness of the task. Secondary outcome measures included withdrawal and craving scales, heart rate, blood pressure, and side effect scales. In the second report (52), the primary outcome was impulsivity, and it was measured by 2 tests. In a Delay-Discounting Task, no significant difference between CBD and placebo was found, while a Go/No-go task showed significantly more errors with CBD than placebo. Memory was measured by a Prose Recall Task (PRT), showing no significant difference between CBD and placebo. Furthermore, an N-Back Task (NBT) showed no difference for correct responses, reaction time, and maintenance and manipulation. Thus, CBD was not shown to improve cognition in the specific condition of nicotine withdrawal.

Cognitive Performance

Several cognitive tests were also assessed in another specific condition, this time the pretreatment with a single dose of 200, 400, or 800 mg CBD prior to smoked cannabis intake (53), along with several VASs exploring the reinforcing and subjective effect of this interaction, during 8 sessions. Once again, no specific significant differences were found between CBD and placebo and neither was there any signal of abuse liability (54).

Abuse Liability

Another team performed the same kind of experiment to assess the abuse liability of oral CBD in healthy recreational polydrug users (55). The investigators compared single administrations of 750, 1,500, and 4,500 mg oral CBD to alprazolam 2 mg (APZ) or dronabinol (THC) 10 and 30 mg. The primary outcome was again the maximum effect (Emax) on a drug-liking VAS scale, with also positive ("feeling high" and "feeling stoned") and negative effects, and there were several other subjective effects as secondary outcome measures. Cognitive, memory, and psychomotor functions were measured by a Divided Attention Test (DAT), the Hopkins Verbal Learning Test Revised (HVLT), and the DSST. Again, this study confirmed that single-dose oral CBD does not show any signal of abuse liability as well as no detectable cognitive effect in this condition.

Facial Emotion Recognition Task

Originally, we identified 1 study conducted by Hindocha et al. (56), which examined the acute effects of THC, CBD, and their combination on facial emotion recognition. This task consists in showing six basic emotions (happiness, sadness, anger, disgust, fearful, surprise, and neutrality) and with an intensity degree in 5 levels. Facial recognition is impaired in mood and anxiety disorders. The reduction of its impairment is proposed as a surrogate endpoint for treatment efficacy in anxiety disorders when screening new molecules (48). Regular cannabis smokers attended 4 sessions with a 1-week washout and were administered by inhalation either THC 8 mg, CBD 16 mg, THC + CBD (8 + 16 mg), or placebo. The results showed that at 60% intensity, participants were more accurate with CBD alone than placebo. At more ambiguous emotion levels, at 40% intensity, participants with THC–CBD were more accurate than participants with THC alone. As a secondary outcome measures, participants also completed the subjective effect VASs for "stoned," "anxiety," "alert," and "happy or sad," among other subjective states. The results did not support the investigators' hypothesis that cannabis users would differ according to their score on a Schizotypal Proneness Questionnaire.

None of those single-administration studies tested if their primary or secondary outcome measures were associated with indirect brain biomarkers of substance use disorder severity or evolution. In the studies presenting time-curve evolution of mood or cognitive effects over some hours, no correlation with plasma CBD level was shown.

Ongoing Studies

Our screening in the American clinical trial registry (clinicaltrials.gov) identified 87 studies. The same screening in the European clinical trial web-base (clinialtrialsregister.eu) identified 2 studies and seven from the Australian and New Zealand clinical trial registry (anzctr.org.au). We did not retain studies not performed in substance use disorders (mostly performed in epilepsy or chronic pain), already published studies (previously included in this review), and studies recorded in several registries. This left 13 studies. Of note, and this is an important change from the past few years, all those studies are evaluating the efficacy of CBD alone as the treatment of interest. The substance use disorder conditions assessed in those studies were as follows: cannabis use disorder (UD) (5 studies), opioid UD (4 studies), alcohol UD (3 studies), and 1 study was also found in cocaine UD. Eight studies were conducted in North America, 2 in Europe, 2 in Oceania, and 1 with unknown location. Protocols, CBD dose, and duration vary according to the study. The duration of CBD administration ranges from four single administrations to 3 months, with the majority of studies assessing 1–2 months of treatment. CBD doses range from 300 to 1,400 mg per day. The primary outcome measures are withdrawal symptoms or craving in the shortest studies (on opioid UD, alcohol UD) and also substance use or relapse, associated with craving in several-week duration trials (cannabis UD, alcohol UD, cocaine UD). Most studies have also secondary outcome measures with various subjective symptoms scales: anxiety, sleep quality, psychotic symptoms, and craving, serving as surrogate endpoints for efficacy. On top of that, those more recent studies add several biomarkers to be tested as surrogate endpoints for efficacy: cannabidiol plasma levels (alcohol UD studies, opioid UD studies, cocaine UD study), combined with endocannabinoid plasma levels (cannabis UD studies and cocaine UD study) composed of both CBD and anandamide plasma levels, sometimes combined with other biomarkers: mono-amine plasma levels or inflammatory biomarkers including plasma cortisol in cocaine UD.

DISCUSSION

Despite the great expectations toward the possible therapeutic effects of CBD in substance use disorders, this review showed that published data are limited. There is no published study demonstrating the efficacy of CBD alone to treat any substance use disorder.

When choosing stringent inclusion criteria, only 3 high-quality randomized placebo-controlled trials can be retained. All those 3 studies tested THC/CBD compounds and proposed to treat cannabis use disorder. Their primary outcome measures were validated scales of withdrawal symptoms or cannabis use reduction. In the context of efficacy trials, validated craving scales, previously associated with relapse, are only secondary outcomes. Those 3 studies did not report on any biomarker that could be used as a useful predictor of efficacy.

Regarding trials assessing CBD alone in treating substance use disorder, none of them can qualify as a high-quality randomized controlled trial. Published data are limited to very short-term or even single-administration crossover designs. In such short-term pilot studies, the efficacy assessment can only rely on primary outcome measures sensitive to short-term change. In that context, series of visual analog scales of various subjective effects, describing the drug effects or anxiety or mood states, are useful and allow repetitive assessments and the establishment of time curves. The adjunction of validated withdrawal or craving scales, as well as scales assessing anxiety or psychotomimetic effects, is an improvement if those scales are validated for such repetitive assessments.

The investigators identified tasks that could be surrogate endpoints for treatment efficacy in substance use disorders, by mimicking conditions associated with relapse: drug-induced craving, attentional bias for the substance, impulsivity, or anxiety. The assessment of the expected procognitive properties of CBD does not target relapse. It is rather a way to rule out the THC-induced cognitive side effects.

There is a shift in the most recently declared clinical trials toward more prolonged efficacy trials and toward targeting more substance use disorders, including alcohol and cocaine use disorders. This shift is also accompanied by a qualitative improvement of the methodology toward the use of biomarkers that could be predictive of CBD efficacy. Above classical pharmacokinetic parameters such as CBD plasma level, which could help to define a therapeutic range, researchers are now adding new peripheral biomarkers assessing the current state of the endocannabinoid system, the mono-amine system, or the immune system. Of note, those biomarkers could be applied to all substance use disorders. Indeed, repetitive drug intake produces homeostatic changes in the common final pathway of the brain reward circuit. The endocannabinoid system plays a role of modulator of this circuit. Those therapeutic trials could benefit from a more general enhancement in research for the identification of valid biomarkers of the reward circuit homeostatic state. They could include peripheral biomarkers, combined with brain imagery or neuropsychological tasks, and eventually drug administration challenges to describe the various stages of substance use disorder. In particular, an entire research era consisting in the design of study protocols able to assess the central nervous system pharmacological target engagement by CBD could emerge in the next years. They could include the association of *CNR1* gene polymorphisms with treatment response, or specific measures of the central nervous system inflammation state through radioactive ligands, or markers of CB1- or 5HT-receptors or TRPV channel activity.

Among the strengths of our review, we would like to point out the stringent definition of included/excluded published studies; the extended search strategy including PubMed, Web of Science, PMC, PsycINFO, EMBASE, and CENTRAL Cochrane Library; the double selection made independently by two reviewers; and the separate presentation of declared ongoing studies.

CONCLUSION

The field of research assessing the efficacy of CBD in substance use disorder is emergent. To date, published randomized controlled trials are limited to THC–CBD compounds. However, pilot studies assessing single administrations or short-term efficacy of CBD alone on surrogate endpoints of efficacy have already been conducted. They targeted cue-induced craving, effort expenditure, attentional bias for the substance, impulsivity, or anxiety. The next generation of trials, already ongoing, will include peripheral biomarkers of the endocannabinoid system homeostatic state as well as immunologic biomarkers as potential predictors of efficacy. Our recommendation for future randomized clinical trials testing the efficacy of CBD to treat substance use disorders would be to combine the repetitive assessment of 3 types of biomarkers of efficacy: peripheral biomarkers of the endocannabinoid system such as cannabinoid plasma level, short-term surrogate endpoints (such as craving or attentional bias reduction), and long-term validated measures of abstinence, dose reduction, or harm reduction.

AUTHOR CONTRIBUTIONS

FV and MF designed the study. AM and PL screened the studies and wrote the first draft. All authors have significantly contributed to the discussion and approved the final manuscript.

FUNDING

This study was funded by the French Ministry of Health (PHRC national 2018) to FV to support a randomized controlled trial of CBD in alcohol use disorder. The study sponsor is the DRCI (Direction de la Recherche Clinique et de l'Innovation) from the Assistance Publique - Hôpitaux de Paris. The funding source as well as the sponsor had no part in the study design, the writing or the choice to submit this work for publication.

REFERENCES

1. Di Marzo V, Bifulco M, De Petrocellis L. The endocannabinoid system and its therapeutic exploitation. *Nat Rev Drug Discov*. (2004) 3:771–84. doi: 10.1038/nrd1495
2. Izgelov D, Davidson E, Barasch D, Regev A, Domb AJ, Hoffman A. Pharmacokinetic investigation of synthetic cannabidiol oral formulations in healthy volunteers. *Eur J Pharm Biopharm*. (2020) 154:108–15. doi: 10.1016/j.ejpb.2020.06.021
3. Davenport S. Price and product variation in Washington's recreational cannabis market. *Int J Drug Policy*. (2019) 102547. doi: 10.1016/j.drugpo.2019.08.004
4. Giroud C, de Cesare M, Berthet A, Varlet V, Concha-Lozano N, Favrat B. E-Cigarettes: a review of new trends in cannabis use. *IJERPH*. (2015) 12:9988–10008. doi: 10.3390/ijerph120809988
5. Morean ME, Lederman IR. Prevalence and correlates of medical cannabis patients' use of cannabis for recreational purposes. *Addict Behav*. (2019) 93:233–9. doi: 10.1016/j.addbeh.2019.02.003
6. Bergamaschi MM, Queiroz RHC, Zuardi AW, Crippa JAS. Safety and side effects of cannabidiol, a *Cannabis sativa* constituent. *Curr Drug Saf*. (2011) 6:237–49. doi: 10.2174/157488611798280924
7. Dalton WS, Martz R, Lemberger L, Rodda BE, Forney RB. Influence of cannabidiol on delta-9-tetrahydrocannabinol effects. *Clin Pharmacol Ther*. (1976) 19:300–9. doi: 10.1002/cpt1976193300
8. Navarro G, Varani K, Lillo A, Vincenzi F, Rivas-Santisteban R, Raïch I, et al. Pharmacological data of cannabidiol- and cannabigerol-type phytocannabinoids acting on cannabinoid CB1, CB2 and CB1/CB2 heteromer receptors. *Pharmacol Res*. (2020) 159:104940. doi: 10.1016/j.phrs.2020.104940
9. Piomelli D. The molecular logic of endocannabinoid signalling. *Nat Rev Neurosci*. (2003) 4:873–84. doi: 10.1038/nrn1247
10. Topol EJ, Bousser M-G, Fox KAA, Creager MA, Despres J-P, Easton JD, et al. Rimonabant for prevention of cardiovascular events (CRESCENDO): a randomised, multicentre, placebo-controlled trial. *Lancet*. (2010) 376:517–23. doi: 10.1016/S0140-6736(10)60935-X
11. Chen X, Williamson VS, An S-S, Hettema JM, Aggen SH, Neale MC, et al. Cannabinoid receptor 1 gene association with nicotine dependence. *Arch Gen Psychiatry*. (2008) 65:816–24. doi: 10.1001/archpsyc.65.7.816
12. Agrawal A, Wetherill L, Dick DM, Xuei X, Hinrichs A, Hesselbrock V, et al. Evidence for association between polymorphisms in the cannabinoid receptor 1. (CNR1) gene and cannabis dependence. *Am J Med Genet B Neuropsychiatr Genet*. (2009) 150B:736–40. doi: 10.1002/ajmg.b.30881
13. Marcos M, Pastor I, de la Calle C, Barrio-Real L, Laso FJ, González-Sarmiento R. Cannabinoid receptor 1 gene is associated with alcohol dependence. *Alcohol Clin Exp Res*. (2012) 36:267–71. doi: 10.1111/j.1530-0277.2011.01623.x
14. Clarke T-K, Bloch PJ, Ambrose-Lanci LM, Ferraro TN, Berrettini WH, Kampman KM, et al. Further evidence for association of polymorphisms in the CNR1 gene with cocaine addiction: confirmation in an independent sample and meta-analysis. *Addict Biol*. (2013) 18:702–8. doi: 10.1111/j.1369-1600.2011.00346.x
15. Zhang P-W, Ishiguro H, Ohtsuki T, Hess J, Carillo F, Walther D, et al. Human cannabinoid receptor 1: 5' exons, candidate regulatory regions, polymorphisms, haplotypes and association with polysubstance abuse. *Mol Psychiatry*. (2004) 9:916–31. doi: 10.1038/sj.mp.4001560
16. Agrawal A, Nelson EC, Littlefield AK, Bucholz KK, Degenhardt L, Henders AK, et al. Cannabinoid receptor genotype moderation of the effects of childhood physical abuse on anhedonia and depression. *Arch Gen Psychiatry*. (2012) 69:732–40. doi: 10.1001/archgenpsychiatry.2011.2273
17. Pasman JA, Verweij KJH, Gerring Z, Stringer S, Sanchez-Roige S, Treur JL, et al. GWAS of lifetime cannabis use reveals new risk loci, genetic overlap with psychiatric traits, and a causal influence of schizophrenia. *Nat Neurosci*. (2018) 21:1161–70. doi: 10.1038/s41593-018-0206-1
18. Demontis D, Rajagopal VM, Thorgeirsson TE, Als TD, Grove J, Leppälä K, et al. Genome-wide association study implicates CHRNA2 in cannabis use disorder. *Nat Neurosci*. (2019) 22:1066–74. doi: 10.1038/s41593-019-0416-1
19. Agrawal A, Chou Y-L, Carey CE, Baranger DAA, Zhang B, Sherva R, et al. Genome-wide association study identifies a novel locus for cannabis dependence. *Mol Psychiatry*. (2018) 23:1293–302. doi: 10.1038/mp.2017.200
20. Luo H, Rossi E, Saubamea B, Chasseigneaux S, Cochois V, Choublier N, et al. Cannabidiol increases proliferation, migration, tubulogenesis, and integrity of human brain endothelial cells through TRPV2 activation. *Mol Pharmaceutics*. (2019) 16:1312–26. doi: 10.1021/acs.molpharmaceut.8b01252
21. Bisogno T, Hanuš L, De Petrocellis L, Tchilibon S, Ponde DE, Brandi I, et al. Molecular targets for cannabidiol and its synthetic analogues: effect on vanilloid VR1 receptors and on the cellular uptake and enzymatic hydrolysis of anandamide: Cannabidiol, VR1 receptors and anandamide inactivation. *Br J Pharmacol*. (2001) 134:845–52. doi: 10.1038/sj.bjp.0704327
22. Izzo AA, Borrelli F, Capasso R, Di Marzo V, Mechoulam R. Non-psychotropic plant cannabinoids: new therapeutic opportunities from an ancient herb. *Trends Pharmacol Sci*. (2009) 30:515–27. doi: 10.1016/j.tips.2009.07.006
23. Hartmann A, Lisboa SF, Sonego AB, Coutinho D, Gomes FV, Guimarães FS. Cannabidiol attenuates aggressive behavior induced by social isolation in mice: involvement of 5-HT1A and CB1 receptors. *Progr Neur Psychopharmacol Biol Psychiatry*. (2019) 94:109637. doi: 10.1016/j.pnpbp.2019.109637
24. Yang K-H, Galadari S, Isaev D, Petroianu G, Shippenberg TS, Oz M. The nonpsychoactive cannabinoid cannabidiol inhibits 5-hydroxytryptamine $_{3A}$ receptor-mediated currents in *Xenopus laevis* oocytes. *J Pharmacol Exp Ther*. (2010) 333:547–54. doi: 10.1124/jpet.109.162594
25. Ibeas Bih C, Chen T, Nunn AVW, Bazelot M, Dallas M, Whalley BJ. Molecular targets of cannabidiol in neurological disorders. *Neurotherapeutics*. (2015) 12:699–730. doi: 10.1007/s13311-015-0377-3
26. Campos AC, Fogaça MV, Sonego AB, Guimarães FS. Cannabidiol, neuroprotection and neuropsychiatric disorders. *Pharmacol Res*. (2016) 112:119–27. doi: 10.1016/j.phrs.2016.01.033
27. Norris C, Loureiro M, Kramar C, Zunder J, Renard J, Rushlow W, et al. Cannabidiol modulates fear memory formation through interactions with serotonergic transmission in the mesolimbic system. *Neuropsychopharmacol*. (2016) 41:2839–50. doi: 10.1038/npp.2016.93
28. Fogaça MV, Campos AC, Coelho LD, Duman RS, Guimarães FS. The anxiolytic effects of cannabidiol in chronically stressed mice are mediated by the endocannabinoid system: Role of neurogenesis and dendritic remodeling. *Neuropharmacology*. (2018) 135:22–33.e28. doi: 10.1016/j.neuropharm.2018.03.001
29. Koob GF, Volkow ND. Neurobiology of addiction: a neurocircuitry analysis. *Lancet Psychiatry*. (2016) 3:760–73. doi: 10.1016/S2215-0366(16)00104-8
30. Fatseas M, Serre F, Swendsen J, Auriacombe M. Effects of anxiety and mood disorders on craving and substance use among patients with substance use disorder: an ecological momentary assessment study. *Drug Alcohol Depend*. (2018) 187:242–8. doi: 10.1016/j.drugalcdep.2018.03.008
31. Zuardi AW, Shirakawa I, Finkelfarb E, Karniol IG. Action of cannabidiol on the anxiety and other effects produced by delta 9-THC in normal subjects. *Psychopharmacology (Berl)*. (1982) 76:245–50. doi: 10.1007/BF00432554
32. Perucca E. Cannabinoids in the treatment of epilepsy: hard evidence at last? *J Epilepsy Res*. (2017) 7:61–76. doi: 10.14581/jer.17012
33. McGuire P, Robson P, Cubala WJ, Vasile D, Morrison PD, Barron R, et al. Cannabidiol (CBD) as an adjunctive therapy in schizophrenia: a multicenter randomized controlled trial. *Am J Psychiatry*. (2018) 175:225–31. doi: 10.1176/appi.ajp.2017.17030325
34. Taylor L, Crockett J, Tayo B, Checketts D, Sommerville K. Abrupt withdrawal of cannabidiol (CBD) a randomized trial *Epilepsy Behav*. (2020) 104:106938. doi: 10.1016/j.yebeh.2020.106938
35. Allsop DJ, Copeland J, Lintzeris N, Dunlop AJ, Montebello M, Sadler C, et al. Nabiximols as an agonist replacement therapy during cannabis withdrawal: a randomized clinical trial. *JAMA Psychiatry*. (2014) 71:281–91. doi: 10.1001/jamapsychiatry.2013.3947
36. Trigo JM, Soliman A, Quilty LC, Fischer B, Rehm J, Selby P, et al. Nabiximols combined with motivational enhancement/cognitive behavioral therapy for the treatment of cannabis dependence: a pilot randomized clinical trial. *PLoS ONE*. (2018) 13:e0190768. doi: 10.1371/journal.pone.0190768
37. Lintzeris N, Bhardwaj A, Mills L, Dunlop A, Copeland J, McGregor I, et al. Nabiximols for the treatment of cannabis dependence: a randomized clinical trial. *JAMA Intern Med*. (2019) 179:1242–53. doi: 10.1001/jamainternmed.2019.1993

38. Gorelick DA, Levin KH, Copersino ML, Heishman SJ, Liu F, Boggs DL, et al. Diagnostic criteria for cannabis withdrawal syndrome. *Drug Alcohol Depend*. (2012) 123:141–7. doi: 10.1016/j.drugalcdep.2011.11.007
39. Heishman SJ, Singleton EG. Assessment of cannabis craving using the marijuana craving questionnaire. *Methods Mol Med*. (2006) 123:209–16. doi: 10.1385/1-59259-999-0:209
40. Trigo JM, Lagzdins D, Rehm J, Selby P, Gamaleddin I, Fischer B, et al. Effects of fixed or self-titrated dosages of sativex on cannabis withdrawal and cravings. *Drug Alcohol Depend*. (2016) 161:298–306. doi: 10.1016/j.drugalcdep.2016.02.020
41. Budney AJ, Novy PL, Hughes JR. Marijuana withdrawal among adults seeking treatment for marijuana dependence. *Addiction*. (1999) 94:1311–22. doi: 10.1046/j.1360-0443.1999.94913114.x
42. Lawn W, Freeman TP, Pope RA, Joye A, Harvey L, Hindocha C, et al. Acute and chronic effects of cannabinoids on effort-related decision-making and reward learning: an evaluation of the cannabis "amotivational" hypotheses. *Psychopharmacology*. (2016) 233:3537–52. doi: 10.1007/s00213-016-4383-x
43. Karschner EL, Darwin WD, McMahon RP, Liu F, Wright S, Goodwin RS, et al. Subjective and physiological effects after controlled Sativex and oral THC administration. *Clin Pharmacol Ther*. (2011) 89:400–7. doi: 10.1038/clpt.2010.318
44. Morgan CJA, Das RK, Joye A, Curran HV, Kamboj SK. Cannabidiol reduces cigarette consumption in tobacco smokers: preliminary findings. *Addict Behav*. (2013) 38:2433–6. doi: 10.1016/j.addbeh.2013.03.011
45. Bond A, Lader M. The use of analogue scales in rating subjective feelings. *Br J Med Psychol*. (1974) 47:211–8. doi: 10.1111/j.2044-8341.1974.tb02285.x
46. Hurd YL, Spriggs S, Alishayev J, Winkel G, Gurgov K, Kudrich C, et al. Cannabidiol for the reduction of cue-induced craving and anxiety in drug-abstinent individuals with heroin use disorder: a double-blind randomized placebo-controlled trial. *Am J Psychiatry*. (2019) 176:911–22. doi: 10.1176/appi.ajp.2019.18101191
47. Crawford JR, Henry JD. The positive and negative affect schedule (PANAS) construct validity, measurement properties and normative data in a large non-clinical sample. *Br J Clin Psychol*. (2004) 43:245–65. doi: 10.1348/0144665031752934
48. Morgan CJA, Freeman TP, Hindocha C, Schafer G, Gardner C, Curran HV. Individual and combined effects of acute delta-9-tetrahydrocannabinol and cannabidiol on psychotomimetic symptoms and memory function. *Transl Psychiatry*. (2018) 8:181. doi: 10.1038/s41398-018-0191-x
49. Mason OJ, Morgan CJM, Stefanovic A, Curran HV. The Psychotomimetic states inventory (PSI) Measuring psychotic-type experiences from ketamine and cannabis. *Schizophr Res*. (2008) 103:138–42. doi: 10.1016/j.schres.2008.02.020
50. Overall JE, Gorham DR. The brief psychiatric rating scale. *Psychol Rep*. (1962) 10:799–812. doi: 10.2466/pr0.1962.10.3.799
51. Hindocha C, Freeman TP, Grabski M, Stroud JB, Crudgington H, Davies AC, et al. Cannabidiol reverses attentional bias to cigarette cues in a human experimental model of tobacco withdrawal. *Addiction*. (2018) 113:1696–1705. doi: 10.1111/add.14243
52. Hindocha C, Freeman TP, Grabski M, Crudgington H, Davies AC, Stroud JB, et al. The effects of cannabidiol on impulsivity and memory during abstinence in cigarette dependent smokers. *Sci Rep*. (2018) 8:7568. doi: 10.1038/s41598-018-25846-2
53. Haney M, Malcolm RJ, Babalonis S, Nuzzo PA, Cooper ZD, Bedi G, et al. Oral cannabidiol does not alter the subjective, reinforcing or cardiovascular effects of smoked cannabis. *Neuropsychopharmacology*. (2016) 41:1974–82. doi: 10.1038/npp.2015.367
54. Babalonis S, Haney M, Malcolm RJ, Lofwall MR, Votaw VR, Sparenborg S, et al. Oral cannabidiol does not produce a signal for abuse liability in frequent marijuana smokers. *Drug Alcohol Depend*. (2017) 172:9–13. doi: 10.1016/j.drugalcdep.2016.11.030
55. Schoedel KA, Szeto I, Setnik B, Sellers EM, Levy-Cooperman N, Mills C, et al. Abuse potential assessment of cannabidio (CBD) in recreational polydrug users: a randomized, double-blind, controlled trial. *Epilepsy Behav*. (2018) 88:162–71. doi: 10.1016/j.yebeh.2018.07.027
56. Hindocha C, Freeman TP, Schafer G, Gardener C, Das RK, Morgan CJA, et al. Acute effects of delta-9-tetrahydrocannabinol, cannabidiol and their combination on facial emotion recognition: a randomised, double-blind, placebo-controlled study in cannabis users. *Eur Neuropsychopharmacol*. (2015) 25:325–34. doi: 10.1016/j.euroneuro.2014.11.014

Conflict of Interest: The authors declare that the research was conducted in the absence of any commercial or financial relationships that could be construed as a potential conflict of interest.

Advantages of publishing in Frontiers

OPEN ACCESS
Articles are free to read for greatest visibility and readership

FAST PUBLICATION
Around 90 days from submission to decision

HIGH QUALITY PEER-REVIEW
Rigorous, collaborative, and constructive peer-review

TRANSPARENT PEER-REVIEW
Editors and reviewers acknowledged by name on published articles

Frontiers
Avenue du Tribunal-Fédéral 34
1005 Lausanne | Switzerland

Visit us: www.frontiersin.org
Contact us: frontiersin.org/about/contact

REPRODUCIBILITY OF RESEARCH
Support open data and methods to enhance research reproducibility

DIGITAL PUBLISHING
Articles designed for optimal readership across devices

FOLLOW US
@frontiersin

IMPACT METRICS
Advanced article metrics track visibility across digital media

EXTENSIVE PROMOTION
Marketing and promotion of impactful research

LOOP RESEARCH NETWORK
Our network increases your article's readership